COLLECTED PAPERS on Off-shell Science

Vol. 37

January 2022 – December 2022

Motoichi OHTSU[1,2]

1 Chief Director
(General Incorporated Association)
Research Origin for Dressed Photon
2 Prof. Emeritus, The University of Tokyo
and Tokyo Institute of Technology

MEMBERS

[I] RESEARCH ORIGIN FOR DRESSED PHOTON (RODreP) *

Chief Director

Motoichi OHTSU** (Dr. Eng.)

Directors

Masayuki NAYA (Dr. Eng.)
Hirofumi SAKUMA (Ph. D.)

Auditor

Satoshi SUGIURA

Advisors

Izumi OJIMA (Dr. Sci.)
Junji MIYAHARA (Dr. Eng.)
Masuo FUKUI (Dr. Eng.)
Naoya TATE (Dr. Eng.)

Senior Researcher

Kazuya OKAMURA (Dr. Sci.)

Visiting Scientists

Hayato SAIGO (Dr. Sci.) (Nagahama Inst. Bio-Sci. and Tech.)
Itsuki BANNO (Univ. Yamanashi)
Suguru SANGU (Dr. Eng.) (Ricoh Co. Ltd.)
Etsuo SEGAWA (Dr. Eng.) (Yokohama National Univ.)
Seiken SAITO (Dr. Sci.) (Kogakuin Univ.)

Secretary

Mari KAZAMA

(*)（General Incorporated Association）Research Origin for Dressed Photon (RODreP)

Phone: 090-1603-0562
E-mail: ohtsu@rodrep.or.jp
URL: https://rodrep.or.jp/
(Labs.)
c/o Bdg.1, Yokohama Research Center, NICHIA Corp.
3-13-19 Moriya-cho, Kanagawa-ku, Yokohama-shi, Kanagawa 221-0022, Japan
(Executive office)
Adthree Publishing Co., Ltd.
4-27-37 Higashi-Nakano, Nakano-ku, Tokyo164-0003, Japan
The 3rd Floor, Sunrise Bldg. II, 5-20 Shin-Ogawa-cho, Shinjuku-ku, Tokyo 162-0814, Japan

（一般社団法人）ドレスト光子研究起点
Phone: 090-1603-0562
E-mail: ohtsu@rodrep.or.jp
URL: https://rodrep.or.jp/
（研究所）
〒221-0022　神奈川県横浜市神奈川区守屋町 3－13－19
日亜化学工業（株）　横浜研究所　1 号館 1 階
（事務局）
〒162-0814　東京都新宿区新小川町 5-20　サンライズビルⅡ ３F
株式会社アドスリー

(**) Professor Emeritus, The University of Tokyo and Tokyo Institute of Technology
東京大学名誉教授、東京工業大学名誉教授

VIDEO LECTURES

[1] (In English) M. Ohtsu, "Energy Transfer of Dressed Photon by a Quantum Walk Model," (December, 2022).

Part 1 https://www.youtube.com/watch?v=gK900FOh67E

Part 2 https://www.youtube.com/watch?v=bNSi6GQdzAY

[2] (In English) M. Ohtsu, "Dressed Photon by Off-shell Science," (August, 2022).

https://www.youtube.com/watch?v=4FUsug8-WXw

(In Japanese) 大津元一、「ドレスト光子とオフシェル科学」

その1 https://www.youtube.com/watch?v=qE2qrAwZWs0

その2 https://www.youtube.com/watch?v=ZcBguqpoOC0

その3 https://www.youtube.com/watch?v=VkzKZzho63E

その4 https://www.youtube.com/watch?v=IrjuRGXSf4U

その5 https://www.youtube.com/watch?v=UZPdNDX1cLE

その6 https://www.youtube.com/watch?v=5lkP57Xje9c

LIST OF PAPERS

[(pp. XX-XX); pages in this issue of the COLLECTED PAPERS**]**

[I] ORIGINAL PAPERS

[1] H. Sakuma, I. Ojima, H. Saigo, and K. Okamura, "Conserved relativistic Ertel's current generating the vortical and thermodynamic aspects of space-time," Int. J. Modern Phys. A, (2022) 2250155.
DOI: 10.1142/S0217751X2250155X

[2] T. Kadowaki, T. Kawazoe, M. Sugeta, M. Sano, and T. Mukai, "Uncooled Si infrared photodetector for 2 μ m wavelength using stimulated emission by dressed photons," *Appl. Phys. Express*, **15**, 045002 (2022).

[II] PRESENTATIONS IN INTERNATIONAL CONFERENCES

[1] M. Ohtsu, E. Segawa, and K. Yuki, "A Quantum Walk Model for the Energy Transfer of a Dressed Photon," Abstracts of the 2022 International Symposium on Nonlinear Theory and its Applications (NOLTA2022), December 12-15, 2022, (Online meeting), paper number A3L-C1, pp.65-68.

[2] K. Okamura, "On the Schroedinger Picture in C*-Algebraic Quantum Theory," Abstracts of the 2022 International Symposium on Nonlinear Theory and its Applications (NOLTA2022), December 12-15, 2022, (Online meeting), paper number A3L-C2, pp.69-72.

[3] M. Ohtsu, "Off-shell Science for Dressed Photons," Abstracts of the 13th Asia-Pacific Conference on Near-Field Optics (APNFO13), July 29-31, 2022, Sapporo, Hokkaido, Japan (also Online meeting), paper number PL29-A1.
[Plenary lecture]

[III] REVIEW PAPERS

[1] M. Ohtsu, "Book review: "A pickled plum and light," by M. Naya, Optronics, Tokyo, May, 2022," *Optronics*, No. 488 (August, 2022). p.111.
【大津元一、「書評：『梅干しとひかり』、納谷昌之著、オプトロニクス社、2022年5月」、オプトロニクス、第488号、2022年8月、p.111】

[IV] PREPRINT DEPOSITORIES

[Original papers]

[1] M. Ohtsu, E. Segawa, K. Yuki, and S. Saito, "Dressed-photon—phonon creation

probability on the tip of a fiber probe calculated by a quantum walk model," *Off-shell Archive* (December, 2022) OffShell: 2212O.001.v1.
DOI 10.14939/2212O.001.v1
https://rodrep.or.jp/en/off-shell/original_2212O.001.v1.html

[2] M. Ohtsu, E. Segawa, and K. Yuki, "Numerical calculation of a dressed photon energy transfer based on a quantum walk model," *Off-shell Archive* (June, 2022) OffShell: 2206O.001.v1.
DOI 10.14939/2206O.001.v1
https://rodrep.or.jp/en/off-shell/original_2206O.001.v1.html

[Review papers]

[1] M. Ohtsu, "Off-shell science theories on interaction for dressed photons," *Off-shell Archive* (January, 2022) OffShell: 2201R.001.v1.
DOI 10.14939/2201R.001.v1
https://rodrep.or.jp/en/off-shell/review_2201R.001.v1.html

[V] PUBLISHED BOOKS

[1] M. Ohtsu (ed), "Quantum Fields and Off-Shell Sciences," (Printed Edition of the Special Issue Published in *Symmetry*), MDPI, Basel, Switzerland (2022). 167 pages.

[2] M. Ohtsu, "Deep-understanding the Dressed Photon," (ed. by S. Sugiura), Adthree, Tokyo (June, 2022). 145 pages.
【大津元一、「ドレスト光子の深わかり」、(杉浦聡　編)、アドスリー、東京、2022年6月、145ページ】

[VI] PRESENTATIONS IN DOMESTIC CONFERENCES

[1] H. Du, H. Takeda, N. Tate, Y. Oki, K. Hayashi, T. Kadowaki, T. Kawazoe, M. Ohtsu, "Evaluation of giant polarization rotation with a SiC spatial light modulator," Abstracts of the Kyushu Chapter, Jpn. Soc. Appl. Phys. Annual Meeting 2022, November 26-27, (Oita Univ.) paper number 26Cp-2.
【Du Haoze、竹田晴信、竪直也、興雄司、林健司、門脇拓也、川添忠、大津元一「SiC 空間光変調器が示す巨大偏光回転機能の評価」、2022年度応用物理学会九州支部学術講演会予稿集、(2022年11月26日−27日）,(大分大学）講演番号26Cp-2】

[2] M. Ohtsu, "Creation and Energy Transfer of Dressed Photon," Abstracts of the Optics & Photonics Japan 2022, November 14-16, 2022, (Utsunomiya Univ. and Online meeting), paper number 16pAS2.
【大津元一、「ドレスト光子の生成過程とそのエネルギー移動」、Optics & Photonics Japan 2022 予稿集、(2022 年 11 月 14-16 日)、(宇都宮大学 & オンライン）講演番号 16pAS2】

[Invited presentation]

[3] E. Segawa, “A convergence time of quantum walk,“ Abstracts of the Optics & Photonics Japan 2022, November 14-16, 2022, (Utsunomiya Univ. and Online meeting), paper number 16pAS3.
【瀬川悦生、「量子ウォークが定常状態になるまでの時間」、Optics & Photonics Japan 2022予稿集、（2022年11月14-16日）、（宇都宮大学 ＆ オンライン）講演番号16pAS3】
[Invited presentation]

[4] H. Saigo, “Category Algebra for describing dressed photons,“ Abstracts of the Optics & Photonics Japan 2022, November 14-16, 2022, (Utsunomiya Univ. and Online meeting), paper number 16pAS4.
【西郷甲矢人、「ドレスト光子記述のための圏代数」、Optics & Photonics Japan 2022予稿集、（2022年11月14-16日）、（宇都宮大学 ＆ オンライン）講演番号16pAS4】
[Invited presentation]

[5] S. Saito, “Quantum Chaos on Graphs,“ Abstracts of the Optics & Photonics Japan 2022, November 14-16, 2022, (Utsunomiya Univ. and Online meeting), paper number 16pAS5.
【斎藤正、「グラフ上の量子カオス」、Optics & Photonics Japan 2022予稿集、（2022年11月14-16日）、（宇都宮大学 ＆ オンライン）講演番号16pAS5】
[Invited presentation]

[6] S. Sangu, “State Transition of Dressed Photons Originating from Defect Structures,“ Abstracts of the Optics & Photonics Japan 2022, November 14-16, 2022, (Utsunomiya Univ. and Online meeting), paper number 16pAS6.
【三宮俊、「欠陥構造を起点とするドレスト光子の状態遷移」、Optics & Photonics Japan 2022予稿集、（2022年11月14-16日）、（宇都宮大学 ＆ オンライン）講演番号16pAS6】
[Invited presentation]

[7] I. Banno, “Dissipative Structure with Immanent Electromagnetic Field attained by the Principle of Least Action, “Abstracts of the 83rd Jpn. Soc. Appl. Phys. Autumn Meeting, September 20-23, 2022, (Tohoku Univ. and Online meeting), paper number 22a-A101-1.
【坂野斎、「最小作用の原理で達成される内在電磁場を伴う散逸構造の理論」、第83回応用物理学会秋季学術講演会予稿集（2022年9月20-23日）、（東北大学川内北キャンパス ＆ オンライン）講演番号22a-A101-1】

[8] H. Sakuma, “Off-shell science” opened up by dressed photon studies: a tangible example, “Abstracts of the 83rd Jpn. Soc. Appl. Phys. Autumn Meeting, September 20-23, 2022, (Tohoku Univ. and Online meeting), paper number 22a-A101-2.

【佐久間弘文、「ドレスト光子研究が拓く”オフシェル科学”：一具体例の考察」、第83回応用物理学会秋季学術講演会予稿集（2022年9月20-23日）、（東北大学川内北キャンパス ＆ オンライン）講演番号22a-A101-2】

[9] H. Saigo, “A category algebraic approach to off-shell sciences,” Abstracts of the 83rd Jpn. Soc. Appl. Phys. Autumn Meeting, September 20-23, 2022, (Tohoku Univ. and Online meeting), paper number 22a-A101-3.
【西郷甲矢人、「オフシェル科学への圏代数アプローチ」、第83回応用物理学会秋季学術講演会予稿集（2022年9月20-23日）、（東北大学川内北キャンパス ＆ オンライン）講演番号22a-A101-3】

[10] S. Saito and E. Segawa, “Quantum Walks related to Dressed Photons: the 1-dimensional case,” Abstracts of the 83rd Jpn. Soc. Appl. Phys. Autumn Meeting, September 20-23, 2022, (Tohoku Univ. and Online meeting), paper number 22a-A101-4.
【斎藤正顕、瀬川悦生、「ドレスト光子の量子ウォークモデル： １次元の場合」、第83回応用物理学会秋季学術講演会予稿集（2022年9月20-23日）、（東北大学川内北キャンパス ＆ オンライン）講演番号22a-A101-4】

[11] E. Segawa, “Estimation of speed of convergence of quantum walks,” Abstracts of the 83rd Jpn. Soc. Appl. Phys. Autumn Meeting, September 20-23, 2022, (Tohoku Univ. and Online meeting), paper number 22a-A101-5.
【瀬川悦生、「量子ウォークとランダムウォークの収束の速さの双対性」、第83回応用物理学会秋季学術講演会予稿集（2022年9月20-23日）、（東北大学川内北キャンパス ＆ オンライン）講演番号22a-A101-5】

[12] M. Ohtsu, E. Segawa, and K. Yuki, “Numerical calculation of a dressed photon energy transfer by a quantum walk model,” Abstracts of the 83rd Jpn. Soc. Appl. Phys. Autumn Meeting, September 20-23, 2022, (Tohoku Univ. and Online meeting), paper number 22a-A101-6.
【大津元一、瀬川悦生、結城謙太、「量子ウォークモデルによるドレスト光子エネルギー移動の数値計算」、第83回応用物理学会秋季学術講演会予稿集（2022年9月20-23日）、（東北大学川内北キャンパス ＆ オンライン）講演番号22a-A101-6】

[13] S. Sangu, H. Saigo, and M. Ohtsu, “Behavior of Dressed Photons in Systems Containing Impurities,” Abstracts of the 83rd Jpn. Soc. Appl. Phys. Autumn Meeting, September 20-23, 2022, (Tohoku Univ. and Online meeting), paper number 22a-A101-7.
【三宮俊、西郷甲矢人、大津元一、「不純物を含む系におけるドレスト光子の振る舞い」、第83回応用物理学会秋季学術講演会予稿集（2022年9月20-23日）、（東北大学川内北キャンパス ＆ オンライン）講演番号22a-A101-7】

[14] M. Ohtsu, “Progress in Off-shell Science,” Abstract of the Special Lecture of the

Japan Physical Society, Hokuriku-branch, August 12, 2022 (Fukui Univ. and Online meeting)
【大津元一、「オフシェル科学の展開」、日本物理学会北陸支部特別講演会(2022年8月12日)、(福井大学 & オンライン)】
[Invited lecture]

[15] S. Saito, "The distribution of the error terms of the number of non-backtracking cycles for a regular graph," Abstracts of Appl. Math. Res. Sect. of Math. Soc. Jpn. Spring Meeting 2022, at Saitama University, March 28--31, 2022, (Online meeting), paper number 20, pp.67-68.
【齋藤正顕、「正則グラフにおける non-backtracking cycle の個数の誤差項の分布」、日本数学会 2022 年度年会(埼玉大学)応用数学分科会予稿集(2022年3月28日—31日)、(オンライン会議)、応用数学分科会 講演アブストラクト、講演番号 20、pp.67-68】

[16] I. Banno, "Dressed Photon / Immanent Electromagnetic Field and the Principle of Least Action," Abstracts of the 69nd Jpn. Soc. Appl. Phys. Spring Meeting, March 22-26, 2022, (Aoyama Gakuin Univ. and Online meeting), paper number 22a-E103-1.
【坂野斎、「ドレスト光子/ 内在電磁場と最小作用の原理」、第69回応用物理学会春季学術講演会予稿集(2022年3月22-26日)、(青山学院大学相模原キャンパス & オンライン)講演番号22a-E103-1】

[17] H. Saigo, "Quantum Fields as Category Algebras," Abstracts of the 69nd Jpn. Soc. Appl. Phys. Spring Meeting, March 22-26, 2022, (Aoyama Gakuin Univ. and Online meeting), paper number 22a-E103-2.
【西郷甲矢人、「圏代数としての量子場」、第69回応用物理学会春季学術講演会予稿集(2022年3月22-26日)、(青山学院大学相模原キャンパス & オンライン)講演番号22a-E103-2】

[18] K. Okamura, "On the Schr¨odinger picture in C*-algebraic quantum theory," Abstracts of the 69nd Jpn. Soc. Appl. Phys. Spring Meeting, March 22-26, 2022, (Aoyama Gakuin Univ. and Online meeting), paper number 22a-E103-3.
【岡村和弥、「C*−代数的量子論におけるシュレディンガー描像」、第69回応用物理学会春季学術講演会予稿集(2022年3月22-26日)、(青山学院大学相模原キャンパス & オンライン)講演番号22a-E103-3】

[19] M. Sabri, E. Segawa, "Sensitivity of quantum walk and dressed photon to perturbtion," Abstracts of the 69nd Jpn. Soc. Appl. Phys. Spring Meeting, March 22-26, 2022, (Aoyama Gakuin Univ. and Online meeting), paper number 22a-E103-4.
【M. Sabri、瀬川悦生、「量子ウォーク・ドレスト光子の摂動に対する感受性」、第69回応用物理学会春季学術講演会予稿集(2022年3月22-26日)、(青山学院大学相模原キャンパス & オンライン)講演番号22a-E103-4】

[20] L. Matsuoka, K. Yuki, H. Lavička, E. Segawa, "The amplitude distribution of

rational numbers trapped in quantum walk networks with exit sinks," Abstracts of the 69nd Jpn. Soc. Appl. Phys. Spring Meeting, March 22-26, 2022, (Aoyama Gakuin Univ. and Online meeting), paper number 22a-E103-5.
【松岡雷士、結城謙太、H. Lavička、瀬川悦生、「出口付き量子ウォークネットワークにおける有理数の残留振幅」、第69回応用物理学会春季学術講演会予稿集（2022年3月22-26日）、（青山学院大学相模原キャンパス ＆ オンライン）講演番号22a-E103-5】

[21] S. Sangu, H. Saigo, M. Ohtsu, "Effect of Impurity Configuration on Dressed-Photon Energy Transfer," Abstracts of the 69nd Jpn. Soc. Appl. Phys. Spring Meeting, March 22-26, 2022, (Aoyama Gakuin Univ. and Online meeting), paper number 22a-E103-6.
【三宮俊、西郷甲矢人、大津元一、「ドレスト光子エネルギー移動における不純物配置の影響」、第69回応用物理学会春季学術講演会予稿集（2022年3月22-26日）、（青山学院大学相模原キャンパス ＆ オンライン）講演番号22a-E103-6】

[22] T. Kadowaki, T. Kawazoe, M. Sugeta, M. Ohtsu, M. Sano, T. Mukai, "Time-resolved photoluminescence of Si light-emitting diode for infrared wavelength using dressed photons," Abstracts of the 69nd Jpn. Soc. Appl. Phys. Spring Meeting, March 22-26, 2022, (Aoyama Gakuin Univ. and Online meeting), paper number 22a-E103-7.
【門脇拓也、川添忠、 菅田雅樹、大津元一、佐野雅彦、向井孝志、「ドレスト光子を用いた赤外Si-LEDの時間分解PL測定」、第69回応用物理学会春季学術講演会予稿集（2022年3月22-26日）、（青山学院大学相模原キャンパス ＆ オンライン）講演番号22a-E103-7】

[23] T.Kawazoe, T. Kadowaki, M. Ohtsu, M. Sano, T. Mukai, "A highly sensitive thermometer fabricated by using DPP annealing," Abstracts of the 69nd Jpn. Soc. Appl. Phys. Spring Meeting, March 22-26, 2022, (Aoyama Gakuin Univ. and Online meeting), paper number 22a-E103-8.
【川添忠、門脇拓也、大津元一、佐野雅彦、向井孝志、「DPPアニールで作製した高感度Si温度計」、第69回応用物理学会春季学術講演会予稿集（2022年3月22-26日）、（青山学院大学相模原キャンパス ＆ オンライン）講演番号22a-E103-8】

[24] M. Ohtsu, "Recent progresses in experimental studies of dressed photons for off-shell science theories," Abstracts of the Workshop on Off-shell mathematical science toward system's analysis and designing (Univ. Kyushu, IMI, February 22-24, 2022: Online meeting), paper number I-1.
【大津元一、「オフシェル科学理論のためのドレスト光子実験研究の進展」、研究会「解析から設計に向けたオフシェル数理科学」、（九州大学IMI、2022年 2月22-24日、オンライン会合、講演番号I-1】

[Keynote speech]

[25] S. Sangu, ”Considerations on dressed and free photon conversion and nanostructure formation,” Abstracts of the Workshop on Off-shell mathematical science toward system’s analysis and designing (Univ. Kyushu, IMI, February 22-24, 2022: Online meeting), paper number I-2.
【三宮俊、「ドレスト光子―自由光子の変換とナノ構造形成に関する考察」、研究会「解析から設計に向けたオフシェル数理科学」、（九州大学IMI、2022年2月22-24日、オンライン会合、講演番号I-2】

[Invited speech]

[26] I. Banno, “Theory of Quantum Dissipative Structure associated with Dressed Photons,” Abstracts of the Workshop on Off-shell mathematical science toward system’s analysis and designing (Univ. Kyushu, IMI, February 22-24, 2022: Online meeting), paper number I-3.
【坂野斎、「ドレスドフォトンが関わる量子的散逸構造の理論」、研究会「解析から設計に向けたオフシェル数理科学」、（九州大学IMI、2022年2月22-24日、オンライン会合、講演番号I-3】

[27] E. Segawa, “Comfortability of quantum walk,” Abstracts of the Workshop on Off-shell mathematical science toward system’s analysis and designing (Univ. Kyushu, IMI, February 22-24, 2022: Online meeting), paper number II-1.
【瀬川悦生、「量子ウォークの Comfortability」、研究会「解析から設計に向けたオフシェル数理科学」、（九州大学 IMI、2022 年 2 月 22-24 日、オンライン会合、講演番号 II-1】

[28] L. Matsuoka, “Maze-solving behavior in the quantum walk model on networks,” Abstracts of the Workshop on Off-shell mathematical science toward system’s analysis and designing (Univ. Kyushu, IMI, February 22-24, 2022: Online meeting), paper number II-2.
【松岡雷士、「ネットワーク量子ウォークモデルにおける迷路解決挙動」、研究会「解析から設計に向けたオフシェル数理科学」、（九州大学IMI、2022年2月22-24日、オンライン会合、講演番号II-2】

[29] H. Saigo, “Quantum Fields as Category Algebras,” Abstracts of the Workshop on Off-shell mathematical science toward system’s analysis and designing (Univ. Kyushu, IMI, February 22-24, 2022: Online meeting), paper number III-1.
【西郷甲矢人、「圏代数としての量子場」、研究会「解析から設計に向けたオフシェル数理科学」、（九州大学IMI、2022年2月22-24日、オンライン会合、講演番号III-1】

[30] K. Okamura, “On the Schrodinger picture in C*-algebraic quantum theory,” Abstracts of the Workshop on Off-shell mathematical science toward system’s analysis and designing (Univ. Kyushu, IMI, February 22-24, 2022: Online meeting),

paper number III-2.
【岡村和弥、「C*-代数的量子論におけるシュレディンガー描像」、研究会「解析から設計に向けたオフシェル数理科学」、（九州大学IMI、2022年2月22-24日、オンライン会合、講演番号III-2】

[31] H. Sakuma, "On the role of duality field for understanding "off-shell physics," Abstracts of the Workshop on Off-shell mathematical science toward system's analysis and designing (Univ. Kyushu, IMI, February 22-24, 2022: Online meeting), paper number IV-1.
【佐久間弘文、「オフシェル物理における双対場の役割について」、研究会「解析から設計に向けたオフシェル数理科学」、（九州大学 IMI、2022 年 2 月 22-24 日、オンライン会合、講演番号 IV-1】

[32] M. Ohtsu, "Dressed photon and its development as off-shell science --- What are required for comparing experiments and theories? ---," Abstracts of the Symposium S05 in the 41st Annual Meeting, The Laser Society of Japan, January 2022, (Online meeting), paper number S05-14p-XII-04.
【大津元一、「ドレスト光子とそのオフシェル科学としての展開 ---実験と理論の対応のために、今何が求められているか？---」、レーザー学会学術講演会第41回年次大会シンポジウムS05予稿集、（2022年1月）、（オンライン会議）講演番号S05-14p-XII-04】
[Invited presentation]

[33] E. Segawa, "Dynamical system of quantum walks and experimental results on dressed photon," Abstracts of the Symposium S05 in the 41st Annual Meeting, The Laser Society of Japan, January 2022, (Online meeting), paper number S05-14p-XII-05.
【瀬川悦生、「量子ウォーク力学系とドレスト光子の実験結果との比較」、レーザー学会学術講演会第41回年次大会シンポジウムS05予稿集、（2022年1月）、（オンライン会議）講演番号S05-14p-XII-05】
[Invited presentation]

[34] H. Saigo, "Category Algebras for the Description of Dressed Photons," Abstracts of the Symposium S05 in the 41st Annual Meeting, The Laser Society of Japan, January 2022, (Online meeting), paper number S05-14p-XII-06.
【西郷甲矢人、「ドレスト光子の記述のための圏代数」、レーザー学会学術演会第 41 回年次大会シンポジウム S05 予稿集、（2022 年 1 月）、（オンライン会議）講演番号 S05-14p-XII-06】
[Invited presentation]

[VII] AWARDS

N.A.

CUMULATIVE LIST: Off-shell Archive

2022

32 Dressed-photon–phonon creation probability on the tip of a fiber probe calculated by a quantum walk model
DOI 10.14939/2212O.001.v1
URL https://rodrep.or.jp/en/off-shell/original_2212O.001.v1.html
Date 2022.12.02

31 Numerical calculation of a dressed photon energy transfer based on a quantum walk model
DOI 10.14939/2206O.001.v1
URL https://rodrep.or.jp/en/off-shell/original_2206O.001.v1.html
Date 2022.06.22

30 Off-shell science theories on interaction for dressed photons
DOI 10.14939/2201R.001.v1
URL https://rodrep.or.jp/en/off-shell/review_2201R.001.v1.html
Date 2022.01.31

2021

29 Progresses in theoretical studies of off-shell science for dressed photons
DOI 10.14939/2110R.002.v1
URL https://rodrep.or.jp/en/off-shell/review_2110R.002.v1.html
Date 2021.10.22

28 Generation Mechanism of Dressed Photon and Unique Features of Converted Propagating Light
DOI 10.14939/2110R.001.v1
URL https://rodrep.or.jp/en/off-shell/review_2110R.001.v1.html
Date 2021.10.01

27 A Quantum Walk Model for Describing the Energy Transfer of a Dressed Photon
DOI 10.14939/2109R.001.v1
URL https://rodrep.or.jp/en/off-shell/review_2109R.001.v1.html

Date 2021.09.03

26 The dressed photon as a member of the off-shell photon family
DOI 10.14939/2103R.001.v1
URL https://rodrep.or.jp/en/off-shell/review_2103R.001.v1.html
Date 2021.03.02

2020

25 Past, present, and future studies on the longitudinal electric field components of light
DOI 10.14939/2008R.001.v1
URL https://rodrep.or.jp/en/off-shell/review_2008R.001.v1.html
Date 2020.08.21

24 Errata: Route to Off-Shell Science
DOI 10.14939/2006R.001.v2
URL https://rodrep.or.jp/en/off-shell/review_2006R.001.v2.html
Date 2020.08.17

23 Route to Off-Shell Science
DOI 10.14939/2006R.001.v1
URL https://rodrep.or.jp/en/off-shell/review_2006R.001.v1.html
Date 2020.06.25

22 Nutation in energy transfer of dressed photons between nano-particles
DOI 10.14939/2005O.001.v1
URL https://rodrep.or.jp/en/off-shell/original_2005O.001.v1.html
Date 2020.05.15

21 Progress in off-shell science in analyzing light–matter interactions for creating dressed photons
DOI 10.14939/2004R.001.v1
URL https://rodrep.or.jp/en/off-shell/review_2004R.001.v1.html
Date 2020.04.25

20 The present and future of numerical simulation techniques for off-shell science
DOI 10.14939/2003R.001.v1

URL https://rodrep.or.jp/en/off-shell/review_2003R.001.v1.html
Date 2020.02.27

2019

19 Note on the physical meaning of the cosmological term
DOI 10.14939/1909O.001.v2
URL https://rodrep.or.jp/en/off-shell/original_1909O.001.v2.html
Date 2019.12.20

18 History, current developments, and future directions of near-field optical science
DOI 10.14939/1912R.001.v1
URL https://rodrep.or.jp/en/off-shell/review_1912R.001.v1.html
Date 2019.12.20

17 Dressed photon phenomena that demand off-shell scientific theories
DOI 10.14939/1911R.001.v1
URL https://rodrep.or.jp/en/off-shell/review_1911R.001.v1.html
Date 2019.11.12

16 Note on the physical meaning of the cosmological term
DOI 10.14939/1909O.001.v1
URL https://rodrep.or.jp/en/off-shell/original_1909O.001.v1.html
Date 2019.09.10

15 Infrared lasers using silicon crystals
DOI 10.14939/1908R.001.v1
URL https://rodrep.or.jp/en/off-shell/review_1908R.001.v1.html
Date 2019.08.01

14 Indications from dressed photons to macroscopic systems based on hierarchy and autonomy
DOI 10.14939/1906R.001.v1
URL https://rodrep.or.jp/en/off-shell/review_1906R.001.v1.html
Date 2019.07.06

13 Novel functions and prominent performance of nanometric optical devices made possible by dressed photons

DOI 10.14939/1904R.001.v1
URL https://rodrep.or.jp/en/off-shell/review_1904R.001.v1.html
Date 2019.04.02

2018

12 Embarking on theoretical studies for off-shell science guided by dressed photons
DOI 10.14939/1811R.001.v1
URL https://rodrep.or.jp/en/off-shell/review_1811R.001.v1.html
Date 2018.12.26

11 Theory of Single Susceptibility for Near-_eld Optics Equally Associated with Scalar and Vector Potentials
DOI 10.14939/1809O.002.v1
URL https://rodrep.or.jp/en/off-shell/original_1809O.002.v1.html
Date 2018.12.26

10 Gigantic Ferromagnetic Magneto-Optical Effect in a SiC Light-emitting Diode Fabricated by Dressed-Photon–Phonon-Assisted Annealing
DOI 10.14939/1809R.001.v1
URL https://rodrep.or.jp/en/off-shell/review_1809R.001.v1.html
Date 2018.12.26

9 Micro-Macro Duality for Inductions/Reductions
DOI 10.14939/1809O.001.v1
URL https://rodrep.or.jp/en/off-shell/original_1809O.001.v1.html
Date 2018.12.26

8 Logical Fallacy of using the Electric Field in Non-resonant Near-field Optics
DOI 10.14939/1808O.001.v1
URL https://rodrep.or.jp/en/off-shell/original_1808O.001.v1.html
Date 2018.12.26

7 Principles and Practices of Si Light Emitting Diodes using Dressed Photons
DOI 10.14939/1805R.001.v1
URL https://rodrep.or.jp/en/off-shell/review_1805R.001.v1.html
Date 2018.12.26

6 Photon localization revisited

DOI 10.14939/1804O.002.v1

URL https://rodrep.or.jp/en/off-shell/original_1804O.002.v1.html

Date 2018.12.26

5 Experimental estimation of the maximum size of a dressed photon

DOI 10.14939/1802R.001.v1

URL https://rodrep.or.jp/en/off-shell/review_1802R.001.v1.html

Date 2018.12.26

4 Creation and Measurement of Dressed Photons: A Link to Novel Theories

DOI 10.14939/1712R.001.v1

URL https://rodrep.or.jp/en/off-shell/review_1712R.001.v1.html

Date 2018.12.26

3 Spatial and Temporal Evolutions of Dressed Photon Energy Transfer

DOI 10.14939/1710R.001.v1

URL https://rodrep.or.jp/en/off-shell/review_1710R.001.v1.html

Date 2018.12.26

2 High-Power Infrared Silicon Light-emitting Diodes Fabricated and Operated using Dressed Photons

DOI 10.14939/1804O.001.v1

URL https://rodrep.or.jp/en/off-shell/original_1804O.001.v1.html

Date 2018.12.24

1 New Routes to Studying the Dressed Photon

DOI 10.14939/OffShell.1709R.001.v1

URL https://rodrep.or.jp/en/off-shell/review_1709R.001.v1.html

Date 2018.12.23

[I] ORIGINAL PAPERS

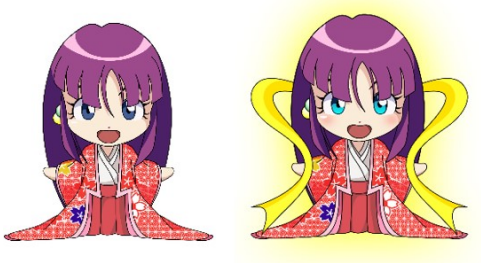

OPEN ACCESS
International Journal of Modern Physics A
(2022) 2250155 (18 pages)

DOI: 10.1142/S0217751X2250155X

World Scientific
www.worldscientific.com

Conserved relativistic Ertel's current generating the vortical and thermodynamic aspects of space–time

Hirofumi Sakuma,[*,§] Izumi Ojima,[*,¶] Hayato Saigo[†,‖] and Kazuya Okamura[*,‡,**]

[*]*Research Origin for Dressed Photon*
3-13-19 Moriya-cho, Kanagawa-ku
Yokohama, Kanagawa 221-0022, Japan

[†]*Nagahama Institute of Bio-Science and Technology*
1266 Tamura, Nagahama, Shiga 526-0829, Japan

[‡]*Graduate School of Informatics, Nagoya University*
Chikusa-ku, Nagoya 464-8601, Japan
[§]*sakuma@rodrep.or.jp*
[¶]*ojima@gaia.eonet.ne.jp*
[‖]*h_saigoh@nagahama-i-bio.ac.jp*
[**]*k.okamura.renormalizable@gmail.com*

Received 17 March 2022
Revised 29 July 2022
Accepted 23 August 2022
Published 28 September 2022

Motivated by Aoki *et al.*'s recent research on conserved charges and entropy current, we reinvestigated the conservation of relativistic Ertel's current, which has received little attention outside the field of geophysical fluid dynamics. Ertel's charge is an important indicator of the correlation between vortex vectors and entropy gradient fields in Earth's meridional heat transport. We first show that in the generalized Hamiltonian structure of baroclinic fluids, the duality between the total energy and the Casimir as a function of Ertel's charge plays an important role in the nonrelativistic case. Then, by extending the result to relativistic cases, we show that this finding has far-reaching implications not only for space–time issues in cosmology but also for the foundation of quantum field theory. An especially important finding is that, as an unreported dual form of the Einstein field equation, we identify a special equation satisfied not only by the vortex tensor field generated by the conserved charge but also by the Weyl tensor in interpreting the physical nature of the metric tensor $g^{\mu\nu}$, which appears in the cosmological term $\Lambda g^{\mu\nu}$.

Keywords: Ertel's charge; entropy; generalized Hamiltonian; cosmological term; Weyl tensor.

PACS numbers: 04.20.Cv, 04.40.Nr, 05.90.+m, 47.10.ab

[§]Corresponding author.

1. Introduction

Two key issues are addressed in this paper: first, we shed new light on the peculiarity of the gravitational field, which has, in addition to its well-documented geometrical nature, an unexpected thermodynamic nature;[1–4] second, we clarify the main cause of the inherent defect in the present form of quantum field theory (QFT), exemplified by Haag's no-go theorem[5] in axiomatic QFT. As we show below, these two seemingly disparate concepts are inextricably linked by the important dynamical role of the spinor field (or the vortical field in the case of classical mechanics), which connects a given physical system to the surrounding space–time as its dynamical environment.

Many issues in nonrelativistic physics require the use of an abstract space to characterize the time-dependent dynamic behaviors of a given physical system, such as the Hilbert space $\mathfrak{H}$ in quantum mechanics and phase space in classical Hamiltonian (H) systems. In general, these spaces are not related to the physics of a given system. The fact that this condition changes drastically in relativistic field theory is well-known and has become common knowledge in physics, while the well-known *wave–particle duality* in quantum mechanics remains a mystery. However, once it is accepted that space–time is a physical entity in which "spacelike" corresponds to wavelike entities, such as the spacelike momentum field required for quantum field interactions (Greenberg–Robinson (GR) theorem[6,7]), while "timelike" corresponds to localized particle-like entities, then the wave–particle duality of quantum entities appears to be a natural consequence of the fact that quantum entities always coexist with embedded space–time; in other words, quantum entities are dynamically integrated with space–time as their environment.

Dirac's finding has played an important role in considering the physicality of space–time, revealing that quantum spin is a feature of relativistic space–time. Since then, the idea that space–time is composed of specific types of spin networks has been investigated, most notably by Penrose[8] and the many researchers that developed loop quantum gravity (LQG) theory. Therefore, an essential question associated with the space–time conundrum is how the thermodynamic properties of space–time fit with this spin network concept. The peculiarity of the space–time problem in relativistic scenarios lies in the fact that space–time not only has a mathematical meaning, which can be used to represent a given physical system, but is also a physical field that must be represented by itself. To explain this reciprocal nature which can be regarded as the interdependent duality (ID) existing between a given physical system and its associated space–time, we must identify the emergent processes of this "physical" space–time.

As an informative example of the ID mentioned above, we briefly refer to micro–macro duality (MMD) theory,[9] which, as briefly explained in a recent review paper[10] on nanophotonics, *can be regarded as a modern version of* "*quantum-classical correspondence*"; *this theory was rigorously derived based on the pertinent generalization of the superselection rule, with the sectors originally formulated by Doplicher–Haag–Roberts.*[11,12] Any efforts to explore unseen microscopic quantum

worlds require experiments that investigate the dynamical interactions between micro-quantum and macro-classical worlds. This simple fact clearly shows that our descriptions of unseen microscopic worlds depend heavily on the "vocabulary" we use in classical physics. Therefore, in the metaphorical sense, classical physics operates not as a static "space" onto which the microscopic world is projected, but rather as an interacting dynamic "space–time" which we use to describe the targeted microscopic world.

This viewpoint is supported as a key element of MMD theory. Among the many noteworthy accomplishments of MMD theory, the following two theoretical results are particularly relevant to the discussion in this paper. First, due to its infinite degrees of freedom, QFT inevitably involves a combination of quantum and classical fields, with the latter emerging due to the existence of disjoint (refined notion of unitary nonequivalent) generalized sectors with nontrivial factor representations acting as order parameters of the emerging classical field. The irrelevance of Schrödinger's cat thought experiment can be easily clarified[10] by the basic results of MMD theory. Second, with the exception of the different algebraic structures of certain physical quantities in their respective fields, i.e. anti-commutativity versus commutativity, we can consider both fields in a unified framework.

The main discussions begin in Sec. 2 with classical physics; however, we show that even in classical fluid dynamics systems, there exists an intriguing ID structure that eventually clarifies the discussed space–time peculiarity. In Secs. 2 and 3, by reviewing the basic structures of barotropic and baroclinic fluids, as well as their generalized Hamiltonian (H) structures, we identify a key conserved dynamical quantity that generates the above-mentioned ID structure. The reason we focus on this conserved quantity is because we found that recent works by Aoki *et al.*,[13,14] particularly on the conservation of entropy in general relativity, are quite informative in the present research. Then, in Sec. 4, we show how the main aims of our paper, as stated in the first paragraph of this introductory section, are achieved based on the results of the previous section. In the final section, we present our conclusions and some novel perspectives on QFT and cosmology.

2. Dynamics of Barotropic and Baroclinic Fluids and H Structures

We begin with the well-known equation of motion of a perfect fluid in nonrelativistic fluid mechanics:

$$D_t v_\mu := \partial_t v_\mu + v^\nu \partial_\nu v_\mu = -\frac{1}{\rho}\partial_\mu p, \tag{1}$$

where the notations are conventional. A fluid is classified as barotropic or baroclinic based on its form of $\partial_\mu p/\rho$; that is, if $p = p(\rho)$ or $\rho = \rho_0 = \text{const}$, the fluid is barotropic; otherwise, the fluid is baroclinic. In other words, the barotropic or baroclinic nature of the fluid is characterized by whether $\partial_\mu p/\rho$ is a conservative force field, which has a decisive influence on whether the associated vorticity field is conservative. Thus, we refer to the *Lagrange's vortex theorem for barotropic flows*, which shows that vortices are free of generation and extinction.

Since we are primarily interested in vorticity and entropy fields, it is useful to rewrite the baroclinic form of Eq. (1) in terms of the vorticity $\zeta_{\mu\nu}$ and specific (i.e. per unit mass) entropy s fields by using the first law of thermodynamics (Eq. (2)) and the vector identity given in Eq. (3):

$$-dp/\rho = Tds - dw, \quad \text{with } \partial_t s + v^\nu \partial_\nu s = 0, \tag{2}$$

$$v^\nu \partial_\nu v_\mu = v^\nu(\partial_\nu v_\mu - \partial_\mu v_\nu) + \partial_\mu(v^\nu v_\nu/2), \tag{3}$$

where T and w are the absolute temperature and specific enthalpy, respectively. From Eqs. (2) and (3), Eq. (1) becomes

$$\partial_t v_\mu + \partial_\mu(w + v^\nu v_\nu/2) - \zeta_{\mu\nu} v^\nu = T\partial_\mu s. \tag{4}$$

The most well-known example of a baroclinic fluid is the atmosphere, for which the ideal gas law can be applied with a high degree of accuracy. The atmosphere is particularly important in our discussion because it provides a useful fluid dynamic system with a nonuniform entropy distribution in both the vertical and meridional directions; furthermore, energetic vortical fields known as baroclinic eddies play important dynamical roles in heat transport along the meridional direction. In the dynamics of this heat transport, there is a strong correlation between the vorticity $\boldsymbol{\zeta}$ and entropy gradient $\boldsymbol{\nabla} s$ fields, which can be described by Ertel's potential vorticity Q,[15] which is defined as

$$Q := \frac{1}{\rho}(\boldsymbol{\zeta} \cdot \boldsymbol{\nabla} s), \quad \partial_t Q + v^\nu \partial_\nu Q = 0. \tag{5}$$

The above is the most important conserved quantity in the field of geophysical fluid dynamics.

It should be noted that the importance of baroclinicity in the atmosphere varies with scale. In general, in typical laboratory experiments using air, such as wind tunnel studies, air flows behave as barotropic flows since the entropy gradient is negligible; however, for air flows with horizontal scales greater than several 100 or a few 1000 km, baroclinicity becomes a nonnegligible dynamical factor. In Sec. 1, we discussed MMD theory, which indicates that the actual world in which we live consists of an ID structure that bridges quantum and classical physics, rather than *the prevailing view that the laws of classical physics are not fundamental but are approximated from "genuine fundamental" quantum mechanics.* We believe that the scale dependency of baroclinicity, represented by Q in the comparison of barotropic and baroclinic flows, is analogous to that of the Planck constant h in the comparison of quantum and classical physics in MMD theory. To show that this resemblance is not superficial but rather has essential implications for the main issue in this paper, we investigated the generalized H structure of baroclinic flows.

The generalized H structure was derived from the so-called noncanonical form of the H formulation, with the seminal work initiated by Arnol'd[16] and further developed by a group of applied mathematicians and physicists.[17–19] For a baroclinic perfect fluid dynamics system with Eulerian representation, the generalized H,

denoted by H_G, has the form[20]

$$H_G := E + C_F, \quad E := \int \langle \rho v^\nu v_\nu/2 + \rho e(\rho, s)\rangle dV, \quad C_F := \int \langle \rho F(s, Q)\rangle dV, \quad (6)$$

where E and C_F are the total energy with $e(\rho, s)$ being the internal energy density, a Casimir constructed by an arbitrary function F of s and Q. Since the given fluid dynamical system can be described by five independent variables, namely, $v^\mu (1 \leq \mu \leq 3)$ and two thermodynamical variables, we choose ρ and s as the thermodynamic variables because Q is expressed in terms of these two variables. First, when we compare the conservative quantity C_F with the total energy E, we can observe that it is not merely an additional constant of motion. This occurs because both E and C_F are "complete" in the sense that they include all five variables. In other words, they are equal pairs of "complete" constants of motion.

The significant advantage of H_G over E becomes clear when we consider the stability of a given steady state of the fluid because any given steady state of the baroclinic flow can be represented by the condition that the first variation in H_G vanishes; that is,

$$\delta H_G = \delta E + \delta C_F = 0, \quad (7)$$

which can be rewritten as the combination of the steady-state version of Eq. (4) and

$$F - Q\frac{\partial F}{\partial Q} + B(s, Q) = 0. \quad (8)$$

Equation (8) shows that an arbitrary function F can be determined by Bernoulli's function $B(s, Q)$, which characterizes the given steady state. Then, we can demonstrate the formal stability of the state[21] (the stability of a given steady state for infinitesimally small amplitude perturbations with arbitrary forms) if the second variation in H_G is sign definite. In our discussion of the ID structure, a particularly important aspect of Eq. (7) is that the balance between δE and δC_F can be regarded as a unique "interaction" between two dynamics with and without explicit forms of Q. It is clear that the phase-space trajectory of a linearly unstable mode, such as those represented by one of the separatrices of H_G, i.e. $\delta^2 H_G = 0$, cannot be described without C_F. Thus, we believe that perturbation methods with only the Hamiltonian as the total energy are not generally adaptable since, as our present discussion shows, these methods cannot cover the dynamic behaviors of certain unstable modes. We also believe that the root cause of Haag's no-go theorem in axiomatic QFT, as discussed in Sec. 1, can be attributed to such an inability inherent in the conventional Hamiltonian approaches. To further show the decisive role of Q in ID structures, we next examine the relativistic expression of Q.

3. Converted Form of the Relativistic Equation of Motion

First, we fix the sign convention as $(+, -, -, -)$ and introduce a nondimensional four-velocity vector u^μ that satisfies the normalization condition $u^\nu u_\nu = 1$. In Secs. 3

and 4, for simplicity, unless otherwise stated, we develop our arguments within the framework of special relativity. The following basic arguments on the relativistic equations from Eqs. (9)–(15) are given by Landau and Lifshitz[22] (pp. 506–508). Regarding the first law of thermodynamics, we have

$$-\frac{dp}{n} = Td\left(\frac{\sigma}{n}\right) - d\left(\frac{w}{n}\right), \tag{9}$$

where n denotes the "particle number" corresponding to the density ρ in the non-relativistic case, and σ/n and w/n are the specific entropy and enthalpy, respectively, as in Eq. (2). The relativistic equation of continuity is given by

$$\partial_\nu(nu^\nu) = 0, \tag{10}$$

and the energy–momentum tensor for a perfect fluid has the following form:

$$T^{\mu\nu} = wu^\mu u^\nu - pg^{\mu\nu}. \tag{11}$$

The tensor divergence of Eq. (11) gives the following equations of motions:

$$\partial_\nu T^\nu_\mu = u_\mu \partial_\nu(wu^\nu) + wu^\nu \partial_\nu u_\mu - \partial_\mu p = 0. \tag{12}$$

The projection of Eq. (12) in the direction u^μ can be calculated by $u^\mu \partial_\nu T^\nu_\mu = 0$; with Eq. (9), this becomes

$$u^\nu \partial_\nu(\sigma/n) = 0, \tag{13}$$

which corresponds to the second equation in Eq. (2). Next, we calculate the component of $\partial_\nu T^\nu_\mu = 0$ perpendicular to u^μ as

$$\partial_\nu T^\nu_\mu - u_\mu u^\nu \partial_\sigma T^\sigma_\nu = 0, \tag{14}$$

which yields

$$wu^\nu \partial_\nu u_\mu - \partial_\mu p + u_\mu u^\nu \partial_\nu p = 0. \tag{15}$$

This equation corresponds to the nonrelativistic form of $\rho D_t v_\mu = 0$ in Eq. (1).

As we have noted with Eq. (4) in Sec. 2, in terms of the vorticity and the entropy field, the form of Eq. (4) is preferable to the form of Eq. (1). The derivation of the relativistic form of Eq. (4) was given by Lichnerowicz[23] (p. 30) and it has the following form:

$$\omega_{\mu\nu} u^\nu = T\partial_\mu(\sigma/n), \quad \omega_{\mu\nu} := \partial_\mu[(w/n)u_\nu] - \partial_\nu[(w/n)u_\mu]. \tag{16}$$

For the sake of readers' convenience, in Appendix A, we give the details of this derivation. Note that Eq. (13) is included in Eq. (16), as shown by $0 = u^\mu \omega_{\mu\nu} u^\nu = Tu^\mu \partial_\mu(\sigma/n)$. We can also observe that Eq. (16) remains valid for curved space–time if we replace ∂_μ with a covariant derivative, denoted as ∇_μ.

4. Ertel's Charge as the Source of an Entropic Vortex Field

To appreciate the importance of Eq. (16), we use an explicit (writing down all the elements) matrix representation of Eq. (17) below to derive the conserved Ertel's current.

$$\omega_{\mu\nu} = \begin{pmatrix} 0 & \omega_{01} & \omega_{02} & \omega_{03} \\ -\omega_{01} & 0 & \omega_{12} & -\omega_{31} \\ -\omega_{02} & -\omega_{12} & 0 & \omega_{23} \\ -\omega_{03} & \omega_{31} & -\omega_{23} & 0 \end{pmatrix}. \tag{17}$$

First, after defining the pseudoscalar Ω in Eq. (18), we introduce ${}^*\omega^{\mu\nu}$, which is the Hodge dual of $\omega_{\mu\nu}$, i.e.

$$\Omega := \omega_{01}\omega_{23} + \omega_{02}\omega_{31} + \omega_{03}\omega_{12}, \tag{18}$$

$${}^*\omega^{\mu\nu} = \begin{pmatrix} 0 & -\omega_{23} & -\omega_{31} & -\omega_{12} \\ \omega_{23} & 0 & -\omega_{03} & \omega_{02} \\ \omega_{31} & \omega_{03} & 0 & -\omega_{01} \\ \omega_{12} & -\omega_{02} & \omega_{01} & 0 \end{pmatrix}. \tag{19}$$

From Eqs. (17) and (19), we obtain

$${}^*\omega^{\mu\kappa}\omega_{\kappa\nu} = \Omega g^{\mu}_{\nu}, \quad {}^*\omega^{\mu\nu}\omega_{\nu\mu} = 4\Omega. \tag{20}$$

According to Eq. (16), we have

$$({}^*\omega^{\mu\kappa}\omega_{\kappa\nu})u^{\nu} = \Omega g^{\mu}_{\nu}u^{\nu} = T({}^*\omega^{\mu\kappa})\partial_{\kappa}(\sigma/n); \tag{21}$$

thus, we can obtain

$$\Omega_T u^{\mu} = {}^*\omega^{\mu\kappa}\partial_{\kappa}(\sigma/n), \quad \text{where } \Omega_T := \Omega/T. \tag{22}$$

By substituting Eq. (19) into Eq. (22) and with a series of manipulations based on the skew symmetry of $\omega_{\mu\nu}$, we can finally derive that

$$\Omega_T \begin{pmatrix} u^0 \\ u^1 \\ u^2 \\ u^3 \end{pmatrix} = \begin{pmatrix} -\partial_1[\omega_{23}(\sigma/n)] - \partial_2[\omega_{31}(\sigma/n)] - \partial_3[\omega_{12}(\sigma/n)] \\ \partial_0[\omega_{23}(\sigma/n)] - \partial_2[\omega_{03}(\sigma/n)] + \partial_3[\omega_{02}(\sigma/n)] \\ \partial_0[\omega_{31}(\sigma/n)] + \partial_1[\omega_{03}(\sigma/n)] - \partial_3[\omega_{01}(\sigma/n)] \\ \partial_0[\omega_{12}(\sigma/n)] - \partial_1[\omega_{02}(\sigma/n)] - \partial_2[\omega_{01}(\sigma/n)] \end{pmatrix}. \tag{23}$$

Based on this expression, we can observe that

$$\partial_{\nu}(\Omega_T u^{\nu}) = 0. \tag{24}$$

In addition, using Eq. (16) again, we have

$$-\Omega u^0 = T[\omega_{23}\partial_1(\sigma/n) + \omega_{31}\partial_2(\sigma/n) + \omega_{12}\partial_3(\sigma/n)]; \tag{25}$$

thus, we obtain

$$\Omega_T = \Omega_Q := -[\omega_{23}\partial_1(\sigma/n) + \omega_{31}\partial_2(\sigma/n) + \omega_{12}\partial_3(\sigma/n)]/u^0, \tag{26}$$

which is the relativistic expression of Ertel's potential vorticity Q given in Eq. (5). Following the convention of theoretical physics, we refer to Ω_T as Ertel's charge. The conservation property of Eq. (24) can be extended to curved space–time by substituting ∂_μ in Eq. (23) with the covariant derivative ∇_μ and using the tensor identity

$$(\nabla_\mu \nabla_\nu - \nabla_\nu \nabla_\mu)\omega_{\kappa\lambda} = -R^{\sigma}_{\kappa\mu\nu}\omega_{\sigma\lambda} - R^{\sigma}_{\lambda\mu\nu}\omega_{\kappa\sigma} \tag{27}$$

to calculate the vector divergence on the right-hand side of Eq. (23), where $R^{\alpha}_{\beta\gamma\delta}$ denotes the Riemann curvature tensor.

Remark 1 A relativistic extension of Ertel's potential vorticity was first done by Katz[24] based on the converted form of a relativistic equation of motion derived by Lichnerowicz referred to at the end of Sec. 3. In his derivation, as in the case of ours, Katz first introduces ${}^*\omega^{\mu\nu}$ (Hodge dual of $\omega_{\mu\nu}$ defined in Eq. (19)). Then, using it, he defines a "vorticity four-vector" $\hat{\omega}^\mu$ of the form

$$\hat{\omega}^\mu = {}^*\omega^{\mu\nu} u_\nu. \tag{28}$$

The conservation law he shows turns out to be

$$\partial_\nu(\Omega_K u^\nu) = 0, \quad \Omega_K := \hat{\omega}^\nu \partial_\nu(\sigma/n), \tag{29}$$

where we have simplified his derivation by confining ourself solely to the case of special relativity. Using Eq. (10), the above equation can be rewritten as

$$u^\nu \partial_\nu[\Omega_K/n] = 0. \tag{30}$$

Based on this advective expression, Katz simply points out that the nonrelativistic limit of Ω_K/n is Q given in Eq. (5). Note, however, that Ω_K in Eq. (29) is defined as the inner-product of four vectors $\hat{\omega}^\nu$ and $\partial_\nu(\sigma/n)$, while the numerator of Q in Eq. (5) is expressed as the inner-product of nonrelativistic three vectors of $\boldsymbol{\zeta}$ and $\boldsymbol{\nabla} s$. In this respect, we do not think that Katz's statement on the nonrelativistic limit is trivial and therefore needs further explanation. In order to prove his statement as well as the equivalence of Katz's and our derivations, we first show that, by direct calculations using Eqs. (16), (19), (26) and (28), we have

$$\Omega_K = \Omega_T (= \Omega_Q). \tag{31}$$

Thus, by comparing Ω_Q/n in the advection equation $u^\nu \partial_\nu[\Omega_Q/n] = 0$ and Q in Eq. (5), we readily see that Q gives the nonrelativistic limit of $\Omega_K/n = \Omega_T/n$.

The advantage of the newly derived expression Ω_T over Ω_K is that the conserved current $\Omega_T u^\mu$ can be shown to be an entropy current tied closely to "space–time dynamics" now we are considering in this paper. According to the second equation in Eq. (16), the physical dimension of Ω in Eq. (18), denoted by $\dim[\Omega]$, becomes $\dim[\Omega] = l^{-2}\dim[(w/n)^2]$, where l denotes the length scale. Since n and w are the particle number and the energy per unit volume, respectively, if we use a natural unit system, then we have $\dim[n] = l^{-3}$ and $\dim[w^2] = l^{-8}$. Thus, it turns out that

$\dim[\Omega] = l^{-1}/l^3$, indicating that $\dim[\Omega] = \dim[T^{\mu\nu}]$ in Eq. (11) and hence, from Eq. (9), *the physical dimension of* Ω_T *is the entropy per unit volume.*

A particularly intriguing property of $\omega_{\mu\nu}$ is that "Dirac's γ matrix" $\hat{\gamma}^{\mu\nu}$ can be constructed from Eq. (20). In fact, if we define $\hat{\gamma}^{\mu}_{\nu}$ such that $\hat{\gamma}^{\mu}_{\nu} := ({}^*\omega^{\mu\sigma})\omega_{\sigma\nu}$, then, according to Eq. (20), we get $\hat{\gamma}^{\mu}_{\nu} = \Omega g^{\mu}_{\nu}$. By raising the suffix ν, we have that $\hat{\gamma}^{\mu\nu} = \Omega g^{\mu\nu}$; thus, we find that

$$\frac{1}{\Omega}(\hat{\gamma}^{\mu\nu} + \hat{\gamma}^{\nu\mu}) = 2g^{\mu\nu}, \tag{32}$$

which is the well-known anti-commutation relation. To further examine the implications of Eq. (32), we investigated the relation between $g^{\mu\nu}$ and ${}^*\omega^{\mu\sigma}\omega^{\nu}_{\sigma}/\Omega$. According to Eq. (20), $g^{\mu\nu}$ can be rewritten as follows:

$$g^{\mu\nu} = \frac{{}^*\omega^{\mu\sigma}\omega^{\nu}_{\sigma}}{\Omega} = \frac{{}^*\omega^{\mu\sigma}\omega^{\nu}_{\sigma}({}^*\omega^{\kappa\lambda}\omega_{\lambda\kappa})}{\Omega({}^*\omega^{\kappa\lambda}\omega_{\lambda\kappa})} = \frac{{}^*\omega^{\mu\sigma}\omega^{\nu}_{\sigma}({}^*\omega^{\kappa\lambda}\omega_{\lambda\kappa})}{({}^*\omega^{\kappa\lambda}\omega_{\lambda\kappa})^2/4}. \tag{33}$$

Recall that, in general, $g^{\mu\nu}$ is not a physical quality but rather a purely mathematical quantity. However, there exists an exceptional case in which $g^{\mu\nu}$ becomes physical, as shown by Eq. (34), which was derived by lengthy straightforward calculations[25,26] on the Weyl conformal tensor $W_{\alpha\beta\gamma\delta}$.

$$W^{\mu\alpha\beta\gamma}W^{\nu}_{\alpha\beta\gamma} - \frac{1}{4}W^2 g^{\mu\nu} = 0, \quad W^2 := W^{\alpha\beta\gamma\delta}W_{\alpha\beta\gamma\delta}. \tag{34}$$

Equation (34) shows that, for nonvanishing W^2, the cosmological term $\Lambda g^{\mu\nu}$ can be interpreted not as vacuum but as (conformal) gravitational energy–momentum tensor. By comparing Eq. (33) with Eq. (34), we find that

$$g^{\mu\nu} = \frac{W^{\mu\alpha\beta\gamma}W^{\nu}_{\alpha\beta\gamma}}{W^2/4} = \frac{{}^*\omega^{\mu\sigma}({}^*\omega^{\kappa\lambda})\omega^{\nu}_{\sigma}\omega_{\kappa\lambda}}{({}^*\omega^{\kappa\lambda}\omega_{\lambda\kappa})^2/4} = \frac{({}^*\omega^{\mu\sigma}){}^*\omega^{\kappa\lambda}\omega^{\nu}_{\sigma}\omega_{\kappa\lambda}}{(4\Omega)^2/4}, \tag{35}$$

which clearly shows that $(4\Omega)^2$ correlates directly with W^2.

As we have referred to at the end of Sec. 1, quite recently, Aoki *et al.* proposed novel mathematical schemes defining precisely a conserved quantity in a curved space–time, that can be applied not only to the energy and momentum for matter but also to the entropy of a given system. And in order to justify the new schemes, they have successfully conducted various verifications for different gravitational systems. We think that one of their new schemes on the entropy conservation provides tantalizing new information revealing the important role played by Weyl tensor in gravitational "entropy dynamics".

A possible connection between gravitational entropy and Weyl tenor was suggested by Penrose in terms of *Weyl curvature hypothesis*[27] which may explain the observed extremely isotropic space–time structure of our early universe. Through their series of studies, of which brief overview is given in the subsequent section, Sakuma *et al.*[25,28] are now pursuing a new study on developing an *extended dark matter* (EDM) model having a form of cosmological term: $\lambda_{\rm dm} g_{\mu\nu}$ where the metric tensor $g_{\mu\nu}$ is related to Weyl tensor field through Eq. (35). The main reason why we

consider an EDM is because we conjecture that, due to the ID structure arising from material fields and their environmental space–time, dark matter phenomena would not be figured out solely in terms of timelike particle dynamics, though *the timelike entity associated with EDM* is our primary concern. We think that the aforementioned studies by Aoki *et al.*[14] are helpful in identifying this timelike entity, because they have proposed a general form of the definition of a timelike entropy current. The key concept in their definition is, what they call, *timelike intrinsic vector* $\hat{\zeta}^\mu$ satisfying

$$T^\mu_\nu \nabla_\mu \hat{\zeta}^\nu = 0 \Rightarrow (\nabla_\mu \hat{\zeta}^\mu = 0, \text{ for } T^\mu_\nu = \lambda_{\rm dm} g^\mu_\nu), \tag{36}$$

where ∇_μ and T^μ_ν, respectively, denote covariant derivative and the energy–momentum tensor under consideration, the latter of which becomes $\lambda_{\rm dm} g^\mu_\nu$ in our present case.

From Eqs. (10) and (13), we have the well-known equation: $\nabla_\nu(\sigma u^\nu) = 0$. Interestingly enough, we have already shown that Ω_Q in Eq. (26) whose physical dimension is exactly the same as that of σ also satisfies the same equation of $\nabla_\nu(\Omega_Q u^\nu) = 0$, though Ω_Q is composed of a certain vortical field while σ is not such a kind of quantity. Since the physical meaning of $\nabla_\nu(\Omega_Q u^\nu) = 0$ must be understood in terms of Eq. (36), we can say that, thanks to it, $\Omega_Q u^\nu$ is a timelike gravitational entropy current associated with Weyl curvature field. A novel proposal of dark matter model based on this timelike gravitational entropy current will be given in Subsec. 5.2.1.

From the definition of Ω_Q in Eq. (26), we see that it is a classical spin field generated by the two-dimensional vortical motion of a fluid particle (or element) confined on a comoving isentropic surface. The equality of the following two expressions $u^\nu \partial_\nu(\sigma/n) = u^\nu \partial_\nu(\Omega_Q/n) = 0$ derived from Eqs. (13) and (30) holds if there exists such a function f as to satisfy $\Omega_Q/n = f(\sigma/n)$. Actually, it is known that this equality holds for a wider class of relation between Ω_Q/n and σ/n called *the fluid element relabeling symmetry* (FERS)[29] leading to the invariance of Casimir functionals referred to in Sec. 2. Thus, as we have stated at the beginning of the abstract of this paper, our reinvestigation on relativistic extension of Ertel's potential vorticity having the property of FERS was set out with the motivation of aiming at a meaningful connection between Aoki *et al.*'s[14] novel achievement of Eq. (36) and our central result of Eq. (35).

5. Brief Conclusions and Novel Perspectives on QFT and Cosmology

5.1. *Conclusions on Ω_T dynamics and its implication for QFT*

By reinvestigating the relativistic form of Ertel's charge Ω_T, of which importance has been largely ignored except in the field of geophysical fluid dynamics, we found that $\Omega_T u^\mu$ is a conserved "entropy current" in the sense of FERS mentioned above. The importance of this finding is that while the physical dimension of Ω_T is the entropy per unit volume, this quantity is not identical to the thermodynamic entropy density;

instead, it is related to both the vortical modes of a given energy–momentum field $T^{\mu\nu}$ in Eq. (11) and the associated space–time $g^{\mu\nu}$ (defined within the framework of conformal gravity (34)). As a result, Ertel's charge Ω_T plays an important role in the ID structure discussed in Sec. 1.

We think that the category-theoretic perspective plays a crucial role in exploring the nature of Ertel's charge in terms of QFT. In thermodynamics, the concept of entropy is understood through the order structure between thermodynamic states and the state transitions between them. Categories are a generalization of both the order and the group-theoretic structure, and they are helpful in capturing the essence of the spatio-temporal structure. In this respect, Saigo[30] proposed the idea of considering the category algebra, which is a noncommutative convolution algebra defined on a spatio-temporal category; furthermore, he considered the states as linear functions on it, as quantum fields and their states. We believe that by reformulating the discussion of Ertel's charge from this perspective, we can naturally "quantize" the contents of this paper. In the context of the quantized theory, the (possibly continuous) sector structure arises, which describes the macroscopic nature of the theory. As we have referred to in the brief explanation of MMD theory given in Sec. 1, so-called *order parameters* distinguish different sectors which have been shown to be treatable in recent quantum measurement theory.[31] We believe that, as a future challenge, it is important to reexamine the role of Ertel's charge from the viewpoint of sector theory.

5.2. *Novel perspective on cosmology*

5.2.1. *On a dark matter model*

In Sec. 4, we showed that $\dim[\Omega] = \dim[T^{\mu\nu}]$ in Eq. (11), and we found that the nonzero value of Ω^2 corresponds to the nonzero value of W^2, which suggests that the nonzero Ω is associated with a special energy field associated with nonzero W^2. In general, in the Einstein field equation (37)

$$R^{\mu\nu} - \frac{1}{2}Rg^{\mu\nu} + \Lambda g^{\mu\nu} = -\frac{8\pi G}{c^4}T^{\mu\nu}, \tag{37}$$

energy–momentum fields are associated directly with Ricci curvature terms; thus, a peculiar energy field such as Ω would be related to the cosmological term $\Lambda g^{\mu\nu}$ we discussed with Eq. (34) to some (or a large) extent. As the first step toward understanding the physical meaning of a conserved "entropy" density $\Omega_T(= \Omega/T)$, we introduce a constant reference temperature T_R, the magnitude of which is immaterial at this point in our discussion but which will become important in our newly proposed hypothesis known as simultaneous conformal symmetry breaking (SCSB) of electromagnetic and gravitational fields. With T_R, we can introduce a nondimensional parameter such as the particle number $\tilde{n} := T_R/T$, which is inversely proportional to the temperature T. With $\tilde{n}$, we can rewrite Eq. (24) as

$$\nabla_\nu(\tilde{n}\Omega u^\nu) = 0. \tag{38}$$

Therefore, if we redefine $\tilde{\Omega}$ as $\tilde{\Omega} := \tilde{n}\Omega$ and introduce $\tilde{T}^{\mu\nu}$ as $\tilde{T}^{\mu\nu} := \tilde{\Omega}u^\mu u^\nu$, we can obtain

$$\nabla_\nu \tilde{T}^{\mu\nu} = 0, \tag{39}$$

since u_μ satisfies the geodesic condition $u^\nu \nabla_\nu u_\mu = 0$ at the galactic scale. Note that the nonzero $\tilde{\Omega}$ does not correspond to the nonzero Ricci scalar curvature R, but instead corresponds to the nonzero Weyl curvature W^2; thus, the nonzero current $\tilde{\Omega}u^\mu$ can exist even in "nearly vacuum" regions where $R^{\mu\nu} \approx 0$. Furthermore, since the magnitude of $\tilde{\Omega}$ is inversely proportional to T, $\tilde{\Omega}$ would become extremely small soon after the beginning phase of the big bang and then increases, which suggests that the current $\tilde{\Omega}u^\mu$ is in a region where $R^{\mu\nu} \approx 0$ is a promising candidate for the (cold) dark matter model.

5.2.2. *Brief review of previous cosmological studies by Sakuma et al.*

In their recent study on the off-shell properties of quantum fields motivated by enigmatic dressed photon research,[10] Sakuma *et al.*[25,28] shed new light on the long-forgotten GR theory (proved in axiomatic QFT) referred to in Sec. 1, which states that interactions among quantum fields must inevitably accompany spacelike momentum supports. Since these findings revealed a novel perspective on cosmology, especially for models of dark energy and dark matter, we will briefly review these findings before we discuss the above-mentioned dark matter model $\tilde{\Omega}u^\mu$ further. First, on the basis of the GR theorem, in previous research, the mathematical form of a spacelike electromagnetic field, which can be regarded as the extension of the charge-free Maxwell equation into spacelike momentum domains, was investigated. The main conclusions can be summarized as follows ((i)–(iv)):

(i) The extended electromagnetic four-vector potential U_μ can be represented by the Clebsch parametrization (CP)[32] with the parameters (λ, ϕ); the former satisfies the spacelike Klein–Gordon (KG) equation $\nabla_\sigma \nabla^\sigma \lambda - (\kappa_0)^2 \lambda = 0$, where κ_0 is the experimentally determined dressed photon constant, while the latter satisfies either the same KG equation or $\nabla_\sigma \nabla^\sigma \phi = 0$, depending on whether U_μ is spacelike or lightlike. The lightlike U_μ can be interpreted as a $U(1)$ gauge boson, while the spacelike U_μ provides the necessary spacelike momentum supports for field interactions. In fluid mechanics, CP is used for canonical H formulations of barotropic fluids. CP is suitable for extended free Maxwell fields because, in sharp contrast to Eq. (18), for the baroclinic case, the pseudoscalar $\Omega_{(ro)}$ defined by Eq. (40) always vanishes:

$$\Omega_{(ro)} := S_{01}S_{23} + S_{02}S_{31} + S_{03}S_{12} = 0, \tag{40}$$

where $S_{\mu\nu} := \nabla_\mu U_\nu - \nabla_\nu U_\mu$ denotes the field strength of the extended electromagnetic field. According to Eq. (40), as in the case of a free electromagnetic wave, the extended "electric" and "magnetic" fields are perpendicular to each other.

(ii) The energy–momentum tensor $\hat{T}^{\mu\nu}$ for both cases can be written in a unified form as

$$\hat{T}^{\mu\nu} = \hat{S}_{\sigma}^{\mu\nu\sigma} - \frac{1}{2}\hat{S}_{\alpha\beta}^{\alpha\beta} g^{\mu\nu}, \quad \hat{S}_{\alpha\beta\gamma\delta} := S_{\alpha\beta} S_{\gamma\delta}. \tag{41}$$

Note that due to the skew-symmetric nature of $S_{\mu\nu}$, $\hat{S}_{\alpha\beta\gamma\delta}$ satisfies exactly the same properties as the Riemann curvature tensor $R_{\alpha\beta\gamma\delta}$; that is,

$$R_{\beta\alpha\gamma\delta} = -R_{\alpha\beta\gamma\delta}, \quad R_{\alpha\beta\delta\gamma} = -R_{\alpha\beta\gamma\delta}, \quad R_{\gamma\delta\alpha\beta} = R_{\alpha\beta\gamma\delta}, \tag{42}$$

$$R_{\alpha\beta\gamma\delta} + R_{\alpha\gamma\delta\beta} + R_{\alpha\delta\beta\gamma} = 0. \tag{43}$$

Equation (43) is known as the first Bianchi identity and corresponds to Eq. (40). Therefore, $\hat{T}^{\mu\nu}$ in Eq. (41) becomes isomorphic to the Einstein tensor $G^{\mu\nu}$, and its divergence vanishes. *Specifically, we can say that $\hat{T}^{\mu\nu}$ naturally fits into the geometrodynamics of general relativity.*

(iii) Since the nonlightlike U^{μ} has a spacelike momentum field parametrized by κ_0 in the aforementioned spacelike KG equation, it forms a submanifold of de Sitter space (a pseudo-hypersphere $\mathfrak{D}$ embedded in R^5) with a geometrical structure similar to the spacelike KG equation, with the radius of $\mathfrak{D}$ corresponding to κ_0 as a scale parameter. According to Sakuma *et al.*,[25,28] the importance of de Sitter space is twofold. First, using a spacelike momentum field in de Sitter space, Snyder[33] derived a space–time quantization with a built-in Lorentz invariance; second, de Sitter space is a solution of the Einstein field equation, which describes the accelerated expansion of the universe. In accordance with Snyder's work, they showed that the quantized form of $\hat{T}^{\mu\nu}$ can be given by a combined form of the Majorana fermion field, which behaves as an energy–momentum tensor with "virtual photons" acting as mediators of electromagnetic field interactions and $\hat{T}^{\mu\nu}$ associated with a unique ground state M_g, which can be regarded as a compound Rarita–Schwinger state with a spin of 3/2. In terms of the accelerated expansion of the universe, they considered the possibility that the trace of the energy–momentum tensor representing M_g can be interpreted as a "reduced cosmological constant" Λ_{DP} (negative in our sign convention) whose magnitude can be evaluated by the new theory of dressed photons. In fact, Λ_{DP} is $-2.47 \times 10^{-53}\,\mathrm{m}^{-2}$, while the observed value of Λ_{obs}, derived from Planck satellite observations,[34] is $-3.7 \times 10^{-53}\,\mathrm{m}^{-2}$.

(iv) The light field, including the newly identified spacelike counterpart U_{μ}, is an essential element in the theory of dressed photons. An especially intriguing aspect of dressed photons is that even in the lightlike field U_{μ} that satisfies $(U_{\nu})^{*}U^{\nu} = 0$, where $(U_{\nu})^{*}$ is the complex conjugate of U_{ν}, the spacelike KG equation $\nabla_{\sigma}\nabla^{\sigma}\lambda - (\kappa_0)^2\lambda = 0$ is "encoded" in this lightlike field through CP. If the conformal symmetry of the lightlike U_{μ} field, which has $W^2 = 0$ and may be related to the Weyl curvature hypothesis proposed by Penrose,[27] breaks, then the spacelike U_{μ} field emerges, along with the above-mentioned M_g, which is responsible for generating de Sitter space. de Sitter space has the unique

structural characteristic of twin universes,[28] with each twin universe separated by the hypersurface of the event horizon embedded in it. Thus, starting from "the big bang" in the respective domains caused by the conformal symmetry breaking of the lightlike U_μ field, the twin universes (with one consisting of ordinary matter and the other consisting of anti-matter in the sense of time reversal) merge eons later at the event horizon and return to the original light phase. In this scenario, the creation and annihilation of the universe can be compared to those of elementary particles according to the intermediation of the light field. We believe that this cyclic twin universe cosmology is similar to the conformal cyclic cosmology[35] proposed by Penrose.

The newly proposed cosmology described above includes two noteworthy features that are missing from current cosmology based on cosmic inflation scenarios. First, in the former, instead of treating vacuum energy as starting from nothing, we assume the infinite cyclicity of the twin universes, with the "nodes" represented as a "lightlike universe" with null distance. One cycle begins with the conformal symmetry breaking of the nodal lightlike universe, and because of the property $W^2 = 0$[28] (the aforementioned Weyl curvature hypothesis) of the nodal universe, the isotropy of the emerging nonlightlike universe can be naturally explained, in sharp contrast to inflation scenarios. Furthermore, the twin structure of the universe provides a simple solution to the missing anti-matter problem.

5.2.3. *On the flatness of the universe and the thermodynamic twin structure*

In addition to the isotropy of the universe, we must consider the flatness problem. Sakuma *et al.*[25] proposed an SCSB hypothesis, which is referred to in the argument immediately before Eq. (38). According to this hypothesis, the twin universes are assumed to be metric space–times emerging from simultaneous transitions from null electromagnetic and gravitational fields that satisfy $(U_\nu)^* U^\nu = 0$ and $W^2 = 0$, respectively, to the symmetry breaking spacelike $(U_\nu)^* U^\nu < 0$ and $W^2 \neq 0$ fields. The key assumption of SCSB is that this transition can be parametrized by κ_0, and our reasoning is based on the following two facts:

(a) The abundance ratio of dark matter to dark energy is approximately 1/3.
(b) The physical meaning of the cosmological term $\Lambda g^{\mu\nu}$ can be explained by Eq. (34).

In Subsec. 5.2.1, we discussed a new plausible form of dark matter; however, given its overwhelming presence over ordinary matter, we do not believe that the dark matter modeled by $\tilde{\Omega} u^\mu$ is the most dominant form of dark matter.

As we explained in item (iii) of Subsec. 5.2.2, in the model of Sakuma *et al.*, the observable effect of dark energy is generated by the reduced cosmological constant Λ_{DP}, which has been shown to be proportional to $3(\kappa_0)^2$. We include the factor 3 in

the expression of $\Lambda_{\rm DP}$ because the spatial dimension of our universe is three. Recall that our original goal, which led to the introduction of $\Lambda_{\rm DP}$, was to properly evaluate the involvement of the spacelike momentum field in quantum field interactions, and the existence of $\Lambda_{\rm DP}$ was derived from electromagnetic field interactions as an important parameter characterizing the ground state of spacelike "virtual photons". The similarity between Newtonian gravity and electromagnetic Coulomb force strongly suggests a possibility that the physical entity similar to spacelike "virtual photons" must be involved in gravitational field interactions. Thus, we believe that it is natural to assume that a similar argument can be extended to gravitational field interactions, although we do not have a satisfactory quantum gravitational theory. In electromagnetism, the spacelike extension of Maxwell theory is given by Eq. (41). For the gravitational case, based on Eq. (39), we introduce a spacelike extension with the form $\tilde{T}^{\mu\nu} = \tilde{\Omega} u^\mu u^\nu$, where u^μ satisfies the spacelike four-vector condition $u^\nu u_\nu = -1$. We investigated this form because the important scalar parameter in our dark matter model must be identified in terms of the "zero-point energy" of the $\tilde{\Omega}$ field, which exists implicitly in the quantum version of Eq. (11).

The energy-quantized version of $\tilde{T}^{\mu\nu}$ is the one in which $\tilde{\Omega}$ is discretized and the minimum value of $\tilde{\Omega}_0 := \text{Min}[|\tilde{\Omega}|] > 0$ exists, which can be compared to the zero-point energy $h\nu/2$ of a harmonic oscillator. As previously stated in the discussion of dark energy by Sakuma *et al.*,[25] the spacelike energy–momentum tensor $\tilde{T}^{\ \mu}_{\nu} = \tilde{\Omega} u^\mu u_\nu$ is not observable, except for its trace, which can be observed as invariant under general coordinate transformations. On the basis of their arguments, we may say that the zero-point energy $-\tilde{\Omega}_0$, as the trace of $(\tilde{T}^{\ \nu}_{\nu})_0$, can be reinterpreted by transferring it from the right-hand side of the Einstein field Eq. (37) to the left-hand side as the *hypothetical cosmological term* $\Lambda(\tilde{\Omega}_0) g^{\mu\nu}$, in which the existence of $g^{\mu\nu}$ is formal and has no physical meanings, where

$$4\Lambda(\tilde{\Omega}_0) := \frac{8\pi G}{c^4} \tilde{\Omega}_0. \tag{44}$$

In contrast to the case of dark energy, however, we can investigate a different possibility in the dark matter model; that is, based on guiding fact (b), we can interpret $\Lambda(\tilde{\Omega}_0) g^{\mu\nu}$ not as *the hypothetical cosmological term* mentioned above but instead as "*a real*" *cosmological term* with the form $\Lambda_{\rm dm} g^{\mu\nu}$, where $\Lambda_{\rm dm} := \Lambda(\tilde{\Omega}_0)$ and $g^{\mu\nu}$ represent the energy–momentum tensor of the conformal gravity field given by Eq. (34). Then, by applying guiding fact (a) to $\Lambda_{\rm dm} = \Lambda(\tilde{\Omega}_0)$, we can introduce a core assumption of the SCSB hypothesis, which has the form

$$\Lambda_{\rm dm} = \Lambda(\tilde{\Omega}_0) = -\Lambda_{\rm DP}/3 > 0. \tag{45}$$

First, we note that the condition of $W^2 \neq 0$ in Eq. (34) is necessary to define $g^{\mu\nu}$ as the energy–momentum tensor of the conformal gravity field, which allows us to hypothesize that $\Lambda_{\rm dm}$ is directly related to the minimum value of quantized $|W^2|$. Recall that the magnitude of $\tilde{\Omega}_0$ depends on the undetermined constant parameter T_R, which was introduced in the argument of Eq. (38). By adjusting this parameter,

we can ensure that $\Lambda(\tilde{\Omega}_0)$ is equal to $\Lambda_{\rm dm}$, which corresponds to the minimum value of quantized $|W^2|$. Second, as previously mentioned, $-\Lambda_{\rm DP}$ is proportional to $3(\kappa_0)^2$; thus, according to Eq. (45), the parameter $\Lambda_{\rm dm}$ of the gravitational field is related to the parameter $(\kappa_0)^2$ of the electromagnetic field. Since the factor of 3 in $-\Lambda_{\rm DP}$ reflects the spatial dimension of our universe, we hypothesize that $\Lambda_{\rm dm} \propto (\kappa_0)^2$ implies the "equipartition of energy" in four-dimensional space–time, which can be concisely represented by a sign convention with the form $(+,-,-,-)$. The overwhelmingly large abundance ratios of dark energy and dark matter to ordinary matter suggest that the space–time structure of our universe is determined by these two dark components. As a result of the above-mentioned "equipartition of energy", our universe has a nearly flat space–time structure. Thus, Eq. (45) relates the parameter of conformal symmetry breaking in an electromagnetic field to that in a gravitational field in a way that it is consistent with observational evidence.

$\Lambda_{\rm dm}$, as defined in Eq. (45), is a unique parameter of anti-de Sitter space (ADS), the theoretical importance of which can be appreciated by ADS/CFT correspondence. Although an expansion-accelerated universe, such as ours, is not ADS itself, it is worth noting that the scale of our universe as one of the pairs is given exactly by $\Lambda_{\rm dm}$;[28] thus, in this sense, ADS must be a genuine scale parameter of our universe. If we choose a natural unit system in which the speed of light c and the Planck constant h have unit magnitude, then the length scale $\sqrt{1/(\kappa_0)^2} \approx 40$ nanometer, called the dressed photon constant, can be shown to be the geometric mean[28] of the smallest Planck length and the largest $\sqrt{1/\Lambda_{\rm dm}}$. It is also worth noting that $\sqrt{1/(\kappa_0)^2}$ provides a rough estimate of the Heisenberg cut for electromagnetic phenomena. We can argue that the dark matter phenomenon can be explained by combining $\tilde{\Omega}u^\mu$ currents in regions where $R^{\mu\nu}$ is negligibly small, which was noted in the argument after Eq. (39), and the result derived of Eq. (45).

Regarding the twin structure of universes and the thermodynamic aspect of space–time, we briefly refer to Tomita–Takesaki theory[36] on the Kubo–Martin–Schwinger (KMS) state, which can be regarded as a generalization of the Gibbs state that covers thermodynamic equilibrium states with infinite degrees of freedom for which we cannot define trace operations. Since the KMS state is a mixed state, its corresponding Gel'fand–Naimark–Segal representation is reducible. Therefore, for $\mathcal{M}$ defined as a von Neumann algebra in Hilbert space $\mathfrak{H}$, there exists a commutant $\mathcal{M}'$ that satisfies the following inversion relation:

$$J\mathcal{M}J = \mathcal{M}', \quad e^{itH}\mathcal{M}e^{-itH} = \mathcal{M}, \quad J^2 = 1, \tag{46}$$

$$JHJ = -H, \tag{47}$$

where H and J denote the Hamiltonian and the anti-unitary operator known as the modular conjugate operator. The spectrum of the Hamiltonian is symmetric with regard to its sign, indicating the existence of states with negative energy, whose stability is known to be greater than that of a vacuum state.[37] Thus, we believe that

the result of Tomita–Takesaki theory applies to the case of twin universes discussed in this paper.

Acknowledgments

We appreciate the anonymous reviewers for their valuable comments which helped us to improve the quality of this paper. This research was partially supported by a collaboration with the Institute of Mathematics for Industry, Kyushu University and the first author is especially thankful for the help of Prof. Y. Fukumoto in promoting this collaboration.

Appendix A

Dividing Eq. (15) by n, we have

$$(w/n)u^\nu\partial_\nu u_\mu - (\partial_\mu p)/n + (u_\mu u^\nu/n)\partial_\nu p = 0. \tag{A.1}$$

The first term on the left-hand side of (A.1) can be rewritten as

$$\begin{aligned} u^\nu(w/n)\partial_\nu u_\mu &= u^\nu[\partial_\nu\{(w/n)u_\mu\} - u_\mu\partial_\nu(w/n)] \\ &= u^\nu[\partial_\nu\{(w/n)u_\mu\} - \partial_\mu\{(w/n)u_\nu\} + \partial_\mu\{(w/n)u_\nu\}] \\ &\quad - u^\nu u_\mu\partial_\nu(w/n). \end{aligned} \tag{A.2}$$

With the new notation for the vorticity field $\omega_{\mu\nu} := \partial_\mu[(w/n)u_\nu] - \partial_\nu[(w/n)u_\mu]$, (A.2) becomes

$$u^\nu(w/n)\partial_\nu u_\mu = -\omega_{\mu\nu}u^\nu + u^\nu\partial_\mu\{(w/n)u_\nu\} - u^\nu u_\mu\partial_\nu(w/n). \tag{A.3}$$

By substituting (A.3) into (A.1), we obtain

$$-\omega_{\mu\nu}u^\nu + u^\nu\partial_\mu\{(w/n)u_\nu\} - (\partial_\mu p)/n - u_\mu u^\nu[\partial_\nu(w/n) - (\partial_\nu p)/n] = 0. \tag{A.4}$$

Next, by applying $u^\nu u_\nu = 1$ to the second term in (A.4), we obtain

$$u^\nu\partial_\mu\{(w/n)u_\nu\} = \partial_\mu\{(w/n)u^\nu u_\nu\} - (w/n)u_\nu\partial_\mu u^\nu = \partial_\mu(w/n). \tag{A.5}$$

In addition, according to Eqs. (9) and (13), the sum of the last two terms in (A.4) becomes $-u_\mu u^\nu T\partial_\nu(\sigma/n) = 0$; thus, we can finally obtain that

$$-\omega_{\mu\nu}u^\nu + \partial_\mu(w/n) - (\partial_\mu p)/n = 0 \Rightarrow \omega_{\mu\nu}u^\nu = T\partial_\mu(\sigma/n). \tag{A.6}$$

References

1. J. Bekenstein, *Lett. Nuovo Cimento* **4**, 737 (1972).
2. S. W. Hawking, *Commun. Math. Phys.* **43**, 199 (1975).
3. W. G. Unruh, *Phys. Rev. D* **14**, 870 (1976).
4. E. Verlinde, *J. High Energy Phys.* **4**, 29 (2011).
5. R. F. Streater and A. S. Wightman, *PCT, Spin and Statistics and all that* (Benjamin, 1964), p. 165.

6. R. Jost, *The General Theory of Quantized Fields* (American Mathematical Society, Providence, 1963).
7. G. F. Dell'Antonio, *J. Math. Phys.* **2**, 759 (1961).
8. R. Penrose, *Quantum Theory and Beyond* (Cambridge University Press, 1971).
9. I. Ojima, Micro-macro duality in quantum physics, in *Proc. 3rd Int. Conf.* "*Stochastic Analysis: Classical and Quantum — Perspectives of White Noise Theory*", ed. T. Hida (World Scientific, 2005), pp. 143–161. arXiv:math-ph/0502038.
10. H. Sakuma, I. Ojima, M. Ohtsu and T. Kawazoe, *J. Eur. Opt. Soc. Rapid Publ.* **17**, 28 (2021). doi:10.1186/s41476-021-00171-w.
11. S. Doplicher, R. Haag and J. E. Roberts, *Commun. Math. Phys.* **13**, 1 (1969); **15**, 173 (1969); **23**, 199 (1971); **35**, 49 (1974).
12. S. Doplicher and J. E. Roberts, *Commun. Math. Phys.* **131**, 51 (1990); *Ann. Math.* **130**, 75 (1989); *Invent. Math.* **98**, 157 (1989).
13. S. Aoki, T. Onogi and S. Yokoyama, *Int. J. Mod. Phys. A* **36**, 2150098 (2021).
14. S. Aoki, T. Onogi and S. Yokoyama, *Int. J. Mod. Phys. A* **36**, 2150201 (2021).
15. H. Ertel, *Meteorol. Z.* **59**, 277 (1942).
16. V. I. Arnol'd, *Dokl. Akad. Nauk SSSR* **162**, 975 (1965) [*Sov. Math. Dokl.* **6**, 773 (1965)] (in Russian).
17. P. J. Morrison and J. M. Greene, *Phys. Rev. Lett.* **45**, 790 (1980).
18. D. D. Holm, B. A. Kuperschmidt and C. D. Levermore, *Phys. Lett. A* **98**, 389 (1983).
19. J. E. Marsden and P. J. Morrison, *Contemp. Math.* **28**, 133 (1984).
20. Y. Kuroda, *Fluid Dyn. Res.* **5**, 273 (1990).
21. H. Sakuma and Y. Fukumoto, *Publ. RIMS Kyoto Univ.* **51**, 605 (2015).
22. L. D. Landau and E. M. Lifshitz, Relativistic fluid dynamics, *Fluid Mechanics*, 2nd edn. (Elsevier, Oxford, UK, 1987), pp. 506–508.
23. A. Lichnerowicz, *Relativistic Hydrodynamics and Magnetohydrodynamics* (Benjamin, New York, 1967).
24. J. Katz, *Proc. R. Soc. Lond. A* **391**, 415 (1984).
25. H. Sakuma, I. Ojima, M. Ohtsu and H. Ochiai, *Symmetry* **12**, 1244 (2020). doi:10.3390/sym12081244.
26. H. Sakuma and H. Ochiai, Note on the physical meaning of the cosmological term, OffShell:1909O.001.v2 (2019), http://offshell.rodrep.org/?p=249.
27. R. Penrose, Singularities and time-asymmetry, *General Relativity: An Einstein Centenary Survey* (Cambridge University Press, 1979), pp. 581–638.
28. H. Sakuma and I. Ojima, *Symmetry* **13**, 593 (2021). https://doi.org/10.3390/sym13040593.
29. N. Padhye and P. J. Morrison, *Phys. Lett. A* **219**, 287 (1996).
30. H. Saigo, *Symmetry* **13**, 1727 (2021). doi:10.3390/sym13091727.
31. K. Okamura, *Symmetry* **13**, 1183 (2021). doi:10.3390/sym13071183.
32. S. H. Lamb, *Hydrodynamics*, Clebsch's Transformation, 6th edn. (Cambridge University Press, Cambridge, UK, 1930), pp. 248–249.
33. H. S. Snyder, *Phys. Rev.* **71**, 38 (1947).
34. H. Liu, https://www.quora.com/What-is-the-best-estimate-of-the-cosmological-constant.
35. R. Penrose, Before the big bang: An outrageous new perspective and its implications for particle physics, in *Proc. EPAC 2006*, Edinburg, Scotland, 2006, pp. 2759–2762.
36. M. Takesaki, *Tomita's Theory of Modular Hilbert Algebras and its Applications*, Lecture Notes in Mathematics, Vol. 128 (Springer, 1970), doi:10.1007/BFb0065832, ISBN:978-3-540-04917-3.
37. O. Bratteli and D. W. Robinson, *Operator Algebras and Quantum Statistical Mechanics*, Vol. 1 (Springer-Verlag, 1979).

Applied Physics Express 15, 045002 (2022)
https://doi.org/10.35848/1882-0786/ac5edc

LETTER

Uncooled Si infrared photodetector for 2 μm wavelength using stimulated emission by dressed photons

Takuya Kadowaki*, Tadashi Kawazoe, Masaki Sugeta, Masahiko Sano, and Takashi Mukai

Nichia Corporation, 3-13-19 Moriya-cho, Kanagawa-ku, Yokohama, Kanagawa, 221-0022, Japan

*E-mail: takuya.kadowaki@nichia.co.jp

Received February 22, 2022; revised March 15, 2022; accepted March 16, 2022; published online April 5, 2022

A Si infrared photodetector that operates without requiring to be cooled was fabricated, and its properties were evaluated. The function of this device is to detect, as an electrical signal, carrier density changes due to stimulated emission utilizing a phonon-assisted process via dressed photons. The photosensitivities of this device were 0.21 A W^{-1}, 0.03 A W^{-1}, and 0.01 A W^{-1} for wavelengths of 1.3 μm, 1.6 μm, and 2.0 μm, respectively, when the forward current density was 50 A cm^{-2}, and the device exhibited a higher sensitivity for wavelengths greater than the cutoff wavelength. © 2022 The Japan Society of Applied Physics

Supplementary material for this article is available online

In recent years, there has been an increase in demand for detectors in near-infrared to mid-infrared bands as advances have been made in such fields as communication, medicine, and chemistry.[1,2] Although Si is often used in a visible-band photodetector, it is not possible to detect infrared light at 1.12 eV or higher with Si due to its bandgap. In general, semiconductors employing compounds such as InGaAs, InSb, and HgCdTe are used as photoelectric conversion materials for such bandwidths;[3,4] however, there are problems due to the toxicity and cost of the materials and the need for a cooling mechanism.

Against such a background, there have been studies on expanding the photodetection bandwidth of Si, which is low cost and nontoxic. In addition, because Si is widely used also in electronic devices, there is an advantage in that a Si device can be fabricated so as to be integrated in an electronic device by being incorporated into existing silicon processes. Si-based near-infrared photodetectors have recently been studied, using the effects such as internal photoemission in Schottky junction,[4–13] surface state absorption,[14,15] and two-photon absorption.[16,17] Also, in these studies, to enhance the infrared light absorption on the devices, the structures such as plasmonic antennas, nano-pillars, resonant cavities, and waveguides are used. Despite numerous studies, for example, the photosensitivity for light having a wavelength of 1.5 μm remains at 36 mA W^{-1}.[14]

We have developed a Si photodetector that operates in the infrared region by utilizing a "dressed photon–phonon-assisted" process, which is understood by describing near-field light in which a light field is localized in a p–n junction interface as dressed photons in which the near-field light is quantized.[18] The "dressed photon–phonon-assisted" process is a transition process of a photon–electron state caused by interactions between dressed photons and phonons. Normally, because Si is an indirect transition semiconductor, interactions between photons and phonons are limited due to the wavenumber conservation law; however, dressed photons localized in a space that is smaller than the wavelength of light are described by a superposition of photons that have a large spread in the wavenumber distributions, and thus, the dressed photons are strongly coupled with phonons, thereby causing the "dressed photon–phonon-assisted" process. Accordingly, with respect to Si, which is an indirect transition semiconductor, we have reported many high-efficiency light-emitting devices that utilize stimulated emission based on phonon-assisted processes.[19–23] The present photodetector is based on a mechanism utilizing carrier density changes due to this stimulated emission. Figure 1(a) shows a band diagram describing the mechanism of the present device. The photodetector applies a forward bias, and detects, as an electrical signal, a change in carriers due to stimulated emission generated by external light. For direct experimental data indicating that stimulated emission is occurring in the Si device, see the supplementary data available online (available online at stacks.iop.org/APEX/15/045002/mmedia). In addition, because this intermediate energy level is caused by dressed photons generated by incident light, the photodetector is not affected by thermally excited electrons, and thus, it can be operated at room temperature. The present study describes a photodetector that employs Si crystal and operates at room temperature in a 2.0 μm band and that is fabricated by using dressed photon technology.

A fabrication process referred to as dressed photon-assisted annealing is required in order to fabricate a device utilizing dressed photons. This annealing method utilizes Joule heat generated as a result of applying a forward current to the p–n homojunction of a crystal of indirect transition semiconductor or the like while irradiating the crystal with light having lower energy than the bandgap of the crystal. Dopant atoms in the crystal are randomly diffused by the heat generated by the forward current. Meanwhile, light having lower energy than the bandgap of the crystal is propagated in the crystal without being absorbed by the crystal. This light generates dressed photons by being coupled with electron–hole pairs in nano regions of the dopant atoms, and is additionally coupled also with phonons in the crystal. The dressed photons possess countless intermediate energy levels due to multimode phonons and emit phonons to generate stimulated emission. As a result, a portion of the Joule energy is converted to light energy, thereby locally cooling the dopant atoms and stopping the diffusion of the dopant atoms. As a result of repeating the above-described processes, the dopant distribution in the crystal is autonomously controlled so as to achieve an optimal distribution for dressed photon generation. As a result, the fabricated device also has a high dressed photon generation efficiency during operation and generates stimulated emission utilizing the phonon-assisted process. Readers are referred to the previous work of the

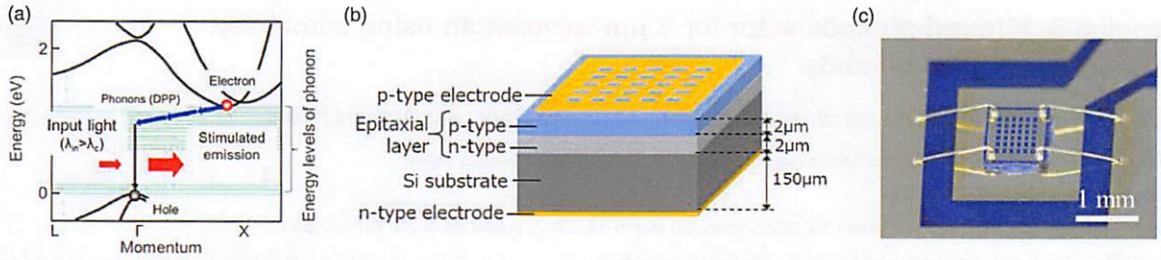

Fig. 1. (Color online) The structure of Si infrared photodetector: (a) band diagram of Si for describing the operating mechanism of the present device; (b) schematic diagram of the device structure of the present device; and (c) micrograph.

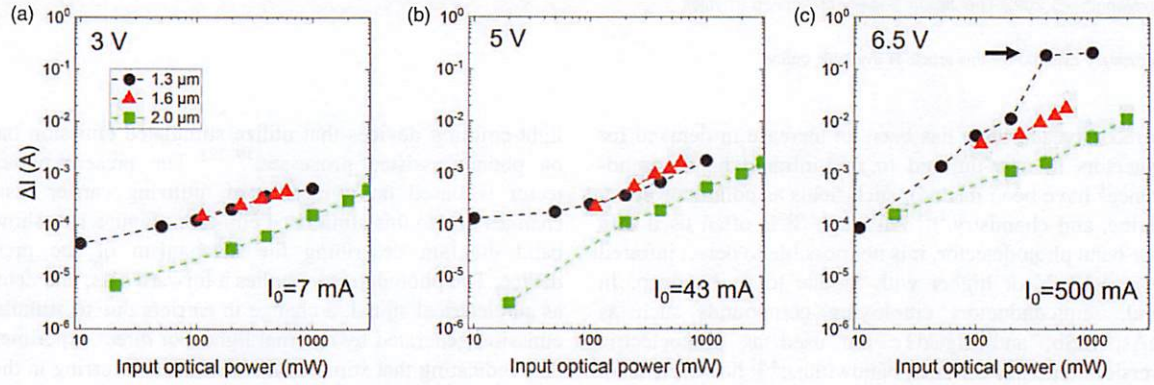

Fig. 2. (Color online) The dependence of changes in the output current on the incident light intensity: (a)–(c) indicate results of applying the forward voltage to the device at 3 V, 5 V, and 6.5 V, respectively. Here, I_0 in the figure shows the value of the forward current without incident light beams. In addition, the individual plots indicate the wavelengths of the incident light beams.

author's group for a further theoretical discussion about dressed photon assisted annealing.[24,25]

Figure 1(b) shows the structure of the employed Si substrate. A high-resistance Si epitaxial layer (the dopant species is As and the concentration is 1×10^{15} cm^{-3}) having a thickness of 4 μm was grown by using CVD on a low-resistance Si single crystal substrate (100) (the dopant species is Sb and the concentration is 1×10^{19} cm^{-3}). Subsequently, a p–n homojunction was formed by injecting its surface with B atoms, which serve as p-type dopants, at a peak concentration of 1×10^{19} cm^{-3} and energy of 700 keV.

On this Si substrate, mesh-like electrodes, shown in the optical micrograph in Fig. 1(c), were formed, and the device was fabricated by dicing the substrate into 1 mm squares. Here, the p electrode was formed of Cr/Au (100 nm/700 nm), and the n electrode was formed of Cr/Pt/Au (30 nm/200 nm/700 nm).

Next, the above-described dressed photon assisted annealing was performed under the following conditions: heating by Joule heat was performed by applying a forward voltage of 5.5 V (15 A cm^{-2}) to the area between the two electrodes; and, at that time, a p-layer surface was irradiated with laser light having a wavelength of 1.3 μm and power of 160 mW (20 W cm^{-2}) for one hour. Doing so makes it possible to arrange the B atoms, which are p-type dopants, in a spatial distribution that is suitable for generating dressed photons.

The present device was used to evaluate changes in the output current with respect to incident light at room temperature, as an example of photodetector properties, and the results are shown in Fig. 2. Specifically, the device was irradiated with light beams having wavelengths of 1.3 μm, 1.6 μm, and 2.0 μm, respectively, in the state in which the forward bias was applied to the device, and changes in the current at that time were measured. Note that this measurement was performed for a time short enough that changes in the spatial distribution of dopant atoms due to annealing, as indicated above, do not occur. Figures 2(a)–2(c) show results for the cases in which the forward bias was 3 V, 5 V, and 6.5 V, respectively, and the plots in the figures represent differences among the incident light beams having different wavelengths. Here, I_0 in the figure shows the value of the forward current without incident light beams. From these plots, changes in the output currents were confirmed for the respective incident light beams having higher wavelengths than the bandgap. Furthermore, an abrupt change in the current value was observed only in the light having a wavelength of 1.3 μm in Fig. 2(c), as indicated by the arrow. This observation will be discussed later.

Figure 3 shows the results of converting the above results so as to show the applied current density on the horizontal axis and the photosensitivity on the vertical axis. The photosensitivity tends to increase with an increase in the injection current density. This trend suggests that stimulated emission occurred via dressed photons.

In particular, corresponding to the result in Fig. 2(c), there was a large increase in the photosensitivity properties when the wavelength was 1.3 μm (indicated by the arrow in the figure). The observed pattern is assumed to be a result of using the light having a wavelength of 1.3 μm for the irradiation in the dressed photon-assisted annealing when fabricating the device. Specifically, there is a correlation

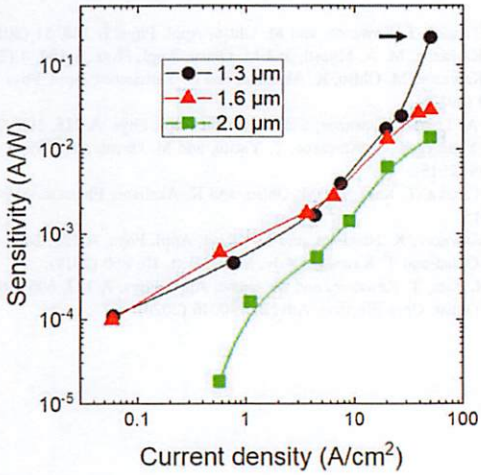

Fig. 3. (Color online) The photosensitivity with respect to the injection current density. The individual plots indicate the wavelengths of the incident light beams.

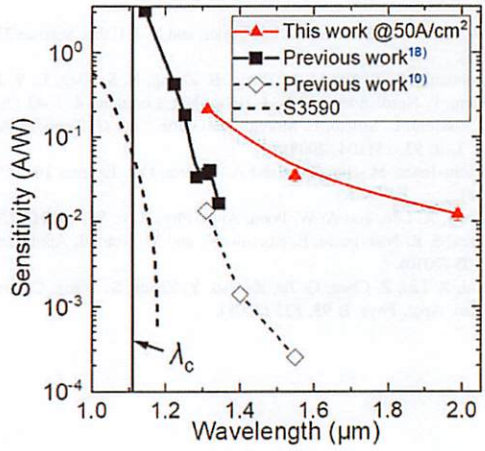

Fig. 4. (Color online) Comparisons with the previous work for the photosensitivity with respect to wavelength. For the present study, the results are shown for a forward current density of 50 A cm^{-2}.

between the wavelength of the irradiation light used when performing the dressed photon assisted annealing and the wavelength of light emitted by utilizing a phonon-assisted process based on the generated dressed photons, and light having the wavelength of the light radiated in the dressed photon assisted annealing tends to be emitted at high efficiency. This phenomenon has been investigated in detail in the previous work of the co-authors, and we refer to it as the photon breeding effect.[26,27]

Next, Fig. 4 shows the photosensitivity with respect to the wavelength. In the figure, the red line indicates the result of the present study at 50 A cm^{-2}, the square symbols (■) indicate the results of the previous work by co-authors, the diamond symbols (◇) indicate the results for a Schottky-type device in the previous work, and the broken line indicates the result for a commercially available Si-PD (Hamamatsu Photonics: S3590). In addition, the vertical line in the figure is the cutoff wavelength λc (1.1 μm) of Si. The photosensitivities of the present device are 0.21 A W^{-1}, 0.03 A W^{-1}, and 0.01 A W^{-1} when the wavelengths are 1.3 μm, 1.6 μm, and 2.0 μm, respectively, and it is clear that a higher sensitivity is observed for a wavelength that is higher than the cutoff wavelength. In addition, as compared with the previous work,[10] a sensitivity that is greater by at least about two orders of magnitude was realized at the wavelength of 1.6 μm. In particular, also at the wavelength of 2.0 μm, the device was shown to exhibit a high photosensitivity of 12 mA W^{-1}.

Finally, the noise equivalent power (NEP) property of the present device is addressed. The NEP represents the incident light intensity at which the S/N becomes 1, and, as a parameter, a lower value indicates a higher performance as a photodetector. As a result of the noise measurement, the NEP of the present device was estimated to be 1.44×10^{-15} W/$Hz^{1/2}$ for the wavelength of 1.3 μm. This value is as high as that of a commercial Si-PD for visible light, and ten times as high as that of a commercial InGaAs-PD for infrared light. This result is due to the fact that the present device is less susceptible to shot noise, as with a normal PD, and the noise energy level of the device is low, because a forward bias is applied and the current flowing in the device is used as a reference. Also, the dynamic range of the present device is addressed. The device has a dynamic range of over 50 dB. Increasing the bias voltage applied to the device increases its photosensitivity, allowing the device to detect incident light of lower power. Therefore, the dynamic range of the device can be made wider by adjusting the bias voltage.

We fabricated a Si infrared photodetector that operates on the basis of stimulated emission via dressed photons, and evaluated its properties. The present study showed that our device exhibits high photosensitivity with respect to light having a wavelength that is higher than the cutoff wavelength. Because the photosensitivity increased with an increase in the forward current density, the observed pattern was interpreted to be a result caused by stimulated emission via dressed photons. In particular, the sensitivity for the wavelength of 2.0 μm was 12 mA W^{-1} at room temperature, thus indicating the feasibility of a Si photodetector that operates at room temperature in the range from near-infrared to mid-infrared.

Acknowledgments The authors would like to express their sincere thanks to Prof. M. Ohtsu for the fruitful discussions and comments on the principles of dressed photons.

1) A. Rogalski, Infrared Phys. Tech. **43**, 187 (2002).
2) A. Karim and J. Y. Andersson, IOP Conf. Series: Material Science and Engineering, 2013, **Vol. 51**, 012001, 10.1088/1757-899X/51/1/012001.
3) C. Cremer, N. Emeis, M. Schier, G. Heise, G. Ebbinghaus, and L. Stoll, IEEE Photon. Tech. Lett. **4**, 108 (1992).
4) A. F. Phillips, S. J. Sweeney, A. R. Adams, and P. J. A. Thijs, IEEE J. Sel. Top. Quantum Electron. **5**, 401 (1999).
5) M. Casalino, L. Sirleto, L. Moretti, and I. Rendina, Semicond. Sci. Technol. **23**, 075001 (2008).
6) M. Casalino, L. Sirleto, M. Iodice, N. Saffioti, M. Gioffrè, I. Rendina, and G. Coppola, Appl. Phys. Lett. **96**, 241112 (2010).
7) S. Zhu, S. M. B. Yu, G. Q. Lo, and D. L. Kwong, Appl. Phys. Lett. **92**, 081103 (2008).
8) A. Akbari and P. Berini, Appl. Phys. Lett. **95**, 021104 (2009).
9) A. Akbari, R. N. Tait, and P. Berini, Opt. Express **18**, 8505 (2010).
10) I. Goykhman, B. Desiatov, J. Khurgin, J. Shappir, and U. Levy, Nano Lett. **11**, 2219 (2011).

11) M. W. Knight, H. Sobhani, P. Nordlander, and N. J. Halas, Science **332**, 702 (2011).
12) A. Sobhani, M. W. Knight, Y. Wang, B. Zheng, N. S. King, L. V. Brown, Z. Fang, P. Nordlander, and N. J. Halas, Nat. Commun. **4**, 1643 (2013).
13) M. Cassalino, L. Sirleto, L. Moretti, M. Gioffre, and G. Coppola, Appl. Phys. Lett. **92**, 251104 (2008).
14) T. Baehr-Jones, M. Hochberg, and A. Scherer, Opt. Express **16**, 1659 (2008).
15) H. Chen, X. Luo, and A. W. Poon, Appl. Phys. Lett. **95**, 171111 (2009).
16) T. Tanabe, K. Nishiguchi, E. Kuramochi, and M. Notomi, Appl. Lett. **96**, 101103 (2010).
17) B. Shi, X. Liu, Z. Chen, G. Jia, K. Cao, Y. Zhang, S. Wang, C. Ren, and J. Zhao, Appl. Phys. B **93**, 873 (2008).
18) H. Tanaka, T. Kawazoe, and M. Ohtsu, Appl. Phys. B **108**, 51 (2012).
19) T. Kawazoe, M. A. Mueed, and M. Ohtsu, Appl. Phys. B **104**, 4 (2011).
20) T. Kawazoe, M. Ohtsu, K. Akahane, and N. Yamamoto, Appl. Phys. B **107**, 659 (2012).
21) M. A. Tran, T. Kawazoe, and M. Ohtsu, Appl. Phys. A **115**, 105 (2014).
22) M. Yamaguchi, T. Kawazoe, T. Yatsui, and M. Ohtsu, Appl. Phys. A **121**, 1389 (2015).
23) H. Tanaka, T. Kawazoe, M. Ohtsu, and K. Akahane, Fluoresc. Mater. **1**, 1 (2015).
24) T. Kawazoe, K. Nishioka, and M. Ohtsu, Appl. Phys. A **121**, 1409 (2015).
25) M. Ohtsu and T. Kawazoe, Adv. Mater. Lett. **10**, 860 (2019).
26) J. H. Kim, T. Kawazoe, and M. Ohtsu, Appl. Phys. A **123**, 606 (2017).
27) M. Ohtsu, Opto-Electron. Adv. **3**, 190046 (2020).

[II] PRESENTATIONS

IN INTERNATIONAL CONFERENCES

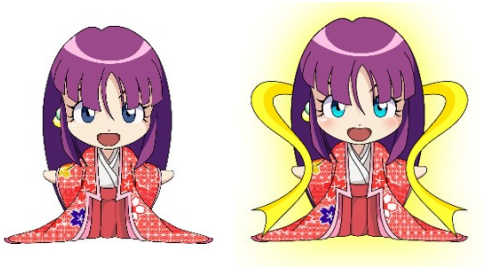

2022 International Symposium on Nonlinear Theory and Its Applications,
NOLTA2022, Virtual, December 12-15, 2022

A Quantum Walk Model for the Energy Transfer of a Dressed Photon

M. Ohtsu†, E. Segawa‡, and K. Yuki*

†Research Origin for Dressed Photon
3-13-19 Moriya-cho, Kanagawa-ku, Yokohama, Kanagawa 221-0022, Japan
‡Graduate School of Environmental Information Sciences, Yokohama National University
79-1 Tokiwadai, Hodogaya-ku, Yokohama, Kanagawa 240-8501 Japan
*Middenii
3-3-13 Nishi-Shinjuku Mizuma Bldg. 6F, Nishishinjuku, Shinjuku, Tokyo 160-0023, Japan
Email: ohtsu@rodrep.or.jp, segawa-etsuo-tb@ynu.ac.jp, k-yuki@middenii.com

Abstract–This paper reports the results of numerical calculation on the dressed photon (DP) energy transfer based on a two-dimensional quantum walk model. In order to compare with the experimental results, the fiber probe was approximated by a two-dimensional right-angled isosceles triangular (RIT) lattice and an equilateral triangular (ET) lattice. The probability of DP creation at the apex of the RIT lattice was higher than that of the ET lattice, which was in agreement with experimental results.

1. Introduction

Experimental studies on dressed photons (DPs) have been actively carried out and applied to produce a variety of advanced technologies [1]. A DP is created in a nano-particle (NP) and on its surface if the NP is irradiated by propagating light (wavelength λ). The size of the DP is equivalent to the size of the NP, and is much smaller than λ. The DP is a quantum field that is created as a result of the interaction among multiple elementary particles such as photons and excitons in a nanometer-sized space. A novel off-shell science theory was built recently and succeeded in describing the fundamental process of the interaction for creating the DP [2,3].

The energy of the created DP transfers to the adjacent NP via a process called DP hopping. In the case where multiple NPs are the atoms in a crystal lattice, the DP excites a lattice vibration during the hopping, resulting in the creation of phonons. Subsequently, the DP exchanges its energy with these phonons to create a dressed-photon—phonon (DPP) quantum field [4]. To achieve further advances, theories on the spatio-temporal behavior of the DP energy transfer should be built to identify the origin of the phenomenon of autonomy that has been experimentally confirmed by the observation of this transfer [5].

The energy is dissipated when the DPP reaches a singularity (for example, at an impurity atom doped in a crystal or at the apex of a sharpened fiber probe). The dissipated energy is transformed to propagating light and can be observed by an external detection system. This means that the singularity serves as an output port to create the propagating light that serves as an output signal.

Figure 1 shows the external forms and cross-sectional structures of fiber probes [1]. The DPP energy dissipates from the taper of the fiber probe. This corresponds to radiating scattered light from the taper. In order to avoid this radiation, an opaque metallic film is formed on the taper (Fig. 1(a)) to realize a high-efficiency fiber probe. This is the prototype of devices that are now popularly used. Figure 1(b) is a basic fiber probe without a metallic film coating, resulting in DPP energy dissipation from the taper. This is a primitive device that has been used only in the early stages of DP science.

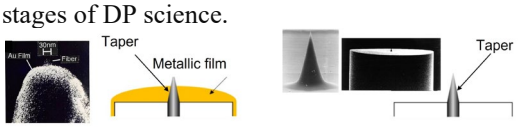

Fig.1 External forms and cross-sectional structures of the fiber probe. (a) A high-efficiency fiber probe. (b) A basic fiber probe.

Employing a quantum walk (QW) model, in which the phonon can be added [6-8], is one promising theoretical method for simultaneously dealing with the issues above.

This paper reports the results of numerical calculation on the DP energy transfer. The results are compared with experimental results on DPP creation at the apex of a fiber probe.

2. Method

For analyzing the spatio-temporal behavior of the DP energy transfer, a system Hamiltonian is assigned by summing the DP energy, the phonon energy, the DP-phonon interaction energy for coupling (the coupling constant χ), and the DP hopping energy (the hopping constant J) [1]. In order to construct a QW model for the two-dimensional lattice, the two traveling directions of the DP (the upper-right and lower-left directions) are assumed, as represented by red and blue broken arrows in Fig. 2(a).

ORCID iDs M. Ohtsu: 0000-0002-4680-9759,
E. Segawa: 0000-0001-8279-9108,
K. Yuki; 0000-0001-5408-5124

While traveling, the DP repeats hopping from one lattice site to its nearest neighbor, as represented by the bent red and blue arrows in this figure. Figures 2(b) and (c) represent the areas around the lattice sites A and B in Fig. 2(a), respectively. A three-row vector is used to express the DPP probability amplitude:

$$\vec{\psi}_{t,(x,y)} = \begin{bmatrix} y_{DP+} \\ y_{DP-} \\ y_{Phonon} \end{bmatrix}_{t,(x,y)}, \quad (1)$$

where [ ] represents the vector at time t and at the position of the lattice site (x, y). y_{DP+} and y_{DP-} are the probability amplitudes of the DPs that travel in the upper-right and lower-left directions, respectively, and y_{Phonon} is that of the phonon.

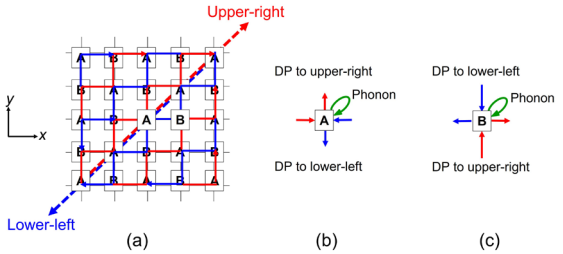

Fig. 2 Two-dimensional lattice.
(a) DP travelling to the upper-right and lower-left. The areas around the lattice sites A and B in (a) are magnified and shown in (b) and (c), respectively. The green loop represents a phonon.

For the lattice sites A and B, the spatial-temporal evolution equations for the vector $\vec{\psi}_{t,(x,y)}$ are

$$\vec{\psi}_{t+1,(x,y)} = P_+\vec{\psi}_{t,(x-1,y)} + P_-\vec{\psi}_{t,(x+1,y)} + P_0\vec{\psi}_{t,(x,y)}, \quad (2)$$

and

$$\vec{\psi}_{t+1,(x,y)} = P_+\vec{\psi}_{t,(x,y-1)} + P_-\vec{\psi}_{t,(x,y+1)} + P_0\vec{\psi}_{t,(x,y)}, \quad (3)$$

respectively. By summing the three matrices on the right-hand sides, one has

$$U = P_+ + P_- + P_0 = \begin{bmatrix} \varepsilon_+ & J & \chi \\ J & \varepsilon_- & \chi \\ \chi & \chi & \varepsilon_0 \end{bmatrix}, \quad (4)$$

which meets a unitarity requirement for the QW model. Diagonal elements ε_+ and ε_- are the eigen-energies of the DPs that travel to the upper-right and lower-left positions, respectively, and ε_0 is that of the phonon.

Figure 3(a) shows a right-angled isosceles triangular (RIT) lattice that approximates the profile of the fiber probe. It schematically explains that, by applying input signals to the sites on the base of the RIT lattice, DPs are created and transferred to the adjacent sites. During this transfer, DPPs are created by the DP-phonon interaction. These DPPs transfer through the RIT lattice and finally reach its apex (the tip of the fiber probe). This apex is assumed to be a sink from which the DPP energy is dissipated. This paper calculates the creation probability P of the DPP at this sink. To cover a broader range of mathematical discussions based on the QW model, a phase angle ξ is introduces to the real-valued matrix in eq. (4). As a result, U is replaced by a complex-valued matrix $U(\xi) = \exp(\xi)U$.

The value of χ / J may be fixed to 1 for simplicity, indicating that the DP-phonon interaction energy is equal to the DP hopping energy. However, to cover a broader range of physical discussions, the present paper employs a wider range of values, i.e., $0.1 \le \chi / J \le 10$.

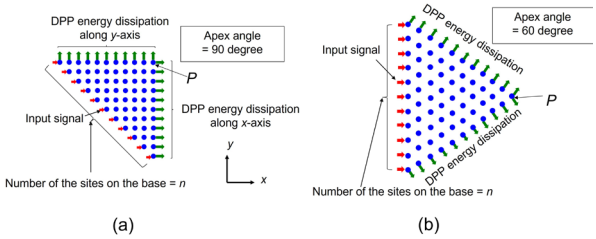

Fig.3 Two-dimensional triangular lattices.
(a) A right-angled isosceles triangle (RIT).
(b)An equilateral triangle (ET).

4. Results and discussion

After the input signals are applied, the value of P increases with time. Preliminary numerical calculations confirmed that the value of P converges to a stationary value within a shorter time compared with a perfect graph, which is advantageous for reducing the computation time and for comparing with experimental results. This section discusses the stationary value of P.

4.1 Dependence on parameters

For comparison with the experimental results derived by using the fiber probes of Figs. 1(a) and (b), this section calculates the value of P without and with DPP energy dissipation, respectively, at the slope of the RIT lattice.

[Case 1: Without DPP energy dissipation]

Figure 4(a) shows the calculated dependence of P on ξ and χ / J (number of the sites on the base of the RIT lattice n=61). Figure 4(b) shows the dependence of P on ξ at χ / J=1 in Fig. 4(a). A lot of bumps are seen on the curve in this figure, which are attributed to interference in the RIT lattice, originating from the reflection at the slope. This curve is symmetrical about ξ=90 degree. Furthermore, the value of P in this figure takes the maximum $P_{\max}$ at ξ =67.5 degree (=(3/8)π). Figure 5 shows the dependence of $P_{\max}$ on n. This figure shows that $P_{\max}$ asymptotically approaches a constant value of 3×10^{-1} as n increases, from which it was confirmed that sufficiently high accuracy

of approximation for numerical calculation was obtained when $n \geq 51$.

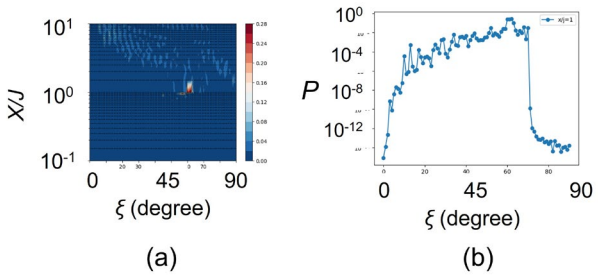

Fig. 4 The value of P in the case without DPP energy dissipation (n=61).
(a) Dependence on ξ and χ / J. (b) Dependence on ξ at χ / J=1 in (a).

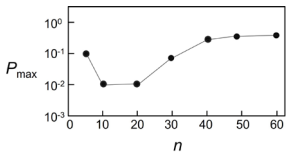

Fig. 5 Dependence of $P_{\max}$ on n in Fig. 4(b).

[Case 2: With DPP energy dissipation]

Figure 6(a) shows the calculated dependence of P on ξ and χ / J (n=61). Crescent-shaped red belts are seen in this figure, in which the value of P is very large in comparison with those outside the belts. The values of P show irregular variations and abrupt increases in the red belts and at their rim. Since these red belts are in the area $\chi / J > 1$, the value of P at χ / J=1 does not suffer any effects from the red belt.

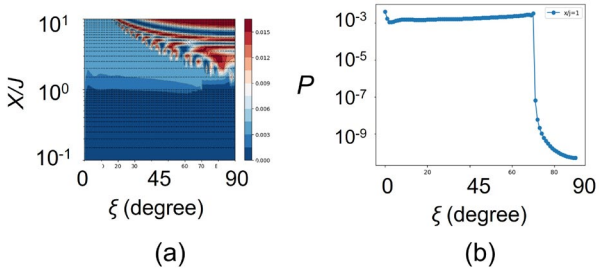

Fig. 6 The value of P in the case with DPP energy dissipation (n=61).
(a) Dependence on ξ and χ / J. (b) Dependence on ξ at χ / J=1 in (a).

Figure 6(b) shows the dependence of P on ξ at χ / J =1 in Fig. 6(a). No bump on the curve is seen in this figure, which indicates that no interference takes place in the RIT lattice. This curve is symmetrical about ξ=90 degree, as was the case of Fig. 6(b). Furthermore, the value of P in this figure takes the maximum $P_{\max}$ at ξ=67.5 degree (=(3/8)π). The value of $P_{\max}$ asymptotically approaches a constant value as n increases, from which it was confirmed that sufficiently high accuracy of approximation for numerical calculation was obtained when $n \geq 51$, as in the Case 1 above. The value of $P_{\max}$ was 3×10^{-3} for $n \geq$ 51, which is 10^{-2} times that in Fig. 5. This indicates that it is effective to suppress the DPP energy dissipation (Case 1) at the slope of the RIT lattice to increase the probability of DPP creation. This indication is in agreement with experimental results in which the taper of a fiber probe is coated with an opaque metallic film to suppress the dissipation and to increase the DPP creation efficiency at the tip of the fiber probe (Fig. 1(a)).

4.2. Dependence on the apex angle of a fiber probe

This section calculates the probability P at the apex of an equilateral triangular (ET) lattice. For reference, experimental studies have found that the value of P was smaller for smaller apex angles [9]. Unlike the 90 degree apex angle of the RIT lattice in Section 4.1, this section deals with a triangular lattice with a smaller apex angle, i.e., an ET lattice (the apex angle of 60 degrees), as an example, as is shown by Fig. 2(b). In the RIT lattice (Fig. 2(a)), each site has four nearest neighbor sites located along the $\pm x$- and $\pm y$- axes. This means that the DPP energy transfers from/to these four sites. In contrast, each site in the ET lattice (Fig. 2(b)) has six nearest-neighbor sites located along the directions of $e^{\pm i\pi/6}$ x-, $e^{\pm i5\pi/6}$ x-, and $\pm y$-axes. The DPP energy transfers from/to these six axes. By noting the number of these nearest-neighbor sites, the tempo-spatial evolution equation for the ET lattice was derived by modifying that for the RIT lattice, and the values of P was calculated for the case without and with DPP energy dissipation.

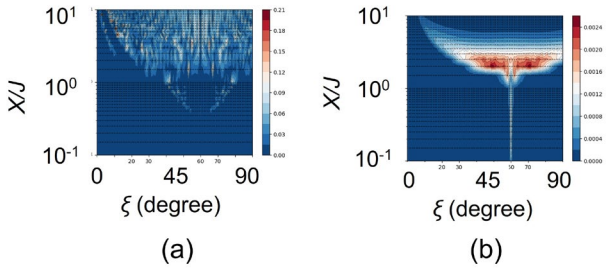

Fig. 7 Dependence of P on ξ and χ / J (n=51).
(a) and (b) are in the cases without and with DPP energy dissipation, respectively.

Figures 7(a) and (b) show the calculated dependence of P on ξ and χ / J without and with DPP energy dissipation, respectively (n=51). In Fig. 7(b), the red belt is seen, as was the case in Fig. 6(a). Since this belt is in the area $\chi / J > 1$, the value of P at χ / J=1 does not suffer

any effects from this belt. Several results were derived from Figs. 7(a) and (b), that are consistent with those of the RIT lattice. They are:

(a) The value of $P_{\max}$ asymptotically approaches a constant value as n increases, from which it was confirmed that sufficiently high accuracy of approximation for numerical calculation was obtained when $n \geq 51$.

(b) The value of $P_{\max}$ of Fig. 7(a) was 1×10^{-2} for $n \geq 51$, which is 10 times that with DPP energy conversion (Fig. 7(b): 1×10^{-3}) This indicates that it is effective to suppress DPP energy dissipation at the slope of the ET lattice to increase the value of P, as was described in Section 4.1. This indication is in agreement with the experimental results.

Table 1 summarizes the calculated values of $P_{\max}$ for χ / J =1. This table shows that the value without DPP energy dissipation is larger than that with DPP energy dissipation, which is in agreement with experimental results. Furthermore, the value is larger for the RIT lattice (an apex angle of 90 degree) than that for the ET lattice (an apex angle of 60 degree), which is also in agreement with experimental results [9].

Table 1. Calculated values of $P_{\max}$

	RIT	ET
Without DPP energy dissipation	3×10^{-1}	1×10^{-2}
With DPP energy dissipation	3×10^{-3}	1×10^{-3}

5. Summary

This paper reported the results of numerical calculation on the dressed photon (DP) energy transfer based on a quantum walk model. In order to compere with the experimental results on DP creation, the fiber probe was approximated by a two-dimensional right-angled isosceles triangular (RIT) lattice and an equilateral triangular (ET) lattice. The sufficiently high accuracy of approximation was obtained when the number of the lattice is larger than 51. The probability of DP creation without DPP energy dissipation was larger than that with DPP energy dissipation, which is in agreement with experimental results. The probability at the apex of the RIT lattice was higher than that of the ET lattice, which was also in agreement with experimental results.

Acknowledgements

The authors express thanks to Prof. S. Saito (Kogakuin Univ.) and Dr. S. Sangu (Ricoh Co. Ltd.) for their supports on numerical calculations.

References

[1] M. Ohtsu, *Off-Shell Applications In Nanophotonics*, Elsevier, Amsterdam (2021).

[2] M. Ohtsu, I. Ojima, and H. Sakuma, "Dressed photon as an off-Shell quantum Field," *Progress in Optics*, ed.by T. D. Visser, Elsevier, Amsterdam, vol.64, pp.45-97., 2019.

[3] H. Sakuma and I. Ojima, "On the dressed photon constant and its implication for a novel perspective on cosmology," *Symmetry*, vol.13, pp.593-611, 2021. https://doi.org/10.3390/sym13040593

[4] Y. Tanaka and K. Kobayashi, "Spatial localization of an optical near field in one-dimensional nanomaterial system," *Physica*, vol. E40, pp.297-300, 2007.

[5] M. Naruse, K. Leibnitz, F. Peper, N. Tate, W. Nomura, T. Kawazoe, M. Murata, and M. Ohtsu, "Autonomy in excitation transfer via optical near-field interactions and its implications for information networking," *Nano Communication Networks*, vol.2, pp.189-195, 2011.

[6] Y. Higuchi, and E. Segawa, "Dynamical system induced by quantum walks," *J. Phys A: Mathematical and Theoretical*, vol.52, 395202, 2009.

[7] N. Konno, E. Segawa, and M. Martin Štefa ˇnák, "Relation between quantum walks with tails and quantum walks with sinks on finite graphs," *Symmetry*, vol.13, pp.1169-1189, 2021. https://doi.org/10.3390/sym13071169

[8] K. Higuchi, T. Komatsu, N. Konno, H. Morioka, and E. Segawa, "A discontinuity of the energy of quantum walk in impurities," *Symmetry*, vol.13, pp.1134-1148, 2021. https://doi.org/10.3390/sym13071134

[9] M. Ohtsu, *Near-Field Nano/Atom Optics and Technology*, Springer, Tokyo/Berlin, pp.71-87, 1998.

2022 International Symposium on Nonlinear Theory and Its Applications,
NOLTA2022, Virtual, December 12-15, 2022

On the Schroedinger picture in C*-algebraic quantum theory

Kazuya Okamura† ‡

†Research Origin for Dressed Photon, 3-13-19 Moriya-cho Kanagawa-ku, Yokohama, 221-0022, Japan
‡Graduate School of Informatics, Nagoya University, Furo-cho, Chikusa-ku, Nagoya 464-8601, Japan
Email: k.okamura.renormalizable@gmail.com

Abstract—We discuss state transitions in C*-algebraic quantum theory and reconsider state changes, usually called the Schrödinger picture in quantum theory. We introduce C*-probability structure and transition probability in C*-algebraic quantum theory. By using them, we define category of state transitions. Next, we explain the historical background of this work related to quantum measurement theory.

1. Introduction

We discuss state transitions in C*-algebraic quantum theory. We define the concept of transition probability in C*-algebraic quantum theory and explain the historical background of this work. The motivation for this paper is twofold. One is to reconsider state changes in C*-algebraic quantum theory, usually called the Schrödinger picture in quantum theory. The other is to connect it with the categorical framework. To achieve these purposes, we introduce the concept of C*-probability structure. In the historical background, we mention quantum measurement theory.

C*-algebraic quantum theory is suitable for the description of quantum systems with infinite degrees of freedom including quantum fields. In quantum systems with infinite degrees of freedom, the nontrivial sector structure emerges, which distinguishes the macroscopic aspect of the system. A C*-probability structure describes the probabilistic nature of the system and specifies sectors involved in the family of situations under consideration. Transition probability is introduced in order to describe the transition between C*-probability structures. In the context of quantum measurement theory, the concept of instrument describes the transition between C*-probability structures and has the axiomatic characterization from the statistical point of view. Typical, nontrivial examples of transition probability are given by the measurement of discrete observables. By contrast, the introduction of instrument is motivated by the operationally valid treatment of the measurement of continuous observables. This is the reason why we actively treat quantum measurement theory.

ORCID iDs Kazuya Okamura: 0000-0001-9223-5920

2. C*-algebraic quantum theory and transition probability

2.1. C*-algebraic quantum theory

Axiom 1 (C*-probability space [1])**.** *All the statistical aspects of a physical system* **S** *are registered in a C*-probablity space* $(\mathcal{X}, \omega)$*, where* $\mathcal{X}$ *is a C*-algebra and* ω *is a state on* $\mathcal{X}$*. Observables of* **S** *are described by self-adjoint elements of the C*-algebra* $\mathcal{X}$*. On the other hand, the state* ω *on* $\mathcal{X}$ *statistically correponds to a physical situation (or an experimental setting) of* **S***.*

This axiom declares that we describe a quantum system in the language of noncommutative (quantum) probability theory (see [2] for noncommutative probability theory, and [3, 4] for operator algebras).

For every C*-algebra $\mathcal{X}$, $\mathcal{S}_{\mathcal{X}}$ denotes the state space of $\mathcal{X}$. We use the weak* topology for the dual space $\mathcal{X}^*$ of $\mathcal{X}$. In the weak* topology, the neighboorhoods of $\omega \in \mathcal{X}^*$ are indexed by finite sets of elements $X_1, \cdots, X_n$ of $\mathcal{X}$, and $\varepsilon > 0$: $U_\omega(X_1, \cdots, X_n, \varepsilon) = \{\varphi \in \mathcal{X}^* \mid |\varphi(X_j) - \omega(X_j)| < \varepsilon,\ j = 1, \cdots, n\}$. The weak* topology for $\mathcal{S}_{\mathcal{X}}$ is the restriction of that for $\mathcal{X}^*$ to $\mathcal{S}_{\mathcal{X}}$. We adopt the Borel structure of $\mathcal{S}_{\mathcal{X}}$ generated by open sets in the weak* topology. $\mathcal{B}(\mathcal{S}_{\mathcal{X}})$ denotes the Borel sets of $\mathcal{S}_{\mathcal{X}}$.

The second dual $\mathcal{X}^{**} := (\mathcal{X}^*)^*$ of $\mathcal{X}$ is a W^*-algebra, a C*-algebra which is a dual space of a Banach space. The isometric embedding $\hat{\cdot}$ of $\mathcal{X}$ into $\mathcal{X}^{**}$ is defined by $\langle \hat{X}, \rho \rangle = \rho(X)$ for all $\rho \in \mathcal{X}^*$. The following axiom is usually assumed.

Axiom 2 (Born statistical formula)**.** *When an observable* A *of* $\mathcal{X}$ *is precisely measured in a state* ω*, the probability* $\Pr\{A \in \Delta \| \omega\}$ *that the spectrum of* A *belonging to* Δ *emerge is given by* $\Pr\{A \in \Delta \| \omega\} = \langle E^{\hat{A}}(\Delta), \omega \rangle$.

2.2. C*-probability structure

Let $\mathcal{X}$ be a C*-algebra and $(\pi, \mathcal{H})$ a representation of $\mathcal{X}$. $\boldsymbol{B}(\mathcal{H})$ denotes the set of bounded linear operators on $\mathcal{H}$. A linear functional ω on $\mathcal{X}$ is said to be π-normal if there exists a trace-class operator ρ on $\mathcal{H}$ such that $\omega(X) = \mathrm{Tr}[\pi(X)\rho]$ for all $X \in \mathcal{X}$. $V(\pi)$ denotes the set of π-normal linear functionals on $\mathcal{X}$. Let $\mathcal{M}$ be a von Neumann algebra on a Hilbert space $\mathcal{K}$. $\mathcal{Z}(\mathcal{M})$ denotes the center of $\mathcal{M}$. $\mathcal{M}_*$ denotes the set of ultraweakly continuous linear functionals on $\mathcal{M}$.

A linear subspace $\mathcal{V}$ of $\mathcal{X}^*$ is said to be central if there exists a central projection C of $\mathcal{X}^{**}$, i.e., $C \in \mathcal{Z}(\mathcal{X}^{**})$, such that $\mathcal{V} = C\mathcal{X}^*$ [5]. The dual space $\mathcal{V}^*$ of a central subspace $\mathcal{V}(= C\mathcal{X}^*)$ is a W^*-algebra (isomorphic to $C\mathcal{X}^{**}$). A central subspace is said to be σ-finite if its dual is σ-finite.

Example 1 (See [4, Chapter III] for example)**.** (1) *Let $\mathcal{X}$ be a C^*-algebra and $(\pi, \mathcal{H})$ a representation of $\mathcal{X}$. There exists a central projection $C(\pi)$ of $\mathcal{X}^{**}$ such that*

$$V(\pi) = C(\pi)\mathcal{X}^* = \{C(\pi)\varphi \mid \varphi \in \mathcal{X}^*\} = \{\varphi \in \mathcal{X}^* \mid C(\pi)\varphi = \varphi\}. \tag{1}$$

(2) *Let $\mathcal{M}$ be a von Neumann algebra on a Hilbert space $\mathcal{H}$. There exists a central projection C of $\mathcal{M}^{**}$ such that $\mathcal{M}_* = C\mathcal{M}^*$. In particular, $\boldsymbol{B}(\mathcal{H})_*$ is a central subspace of $\boldsymbol{B}(\mathcal{H})^*$.*

Definition 1 (C^*-probability structure)**.** *$a = (\mathcal{X}_a, \mathcal{V}_a)$ is called a C^*-probability structure if it is the pair of a C^*-algebra $\mathcal{X}_a$ and a central subspace $\mathcal{V}_a$ of $\mathcal{X}_a^*$.* **C^*-PS** *denotes the class of C^*-probability structures. For each $a = (\mathcal{X}_a, \mathcal{V}_a) \in$* **$C^*$-PS***, we put $\mathcal{S}_a = \mathcal{S}_{\mathcal{X}_a} \cap \mathcal{V}_a$.*

Here we adopt the next axiom, a sequel to Axiom 1.

Axiom 3. *A quantum system in physical situations (or experimental settings) contained in a fixed category is statistically specified by a C^*-probability structure.*

2.3. Definition

We shall define the concept of transition probability by using C^*-probability structure.

Definition 2 (Transition probability)**.** *Let $a, b \in$* **C^*-PS***. A map $P(\cdot \leftarrow \cdot) : \mathcal{B}(\mathcal{S}_{\mathcal{X}_b}) \times \mathcal{S}_a \to [0, 1]$ is called a transition probability for (a, b) if it satisfies the following two conditions:*
(1) *For every $\omega \in \mathcal{S}_a$, $P(\cdot \leftarrow \omega)$ is a probability measure on $\mathcal{S}_{\mathcal{X}_b}$.*
(2) *For any pair $\omega \in \mathcal{S}_a$ and $\Delta \in \mathcal{B}(\mathcal{S}_{\mathcal{X}_b})$ such that $P(\Delta \leftarrow \omega) \neq 0$, $\omega_{(P,\Delta)} \in \mathcal{S}_b$, where, for any pair $\omega \in \mathcal{S}_a$ and $\Delta \in \mathcal{B}(\mathcal{S}_{\mathcal{X}_b})$ such that $P(\Delta \leftarrow \omega) \neq 0$, we define a state $\omega_{(P,\Delta)}$ on $\mathcal{X}_b$ by*

$$\omega_{(P,\Delta)}(X) = \int_\Delta \rho(X)\, \frac{dP(\rho \leftarrow \omega)}{P(\Delta \leftarrow \omega)}, \qquad X \in \mathcal{X}_b. \tag{2}$$

When $a = b$, a transition probability for (a, b) is also called a transition probability for a for simplicity. For every one element set $\{\varphi\}$, $P(\{\varphi\} \leftarrow \omega)$ is denoted by $P(\varphi \leftarrow \omega)$.

Example 2 (Deterministic transition)**.** (1) *Let $a_\mathcal{X} = (\mathcal{X}, \mathcal{X}^*) \in$* **$C^*$-PS** *and α be a *-automorphism of $\mathcal{X}$. A transition probability $P^{(\alpha)}$ for $a_\mathcal{X}$ is defined by $P^{(\alpha)}(\Delta \leftarrow \omega) = \delta_{\omega\circ\alpha}(\Delta)$.*
(2) *Let $a, b \in$* **C^*-PS***, and $T : \mathcal{V}_a \to \mathcal{V}_b$ a unital positive linear map. A transition probability $P^{(T)}$ for (a, b) is defined by $P^{(T)}(\Delta \leftarrow \omega) = \delta_{T\omega}(\Delta)$ for all $\omega \in \mathcal{S}_a$ and $\Delta \in \mathcal{B}(\mathcal{S}_{\mathcal{X}_b})$.*

2.4. Composition of transition probabilities

Definition 3. *A transition probability P for (a, b) is said to be discrete if, for every $\omega \in \mathcal{S}_a$, $P(\cdot \leftarrow \omega)$ is a discrete probability measure on $\mathcal{S}_{\mathcal{X}_b}$.*

Definition 4 (Composition)**.** *Let $a, b, c \in$* **C^*-PS***, and Q and P be transition probabilities for (b, c) and (a, b), respectively. Suppose that P is discrete. The product $Q * P$ of Q and P is defined as follows: for every $\omega \in \mathcal{S}_a$,*

$$(Q * P)(\Gamma \times \Delta|\omega) = \sum_{\rho \in \Delta \cap S_{P,\omega}} Q(\Gamma \leftarrow \rho)\, P(\rho \leftarrow \omega) \tag{3}$$

for all $\Gamma \in \mathcal{B}(\mathcal{S}_{\mathcal{X}_c})$ and $\Delta \in \mathcal{B}(\mathcal{S}_{\mathcal{X}_b})$.

To extend the product into the case where P is not discrete, we use Riesz-Markov-Kakutani theorem stating the one-to-one correspondence between probability measures on a compact Hausdorff space S and states on the set $C(S)$ of continuous functions on S.

Definition 5 (Composition; continued)**.** *Let $a, b, c \in$* **C^*-PS***, and Q and P be transition probabilities for (b, c) and (a, b), respectively. Q and P are composable if the following two conditions hold:*
(1) *For every $\omega \in \mathcal{S}_a$ and net $\{P_\alpha\}_{\alpha\in A}$ of discrete transition probabilities for (a, b) convergent to P, the net $\{Q * P_\alpha(\cdot|\omega)\}_{\alpha\in A}$ of states on $C(\mathcal{S}_{\mathcal{X}_c} \times \mathcal{S}_{\mathcal{X}_b})$ weakly converges to a state on $C(\mathcal{S}_{\mathcal{X}_c} \times \mathcal{S}_{\mathcal{X}_b})$.*
(2) *For every $\omega \in \mathcal{S}_a$, the limit of the net $\{Q * P_\alpha(\cdot|\omega)\}_{\alpha\in A}$ is independent of the choice of the net $\{P_\alpha\}_{\alpha\in A}$ of discrete transition probabilities for (a, b) convergent to P. Then the limit is denoted by $Q * P$.*

When Q and P are composable, we define a transition probability $Q \triangleleft P$ for (a, c), called the composition of Q and P, by $(Q \triangleleft P)(\Gamma \leftarrow \omega) = (Q * P)(\Gamma \times \mathcal{S}_{\mathcal{X}_b}|\omega)$ for all $\omega \in \mathcal{S}_a$ and $\Gamma \in \mathcal{B}(\mathcal{S}_{\mathcal{X}_c})$.

We use this composition to define category of state transitions: Objects and arrows are C^*-probability structures and transition probabilities, respectively. The latter must satisfy the associative law of the composition of transition probabilities.

Definition 6 (Category of state transitions)**.** *C is a category of state transitions if it has*

Objects *C^*-probability structures $a = (\mathcal{X}_a, \mathcal{V}_a)$, and*

Arrows *$b \leftarrow a : f$ with transition probability P_f for (a, b). For every object a, the identity arrow $a \leftarrow a : 1_a$ of a has a transition probability P_{1_a} for a such that $P_{1_a}(\Delta \leftarrow \omega) = \delta_\omega(\Delta)$ for all $\omega \in \mathcal{S}_a$ and $\Delta \in \mathcal{B}(\mathcal{S}_{\mathcal{X}_a})$.*

The composition of arrows involves that of transition probabilities and satisfies the associative law.

3. Historical remarks and instrument

We assume that $\mathcal{H}$ is a separable Hilbert space. We do not distinguish density operators ρ on $\mathcal{H}$ and normal states $\tilde{\rho}$ on $\boldsymbol{B}(\mathcal{H})$ via the isomorphism $\tilde{\cdot} : \boldsymbol{T}(\mathcal{H}) \to \boldsymbol{B}(\mathcal{H})_*$ such that $\tilde{\rho}(X) = \mathrm{Tr}[\rho X]$ for all $X \in \boldsymbol{B}(\mathcal{H})$. We put $a_{\mathcal{H}} = (\boldsymbol{B}(\mathcal{H}), \boldsymbol{T}(\mathcal{H}))$. By using transition probabilities, state transitions by the measurement of discrete observables in the traditional context are given by the following axiom.

Postulate 1. *Let $A = \sum_{a\in\mathbb{R}} aE^A(\{a\})$ be a discrete observable of $\boldsymbol{B}(\mathcal{H})$ to be measured. When a density operator ρ is prepared, the state $\rho_{\{A=a\}}$ after the measurement is uniquely determined for each $a \in Sp(A;\rho) = \{a \in \mathbb{R} \mid \mathrm{Tr}[E^A(\{a\})\rho] > 0\}$, and the transition probability* Pr *for $a_{\mathcal{H}}$ is given by*

$$\Pr(\Delta \leftarrow \rho) = \sum_{a\in Sp(A;\rho)} \mathrm{Tr}[E^A(\{a\})\rho]\delta_{\rho_{\{A=a\}}}(\Delta). \tag{4}$$

In particular, for every $a \in Sp(A;\rho)$,

$$\Pr(\rho_{\{A=a\}} \leftarrow \rho) = \mathrm{Tr}[E^A(\{a\})\rho]. \tag{5}$$

Postulate 2 (von Neumann-Lüders projection postulate)**.** *For each $a \in Sp(A;\rho)$, $\rho_{\{A=a\}}$ in Postulate 1 is given by*

$$\rho_{\{A=a\}} = \frac{E^A(\{a\})\rho E^A(\{a\})}{\mathrm{Tr}[E^A(\{a\})\rho]}. \tag{6}$$

J. von Neumann [6] considered this postulate only for non-degenerate observables, and Lüders [7] generalized it for the degenerate case. Dirac's transition probability [8] motivated the above postulates. Under the above postulates, we have the following lemma.

Lemma 1. *When ρ is a prepared state and values of A not contained in Δ are ignored, the state $\rho_{\{A\in\Delta\}}$ after the measurement of A is given by*

$$\frac{\sum_{a\in\Delta} E^A(\{a\})\rho E^A(\{a\})}{\mathrm{Tr}[\rho E^A(\Delta)]} = \frac{\left(\sum_{a\in\mathbb{R}} E^A(\{a\})\rho E^A(\{a\})\right)\cdot E^A(\Delta)}{\mathrm{Tr}[\rho E^A(\Delta)]}.$$

For nondegenerate discrete observables, von Neumann [6] derived Postulate 2 from

Postulate 3 (Repeatability hypothesis [6, 9])**.** *If an observable A is measured twice in succesion in the object system, then we get the same value each time.*

From Postulates 1 and 3, we have $\mathrm{Tr}[E^A(\{b\})\rho_{\{A=a\}}] = \delta_{ab}$ for all $a \in Sp(A;\rho)$ and $b \in \mathbb{R}$. Under Postulate 1, Postulate 2 implies Postulate 3.

Nakamura and Umegaki [10] pointed out that the map

$$\mathcal{E}_A : \boldsymbol{B}(\mathcal{H}) \ni X \mapsto \sum_{a\in\mathbb{R}} E^A(\{a\})XE^A(\{a\}) \in \{A\}' \tag{7}$$

is nothing but the conditional expectation of $\boldsymbol{B}(\mathcal{H})$ onto the von Neumann algebra $\{A\}' = \{B \in \boldsymbol{B}(\mathcal{H}) \mid AB = BA\}$, and conjectured that the same argument holds for continuous observables. Arveson [11] proved that their conjecture does not hold. Following those investigations, Davies and Lewis [12] introduced the notion of instrument which describes general state changes caused by the measurement in order to formulate measurement theory *not* based on the repeatability hypothesis (Postulate 3).

Let $\mathcal{V}_1$ and $\mathcal{V}_2$ be central subspaces of the dual spaces of C*-algebras $\mathcal{X}_1$ and $\mathcal{X}_2$, respectively. $P(\mathcal{V}_1, \mathcal{V}_2)$ denotes the set of positive linear maps of $\mathcal{V}_1$ into $\mathcal{V}_2$. Also, $\langle\cdot,\cdot\rangle$ denotes the pairing of $\mathcal{V}_1^*$ and $\mathcal{V}_1$.

Definition 7 (instrument)**.** *Let $a, b \in$ **C*-PS** and $(S, \mathcal{F})$ a measurable space. $\mathcal{I}$ is called an instrument for (a, b, S) if it satisfies the following three conditions:*
(1) *$\mathcal{I}$ is a map of $\mathcal{F}$ into $P(\mathcal{V}_a, \mathcal{V}_b)$.*
(2) *$\langle 1, \mathcal{I}(S)\rho\rangle = \langle 1, \rho\rangle$ for all $\rho \in \mathcal{V}_a$.*
(3) *For every $\rho \in \mathcal{V}_a$, $M \in \mathcal{V}_b^*$ and mutually disjoint sequence $\{\Delta_j\}_{j\in\mathbb{N}}$ of $\mathcal{F}$, $\langle M, \mathcal{I}(\cup_j\Delta_j)\rho\rangle = \sum_{j=1}^{\infty}\langle M, \mathcal{I}(\Delta_j)\rho\rangle$.*
An instrument $\mathcal{I}$ for (a, b, S) is said to be completely positive (CP) if $\mathcal{I}(\Delta)$ is completely positive for all $\Delta \in \mathcal{F}$.

Davies and Lewis [12] defined instrument more abstractly. Their definition uses "state space" and includes our definition in some sense. However, we cannot reach our definition from their one without the understanding for sector theory [13, 14]. The theory of CP instrument was developed in [15, 16] in the von Neumann algebraic setting. The theory in the setting of the paper is a future task.

We shall define category of instruments. As defined below, instruments become arrows in the category.

Definition 8 (Category of instruments)**.** *C is a category of state transitions if it has*

Objects *C*-probability structures $a = (\mathcal{X}_a, \mathcal{V}_a)$, and*

Arrows *$b \leftarrow a : \mathcal{I}$ is an instrument $\mathcal{I}$ for $(a, b, \mathbb{R}^d)$, where $d = 0, 1, 2, \cdots$.*

The composition of arrows is given by the product of instruments (see [12] for the definition of the product).

4. Central instrument

In the C*-algebraic setting, there exists a nontrivial example of instrument, called a central instrument. It gives the simultaneous central decomposition of states belonging to the given central subspace. Thus the unification of sector theory and quantum measurement theory is achieved by the use of central instruments.

Let $a \in$ **C*-PS**, $(S, \mathcal{F})$ be a measurable space, and $C : \mathcal{F} \to \mathcal{Z}(\mathcal{V}_a^*)$ a projection valued measure (PVM). For every $M_1, M_2 \in \mathcal{V}_a^*$ and $\rho \in \mathcal{V}_a$, we define $M_1\rho M_2 \in \mathcal{V}_a$ by $\langle M, M_1\rho M_2\rangle = \langle M_2 M M_1, \rho\rangle$ for all $M \in \mathcal{V}_a^*$. An instrument $\mathcal{I}_C$ for (a, S) is defined by $\mathcal{I}_C(\Delta)\rho = C(\Delta)\rho$ for all $\rho \in \mathcal{V}_a$ and $\Delta \in \mathcal{F}$.

Theorem 2 ([5, Theorem 10]). *$\mathcal{I} = \mathcal{I}_C$ defined above satisfies the following conditions:*
(1) *$\mathcal{I}(S)\rho = \rho$ for all $\rho \in \mathcal{V}_a$.*
(2) *It is repeatable, i.e., it satisfies $\mathcal{I}(\Delta)\mathcal{I}(\Gamma) = \mathcal{I}(\Delta \cap \Gamma)$ for all $\Delta, \Gamma \in \mathcal{F}$.*
(3) *For every $\rho \in \mathcal{S}_a$ and $\Delta \in \mathcal{F}$, $\mathcal{I}(\Delta)\rho$ and $\mathcal{I}(\Delta^c)\rho$ are mutually disjoint.*
(4) *For every $\Delta \in \mathcal{F}$, $\mathcal{I}(\Delta)$ is $\mathcal{V}_a^*$-bimodule map, i.e., for every $\Delta \in \mathcal{F}$, $\rho \in \mathcal{V}_a$ and $M_1, M_2 \in \mathcal{V}_a^*$,*

$$\mathcal{I}(\Delta)(M_1\rho M_2) = M_1(\mathcal{I}(\Delta)\rho)M_2. \tag{8}$$

Conversely, if an instrument $\mathcal{I}$ for (a, S) satisfies the conditions (2) *and* (4)*, then there exists a spectral measure $C : \mathcal{F} \to \mathcal{Z}(\mathcal{V}_a^*)$ such that $\mathcal{I} = \mathcal{I}_C$.*

An instrument $\mathcal{I}$ for (a, S) is said to be subcentral if it satisfies the conditions (2) and (4) in Theorem 2. An instrument $\mathcal{I}$ for (a, S) is said to be central if it is the maximum in the set of subcentral instruments defined on a, where the maximum is due to the preorder $\prec$ on instruments defined as follows: For instruments $\mathcal{I}_1$, $\mathcal{I}_2$ for (a, S_1) and (a, S_2), respectively, $\mathcal{I}_1 \prec \mathcal{I}_2$ if $\mathcal{I}_1(\mathcal{F}_1) \subset \mathcal{I}_2(\mathcal{F}_2)$ for all $\rho \in \mathcal{S}_a$, where $\mathcal{I}_i(\mathcal{F}_i)$, $i = 1, 2$, is the subset of $\mathcal{P}(\mathcal{V}_a, \mathcal{V}_a)$ defined by $\mathcal{I}_i(\mathcal{F}_i) = \{\mathcal{I}_i(\Delta_i) \mid \Delta_i \in \mathcal{F}_i\}$.

Theorem 3 ([5, Theorem 11]). *$\mathcal{I}_C$ is central if and only if the abelian von Neumann algebra generated by $\{C(\Delta) \mid \Delta \in \mathcal{F}\}$ is isomorphic to $\mathcal{Z}(\mathcal{V}_a^*)$.*

5. Discussion and perspective

The content of the paper can be summarized as the following axiom.

Axiom 4. *A quantum system is specified by a category; its objects are C^*-probability structures and its arrows describe transitions between them. Category of state transitions and that of instruments are such examples.*

The paper [17] by Saigo et al. motivates this work and suggests further development. For example, we do not treat the composite system related to the complete positivity of instrument in the paper yet. The concept of transition probability has room for development. We believe that it is important to establish the formulation of category of state transitions applicable to quantum field theory in the future.

References

[1] I. Ojima, K. Okamura & H. Saigo, "Derivation of Born Rule from Algebraic and Statistical Axioms," *Open Sys. Inform. Dyn.* **21** (2014), 1450005.

[2] A. Hora & N. Obata, *Quantum probability and spectral analysis of graphs*, (Springer, Berlin, 2007).

[3] O. Bratteli & D.W. Robinson, *Operator Algebras and Quantum Statistical Mechanics* Vol.1 (2nd printing of 2nd ed.), (Springer, 2002).

[4] M. Takesaki, *Theory of Operator Algebras I*, (Springer, Berlin, 1979).

[5] K. Okamura, "Towards a Measurement Theory for Off-Shell Quantum Fields," *Symmetry* **13**, (2021) 1183.

[6] J. von Neumann, *Mathematische Grundlagen der Quantenmechanik*, (Springer, Berlin, 1932); *Mathematical Foundations of Quantum Mechanics*, (Princeton UP, Princeton, 1955).

[7] G. Lüders, "Über die Zustandsänderung durch den Meßprozeß," *Ann. Phys. (Leipzig)* **8** (1951), 322–328.

[8] P.A.M. Dirac, *The Principles of Quantum Mechanics*, Fourth Edition, (Oxford UP, Oxford, 1958).

[9] M. Ozawa, "Heisenberg's original derivation of the uncertainty principle and its universally valid reformulations," *Current Science* **109**, 2006–2016, (2015).

[10] M. Nakamura & H. Umegaki, "On von Neumann's theory of measurements in quantum statistics," *Math. Japon.* **7** (1962), 151–157.

[11] W. Arveson, "Analyticity in operator algebras," *Amer. J. Math.* **89** (1967), 578–642.

[12] E.B. Davies & J.T. Lewis, "An operational approach to quantum probability," *Commun. Math. Phys.* **17** (1970), 239–260.

[13] I. Ojima, "A unified scheme for generalized sectors based on selection criteria –Order parameters of symmetries and of thermality and physical meanings of adjunctions–," *Open Sys. Inform. Dyn.* **10** (2003), 235–279.

[14] I. Ojima, "Micro-Macro Duality in Quantum Physics,"pp.143–161 in *Proc. Intern. Conf. on Stochastic Analysis, Classical and Quantum*, (World Scientific, 2005), arXiv:math-ph/0502038.

[15] M. Ozawa, "Quantum measuring processes of continuous obsevables," *J. Math. Phys.* **25** (1984), 79–87.

[16] K. Okamura & M. Ozawa, "Measurement theory in local quantum physics," *J. Math. Phys.* **57** (2016), 015209.

[17] H. Saigo, M. Naruse, K. Okamura, H. Hori & I. Ojima, "Analysis of Soft Robotics Based on the Concept of Category of Mobility," *Complexity* **2019** (2019), 1490541.

Off-shell Science for Dressed Photons

M. Ohtsu
Research Origin for Dressed Photon
3-13-19 Moriya-cho, Kanagawa-ku, Yokohama, Kanagawa 221-0022 Japan
E-mail 1 : ohtsu@rodrep.or.jp
E-mail 2 : ohtsu@nanophotonics.t.u-tokyo.ac.jp

Abstract: Based on a Clebsch dual field theoretical model, it is made clear that a dressed photon (DP) originates from a transition of the spacelike momentum of the Majorana field to a timelike one. This model derives a maximum size of the DP that has already been found by experimental studies. It is pointed out that, in the case where the timelike Majorana particle and anti-particle have anti-parallel spins, the pair annihilation creates a DP with a spin 0. The light converted from this DP can be a unique light field with spin 0, which behaves as a particle. It is experimentally confirmed that a cluster of photons emitted from an Si-LED behaves as such a particle.

1. Introduction

Dressed photon (DP) is a quantum field created as the result of the light–matter interaction that is induced by irradiating a nanometer-sized particle with light [1,2]. Thus, an interacting quantum field must be studied for constructing a theorical model for the DP. However, the existence of a nontrivial interacting quantum field model defined on a four-dimensional Minkowski spacetime has not yet been proven. Axiomatic approaches to quantum field theories have derived many fundamental theorems, including the Haag theorem [3,4]. It is a no-go theorem, implying that an "interaction picture exists only if there is no interaction" [5,6]. To put it roughly, we cannot go beyond the theories for free fields if we stick to the axioms for conventional quantum field theories. Intensive discussions on the theoretical methods based on classical Clebsch dual (CD) fields have been made in order to go beyond free fields, and a mechanism of DP creation has been made clear recently. These discussions have also succeeded in describing several experimental results by quantizing the DP energy [7].

2. Off-shell science theories for dealing with interaction

The DP originates from an off-shell electromagnetic field. Furthermore, this field is associated with the longitudinal Coulomb mode, which plays an important role in light–matter interaction [7-9]. A theory for the DP has to meet the requirement that has been stated by the Greenberg-Robinson (GR) theorem [10,11]. This theorem claims that not only the timelike and lightlike momenta but also the spacelike momenta are required for the interaction. The Maxwell equations can be expanded to the spacelike momentum region by using the CD field because it can introduce the longitudinal mode into the electromagnetic theoretical formulation. By this expansion, the conventional Maxwell equations can be analytically connected to the spacelike momentum region, and the longitudinal mode can be dealt with. Then, space-time can be quantized, which is consistent with the Lorentz covariance. Thus, the quantization of the spacelike CD field is consistent with the space-time quantization. This means that the classical Maxwell equations were successfully expanded from the lightlike to spacelike momentum region. Another important aspect of the quantization is that the length (or wavenumber) must be quantized in the Majorana field [9]. This corresponds to the successful derivation of space-time quantization performed by Snyder [12]. As a result, it is confirmed that a small DP field originates from a transition of the spacelike momentum of the Majorana field into a timelike one. However, this DP cannot be observed in the macroscopic area because it is much smaller than the wavelength of conventional propagating light. For measurement, the DP field must be disturbed to create free photons by inserting a probe into the DP field.

3. Maximum size of the dressed photon

The quantization of the Majorana field suggests that there exists a maximum size of the DP, whose value has been evaluated experimentally to be 40–70 nm [13]. This size is called the DP constant [14]. It is given by the geometrical mean of the smallest Planck length and the largest length associated with a newly modified cosmological constant. They are related to their dark energy model defined by the ground state of a spacelike Majorana field and to their novel dark matter model defined solely by the Weyl conformal tensor field, respectively [7-9].

4. Conversion from dressed photon to bullet-like propagating light

In the case of a pair annihilation of the timelike Majorana field involving anti-parallel spins, the created DP has a spin 0. Specifically, the light converted from the DP can be a unique light field with spin 0, which behaves as a particle. This particle-like behavior has been supported by the Wightman theorem [15] stating that: *A Lorentz or*

Galilei covariant massive system is always localizable. For the Lorentz case, the only localizable massless elementary system (i.e., irreducible representation) has spin 0. Here, localizability means that a position operator can be defined for this system. Quantum mechanically, the bivector for the CD field represents a Majorana field with spin 1/2; thus, a couple of anti-parallel vibector fields with spins 1/2 and −1/2 can be combined to yield a null energy–momentum current with spin 0, which can be regarded as a unique bullet-like light field with spin 0.

A silicon-LED (1.3–1.6 μm wavelength) [16] was used to verify the bullet-like behaviors of emitted light described above [7]. The values of the second-order cross-correlation coefficient (CC), measured by the Hanbury Brown-Twiss method [17], were less than unity in the range of time difference shorter than 20 ns. This indicates the photon anti-bunching, which is an inherent feature of a single photon. However, the CC took a nonzero value at null time difference even though it is less than 1×10^{-2}. This nonzero value is attributed to the photons emitted from multiple light sources located in close proximity with each other in the LED. These features suggest that a cluster of photons emitted from the LED behaves as a single photon. It is named DP-cluster light and is closely related to the localizable property of the spin 0 particle. Namely, if the observable positions of given spin 0 quantum particles are sufficiently close, the cluster of these particles would behave as if it were a single quantum particle with the accumulated amount of energy.

The experimental verification above suggests that such a peculiar propagating light field exists, whose energy-momentum tensor has exactly the same form as a free particle. If that is the case, a light beam consisting of such a light field would behave as a bullet and be free from diffraction. In regard to this peculiar light field, it is further conjectured that the mechanism of DP-cluster light may be involved in gamma ray bursts, one of the cosmological enigmas, as an intermittent extremely high-energy radiation with strong directionality that reaches the earth after travelling over an enormous distance of several billions of light years.

5. Summary

Based on a CD field theoretical model, it was made clear that a DP originates from a transition of the spacelike momentum of the Majorana field to a timelike one. This model succeeded in deriving a maximum size of the DP. This size was named the DP constant. It was found that, in the case where timelike Majorana particle and anti-particle have anti-parallel spins, pair annihilation creates a DP with a spin 0. The light converted from this DP can be a unique light field with spin 0, which behaves as a particle. It was experimentally confirmed that a cluster of photons emitted from an Si-LED behaved as such a particle and was named DP-cluster light [18].

Acknowledgements

The author thanks Drs. I. Ojima and H. Sakuma (Research Origin for Dressed Photon) or their support in theoretical studies.

[1] M.Ohtsu: *Dressed Photons*, Springer, Heidelberg, 2014.
[2] M. Ohtsu: *Off-Shell Application in Nanophotonics*, Elsevier, Amsterdam, 2021.
[3] R. Haag: On Quantum Field Theory. *Dan. Mat. Fys. Medd*. **29**,12 (1955).
[4] D. Hall and A. S. A. Wightman: Theorem on Invariant Analytic Functions with Applications to Relativistic Quantum Field Theory. *Mat. Fys. Medd. Dan. Vid. Selsk.* **31**, 5(1957).
[5] R. F. Streater and A.S.Wightman: *PCT, Spin and Statistics, and All That*, Princeton University Press, 2000.
[6] R. Haag, *Local Quantum Physics*, second edition, Springer Verlag, 1996.
[7] H.Sakuma, I. Ojima, M. Ohtsu, and T. Kawazoe: Drastic advancement in nanophotonics achieved by a new dressed photon study. *J. European Opt. Soc.: RP*. **17**, 28 (2021).
[8] M. Ohtsu, I, Ojima, and H. Sakuma: Dressed Photon as an Off-Shell Quantum Field, in *Prog. Opt.* (ed. By T.D. Visser), vol.64, (2019).
[9] H, Sakuma, I. Ojima, M. Ohtsu, and H. Ochiai: Off-shell quantum fields to connect dressed photons with cosmology. *Symmetry*, **12**, 1244 (2020).
[10] R. Jost: The General Theory of Quantized Fields. *Amer. Math. Soc. Publ.*, Providence (1963).
[11] G.F. Dell'Antonio: Support of a field in p space. *J. Math. Phys.* **2**, 759 (1961).
[12] H.S.Snyder: Quantized space-time. *Phys. Rev.* **71**, 38 (1947).
[13] M. Ohtsu: History, current development, and future directions of near-field optical science. *Opto-Electronic Advances*, **3**, 190046 (2020).
[14] H. Sakuma and I. Ojima: On the Dressed Photon Constant and Its Implication for a Novel Perspective on Cosmology. *Symmetry*, **13**, 593 (2021).
[15] A.S. Wightman: On the localizability of quantum mechanical systems. *Rev. Mod. Phys*. **34**, 845 (1962).
[16] M. Ohtsu, *Silicon Light-Emitting Diodes and Lasers*, Springer, Heidelberg, 2016.
[17] R. Hanbury Brown, and R.Q. Twiss: A Test of New Type of Stellar Interferometer on Sirius, *Nature*. **178** ,1046 (1956).
[18] For the present status of the theoretical studies on off-shell science, please refer to the Special Issue "Quantum Fields and Off-Shell Sciences", *Symmetry*, 2021, guest-edited by M. Ohtsu.

[III] REVIEW PAPERS

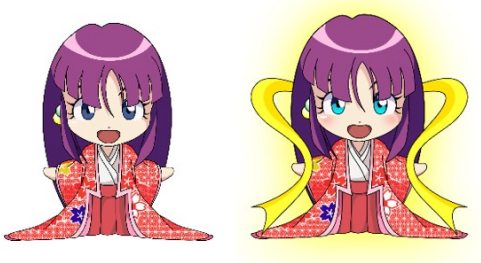

納谷昌之著 「梅干しとひかり」 書評

東京大学名誉教授　大津元一（(一社)ドレスト光子研究起点）

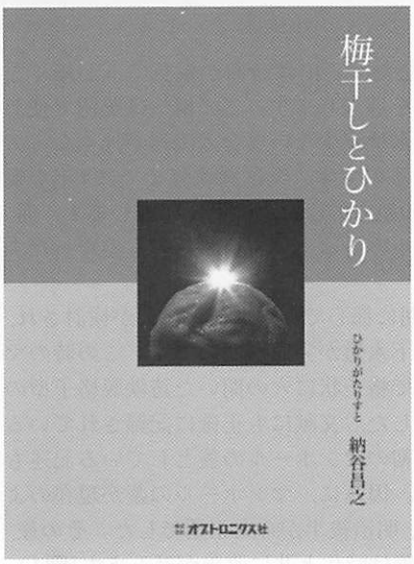

70編に達しようという多くの話題からなるこのユニークな書物を読みつつ，「このような本を書く人はどんな才能，感性を持っているのだろう」と驚愕しています。まえがきには「この本は教本ではない」とありますが，いやはやどうして，これはまさに光に関する優れた教本ですよ。ところで技術開発に従事する人が新しい技術ネタを探す際，欧米先進国で流行している技術を「習う」ことからネタを「作る」ことへと意識を切り替える必要がありますが，「作る」ためにはある種の感性が必要です。本書はまさにこの感性が身につく教本でしょう。ついに光の書籍の新ジャンルが開拓されましたね。

光にまつわるエッセイはこれまでいくつか目にしましたが，本書はそれらとは大きく異なります。優れた独創技術を実用化した技術者として産業界で高く評価されている著者の筆によるもので，光に関する深い造詣にもとづく話題が満載です。各話題の前半では国内外の文学，自然現象，旅行，そして新技術などと光とのつながりが紹介されており，著者の視点の広さが光ります。まさに「どんな才能？感性？」と驚きつつ楽しく読み進められます。しかし後半になるとこれらを科学的に鋭く（かつ奥ゆかしく）分析することへ進むので，「しっかり習わなければ」と少し緊張します。そして全部読み終わると何かを「作る」勇気が湧き，一服の清涼剤を味わった気分になるのです。いや，まさに「梅干し」を一口かじった気分かな。

本書はどこから読み始めても良いですが，一旦読み始めると止まらなくなります。題名の「梅干しとひかり」も秀逸で，その由来も本書に記されています。「日本人として生まれてよかった」と実感します。光の多くの現象を扱っているのに図や写真が一枚もありませんが，これもまた良いのです。文章を読むと自ずから画像が浮かび上がってきますので。（そうそう，唯一，表紙カバーに「梅干しとひかり」のきれいな写真がありますね）。書評執筆者としての私は「ラマン」，「ステンドグラスは…」，「やっぱり百聞は…」など，いくつかの話題の現場に立ち会った記憶があり，読みながら思わず「ニンマリ」しました。

幅広い世代の方々に本書をお勧めします。学生諸君，本書は将来の勉強や仕事の方向を探る栄養，活力となりますよ。さわやかな「梅干し」をご賞味あれ。

『梅干しとひかり』
■著者：納谷昌之
■A5判 200頁
■定価：2,400円＋税
http://shop.optronics.co.jp/products/detail.php?product_id=787
※Amazonでも絶賛販売中です！

[IV] PREPRINT DEPOSITORIES

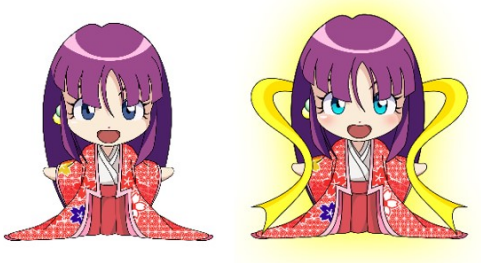

Dressed-photon–phonon creation probability on the tip of a fiber probe calculated by a quantum walk model

M. Ohtsu[1], E. Segawa[2], K. Yuki[3], and S. Saito[4]

[1]Research Origin for Dressed Photon,3-13-19 Moriya-cho, Kanagawa-ku, Yokohama, Kanagawa 221-0022, Japan

[2]Yokohama National University, 79-8 Tokiwadai, Hodogaya-ku, Yokohama, Kanagawa 240-8501, Japan

[3]Middenii, 3-3-13 Nishi-shinjuku, Sinjuku-ku, Tokyo 160-0023, Japan

[4]Kogakuin University, 2665-1, Nakano-machi, Hachioji, Tokyo 192-0015, Japan

Abstract

To study the probability of a dressed-photon–phonon (DPP) created on the tip of a fiber probe based on a quantum walk (QW) model, the creation probability of the DPP at the apex of a triangle is numerically calculated by substituting several values of mathematical and physical parameters. Two cases are dealt with: One is the case in which the DPP energy does not dissipate from the slope of the triangular lattice; and the other is the case in which the DPP energy dissipates. Sufficiently high accuracy of the approximation was obtained when the number of sites on the base of the triangle was larger than 51. The probability of DPP creation at the apex of the triangle was larger in the case without DPP energy dissipation at the slope of the triangle than that in the case with dissipation; furthermore, it was larger for a triangle with a larger apex angle. The derived results were in agreement with experimental results.

1. Introduction

A dressed photon (DP) is a quantum field that is created as the result of an interaction between photons and excitons (pairs consisting of electrons and positive holes) in a nanometer-sized particle (NP). After the DP is created on an NP, it hops to adjacent NPs, where it creates a phonon. The created phonon interacts with the DP to form a new quantum field, which is called a dressed-photon–phonon (DPP) [1]. A quantum walk (QW) model was employed to analyze the tempo-spatial behavior of the DPP energy transfer [2].

In the present paper, the probability of DPP creation on the tip of a fiber probe was numerically calculated based on the QW model, and the calculated results were compared with experimental ones. The results of preliminary calculations have been reported by ref. [3]. In Section 2, the purpose and method of calculation are reviewed. In Section 3, the profile of the fiber probe is approximated by a right-angled isosceles triangle, in which a part of a square lattice is embedded. The dependence of the calculated results on the number of the sites in the triangle is discussed. In Section 4, the fiber probe is approximated by an equilateral triangle, in which a part of a triangular lattice is embedded. The dependence of the probability of DPP creation on the apex angle of the fiber probe is discussed by comparing the calculated results with those in Section 3. Section 5 summarizes

the results derived in the present paper.

2. Purpose and method

The present calculations are based on a two-dimensional QW model for simplicity. Figure 1 shows a right-angled isosceles triangle, in which a part of a square lattice is embedded. Here, the number of the sites on the base of the triangle is n, and this triangle is expressed as $\mathrm{T_R}(n)$. This figure schematically explains that, by applying input signals to all the sites on the base of the $\mathrm{T_R}(n)$, DPs are created and transferred to the adjacent sites. During this transfer, DPPs are created by the DP–phonon interaction. These DPPs transfer through the $\mathrm{T_R}(n)$ and finally reach its apex (the tip of the fiber probe). This apex is assumed to be a sink from which the DPP energy is dissipated. This paper calculates the creation probability P of the DPP at this sink. It should be pointed out that each site in the $\mathrm{T_R}(n)$ has four nearest-neighbor sites located along the $\pm x$-, and $\pm y$-axes originated from the embedded square lattice. This means that the DPP energy transfers from/to these four sites.

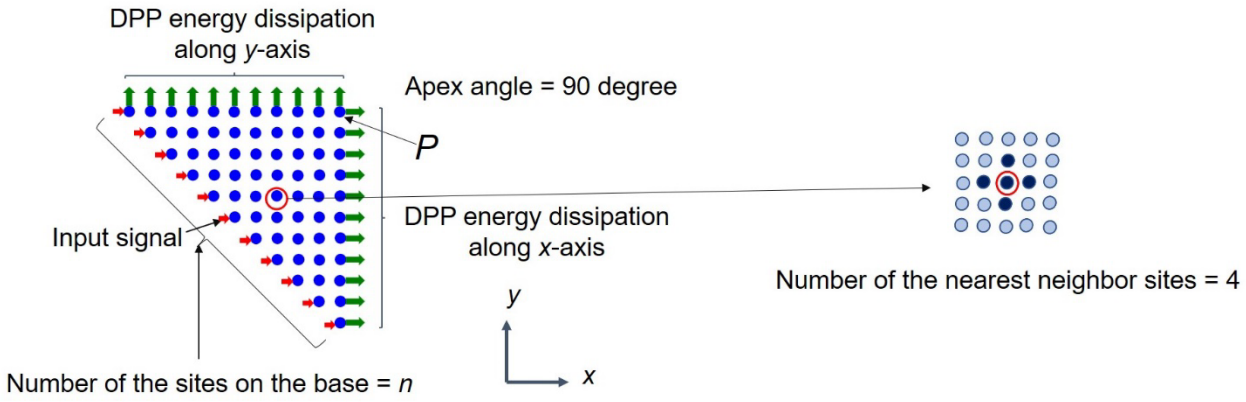

Fig. 1 A right-angled isosceles triangle $\mathrm{T_R}(n)$, in which a part of a square lattice is embedded.

Three parameters are used for the calculation:

(1) Mathematical parameter ξ:

To cover a broader range of mathematical discussions based on the QW model, a phase angle ξ is introduced to the real-valued unitary matrix in eq. (6) of ref. [2]:

$$U = \begin{bmatrix} \varepsilon_+ & J & \chi \\ J & \varepsilon_- & \chi \\ \chi & \chi & \varepsilon_0 \end{bmatrix}. \quad (1)$$

As a result, U is replaced by a complex-valued matrix

$$U(\xi) = \exp(i\xi)U\,. \quad (2)$$

Here, ξ is regarded as a mathematical parameter.

(2) Physical parameter χ / J:

Since the quantities J and χ in eq. (1) represent the energies of the DP-hopping to the adjacent NP (an atom in the fiber probe) and of the DP–phonon interaction, respectively, their ratio χ / J is regarded as a physical parameter. The value of χ / J may be fixed to 1 for simplicity, as was recommended in ref. [2]. However, to cover a broader range of physical discussions, the present paper employs a wider range of values, i.e., $0.1 \le \chi / J \le 10$.

(3) Parameter n for numerical calculation:

The total number of sites increases as the number n of sites on the base of the $\mathrm{T_R}(n)$ increases. Since this increase can improve the accuracy of approximating the fiber probe by the $\mathrm{T_R}(n)$, n is regarded as a parameter for the numerical calculation.

The probability P is numerically calculated by substituting several values of ξ and χ / J into eqs. (1) and (2). The parameter n was fixed to 5 – 61 due to the limit of the computation time.

Two cases are dealt with: One is the case in which the DPP energy does not dissipate from the slope of the $\mathrm{T_R}(n)$. The other is the case in which the DPP energy dissipates. For the former case, the tempo-spatial evolution equation at the slope is given by eq. (12a) in ref. [2], which is

$$\vec{\psi}^{\Leftrightarrow}_{t+1,(x,y)} = \sigma P^{\Updownarrow}_{-}\vec{\psi}^{\Updownarrow}_{t,(x,y)} + P^{\Updownarrow}_{-}\vec{\psi}^{\Updownarrow}_{t,(x+1,y)} + P^{\Updownarrow}_{0}\vec{\psi}^{\Updownarrow}_{t,(x,y)} . \quad (3)$$

Here, the matrix σ represents the DPP energy reflection at the slope. For the latter, the equation, given by eq. (10b) in ref. [2], is

$$\vec{\psi}^{\Updownarrow}_{t+1,(x,y)} = P^{\Leftrightarrow}_{+}\vec{\psi}^{\Leftrightarrow}_{t,(x,y-1)} + P^{\Leftrightarrow}_{-}\vec{\psi}^{\Leftrightarrow}_{t,(x,y+1)} + P^{\Leftrightarrow}_{0}\vec{\psi}^{\Leftrightarrow}_{t,(x,y)} . \quad (4)$$

3. Dependence on number of sites

Figure 2 shows an example of the calculated temporal behavior of the value of P. After the input signals are applied to all the sites on the base of the $T_R(n)$ simultaneously, the value of P increases with time and reaches a stationary value. Recent QW theoretical studies have found that the temporal behavior of the value of P on a complete graph exhibits pulsation prior to converging to the stationary value [4]. They have also found that the pulsation interval T_p is proportional to $\pi\sqrt{2N}$. Furthermore, the time T_s required to converge to the stationary value is proportional to $N \log N$. Here, N is the total number of sites in a lattice, that is equal to $n(n+1)/2$ in the case of the RIT lattice. The profile of the curve in Fig. 2 qualitatively agrees with the results of these theoretical studies. The present paper discusses the dependence of the stationary value of P on the parameters in eqs. (1) -(4).

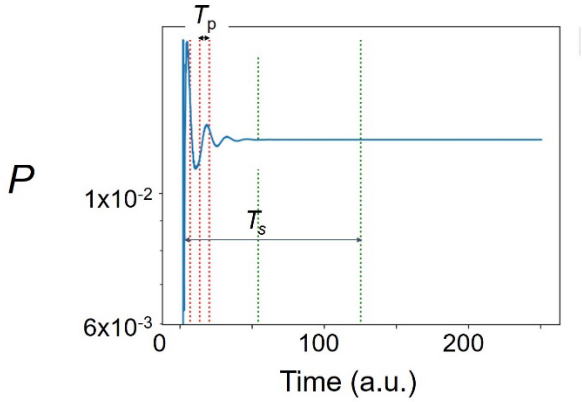

Fig. 2 An example of the calculated temporal behavior of the value of P.

Figure 3 shows the external forms and cross-sectional structures of fiber probes [5]. The DPP energy dissipates from the taper of the fiber probe. This corresponds to radiating scattered light from

the taper. In order to avoid this radiation, an opaque metallic film is coated on the taper to realize a high-efficiency fiber probe (Fig. 3(a)). This is the prototype of devices that are now popularly used. Figure 3(b) is a basic fiber probe without a metallic film coating, resulting in DPP energy dissipation from the taper. This is a primitive device that was used only in the early stages of DP science. Corresponding to Figs. 3(a) and (b), numerical calculations are carried out for the two cases below.

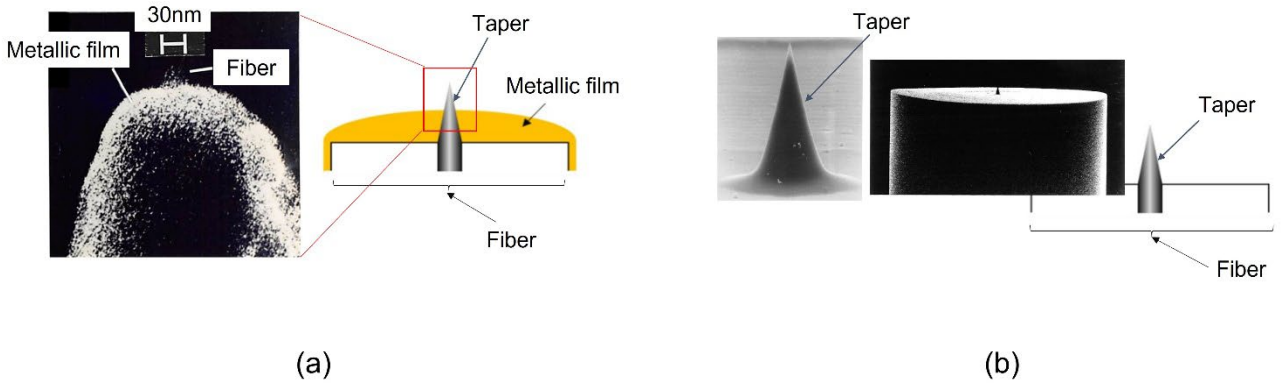

Fig. 3 External forms and cross-sectional structures of the fiber probes.
(a) A high-efficiency fiber probe with an opaque metallic film on the taper. (b) A basic fiber probe.

Case 1: Without DPP energy dissipation

Figure 4 shows the calculated results of the dependence of the probability P on the parameters ξ and χ / J. The parameter n was fixed to 5, 11, 21, 31, 41, 51, and 61 in Figs. 4(a)-(g). The values of P at χ / J=1 (as was recommended in ref. [2]) are extracted from these figures, and their dependences on ξ are shown in Figs. 5(a) – (g). The curves in these figures show a lot of bumps that are attributed to interference in the $T_R(n)$ originating from reflection at the slope.

Figure 5 shows that the value of P takes the maximum P_{max} at ξ=67.5 degree. This value of ξ is equal to (3/8)π. The reason why the rational number 3/8 appears here should be studied in

the future. Figure 6 shows the dependence of this maximum $P_{\max}$ on n. This figure shows that $P_{\max}$ asymptotically approaches a constant value of 3×10^{-1} as n increases, from which it was confirmed that a sufficiently high accuracy of approximation for the numerical calculation was obtained when $n \geq 51$. Figure 7 shows the dependence of the ratio between the maximum $P_{\max}$ and the minimum $P_{\min}$ (of the curves in Fig. 5) on n. The ratio in this figure also shows an asymptotic approach to a constant value, from which it was confirmed again that sufficiently high accuracy was obtained when $n \geq 51$.

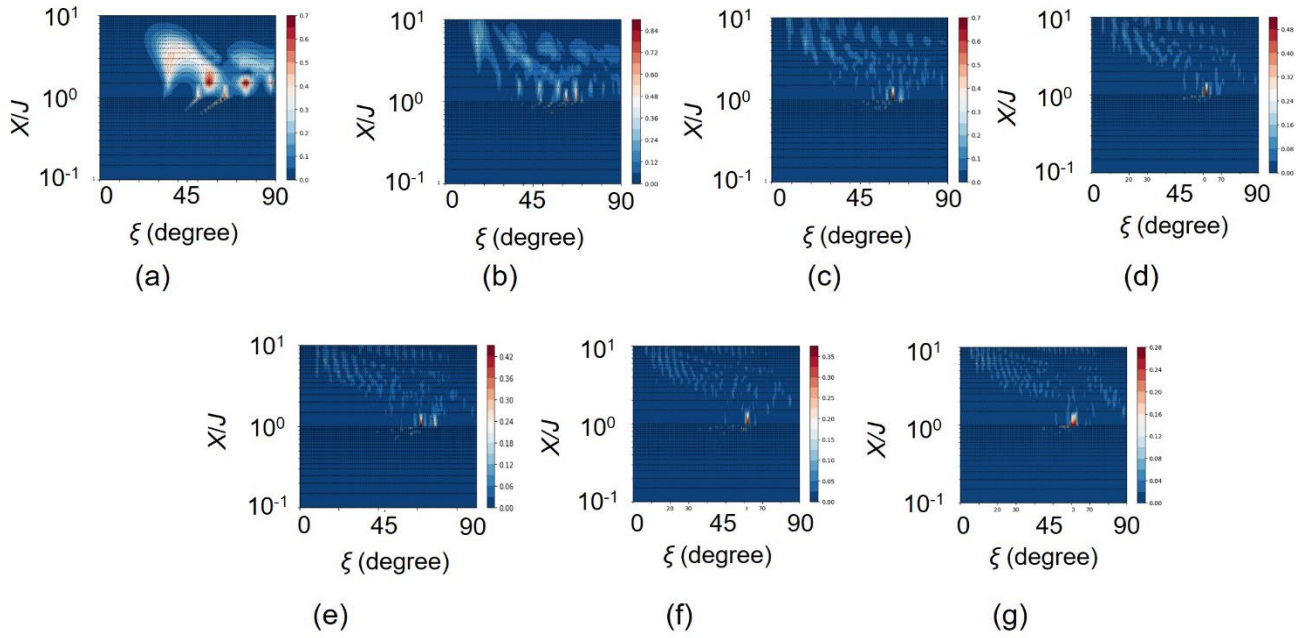

Fig.4 Dependence of P on ξ and χ/J in the case without DPP energy dissipation.

n is 5 (a), 11 (b), 21 (c), 31 (d), 41 (e), 51 (f), and 61 (g).

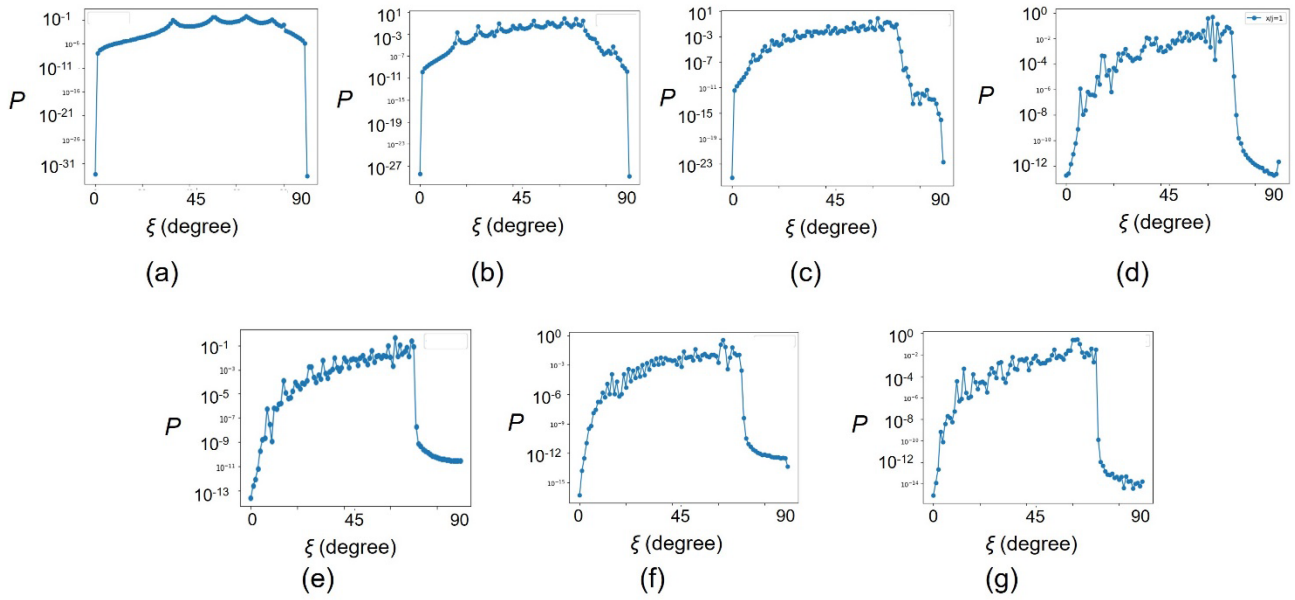

Fig.5 Dependence of P on ξ at χ / J =1.

n is 5 (a), 11 (b), 21 (c), 31 (d), 41 (e), 51 (f), and 61 (g).

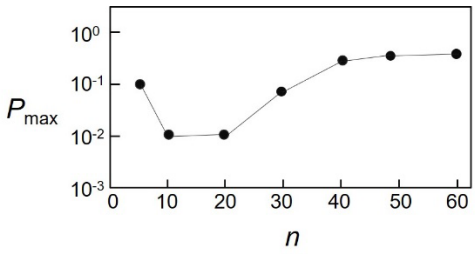

Fig. 6 Dependence of the maximum $P_{\max}$ on n.

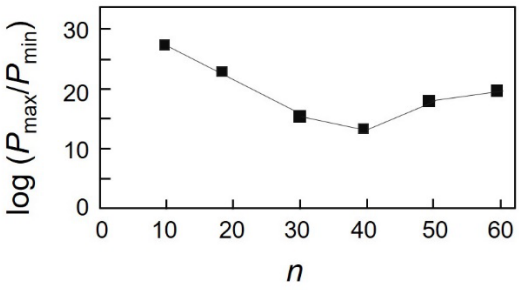

Fig. 7 Dependence of the ratio between the maximum $P_{\max}$ and minimum $P_{\min}$ on n.

Case 2: With DPP energy dissipation

Figure 8 shows the calculated results of the dependence of P on ξ and χ/J. In Figs. 8(a)-(g), n is fixed to 5, 11, 21, 31, 41, 51, and 61. Crescent-shaped red belts are seen in the upper right parts of these figures, in which the value of P is very large in comparison with those outside the red belts. It takes the maximum value at the position □. The origin of these red belts is attributed to intrinsic properties of the QW or dispersive features of the phonon energy. The values of P show irregular variations and abrupt increases in the red belts and at their rims. The value of χ/J at □ increases with the increases of n, as is shown by Fig. 9. It increases to $\chi/J \gg 1$, which means that the value of P at $\chi/J=1$ (as was recommended in ref.[2]) does not vary irregularly with ξ.

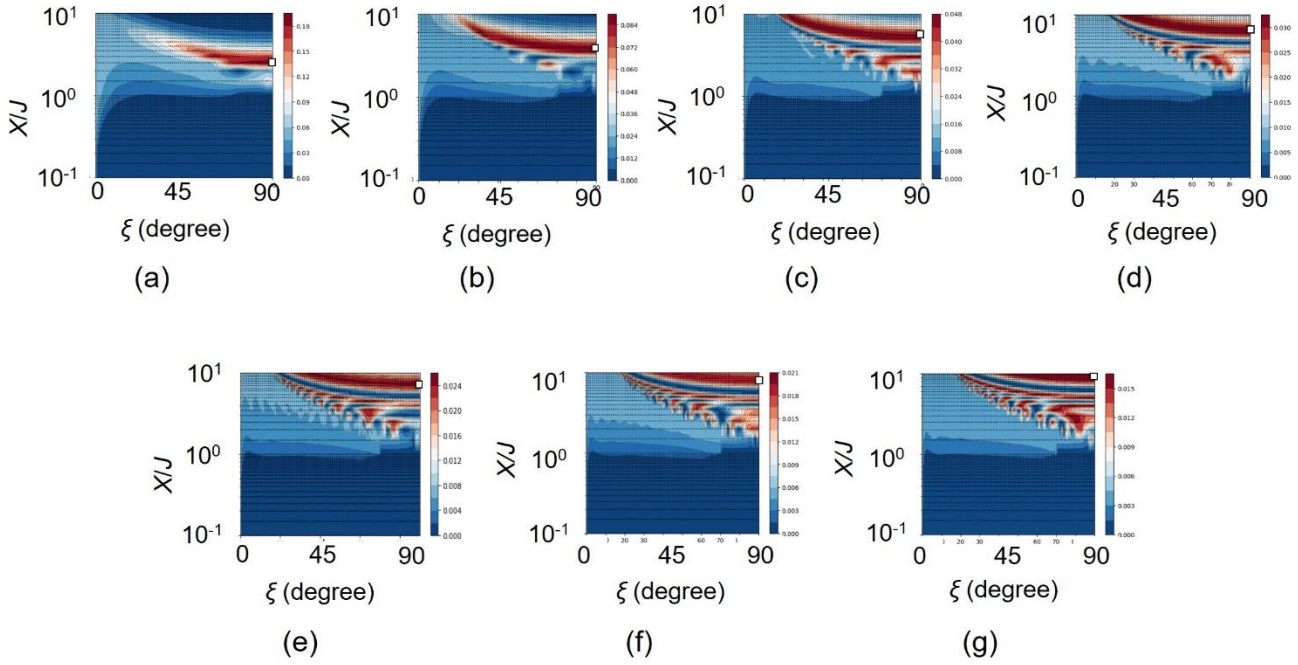

Fig.8 Dependence of P on ξ and χ/J in the case with DPP energy dissipation.

n is 5 (a), 11 (b), 21 (c), 31 (d), 41 (e), 51, (f), and 61 (d).□ is the position for P_{max} in the red belt.

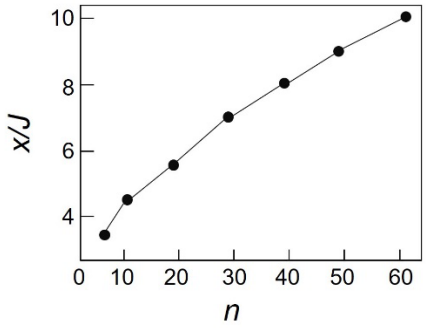

Fig. 9 Dependence of χ / J on n at the position □ in Fig. 8.

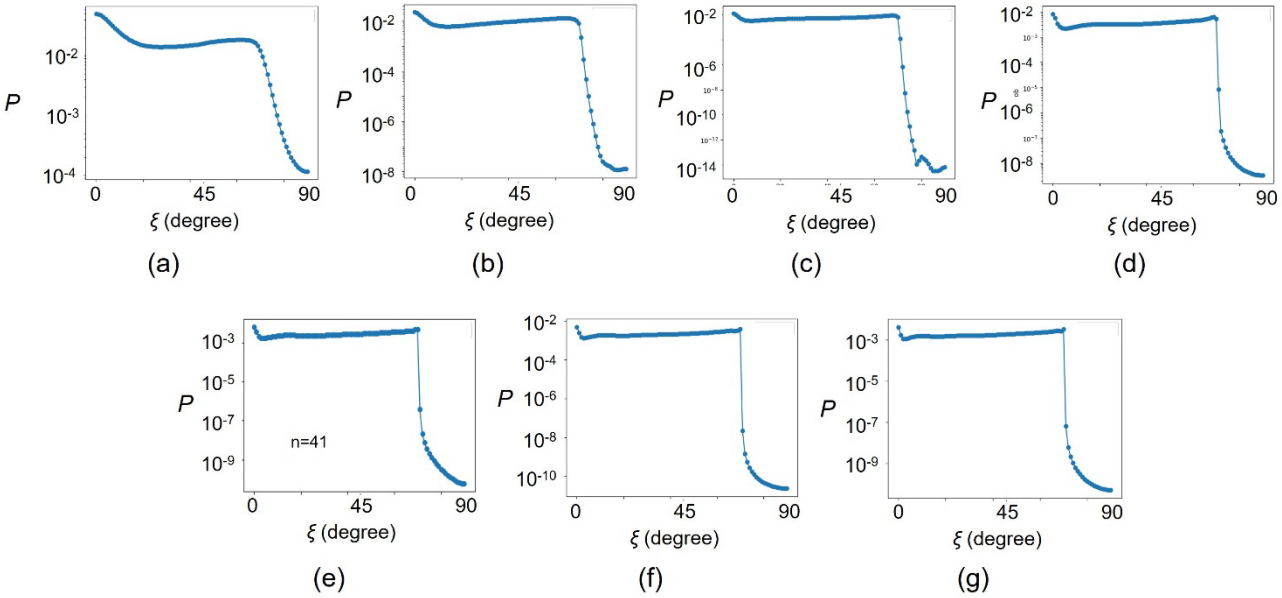

Fig. 10 Dependence of P on ξ at χ / J =1.

n is 5 (a), 11 (b), 21 (c), 31 (d), 41 (e), 51, (f), and 61 (d).

The value of P at the area isolated from the red belt is now evaluated for studying its regular and smooth variations. For this evaluation, χ / J is fixed to 1 (as was recommended in ref. [2]), and the dependence of on ξ and n is derived as shown by Fig. 10. In contrast to Fig. 5, no bumps are seen on the curves in this figure, which indicates that no interference takes place in the RIT lattice. This is due to the absence of reflection at the slope.

As in Case 1, the value of P in Fig. 10 takes the maximum $P_{\max}$ at ξ =67.5 degree. Figure

11 shows the dependence of P_{max} on n. This figure shows that the value of P_{max} asymptotically approaches a constant value as n increases, from which it was confirmed that sufficiently high accuracy of approximation was obtained when $n \geq 51$, as in Case 1 above. The value of P_{max} was 3 $\times 10^{-3}$ for $n \geq 51$, which is 10^{-2} times that in Fig. 6. This indicates that it is effective to suppress DPP energy dissipation (Case 1) at the slope of the RIT lattice to increase the probability of DPP creation. This indication is compatible with experimental results in which the taper of a fiber probe is coated with an opaque metallic film to suppress dissipation and to increase the DPP creation efficiency at the tip of the fiber probe (refer to Fig. 3(a)).

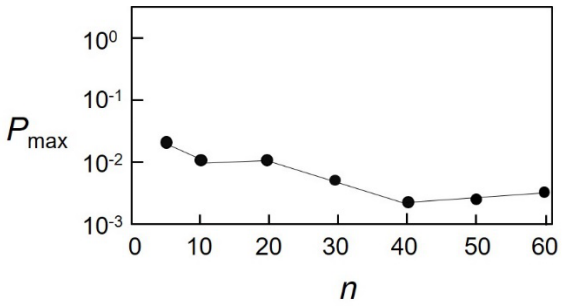

Fig. 11 Dependence of the maximum P_{max} on n.

Figure 12 shows the dependence of the ratio between the maximum P_{max} and the minimum P_{min} (of the curves in Fig. 10) on n. The curve in this figure also shows an asymptotic approach to a constant value, from which it was confirmed that sufficiently high accuracy was obtained when $n \geq$ 51.

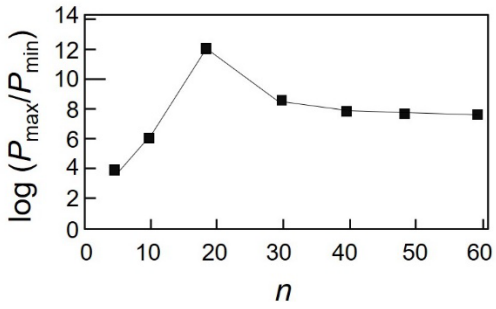

Fig. 12 Dependence of the ratio between the maximum P_{max} and minimum P_{min} on n.

4. Dependence on apex angle of fiber probe

Experimental studies have found that the value of P was smaller for smaller apex angles [6]. Unlike the 90 degree apex angle of the $T_R(n)$ in Section 3, this section deals with a triangle with a smaller apex angle, i.e., an equilateral triangle $T_E(n)$ (apex angle of 60 degrees), as an example, as is shown in Fig. 13. The calculated results are compared with those in Section 3.

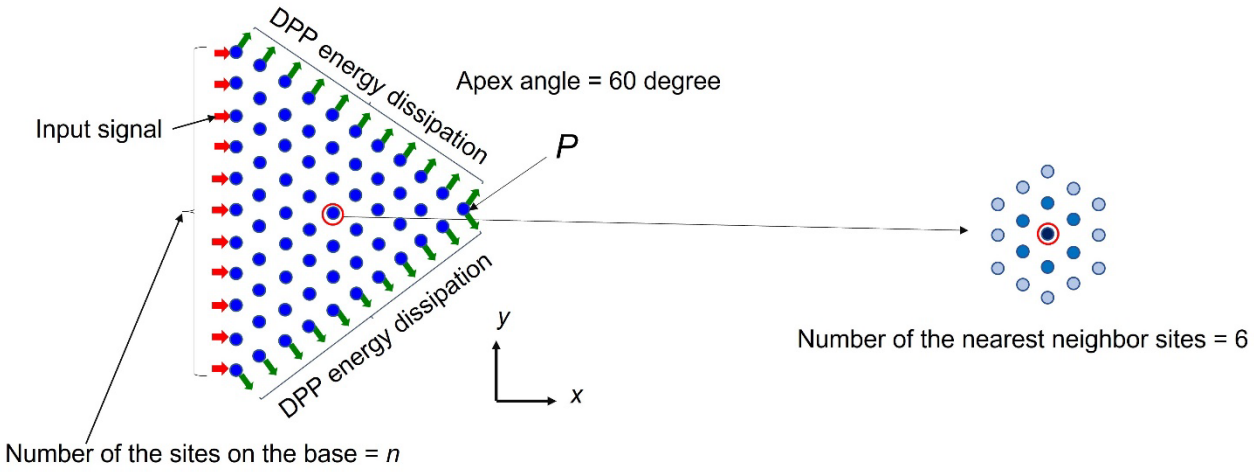

Fig. 13 An equilateral triangle $T_E(n)$, in which a part of a triangular lattice is embedded.

Being different from the $T_R(n)$, each site in the $T_E(n)$ in Fig. 13 has six nearest-neighbor sites located along the directions of the $e^{\pm i\pi/6}x$-, $e^{\pm i5\pi/6}x$-, and $\pm y$-axes originated from the embedded triangular lattice. The DPP energy transfers from/to these six sites. By noting the number of these nearest-neighbor sites, the tempo-spatial evolution equation for the $T_E(n)$ was derived by modifying that for the $T_R(n)$, and the probabilities P were calculated for the cases without and with DPP energy dissipation.

Case 1: Without DPP energy dissipation

Figure 14 shows the dependence of P on ξ and on χ/J. Figure 15 shows the dependence of P in Fig. 14 on ξ at χ/J=1. A lot of bumps are seen on the curves in this figure, which are attributed to interference in the triangular lattice, originating from the reflection at the slope, as were seen in Fig. 5. It was confirmed that these curves are symmetrical about ξ=60 degree. Furthermore, the value of P in these figures takes the maximum $P_{\max}$ at $\xi = 60$ degree (=$(1/3)\pi$).

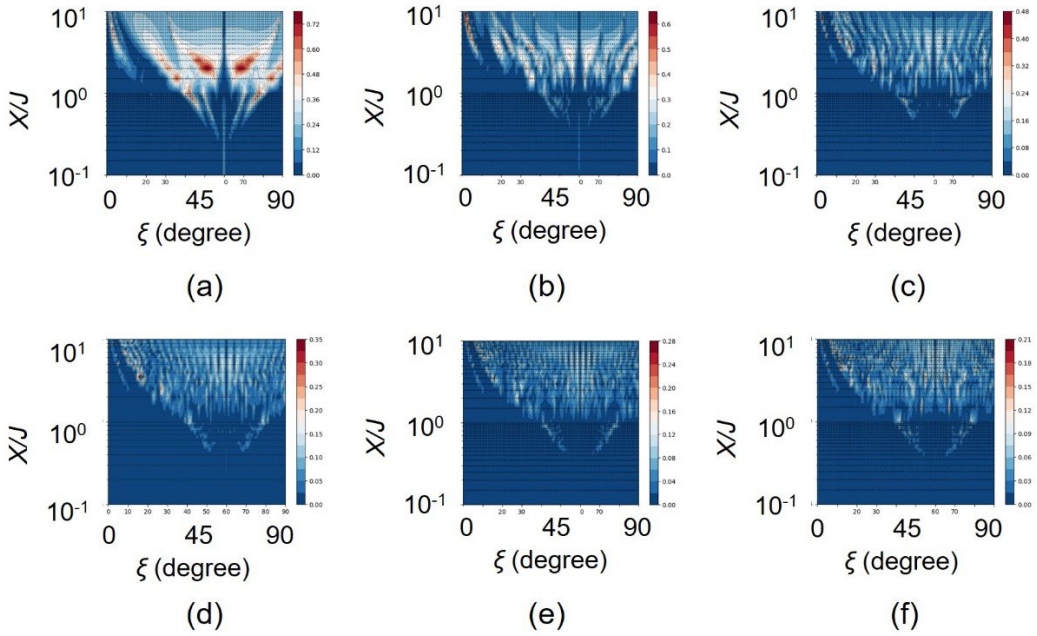

Fig. 14 Dependence of P on ξ and χ/J in the case with DPP energy dissipation.

(a) n=5, (b) 11, (c) 21, (d) 31, (e) 41, and (f) 51.

Figure 16 shows the dependence of $P_{\max}$ on n, in which the value at n=61 was not obtained due to the upper limit of the computation time. This figure shows that the value of $P_{\max}$ asymptotically approaches a constant value as n increases, from which it was confirmed that sufficiently high accuracy of approximation was obtained when $n \geq 51$. Figure 17 shows the

dependence of the ratio between the maximum $P_{\max}$ and the minimum $P_{\min}$ (of the curves in Fig. 15) on n. The ratio in this figure also shows an asymptotic approach to a constant value, from which it was confirmed again that sufficiently high accuracy of approximation was obtained when $n \geq 51$.

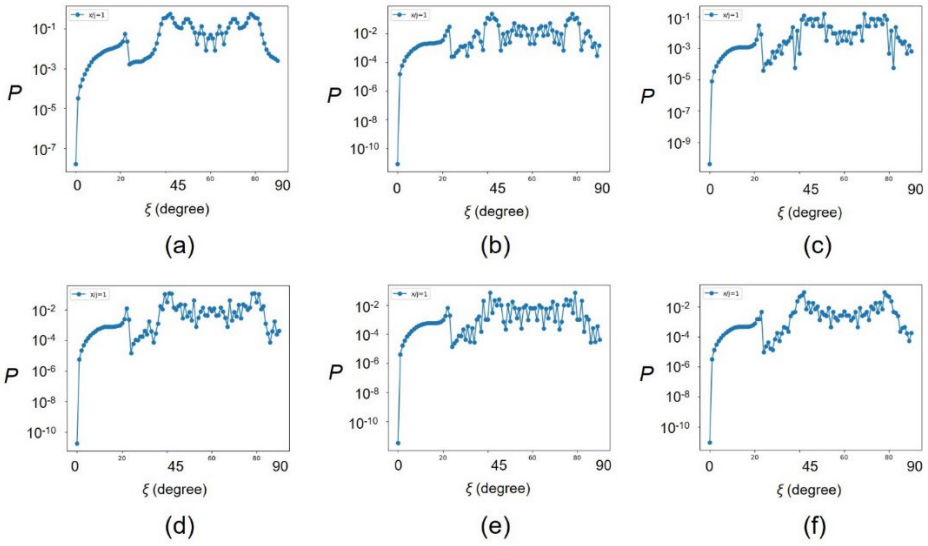

Fig. 15 Dependence of P on ξ at χ / J =1 in Fig. 14.

(a) n =5 , (b) 11, (c) 21, (d) 31, (e) 41, and (f) 51.

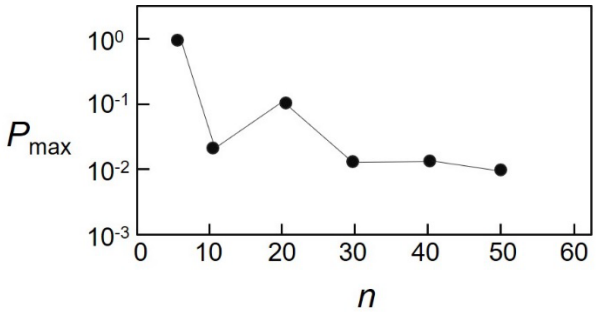

Fig. 16 Dependence of $P_{\max}$ on n in Fig. 14.

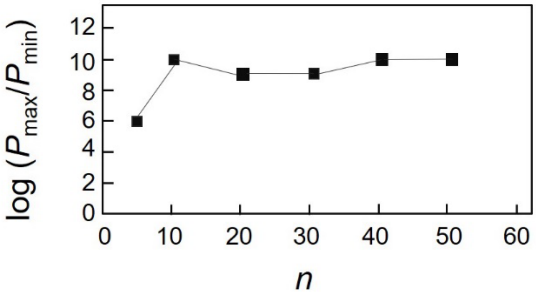

Fig. 17 Dependence of the ratio between the maximum $P_{\max}$ and minimum $P_{\min}$ on n in Fig. 15.

It is found that the value of $P_{\max}$ in Fig. 16 is 1×10^{-2} for $n\geq51$, which is smaller than the value 3×10^{-1} in Fig. 6. This smaller value indicates that the efficiency of DPP creation is lower for a smaller apex angle of the fiber probe, which is in agreement with the experimental results [6], as was described at the beginning of this section.

Case 2: With DPP energy dissipation

Figure 18 shows the dependence of P on ξ and on χ/J. A red belt is seen in this figure, as was the case in Fig. 8, in which the value of P is very large in comparison with those outside the belts. The value of P is integrated over the range $0\leq\xi\leq90.0$ degree, and Fig. 19 shows the dependence of χ/J on n at which the integrated value of P takes the maximum in the red belt, indicating that χ/J takes a constant value as n increases. Furthermore, this value of χ/J is larger than 2, which means that the value of P at $\chi/J=1$ (as was recommended in ref. [2]) does not suffer any effects from the red belt.

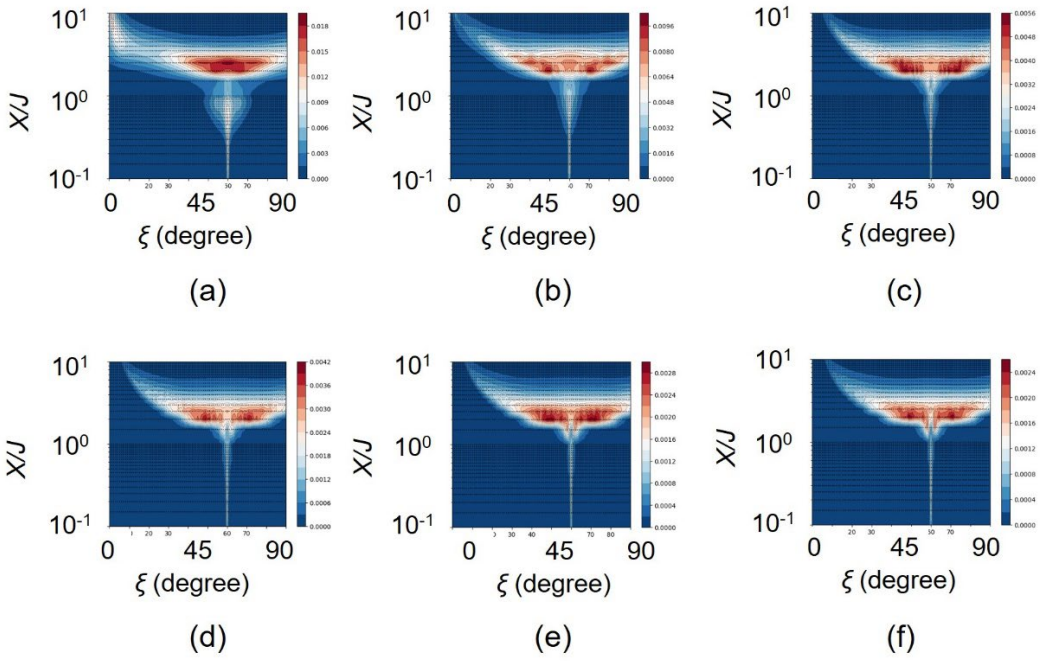

Fig. 18 Dependence of P on ξ and χ / J in the case with DPP energy dissipation.

(a) n =5, (b) 11, (c) 21, (d) 31, (e) 41, and (f) 51.

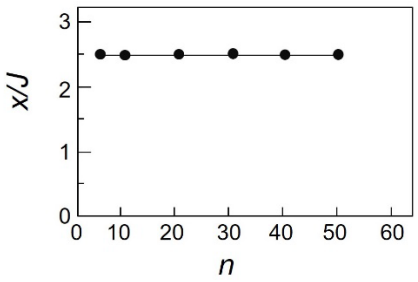

Fig. 19 Dependence of χ / J on n at which the integrated value of P takes the maximum value in the red belt in Fig. 18.

Figure 20 shows the dependence of P on ξ at the position χ / J =1 in Fig. 18. No bump on the curves is seen in this figure, which indicates that no interference takes place in the $\mathrm{T\{E\}}(n)$, as was the case in Fig. 10. It was confirmed that these curves were symmetrical about ξ =60 degree, as was the case in Fig.15. Furthermore, the value of P in these figures takes the maximum $P_{\max}$ at $\xi = 60$ degree (=$(1/3)\pi$). Figure 21 shows the dependence of $P_{\max}$ on n. This figure shows that the value of $P_{\max}$ asymptotically approaches a constant value as n increases, from which it was confirmed that sufficiently high accuracy of approximation for the numerical calculation was obtained when $n \geq 51$, as was the case in Fig. 16. The value of $P_{\max}$ was 1×10^{-3} for $n \geq 51$, which is 10^{-1} times that in Fig. 16. This indicates that it is effective to suppress DPP energy dissipation (Case 1) at the slope of the $\mathrm{T}_E(n)$ to increase the probability of DPP creation, as was described in Section 3. This indication is in agreement with the experimental results.

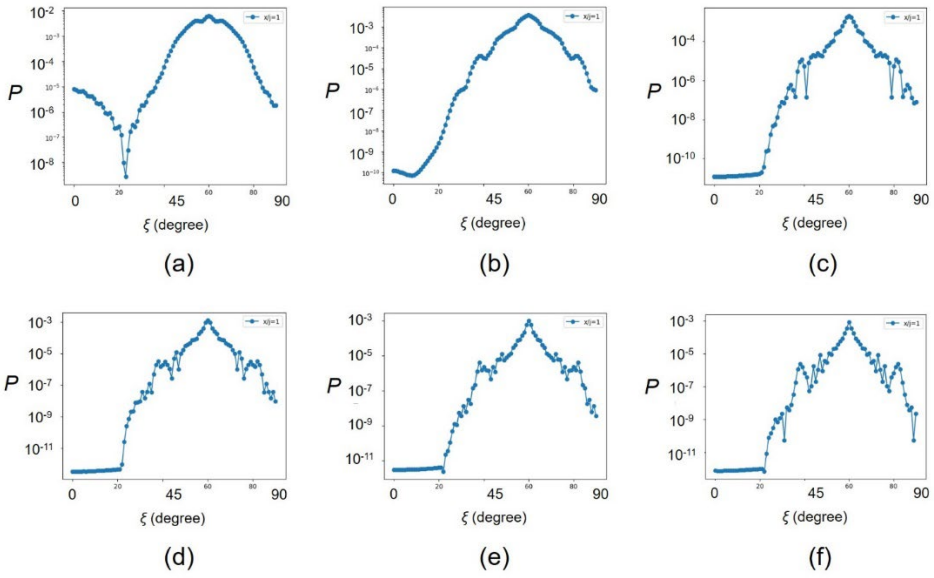

Fig. 20 Dependence of P on ξ at the position at χ / J =1 in Fig. 18.

(a) n =5, (b) 11, (c) 21, (d) 31, (e) 41, (f) 51.

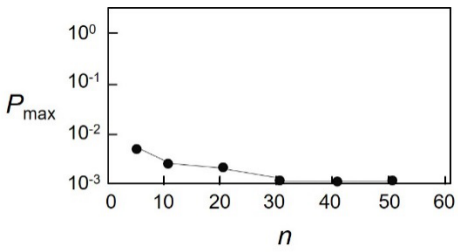

Fig. 21 Dependence of the maximum $P_{\max}$ on n.

Figure 22 shows the dependence of the ratio between the maximum $P_{\max}$ and the minimum $P_{\min}$ (of the curves in Fig. 20) on n. The curve in this figure also shows an asymptotic approach to a constant value, from which it was confirmed again that sufficiently high accuracy was obtained when $n \geq 51$.

It is found that the value of $P_{\max}$ in Fig. 21 is 1×10^{-3} for $n \geq 51$, which is smaller than the value 3×10^{-3} in Fig. 11. As with the discussion in Case 1, this smaller value indicates that the efficiency of DPP creation is lower for a smaller apex angle of the fiber probe, which is in agreement with the experimental results.

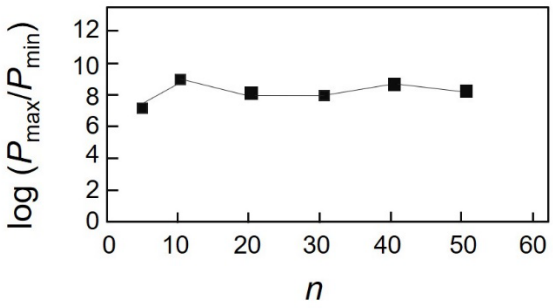

Fig. 22 Dependence of the ratio between the maximum $P_{\max}$ and minimum $P_{\min}$ on n.

5. Summary

To calculate the probability of DPP creation on the tip of a fiber probe on the basis of a QW model, the profile of the fiber probe was approximated by a two-dimensional right-angled isosceles triangle $\mathrm{T_R}(n)$ and an equilateral triangle $\mathrm{T}_E(n)$. The calculations were carried out for cases without and with DPP energy dissipation at the slope of the triangular lattice. In both cases, the calculated maximum probability $P_{\max}$ converged to a constant value when $n \geq 51$, where n is the number n of the sites on the base of the triangle. This indicates that sufficiently high accuracy of the approximation above was obtained when $n \geq 51$.

Table 1 summarizes the calculated values of $P_{\max}$ for the physical parameter $\chi / J = 1$. This table shows that the value without DPP energy dissipation is larger than that with DPP energy dissipation, which is in agreement with experimental results. Furthermore, the value is larger for the $\mathrm{T_R}(n)$ (an apex angle of 90 degree) than that for the $\mathrm{T}_E(n)$ (an apex angle of 60 degree), which is also in agreement with experimental results.

Table 1 Calculated values of $P_{\max}$ for $\chi / J = 1$.

	Right-angled isosceles triangle $\mathrm{T_R}(n)$	Equilateral triangle $\mathrm{T}_E(n)$
Without DPP energy dissipation	3×10^{-1}	1×10^{-2}
With DPP energy dissipation	3×10^{-3}	1×10^{-3}

Acknowledgements

The authors thank Dr. S. Sangu (Ricoh Co. Ltd.) for his valuable comments on this study.

References

[1] M. Ohtsu, *Dressed Photons*, Springer, Heidelberg (2014).

[2] M. Ohtsu, "A Quantum Walk Model for Describing the Energy Transfer of a Dressed Photon," *Off-shell Archive* (September, 2021) OffShell: 2109R.001.v1., **DOI** 10.14939/2109R.001.v1

[3] M. Ohtsu, E. Segawa, and K.Yuki, "Numerical calculation of a dressed photon energy transfer based on a quantum walk model," *Off-shell Archive* (June, 2022) OffShell: 2206R.001.v1., **DOI** 10.14939/2206R.001.v1

[4] Y. Higuchi, M. Sabri, and E. Segawa, "Toward fixed point and pulsation quantum search on graphs driven by quantum walks with in- and out-flows: a trial to the complete graph", arXiv:2207.10633

[5] M. Ohtsu, *Off-shell Applications in Nanophotonics*, Elsevier, Amsterdam (2021), p.9.

[6] M. Ohtsu, *Near-Field Nano/Atom Optics and Technology*, Springer, Tokyo/Berlin (1998), pp.71-87.

Numerical calculation of a dressed photon energy transfer based on a quantum walk model

M. Ohtsu[1], E. Segawa[2], and K. Yuki[3]

[1]Research Origin for Dressed Photon,3-13-19 Moriya-cho, Kanagawa-ku, Yokohama, Kanagawa 221-0022, Japan

[2]Yokohama National University, 79-8 Tokiwadai, Hodogaya-ku, Yokohama, Kanagawa 240-8501, Japan

[3]Middenii, 3-3-13 Nishi-shinjuku, Sinjuku-ku, Tokyo 160-0023, Japan

Abstract

To study the probability of a dressed-photon–phonon (DPP) created on the tip of a fiber probe based on a quantum walk (QW) model, the creation probability of the DPP at the apex of a two-dimensional triangular lattice is numerically calculated by substituting several values of mathematical (ξ) and physical (χ / J) parameters. Two cases are dealt with: One is the case in which the DPP energy does not dissipate from the slope of the triangular lattice; and the other is the case in which the DPP energy dissipates. It is found that the optimum value of ξ is 67.5 degree, and the value of χ / J can be fixed to 1. The calculated temporal behaviors agree with the results derived by QW theory.

1. Introduction

A dressed photon (DP) is a quantum field that is created as the result of an interaction between photons and excitons (pairs consisting of electrons and positive holes) in a nanometer-sized particle (NP). It localizes on the NP and its size is much smaller than the wavelength of light. It is an off-shell field because its momentum has a large uncertainty originating from its sub-wavelength size [1,2]. Conventional on-shell scientific theories cannot be used to analyze this field because no thorough studies of this light–matter interaction have been made in the long history of on-shell science. Fortunately, however, studies of this interaction in off-shell science have commenced recently, resulting in a precise description of the mechanism of DP creation [3,4].

After the DP is created on a NP, it hops to adjacent NPs. During this hopping, the DP excites a crystal lattice vibration, resulting in the creation of a phonon. The created phonon interacts with the DP to form a new state of the DP, which is called a dressed-photon–phonon (DPP) [5]. The DPP energy transfers through adjacent NPs. Although the tempo-spatial behavior of this transfer has been experimentally evaluated, it has not been fully described by conventional theories of a random walk process [6]. In order to describe the behavior, a quantum walk (QW) model was recently employed, allowing the unique properties of the DPP to be analyzed [7].

In this article, the probability of DPP creation on the tip of a fiber probe is numerically calculated based on the QW model, and the results are compared with experimental results.

2. Purpose and method

The present calculations are based on a two-dimensional QW model for simplicity. Figure 1(a) shows a right-angled isosceles triangular lattice that approximates the profile of the fiber probe. Figure 1(b) schematically explains that, by applying input signals to all the sites on the base of the triangular lattice, DPs are created and transferred to the adjacent sites. During this transfer, DPPs are created by the DP–phonon interaction. These DPPs transfer through the triangular lattice and finally reach its apex (the tip of the fiber probe). This apex is assumed to be a sink from which the DPP energy is dissipated. This article calculates the creation probability P of the DPP at this sink.

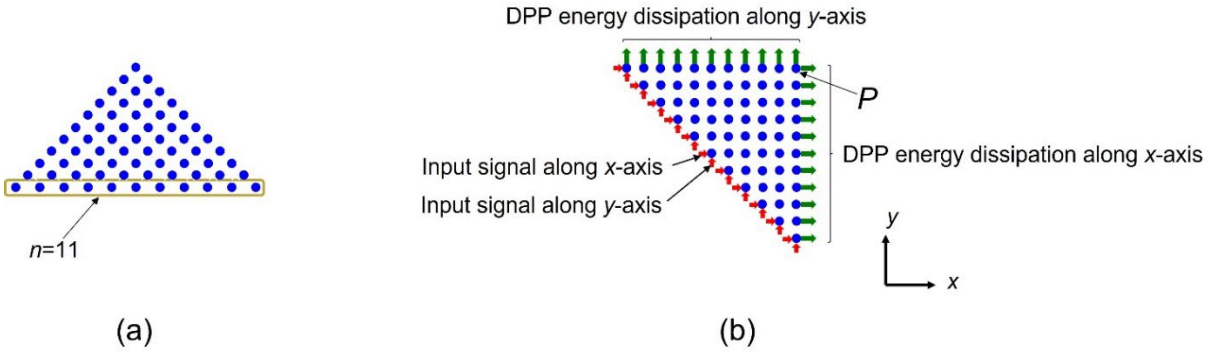

Fig. 1 A two-dimensional right-angled isosceles triangular lattice.
(a) The case of n =11. (b) The lattice illustrated after rotating that in (a) by 45 degree for convenience of the numerical calculation.

Three parameters are used for the calculation:

(1) Mathematical parameter ξ:

To cover a broader range of mathematical discussions based on the QW model, a phase angle ξ is introduced to the real-valued matrix in eq. (6) of ref. [7]:

$$U = \begin{bmatrix} \varepsilon_+ & J & \chi \\ J & \varepsilon_- & \chi \\ \chi & \chi & \varepsilon_0 \end{bmatrix}. \qquad (1)$$

As a result, U is replaced by a complex-valued matrix

$$U(\xi) = \exp(i\xi)U\,. \qquad (2)$$

Here, ξ is regarded as a mathematical parameter.

(2) Physical parameter χ / J:

Since the quantities J and χ in eq. (1) represent the energies of the DP-hopping to the adjacent NP (an atom in the fiber probe) and of the DP–phonon interaction, respectively, their ratio χ / J is regarded as a physical parameter. The value of χ / J may be fixed to 1 for simplicity, as was

recommended in ref. [7]. However, to cover a broader range of physical discussions, the present article employs a wider range of values, i.e., $0.1 \le \chi / J \le 10$.

(3) Parameter n for numerical calculation:

The total number of sites increases as the number n of sites on the base of the triangular lattice increases. Since this increase can improve the accuracy of approximating the fiber probe by the triangular lattice, n is regarded as a parameter for the numerical calculation.

The probability P is numerically calculated by substituting several values of ξ and χ / J into eqs. (1) and (2).

Section 3 deals with two cases: One is the case in which the DPP energy does not dissipate from the slope of the triangular lattice. The other is the case in which the DPP energy dissipates. For the former case, the tempo-spatial evolution equation at the slope is given by eq. (12a) in ref. [7], which is

$$\vec{\psi}^{\Leftrightarrow}_{t+1,(x,y)} = \sigma P_{-}^{\Updownarrow} \vec{\psi}^{\Updownarrow}_{t,(x,y)} + P_{-}^{\Updownarrow} \vec{\psi}^{\Updownarrow}_{t,(x+1,y)} + P_{0}^{\Updownarrow} \vec{\psi}^{\Updownarrow}_{t,(x,y)} . \tag{3}$$

Here, the matrix σ represents the DPP energy reflection at the slope. For the latter, the equation, given by eq. (10b) in ref. [7], is

$$\vec{\psi}^{\Updownarrow}_{t+1,(x,y)} = P_{+}^{\Leftrightarrow} \vec{\psi}^{\Leftrightarrow}_{t,(x,y-1)} + P_{-}^{\Leftrightarrow} \vec{\psi}^{\Leftrightarrow}_{t,(x,y+1)} + P_{0}^{\Leftrightarrow} \vec{\psi}^{\Leftrightarrow}_{t,(x,y)} . \tag{4}$$

3. Results and discussion

After the input signals are applied to all the sites on the base of the triangular lattice simultaneously, the value of P increases with time and reaches a stationary value. Subsection 3.1 discusses the dependence of the stationary value of P on the parameters in eqs. (1) to (3) in Section 2. Subsection 3.2 presents temporal behaviors of P prior to converging to the stationary value.

3.1 Dependences of the probability on mathematical and physical parameters

Figure 2 shows the external forms and cross-sectional structures of fiber probes [8]. The DPP energy dissipates from the taper of the fiber probe. This corresponds to radiating scattered light from the taper. In order to avoid this radiation, an opaque metallic film is formed on the taper (Fig. 2(a)) to realize a high-efficiency fiber probe. This is the prototype of devices that are now popularly used. Figure 2(b) is a basic fiber probe without a metallic film coating, resulting in DPP energy dissipation from the taper. This is a primitive device that was used only in the early stages of DP science. Figures 2(c) and (d) are for advanced devices, i.e., asymmetric and triple-tapered fiber probes, respectively, for future numerical calculations (cf. Section 4). Corresponding to Figs. 2(a) and (b), numerical calculations are carried out for the two cases presented in Section 2.

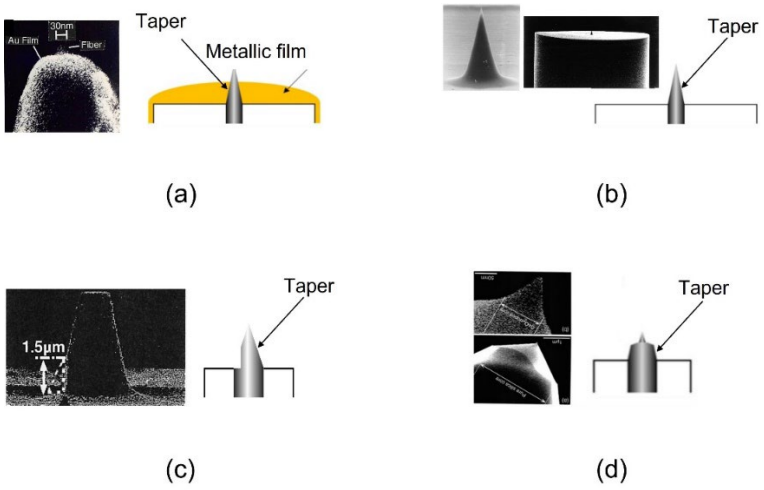

Fig. 2 External forms and cross-sectional structures of the fiber probes.
(a) A high-efficiency fiber probe with an opaque metallic film on the taper. (b) A basic fiber probe. (c) An asymmetric fiber probe. (d) A triple-tapered fiber probe.

Case 1: Without DPP energy dissipation

Figure 3 shows the calculated results of the dependence of the probability P on the parameters ξ and χ / J. The parameter n was fixed to 5, 11, 21, and 41 in Figs. 3(a)-(d). The values of P at χ / J =1 are extracted from these figures, and their dependences on ξ are shown in Figs. 4(a) – (d). The curves in these figures show a lot of bumps that are attributed to interference in the triangular lattice originating from reflection at the slope. The interval between the adjacent bumps (indicated by horizontal double arrows) decreases as n increases, as is shown by Fig. 5. These decreases indicate that the magnitude of the interference decreases with an increase in the size of the triangular lattice. Since this interference had not been experimentally observed, the present calculation results are quite reasonable.

Figure 4 shows that the value of P takes the maximum $P_{\max}$ at ξ =67.5 degree. This value of ξ is equal to (3/8)π. The reason why the rational number 3/8 appears here should be studied in the future. Figure 6 shows the dependence of this maximum $P_{\max}$ on n. It is found from this figure that the maximum $P_{\max}$ increases roughly monotonically with the increase of n. This means that the DPP energy is effectively confined in the triangular lattice due to reflection at the slope, which agrees with the characteristics of the actual high-efficiency fiber probe in Fig. 2(a). However, the values deviate from this monotonic increase in the range $n < 21$, which may be due to interference inside the triangle.

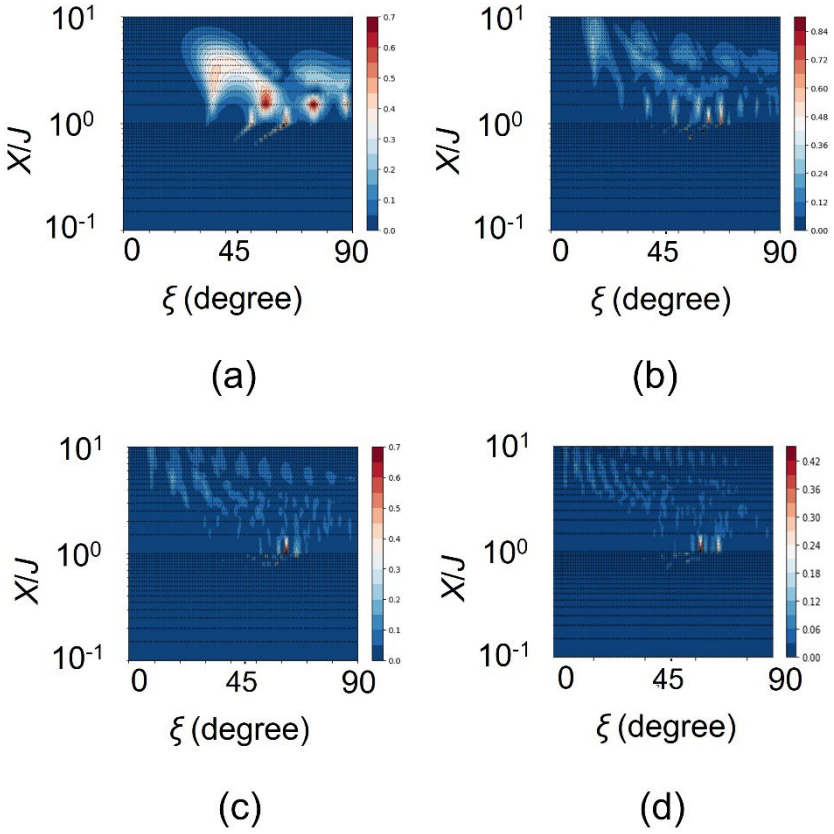

Fig.3 Dependence of P on ξ and χ / J in the case without DPP energy dissipation. n is 5 (a), 11 (b), 21 (c), and 41 (d).

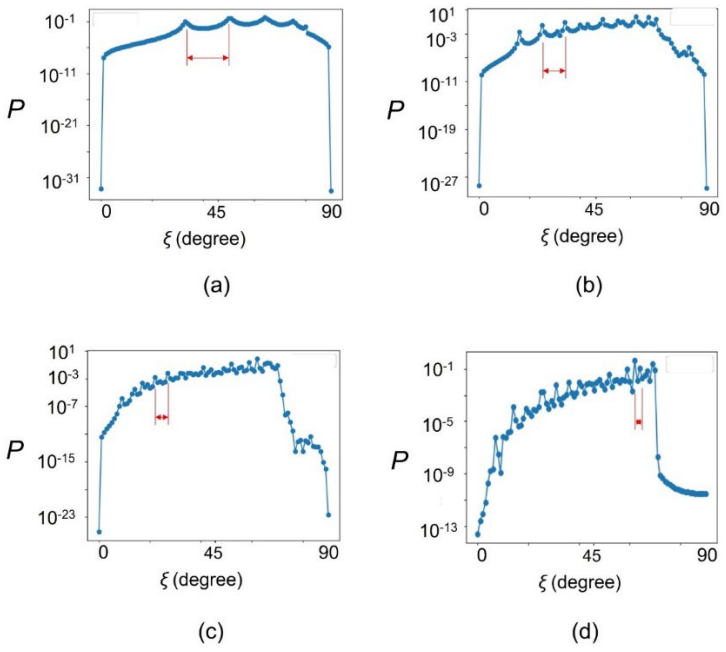

Fig.4 Dependence of P on ξ at χ / J =1. n is 5 (a), 1 1(b), 21 (c), and 41 (d). Horizontal double arrows indicate the interval of the adjacent bumps.

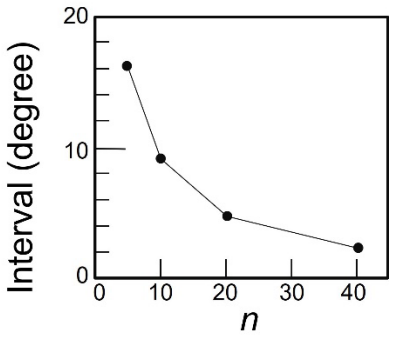

Fig. 5 Dependence of the interval between the adjacent bumps on n.

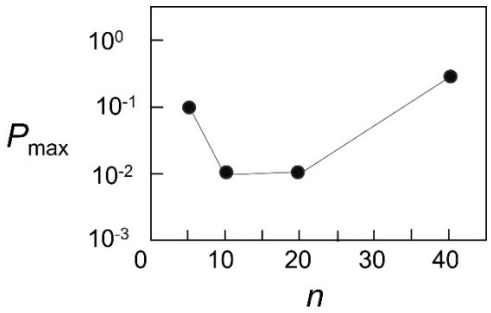

Fig. 6 Dependence of the maximum $P_{\max}$ (in Fig. 4) on n.

Figure 7 shows the ratio between the maximum $P_{\max}$ and minimum $P_{\min}$ of the curves in Figs. 4(a) – (d). The ratio monotonically decreases with the increases of n. This decrease also indicates that the effects of reflection and interference become less conspicuous, which means that the present calculation results agree with the experimental results.

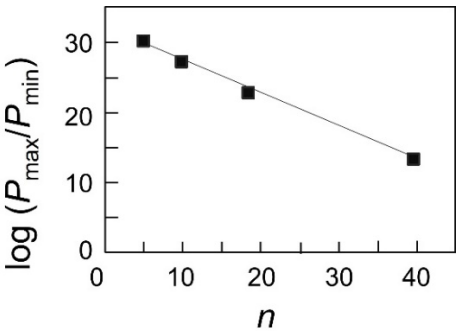

Fig. 7 Dependence of the ratio between the maximum $P_{\max}$ and minimum $P_{\min}$ (in Fig. 4) on n.

Case 2: With DPP energy dissipation

Figure 8 shows the calculated results of the dependence of P on ξ and χ / J. In Figs. 8(a)-(d), n is fixed to 5, 11, 21, and 41. Crescent-shaped red belts are seen in the upper right parts of these figures, in which the value of P is very large in comparison with those outside the red belts. It takes the maximum value at the position □ at ξ=90 degree. The origin of these red belts is attributed to

intrinsic properties of the QW or dispersive features of the phonon energy. The values of P show irregular variations and abrupt increases in the red belts and at their rims. The value of χ/J at □ increases with the increases of n, as is shown by Fig. 9. It increases to $\chi/J \gg 1$, which means that the value of P at $\chi/J=1$ (as was recommended in ref.[7]) does not vary irregularly with ξ. For reference, the value of P at χ/J=5 takes the maximum at the position ○ in Fig. 8. The value of ξ at this position ○ irregularly varies with the increase of n, as is shown by Fig. 10. A possible reason for this irregularity is that the red belt passes through the horizontal line χ/J=5 in Fig. 8 when n varies from 11 to 41.

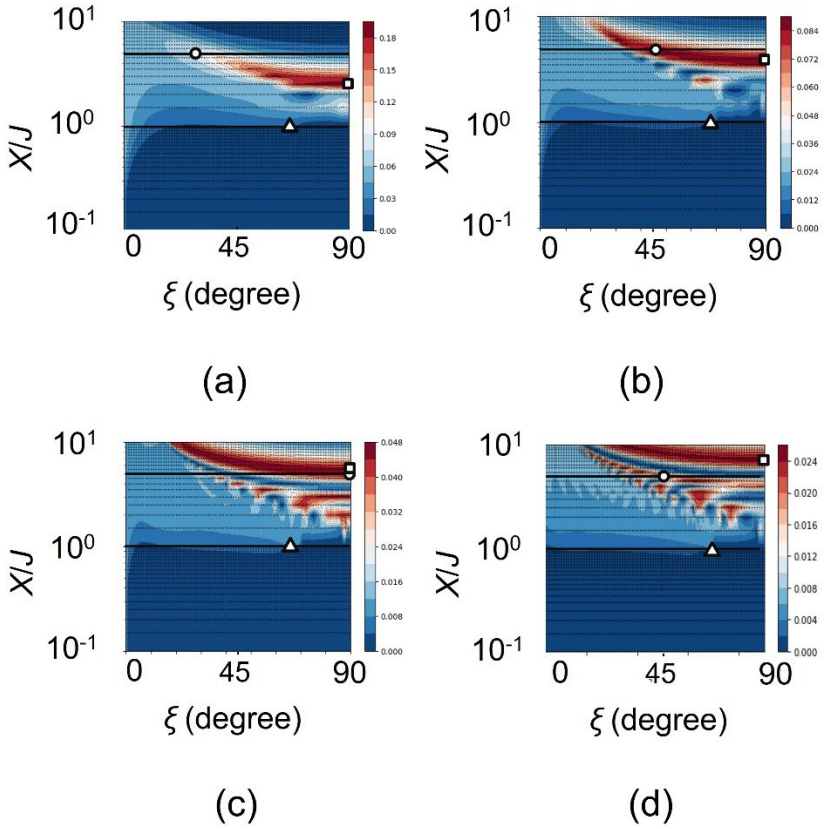

Fig.8 Dependence of P on ξ and χ/J in the case with DPP energy dissipation.
n is 5 (a), 11 (b), 21 (c), and 41 (d). △ and ○ on the horizontal line of χ/J=1 and 5, respectively, represent the position at which P takes the maximum P_{max}. □ is the position for P_{max} in the red belt.

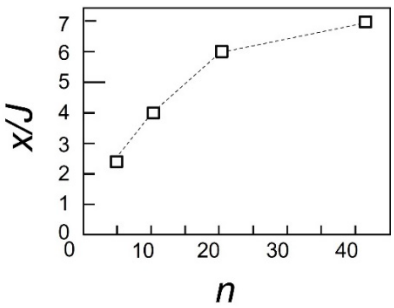

Fig. 9 Dependence of the value of χ / J at the position □ in Fig. 8 on n.

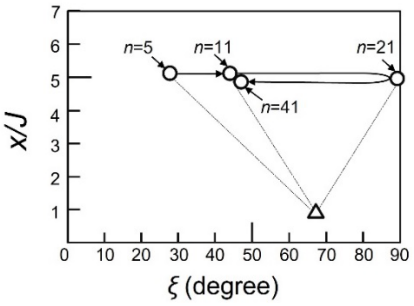

Fig.10 The value of ξ (at the position ○ in Fig. 8) at which P takes the maximum $P_{\max}$ at χ / J=5.

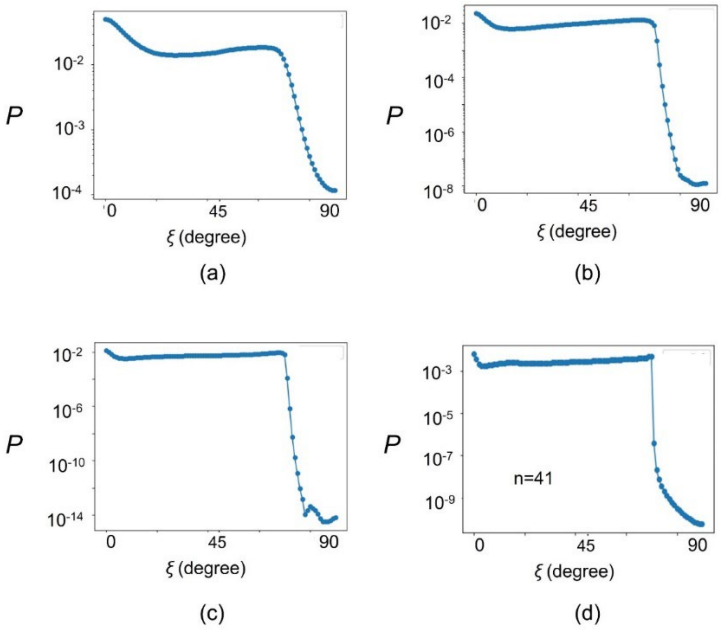

Fig. 11 Dependence of P on ξ at χ / J=1.
n is 5 (a), 11 (b), 21 (c), and 41 (d).

The value of P at the area isolated from the red belt is now evaluated for studying its regular and smooth variations. For this evaluation, χ / J is fixed to 1 (as was recommended in ref. [7]), and the dependence of P on ξ and n is derived as shown by Fig. 11. In contrast to Fig. 4, no bumps are seen on the curves in this figure, which indicates that no interference takes place in the triangular lattice. This is due to the absence of reflection at the slope and indicates that the present calculation results agree with the experimental results for the basic fiber probe in Fig. 2(b).

As in Case 1, the value of P in Fig. 11 takes the maximum $P_{\max}$ at ξ=67.5 degree (also at 0 degree), being independent of n. Figure 12 shows the dependence of the maximum $P_{\max}$ at ξ

=67.5 degree (and also at 0 degrees, for reference) on the value n. In contrast to Fig. 6, this figure shows that the maximum $P_{\max}$ decreases nearly monotonically with the increase of n. This is because the magnitude of the energy dissipation on the slope of the triangular lattice increases with the increase of n. However, the maximum $P_{\max}$ does not decrease drastically even though the value of n varies from 5 to 41. This indicates that a sufficiently high-energy DPP reaches the tip of the fiber probe even though the DPP energy dissipates from the slope. This is advantageous for practical applications.

Figure 13 shows the ratio between the maximum $P_{\max}$ and minimum $P_{\max}$ of each curve of Fig. 11. In contrast to Fig. 7, the ratio increases with the increase of n. Here, it should be noted that the values at n=21 deviates from the monotonically decreasing and increasing sequential lines in Figs. 12 and 13, respectively. In addition, the value of the ratio in Fig. 13 is much smaller than that in Fig. 7. Further discussions on Figs. 12 and 13 are required to compare them with Figs. 6 and 7.

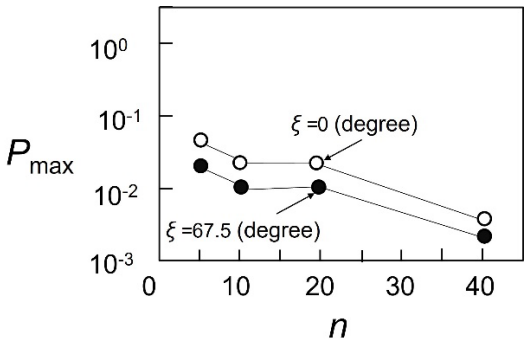

Fig. 12 Dependence of the maximum $P_{\max}$ (in Fig. 11) on n.

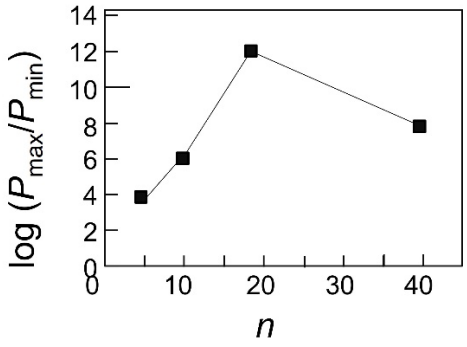

Fig. 13 Dependence of the ratio between the maximum $P_{\max}$ and minimum $P_{\min}$ (in Fig. 11) on n.

From the results and discussions for Case 1 and Case 2 above, the optimum value of the parameter ξ was found to be 67.5 degree, being independent of n. Furthermore, it was found that the value of the parameter χ / J can be fixed to 1, as was recommended in ref. [7]. It is expected that this value can be used even when the value of n is increased to $n > 41$ to increase the accuracy of approximating the fiber probe.

3.2. Temporal behaviors

Recent QW theoretical studies have found that the temporal behavior of the value of P exhibits pulsation prior to converging to the stationary value [9]. They have also found that the pulsation interval T_p is proportional to $\pi\sqrt{2N}$. Furthermore, the time T_s required to converge to the stationary value is proportional to $N \log N$. Here, $N\,(=n(n+1)/2)$ is the total number of sites in the triangle. Figure 14 shows an example of the temporal behavior of the value of P derived by the present calculations. The horizontal axis represents time. Figures 15 (a) and (b) show the values of T_p and T_s, respectively, calculated for **Case 2**. The horizontal axes represent the total number N of sites. The theoretical values above are represented by the curve A that monotonically increases with the increase of N. The curve B is the calculated result for χ/J=1. The curves C to E represent the calculated results for χ/J=5, in which the values of T_p and T_s increase with the increase of N, without exhibiting any irregular variations. This means that they do not suffer any effects from the red belt in Fig. 8, which is advantageous for comparing the results with the curve A.

By comparing the curves B to E with curve A, it can be concluded that the calculated temporal behaviors agree with the results derived by the QW theory, from which the validity of the present calculation is confirmed.

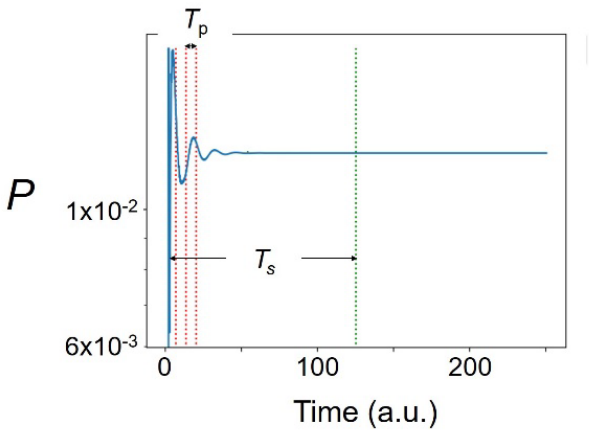

Fig. 14 An example of the calculated temporal behavior of the value of P.
The horizontal axis is proportional to time.

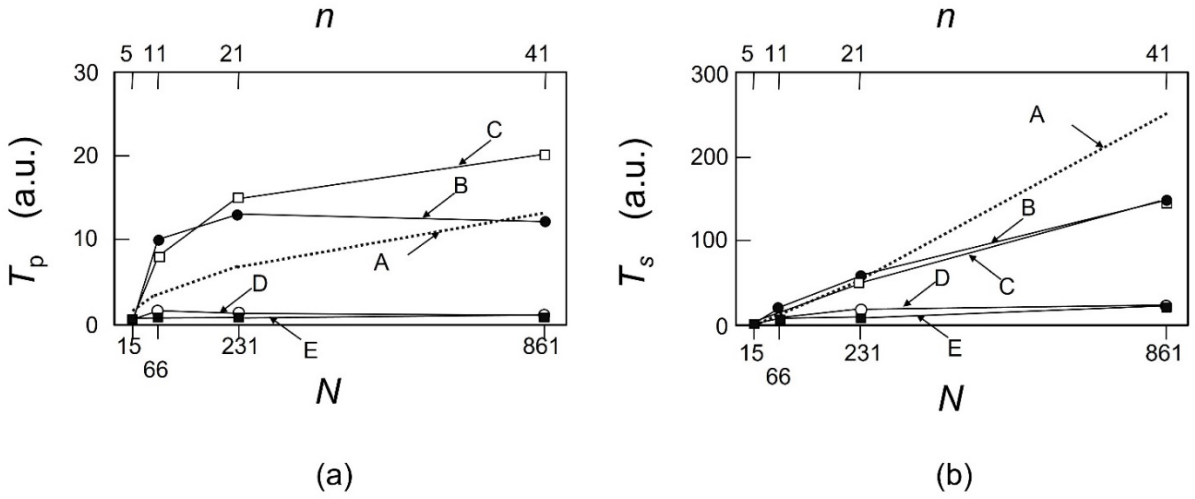

Fig. 15 Calculated values of the pulsation interval T_p (a) and the time T_s (b) required to converge to the stationary value.

The horizontal axis represents the total number N of sites in the triangular lattice. Curve A represents the theoretical values. Curve B represents the calculated values for χ / J =1. Curves C to E are the calculated values for χ / J =5 (at ξ =30, 60, and 90 degrees, respectively).

4. Summary

The present calculations successfully reproduced the DPP creation phenomena at the tip of a fiber probe. In particular, it was found that the value of the mathematical (ξ) and physical (χ / J) parameters could be fixed to 67.5 degree and 1, respectively, being independent of the parameter (n) for numerical calculation. It is expected that these values can be used to calculate the probability of the DPP creation at the tip of advanced high-throughput fiber probes, such as the asymmetric and triple-tapered fiber probes in Figs. 2(c) and (d), respectively. The calculated temporal behaviors agree with the results derived by the QW theory. It is expected that design criteria for novel fiber probes will be established in the near future based on the results of these calculations.

References

[1] M. Ohtsu, I. Ojima, and H. Sakuma, "Dressed Photon as an Off-Shell Quantum Field," *Progress in Optics* Vol.64, (ed. T.D. Visser) pp.45-97 (Elsevier, 2019).

[2] M. Ohtsu, *Off-Shell Applications In Nanophotonics*, Elsevier, Amsterdam (2021).

[3] H. Sakuma and I. Ojima, "On the Dressed Photon Constant and Its Implication for a Novel Perspective on Cosmology," *Symmetry* **2021**, 13, 593. https://doi.org/10.3390/sym13040593

[4] H. Sakuma, I. Ojima, M. Ohtsu and T. Kawazoe, "Drastic advancement in nanophotonics achieved by a new dressed

photon study, " *JEOS-RP* (2021)**17**:28.
https://jeos.springeropen.com/articles/10.1186/s41476-021-00171-w
[5] M. Ohtsu, *Dressed Photons*, Springer, Heidelberg (2014).
[6] M. Ohtsu, T. Kawazoe, and H. Saigo, "Spatial and Temporal Evolutions of Dressed Photon Energy Transfer," Offshell:1710R.001.v1.
DOI 10.14939/1710R.001.v1, http://offshell.rodrep.org/?p=79
[7] M. Ohtsu, "A Quantum Walk Model for Describing the Energy Transfer of a Dressed Photon," *Off-shell Archive* (September, 2021) OffShell: 2109R.001.v1.
DOI 10.14939/2109R.001.v1, http://offshell.rodrep.org/?p=345
[8] M. Ohtsu, Off-shell applications, Elsevier, 2021,p.9 (Fig.1.5)]
[9] M. Sabri, E. Segawa, "Sensitivity of quantum walk and dressed photon to perturbation," Abstracts of the 69nd Jpn. Soc. Appl. Phys. Spring Meeting, March 22-26, 2022, (Aoyama Gakuin Univ. and Online meeting), paper number 22a-E103-4.

Off-shell science theories on interaction for dressed photons

M. Ohtsu

Research Origin for Dressed Photon,

3-13-19 Moriya-cho, Kanagawa-ku, Yokohama, Kanagawa 221-0022 Japan

Abstract

This article, first, proposes a new approach to quantum fields in terms of category algebras and states on categories. Quantum fields and their states are respectively defined as category algebras and states on causal categories with partial involution structures. It is pointed out that, by utilizing category algebra and states on categories, relativity and quantumness can be directly integrated as a category theoretic structure and as a noncommutative probabilistic structure, respectively. Second, based on a Clebsch dual field theoretical model, it is made clear that a dressed photon (DP) field originates from a transition of the spacelike momentum of the Majorana field to a timelike one. This model derives a maximum size of the DP that has already been found by experimental studies. It is pointed out that, in the case where the paired timelike Majorana particle and anti-particle have anti-parallel spins, the pair annihilation creates a DP with a spin 0. The light converted from this DP can be a unique light field with spin 0, which behaves as a particle. It is experimentally confirmed that a cluster of photons emitted from an Si-LED behave as such a particle. Finally, a quantum walk model is employed to analyze the experimentally confirmed phenomena of DP energy transfer between nano-particles. Its theoretical bases are described based on the theory of category.

1. Introduction

It has been known that the dressed photon (DP) is a quantum field created as the result of the light–matter interaction that is induced by irradiating a nanometer-sized particle (NP) with light [1]. Thus, an interacting quantum field must be studied for constructing an accurate theorical model for the DP. However, the existence of a nontrivial interacting quantum field model defined on a four-dimensional Minkowski spacetime has not yet been proven. Axiomatic approaches to quantum field theories have derived many fundamental theorems, including the Haag theorem [2,3]. It is a no-go theorem, implying that an "interaction picture exists only if there is no interaction", through clarification of the concept of a quantum field [4,5]. To put it roughly, we cannot go beyond the theories for free fields if we stick to the axioms for conventional quantum field theories.

Intensive discussions on the theoretical methods based on classical Clebsch dual (CD) fields have been made in order to go beyond free fields, and a possible mechanism of DP creation has been made clear recently. These discussions have also succeeded in describing several experimental results by quantizing the DP energy [6]. Furthermore, a quantum walk (QW) model has been employed to analyze the spatio-temporal behaviors of the DP energy transfer.

Section 2 reviews the progress in theoretical studies based on category algebras, which serve as the bases of studying the DP [7-9]. Section 3 reviews the mechanism of DP creation based on CD fields. Section 4 reviews the relation between the QW model and the topics in Sections 2 and 3. Section 5 summarizes the discussions in this article.

2. Approaches based on category algebras

A new approach to quantum fields is proposed here to go beyond the free fields mentioned in the previous section [7-9]. The core idea is to deal with quantum fields in terms of noncommutative category algebra over a rig (ring without negatives). It is an algebraic system equipped with addition and multiplication, where the category and the rig correspond to the relativity aspect and the quantum aspect of nature, respectively. By utilizing category algebra and states on categories instead of simply considering categories, the two aspects above can be directly integrated as a category theoretic structure and as a noncommutative probabilistic structure, respectively. Through this integration, it is expected that quantum fields can be understood as the most fundamental entities in modern physics.

2.1 Treating relativity

Since the essence of relativity is nothing but the structure of possible relationships between possible events, what really matters are causal relationships [10]. For these relationships, there is an interesting order-theoretic approach to spacetime (for example, the causal set approach [11]). Furthermore, to deal with the off-shell nature of quantum fields, which seems to be essential in modelling interacting fields in space-time, one needs to take into consideration not only causal relationships but also more general relationships between spacelike events.

The strategy proposed here is to use a category C, which is a generalization of both ordered sets (causality structures) and groups (symmetry structures), as relativity in a generalized sense.
More concretely, the notion of causal category equipped with a partial involution structure is identified as the generalized relativity structure.

2.2 Treating quantum fields

To combine the relativity structure above with quantum theory (which can be modelled by noncommutative rigs, effectively by noncommutative algebras over C), noncommutative algebras are required to reflect the structures of categories. Category algebras are just such algebras. They are generalized group algebras because categories are generalized groups.

Importantly, the category algebras can be considered as generalized matrix algebras over R as well as generalized polynomial algebras [9], which provides a platform for concrete and flexible studies and calculations. The category algebras have rich structure as covariance and local structure of

subalgebras that reflect the causal and partial involution structure of the category. By focusing on these structures, one can also see the conceptual relationship between the present approach and the preceding approaches, such as algebraic quantum field theory [12,13] and topological quantum field theory [14,15].

After a quantum field is identified as a category algebra over a rig, the next problem is how to define a state of it. In general, the notion of state on *-algebra over C is defined as a positive normalized linear functional. The states on category algebras are called states on categories. More generally, defining a state on category (whose support is contained in a subcategory with finite numbers of objects) is equivalent to defining the corresponding function that assigns the weight to each arrow. By considering such states, a quantum mechanical system can be seen as an aspect of the quantum field.

For the study of quantum fields, a localized notion of state or a local state [16,17] is a key concept. The counterpart of the notion can be defined as the system of states on certain subalgebras of category algebras, called local algebras.

3 A novel theoretical model for dealing with interaction and longitudinal mode

As was pointed out at the beginning of Section 1, the DP is a localized quantum field whose size is much smaller than the wavelength of light. That is to say, the DP originates from an off-shell electromagnetic field. Furthermore, it should be pointed out that this field is associated with the longitudinal Coulomb mode, which plays an important role in light–matter interaction [6,18].

On the other hand, conventional propagating light is an on-shell electromagnetic field that can be observed in a macroscopic-sized region. It belongs to the visible sector and corresponds to a transverse mode photon. Conventional quantum electrodynamics have treated this mode, while the longitudinal mode has been excluded as an unphysical quantity. However, Ojima re-examined the quantization processes of the electromagnetic field and found that the longitudinal mode had to be included as a physically indispensable non-particle mode that plays an essential role in electromagnetic interaction [19,20]. This section reviews the novel theory constructed to deal with the interaction and the longitudinal mode [6].

3.1 Requiring spacelike momenta

Such a novel theory has to meet the requirement that has been stated by the Greenberg-Robinson (GR) theorem [21,22]. This theorem has been used to distinguish nonlinear field interactions from the free time evolutions of non-interacting modes. It states that *if the Fourier transform* $\phi(p)$

$\phi(x)$ *(p and* x

p_μ *with* $p_\nu p^\nu < 0$ (the sign convention of the Lorentzian metric

signature $(+---)$ is employed), *then* $\phi(x)$ *is a generalized free field*. Although spacelike momenta are often associated with tachyons breaking Einstein causality, it is known that there exist certain types of causal motions having spacelike momenta.

The arguments above have revealed that spacelike momenta must be considered, while the classical longitudinal mode is closely related to virtual photons as the mediator of the longitudinal Coulomb force. More concretely, if the field is represented by a four-dimensional momentum p^μ, the GR theorem claims that not only the timelike and lightlike momenta ($p_\nu p^\mu \geq 0$) but also the spacelike momenta ($p_\nu p^\mu < 0$) are required for the interaction,.

Furthermore, the Haag theorem in Section 1 has claimed that such an interacting field (i.e., the Heisenberg field [23]) cannot be analytically connected to the propagating linear wave with unitary time evolution. Thus, it is a "no-go theorem" for the theoretical description of "interaction". In other words, no theories for "interaction" have ever existed so far.

3.2 Augmented electromagnetic theory for connecting to the spacelike region

The Maxwell equations can be expanded to the spacelike momentum region by using the CD field because this can introduce the longitudinal mode into the electromagnetic theoretical formulation. By this expansion, the conventional Maxwell equations can be analytically connected to the spacelike momentum region, and the longitudinal mode can be dealt with.

The lightlike CD field is represented by [1,6,18]:

$$\hat{T}_\mu^\nu = S_{\mu\sigma} S^{\nu\sigma} = \rho C_\mu C^\nu , \tag{1a}$$

$$\partial_\nu \hat{T}_\mu^\nu = 0 , \tag{1b}$$

and

$$\rho \equiv L_\tau L^\tau < 0 , \tag{1c}$$

where $S_{\mu\sigma}$ is the field strength. C_μ and L_μ are gradient vectors of the Clebsch variables that are introduced by

$$\partial_\nu \hat{T}_\mu^\nu = F_{\mu\nu} \partial_\sigma F^{\nu\sigma} = F_{\mu\nu} (-\partial^\sigma \partial_\sigma A^\nu + \partial^\nu (\partial_\sigma A^\sigma)) = 0 , \tag{2a}$$

$$\phi := \partial_\sigma A , \ \ \partial^\tau \partial_\tau \phi = 0 , \ \ C_\mu := \partial_\mu \phi , \tag{2b}$$

$$\partial^{\tau}\partial_{\tau}\lambda-\left(\kappa_0\right)^2\lambda=0\,,\;\; L_{\mu}\coloneqq\partial_{\mu}\lambda\,,\;\; C^{\nu}L_{\nu}=0\,, \tag{2c}$$

and

$$U_{\mu}=\lambda C_{\mu}\,,\;\; S_{\mu\nu}=\partial_{\mu}U_{\nu}-\partial_{\nu}U_{\mu}=L_{\mu}C_{\nu}-C_{\mu}L_{\nu}\,. \tag{2d}$$

It should be noted that the term $\partial_{\sigma}A^{\sigma}$ in the Lagrangian

$$L^{*}=L+L_{GF}=-\frac{1}{4}F_{\mu\nu}F^{\mu\nu}-\frac{1}{2}\left(\partial_{\nu}A^{\nu}\right)^2, \tag{3a}$$

and

$$(-\partial_{\sigma}F^{\nu\sigma}+\partial^{\nu}(\partial_{\sigma}A^{\sigma}))\delta A_{\nu}=0\,, \tag{3b}$$

introduced by Fermi, is identical to eqs. (2a) –(2d) if $F_{\mu\nu}\partial^{\nu}(\partial_{\sigma}A^{\sigma})=0$. That is, this term is identical to the classical longitudinal mode that follows the energy–momentum conservation law. Here, by referring to the Nakanishi-Lautrup (NL) formalism on the covariant quantization of the electromagnetic field [20], L_{GF} in eq. (3a) is expressed as

$$L_{GF}=B\partial_{\mu}A^{\mu}+\frac{\alpha B^2}{2}, \tag{4a}$$

$$\partial_{\mu}A^{\mu}+\alpha B=0\,, \tag{4b}$$

and

$$\partial^{\tau}\partial_{\tau}B=0\,. \tag{4c}$$

Since eqs. (3a) and (3b) above can be derived by setting $\alpha=1$ in eqs. (4a) and (4b), the Feynman gauge given by the NL formalism claims that $\partial_{\nu}A^{\nu}$ in eqs. (3a) and (3b) represents the longitudinal mode.

If the four-dimensional vector potential U_{μ} is re-defined by

$$U_{\mu}=\frac{1}{2}(\lambda C_{\mu}-\phi L_{\mu})\,, \tag{5a}$$

$$\partial^{\tau}\partial_{\tau}\lambda-(\kappa_0)^2\lambda=0\,, \tag{5b}$$

$$\partial^{\tau}\partial_{\tau}\phi-(\kappa_0)^2\phi=0\,, \tag{6a}$$

and

$$C^{\tau} L_{\tau} = 0 \tag{6b}$$

for expanding the electromagnetic field from the lightlike to spacelike region, the spacelike U_{μ} with $U^{\tau} U_{\tau} < 0$ satisfies the equation $U^{\tau} \partial_{\tau} U_{\mu} = 0$ that represents motion along a geodesic. Furthermore, the energy–momentum tensor $\hat{G}_{\mu}^{\nu}$, following the conservation law $\partial \nu \hat{G}_{\mu}^{\nu} = 0$, satisfies

$$\hat{G}_{\mu}^{\nu} = -\hat{S}_{\mu\sigma}^{\nu\sigma} + \frac{1}{2} \hat{S}_{\alpha\beta}^{\alpha\beta} g_{\mu}^{\nu} \tag{7a}$$

and

$$\hat{S}_{\mu\nu}^{\sigma\rho} \equiv S_{\mu\nu} S^{\sigma\rho}. \tag{7b}$$

They are isomorphic to the Einstein equation of eqs. (8a) and (8b) below that are represented by the Riemann curvature tensor $R_{\mu\nu}^{\sigma\rho}$:

$$G_{\mu}^{\nu} = \kappa T_{\mu}^{\nu}, \tag{8a}$$

and

$$G_{\mu}^{\nu} = -R_{\mu\sigma}^{\nu\sigma} + \frac{1}{2} R_{\alpha\beta}^{\alpha\beta} g_{\mu}^{\nu}. \tag{8b}$$

By noting the relation between eqs. (7) and (8), and the "quantized space-time" introduced by Snyder [24], and furthermore, by noting the momentum vector

$$\hat{p}^{\nu} (\hat{p}_{\nu})^{*} = -\Lambda_{dS} = const. < 0 \tag{9}$$

in the de Sitter space, it is found that the quantity L_{ν} in the spacelike CD field is the submanifold in the de Sitter space.

If the momentum field satisfies eq. (9), space-time can be quantized, which is consistent with the Lorentz covariance. Therefore, the fact that eqs. (7) and (8) are isomorphic means that the quantization of the spacelike CD field is consistent with the space-time quantization. This means that the classical Maxwell equations were successfully expanded from the lighlike to spacelike momentum region.

3.3 Creation of Majorana field

It should be pointed out that the quantized field corresponding to the spacelike Klein-Gordon equation

$$(\partial^{\nu}\partial_{\nu} - (\kappa_0)^2)\lambda = 0 \tag{10}$$

is given by the Majorana field. To confirm this, let us consider the Dirac equation

$$(i\gamma^{\nu}\partial_{\nu} + m)\Psi = 0, \tag{11}$$

which can be regarded as the "square root" of the timelike Klein-Gordon equation ($(\partial^{\nu}\partial_{\nu} + m^2)\Psi = 0$).

Thus, it can be readily seen that the Dirac equation for eq. (10) is expressed as $i(\gamma^{\nu}\partial_{\nu} + \kappa_0)\Psi = 0$.

It has been reported that for eq. (11), there exists an electrically neutral Majorana representation in which all the components of the matrix γ take purely imaginary values such that it takes the form $((\gamma_{(M)})^{\nu}\partial_{\nu} + m)\Psi = 0$. This equation clearly shows that a Majorana field λ satisfying $(\gamma^{\nu}\partial_{\nu} + \kappa_0)\lambda = 0$ corresponds to the spacelike Klein-Gordon equation (eq. (10)). Reference [25] has explained how a couple of fermionic Majorana fields λ and φ (spin 1/2) can form a bosonic field (spin 1) that corresponds to the CD field. This explanation is based on Pauli`s exclusion principle and corresponds to the orthogonal condition $C^{\tau}L_{\tau} = 0$ (eq. (6b)).

Another important aspect of the quantization is that the length (or wavenumber) must be quantized in the Majorana field [25]. This corresponds to the successful derivation of space-time quantization performed by Snyder [24], who worked on the spacelike momentum field defined on the de Sitter space. As a result, it is confirmed that the Majorana field was derived through this discussion of the CD field.

3.4 Mechanism of dressed photon creation

Since the DP field is created at a point-like singularity, let us consider a case in which a spacelike field λ in eq. (10) is perturbed by the interaction with a point source of the form $\delta(x^0)\delta(r)$, where x^0 and r respectively denote time and the radial coordinate of a spherical coordinate system. The solution can be expressed by the superposition of a spacelike stable oscillatory mode and a timelike unstable mode whose combined amplitude moves at a speed less than the velocity of light. A timelike unstable mode of the solution has the form $\lambda(x^0, r) = \exp(\pm k_0 x^0)R(r)$, where $R(r)$ satisfies

$$R'' + \frac{2}{r}R' - (\hat{\kappa}_r)^2 R = 0, \tag{12a}$$

and

$$(\hat{\kappa}_r) \coloneqq (k_0)^2 - (\kappa_0)^2 > 0 . \tag{12b}$$

Here, $R(r)$ is known as the Yukawa potential

$$R(r) = \exp(-\hat{\kappa}_r)/r , \tag{13}$$

which rapidly falls off as r increases.

A crucial kinematic property that distinguishes quantum mechanics from classical mechanics is the temporal directions of a moving particle and anti-particle. For an electrically neutral Majorana particle field, this property corresponds directly to time reversal, which means that a couple of unstable fields $\lambda(x^0, r) = \exp(\pm k_0 x^0) R(r)$ in the classical system can be reinterpreted as a particle and anti-particle pair in a quantum mechanical system. Thus, the argument above shows that a pair consisting of a timelike Majorana particle and an anti-particle pops up at the origin $r = 0$ as a result of field interactions between the field given by eq. (10) and $\delta(x^0)\delta(r)$. However, since these particle fields are non-propagating, the mechanism of pair annihilation would occur instantly to produce a small light field with a spatial distribution $R(r)$. This light field, which is the genesis of the DP, is a timelike quantum field and belongs to the visible sector. It should be noted again that such a small spatial DP field originates from a transition of the spacelike momentum of the Majorana field into a timelike one.

However, this small DP cannot be observed in the macroscopic area because it is much smaller than the wavelength of conventional propagating light. That is, its size is beyond the diffraction-limit for measurement. For measurement, the DP field must be disturbed to create free photons (propagating light) by inserting a probe into the DP field.

3.5 Maximum size of the dressed photon

Since a quantum mechanical discussion has shown that k_0 in $\exp(\pm k_0 x^0)$ and in eq. (12b) is the energy of a given system, the quantization of the Majorana field suggests that the wavenumber quantization with $Min[k_0] = \kappa_0$ $(, \Delta k_0 = \kappa_0)$ is advantageous because it is similar to the well-known energy quantization $E = h\nu$. Thus, it is found that this wavenumber quantization is valid for the quantum version of eq. (12b). That is, the quantized DP energy $E_{DP,n}$ is expressed as $E_{DP,n} \propto (\kappa_r)^2 = n(\kappa_0)^2$, where $n(= 1, 2, 3, - - -)$ is a quantum number.

The advantage of the radial distribution given by $R(r)$ (eq. (13)) shows that this distribution has a clear-cut minimum value κ_0 of $\hat{\kappa}_r$ (refer to eq. (12b)). The existence of such a minimum wavenumber κ_0 means that there exists a maximum size of the DP defined by

$$L_{\max}^{DP} \coloneqq \frac{1}{\kappa_0} \tag{14}$$

whose value has been evaluated experimentally to be 40–70 nm [26]. Here, $L_{\max}^{DP}$ is called the DP constant [6,18]. From the viewpoint of a new natural unit system in which all the magnitudes of the Planck constant h, light velocity c, and $L_{\max}^{DP}$ are set to unity, the importance of this length has been discussed by Sakuma and Ojima [27]. They showed that $L_{\max}^{DP}$ gives the geometrical mean of the smallest Planck length and the largest length associated with a newly modified cosmological constant, related to their dark energy model defined by the ground state of a spacelike Majorana field and to their novel dark matter model defined solely by the Weyl conformal tensor field, respectively.

3.6 Conversion from dressed photon to bullet-like propagating light

In the case of a pair annihilation involving anti-parallel spins, the created DP has a spin 0. Specifically, the discussions of the DP in the preceding sections suggest the possibility that the light converted from the DP can be a unique light field with spin 0, which behaves as a particle. This particle-like behavior has been supported by the Wightman theorem [28] stating that: *A Lorentz or Galilei covariant massive system is always localizable. For the Lorentz case, the only localizable massless elementary system (i.e., irreducible representation) has spin 0.* Here, localizability means that a position operator can be defined for this system.

The lightlike CD field can be described by the system of eqs. (1) and (2), in which the field strength $S_{\mu\nu}$ is given by bivectors C_ν and L_ν, that satisfy the orthogonality condition $C_\nu L_\nu = 0$ (eq. (6b)). In this case, it is assumed that L_ν is a spacelike vector. Notice, however, that the orthogonality condition $C_\nu L_\nu = 0$ is also satisfied in the case of $L_\nu = C_\nu$ since C_ν is a null vector. Of course, in this case, the vortical field strength $S_{\mu\nu}$ vanishes. Recall that, quantum mechanically, the C_ν field is a Majorana field with spin 1/2; thus, a couple of anti-parallel C_ν fields with spins 1/2 and −1/2 can be combined to yield a null energy–momentum current $C_\mu C^\nu$ ($\hat{T}_\mu^\nu = \rho C_\mu C^\nu$ in eq. (1a)) with spin 0, which can be regarded as a unique bullet-like light field with spin 0.

3.7 Experimental verification

This subsection reviews results of experiments that were carried out to verify the behaviors of emitted light described in the previous section [6]. As background information for the present experiment, Wada et al. [29] showed that a silicon-LED (1.3–1.6 μm wavelength), successfully fabricated by a novel fabrication technology named DPP-assisted annealing, worked as a relaxation oscillator upon

the injection of direct current to emit an optical pulse train whose duration and repetition frequency were about 50 ps and 1 GHz, respectively.

The experiments were carried out by following the well-known Hanbury Brown-Twiss method [30]. A similar experiment has been carried out to check the behavior of a single photon in a nanometer-sized semiconductor logic gate whose signal was controlled by using DPs [31]. For the present experiment, highly sensitive superconducting single-photon detectors were used to measure the temporal behavior of the infrared light emitted from small light sources in the LED.

The values of the second-order cross-correlation coefficient (CC) were measured as a function of the difference τ between the arrival times of the photons at the two independent photon detectors. The measured results showed two features: One was that the value of CC was smaller than unity in the range of time difference $|\tau| < 20$ ns. This indicates the photon anti-bunching phenomenon, which is an inherent feature of a single photon. The other was that the CC took a nonzero value at $\tau = 0$ even though it is smaller than 1×10^{-2}. This nonzero value is attributed to the photons emitted from multiple light sources located in close proximity with each other in the LED.

These two features suggest that a cluster of photons emitted from the LED behaves as a single photon. It is named DP-cluster light and is closely related to the localizable property of the spin 0 particle. Namely, if the observable positions of given spin 0 quantum particles are sufficiently close, the cluster of these particles would behave as if it were a single quantum particle with the accumulated amount of energy.

The original motivation of embarking on the DP study was to generate a diffraction-free small light field. However, the experimental verification above gives another suggestion, that is, such a peculiar propagating light field exists, whose energy-momentum tensor has exactly the same form as a free particle. If that is the case, a light beam consisting of such a light field would behave as a bullet and be free from diffraction. It is well known that a laser beam employing conventional transverse light waves is unavoidably diffracted. Although there exists a certain class of diffraction-free mode-solutions [32] for transverse light waves, these solutions should not be confused with the above-mentioned peculiar light field that is intrinsically diffraction-free. In regard to this peculiar light field, it is further conjectured that the mechanism of DP-cluster light may be involved in γ -ray bursts, one of the cosmological enigmas, as an intermittent extremely high-energy radiation with strong directionality that reaches the earth after travelling over an enormous distance of several billions of light years.

4. Quantum walk model for the energy transfer of dressed photon

Experimental studies have confirmed that the DP, created on one NP by light irradiation, hops to the adjacent NP. That is, the DP energy transfers from one NP to the adjacent one. This transfer originates from the interaction between the NPs mediated by the DP.

Creation and annihilation operators for the DP are required to describe this transfer. However, conventional quantum field theories have never succeeded in deriving them. This is because the DP is an interacting quantum field, for which the interaction is a nonlinear event. Conventional creation and annihilation operators have been derived only for the linear system. As long as these operators are not derived for the nonlinear interacting field, the origin of the pair-annihilation of the aforementioned Majorana particle and anti-particle will remain unknown.

However, since the created DP is a timelike boson field and since it spatially localizes at the NP, it is expected that experimentally confirmed spatio-temporal behaviors of the DP energy transfer can be described by using a QW model. A QW model for a quasi-particle, whose behavior is described by the Klein-Gordon equation, has been studied [33]. With future progress in this study, it is expected that the theory of DP creation described in the previous section and the QW model for DP energy transfer can be connected consistently. Furthermore, it is expected that this connection will enable the construction of a novel theory that can systematically describe the creation, energy transfer, and detection of the DP to identify the origins of a variety of experimentally confirmed phenomena.

Concrete dynamics of quantum fields can be modeled as a sequence or flow of the states on a category. A QW is a typical example of describing such dynamics [34,35]. The notion of a QW on general *-algebras and quantum walks on +-categories can be defined as follows: Let A be a *-algebra. A sequence of states given by $\varphi^t(\alpha) = \varphi((\omega^*)^t \alpha \omega^t)$ where $t = 0,1,2,3,...$ generated by a unitary element $\omega \in R[C]$, i.e. an element satisfying $\omega^* \omega = \omega \omega^* = \varepsilon$, is called a quantum walk on A.

A QW can be considered as a sequence of state vectors through a Gel'fand-Naimark-Segal (GNS) construction. Numerical calculations have been embarked on [36] to analyze the DP energy transfer phenomena. It should be noted that the DP cannot be understood without focusing on the off-shell nature of quantum fields [37]. This means that the aspects of quantum fields cannot be described as a collection of the modes which satisfies the on-shell condition, and that a QW on categories may become important in quantum field theory.

5. Summary

A new approach to quantum fields was proposed in terms of category algebras and states on categories. Quantum fields and their states were respectively defined as category algebras and states on causal categories with partial involution structures. It was pointed out that, by utilizing category algebra and states on categories, relativity and quantumness can be directly integrated as a category theoretic structure and as a noncommutative probabilistic structure, respectively.

Based on a CD field theoretical model, it was made clear that a DP field originates from a transition of the spacelike momentum of the Majorana field to a timelike one. This model succeeded in deriving a maximum size of the DP that has been already found by experimental studies. This size

was named the DP constant. It was found that, in the case where paired timelike Majorana particle and anti-particle have anti-parallel spins, pair annihilation creates a DP with a spin 0. The light converted from this DP can be a unique light field with spin 0, which behaves as a particle. It was experimentally confirmed that a cluster of photons emitted from an Si-LED behaved as such a particle and is named DP-cluster light.

A QW model was employed to analyze the experimentally confirmed phenomena of DP energy transfer between NPs. Its theoretical bases were reviewed based on the theory of category.

Acknowledgements

The author thanks Drs. H. Sakuma (Research Origin for Dressed Photon), H. Saigo (Nagahama Inst. Bio-Sci. and Tech.), and T. Kawazoe (Nichia Corp.) for their support in theoretical and experimental studies, respectively.

References

[1] Ohtsu, M. *Off-Shell Application in Nanophotonics,* Elsevier, Amsterdam, Netherland, 2021.

[2] Haag, R. On Quantum Field Theory. Dan. Mat. Fys. Medd.1955,29,12.

[3] Hall, D. and Wightman, A. S. A Theorem on Invariant Analytic Functions with Applications to Relativistic Quantum Field Theory. Mat. Fys. Medd. Dan. Vid. Selsk.1957, 31,5.

[4] Streater, R. F. and Wightman, A.S. PCT, Spin and Statistics, and All That, Princeton University Press, 2000.

[5] Haag, R. *Local Quantum Physics*, second edition, Springer Verlag, 1996.

[6] Sakuma, H., Ojima, I., Ohtsu, M. and Kawazoe, T: Drastic advancement in nanophotonics achieved by a new dressed photon study. *J. European Opt. Soc.: RP*. (2021) **17**:28.
https://jeos.springeropen.com/articles/10.1186/s41476-021-00171-w

[7] Saigo, H. Quantum Fields as Category Algebras. Symmetry 2021, 139, 1727. https://doi.org/10.3390/sym13091727

[8] Saigo, H. and Nohmi, J. Categorical Nonstandard Analysis. Symmetry 2021, 13, 1573.
https://doi.org/10.3390/sym13091573

[9] Saigo, H. Category Algebras and States on Categories. Symmetry 2021, 13 7, 1172.
https://doi.org/10.3390/sym13071172

[10] Gogioso, S., Stasinou, E. and Coecke, B. Functorial Evolution of Quantum Fields. Front. Phys. 2021, 9:534265.

[11] Bombelli, L., Lee, J., Meyer, D. and Sorkin, R. D. Space-time as a causal set. Physical review letters 1987, 59(5):521.

[12] Haag R. and Kastler D. An algebraic approach to quantum field theory. J. Math. Phys. 1964, 5 848-861.

[13] Haag, R. *Local Quantum Physics*, second edition, Springer Verlag, 1996.

[14] Atiyah, M. Topological Quantum Field Theories. Publications Math_ematiques de l'Institut des Hautes Scienti_ques 1988, 68 175-186.

[15] Witten, E. Topological Quantum Field Theory. Commun. Math. Phys. 1988, 117 353-186.

[16] Werner, R. F. Local preparability of states and the split property in quantum field theory. Lett. Math. Phys. 1987 13, 325-329.

[17] Ojima, I., Okamura, K. and Saigo, H. Local State and Sector Theory in Local Quantum Physics. Lett. Math. Phys.

2016 106, 741-763.

[18] Sakuma, H, Ojima, I, Ohtsu, M, Ochiai, H: Off-shell quantum fields to connect dressed photons with cosmology. Symmetry 12, 1244 (2020). Doi:10.3390/sym12081244.

[19] Ojima, I: Nakanishi-Lautrup B-Field, Crossed Product & Duality. RIMS Kokyuroku 1524, 29–37 (2006).

[20] Nakanishi, N, Ojima, I: *Covariant Operator Formalism of Gauge Theories and Quantum Gravity*. World Scientific, Singapore (1990).

[21] Jost, R: The General Theory of Quantized Fields. Amer. Math. Soc. Publ., Providence (1963).

[22] Dell'Antonio, GF: Support of a field in p space. J. Math. Phys. 2, 759–766 (1961).

[23] Lehmann, H., Symanzik, K. and Zimmermann, W., Zur Formulierung quantisierter Feldtheorem, Nuovo Chim. **1**, 425 (1955).

[24] Snyder, H.S.: Quantized space-time. Phys. Rev. 71, 38 (1947).

[25] Sakuma, H., Ojima, I., Ohtsu, M. and H. Ochiai, "Off-Shell Quantum Fields to Connect Dressed Photons with Cosmology," *Symmetry*, vol.12, no.8 (2020) 1244. DOI:10.3390/sym12081244

[26] Ohtsu, M. "History, current development, and future directions of near-field optical science," *Opto-Electronic Advances*, vol.3, no.3 (2020)190046. DOI: 10.29026/oea.2020.190046

[27] Sakuma, H. and Ojima, I. "On the Dressed Photon Constant and Its Implication for a Novel Perspective on Cosmology," *Symmetry* **2021**, 13, 593. https://doi.org/10.3390/sym13040593

[28] Wightman, A.S.: On the localizability of quantum mechanical systems. Rev. Mod. Phys. 34, 845 (1962).

[29] Wada, N., Kawazoe, T. and Ohtsu, M. "An optical and electrical relaxation oscillator using a Si homojunction structured light emitting diode." *Appl. Phys. B*, 108(2012) 25-29.

[30] Hanbury Brown, R. and Twiss, R.Q. "A Test of New Type of Stellar Interferometer on Sirius." *Nature*. 178 (4541) (1956) 1046-1048.

[31] Kawazoe, T., Tanaka, S. and Ohtsu, M. "A single-photon emitter using excitation energy transfer between quantum dots". *J. Nanophotoics* 2 (2008) 029502 1-6.

[32] Durnin, J., Miceli, J. J. Jr., Eberly, J. H.: Diffraction-free beams. *Phys. Rev. Lett.* **58**, 1499 (1987).

[33] Arrighi, P. and Facchini, S. "Decoupled Quantum Walks, models of the Klein-Gordon and wave equation," arXiv:1309.773v1 [quanut-ph] 30 Sep 2013

[34] Ambainis, A. Quantum walk algorithm for element distinctness. In: Proc. of the 45th IEEE Symposium on Foundations of Computer Science (FOCS), 22-31. (2004)

[35] Konno, N. Quantum Walks. In: *Quantum Potential Theory*, Franz, U., and Schürmann, M., Eds., Lecture Notes in Mathematics, 1954, 309-452, Springer-Verlag, Heidelberg, 2008.

[36] Ohtsu, M. "A Quantum Walk Model for Describing the Energy Transfer of a Dressed Photon," *Off-shell Archive* (September, 2021) OffShell: 2109R.001.v1.

DOI 10.14939/2109R.001.v1, http://offshell.rodrep.org/?p=345

[37] Hamano, M. and Saigo, H, Quantum Walk and Dressed Photon. Electronic Proceedings in Theoretical Computer Science 2020, 315, 93-99.

[V] PUBLISHED BOOKS

symmetry

Quantum Fields and Off-Shell Sciences

Edited by

Motoichi Ohtsu

Printed Edition of the Special Issue Published in *Symmetry*

www.mdpi.com/journal/symmetry

MDPI

Quantum Fields and Off-Shell Sciences

Quantum Fields and Off-Shell Sciences

Editor

Motoichi Ohtsu

MDPI • Basel • Beijing • Wuhan • Barcelona • Belgrade • Manchester • Tokyo • Cluj • Tianjin

Editor
Motoichi Ohtsu
Research Origin for Dressed
Photon, 3-13-19 Moriya-cho,
Kanagawa-ku, Yokohama,
Kanagawa 221-0022, Japan

Editorial Office
MDPI
St. Alban-Anlage 66
4052 Basel, Switzerland

This is a reprint of articles from the Special Issue published online in the open access journal *Symmetry* (ISSN 2073-8994) (available at: https://www.mdpi.com/journal/symmetry/special_issues/Quantum_Fields_Off-Shell_Sciences).

For citation purposes, cite each article independently as indicated on the article page online and as indicated below:

LastName, A.A.; LastName, B.B.; LastName, C.C. Article Title. *Journal Name* **Year**, *Volume Number*, Page Range.

ISBN 978-3-0365-5197-5 (Hbk)
ISBN 978-3-0365-5198-2 (PDF)

Contents

About the Editor

Motoichi Ohtsu

Motoichi Ohtsu (Director-in-chief of the Research Origin for Dressed Photon; Professor Emeritus, University of Tokyo and Tokyo Institute of Technology) received his Dr. Eng. Degree from the Tokyo Institute of Technology, Tokyo, in 1978. He was first appointed as a research associate, then an associate professor in 1982. From 1986 to 1987, while on leave from the Tokyo Institute of Technology, he joined the Crawford Hill Laboratory, AT&T Bell Laboratories, Holmdel, New Jersey, USA. In 1991, he became a professor at the Tokyo Institute of Technology. In 2004, he moved to the University of Tokyo as a professor. He has been the leader of the "Photon Control" project (1993–1998: the Kanawaga Academy of Science and Technology, Kanagawa, Japan), the "Localized Photon" project (1998–2003: ERATO, JST, Japan), the "Terabyte Optical Storage Technology" project (2002–2006: NEDO, Japan), the Near Field Optical Lithography System" project (2004–2006: Ministry of Education, Japan), the "Nanophotonics" team (2003–2009: SORST, JST, Japan), the "Innovative Nanophotonics Components Development" project (2006–2011: NEDO, Japan), the "Nanophotonics Total Expansion: Industry-University Cooperation and Human Resource Development" project (2006–2011: NEDO, Japan), and the "Development of a solar cell technology using dressed photons" project (2012–2014, NEDO, Japan).

Dr. Ohtsu has written over 588 papers and received 83 patents. He is the author, co-author, and editor of 85 books, including 46 in English. In 2000, He was appointed as President of the IEEE LEOS Japan Chapter. From 2000, he has been an executive director of the Japan Society of Applied Physics. His main fields of interests are off-shell science and dressed photon technology. He is a fellow of the Optical Society of America. He is also a fellow and life member of the Japanese society of Applied Physics. He is a member of the American Physical Society and the Laser Society of Japan. He has been awarded 21 prizes from academic institutions, including the Issac Koga Gold Medal of URSI in 1984; the Japan IBM Science Award in 1988; two awards from the Japan Society of Applied Physics in 1982 and 1990; the Inoue Science Foundation Award in 1999; the Japan Royal Medal with Purple Ribbon from the Japanese Government in 2004; the H. Inoue Award From JST in 2005; the Distinguished Achievement Award from the Institute of Electronics, Information and Communication, Engineering of Japan in 2007; the Julius Springer Prize for Applied Physics in 2009; the Okawa Publications Prize in 2016; and the IAAM Medal from the International Association of Advanced Materials in 2018.

He served as the committee member of 18 international conferences, including the Chair of the Executive Committee, the German–Japanese Symposium on Nanophotonics; the Chair of the Executive Committee, The US–Japan Symposium on Nanophotonics; the Chair of the Program Committee, the International Near-Field Optics Conference; the Chair of the Organizing Committee, the Asia-Pacific Near Field Optics Workshop; and the Chair of the Program Committee, the Pacific Rim Conference on Lasers and Electro-Optics.

Preface to "Quantum Fields and Off-Shell Sciences"

Intensive experimental studies on light–matter interactions and their associated technological breakthroughs, especially conducted in the field of dressed photon research, have led to a growing concern regarding unsettled off-shell quantum field interactions. In order to respond to the demand of this new tide of scientific progress, a new initiative has been recently launched. The Special Issue, entitled "Quantum Fields and Off-Shell Sciences", was organized in the academic journal *Symmetry* to promote the progress of such research activities from a wider perspective, not necessarily limited to dressed photon studies. The scope of the Special Issue covered quantum probability theory, quantum walk modeling, quantum measurement theory, micro–macro duality, category theory, dynamics, the vortex structure of spacetime, off-the-mass-shell property of quantum field and symmetry, and/or symmetry breaking in quantum fields.

Eleven excellent original papers were successfully accepted for publication via an impartial peer-review process. This book contains these published papers. It will provide scientific and technical information on the quantum fields and off-shell sciences to scientists, engineers, and students who are and will be engaged in this field.

Motoichi Ohtsu
Editor

ドレスト光子の深わかり

異次元の光の科学と技術を味わう

大津 元一　著

杉浦　聡　編

ナノフォトニクス工学推進機構　発行

まえがき

2014年に上梓した前著『ドレスト光子はやわかり』(丸善プラネット)は、ナノ寸法の小さな光であるドレスト光子(dressed photon：DP)の原理と応用を駆け足で紹介する読み物でした。その後、読者諸兄からもう一歩踏み込み「深わかり」するための読み物が欲しいとの希望が寄せられました。それに応え、紹介書と専門書の間をつなぐ書籍として記したのが本著です。前著の続編と考え、前著と同様、まず第Ⅰ部では原理について、しかし前著より少し詳しく説明しています。第Ⅱ部では応用技術について、前著との重複を避けつつ前著出版後にさらに進展した技術を中心に説明してあります。これにより前著の副題であった「異次元の光技術」をさらに実感していただければ幸いです。

さて、前著との違いは第Ⅲ部を加えたことです。ここでは第Ⅰ部の原理の説明では実は不十分なので、DPをきちんと説明するための新しい科学を紹介します。それは「オフシェル科学」と呼ばれていて、従来の光科学である「オンシェル科学」とは相互補完の関係にあります※。すなわち両者は重複せず、非なるものです。実は第Ⅰ部での説明には、オンシェル科学を修正して使ったのでした。オフシェル科学によりDPの素性が明らかになり、そしてさらなるアイディアが形になり、従来の光技術の限界を超えて未来を拓くのです。

最後に、オフシェル科学研究にご協力いただいた小嶋泉氏、佐久間弘文氏（一般社団法人ドレスト光子研究起点）、西郷甲矢人氏（長浜バイオ大学）、瀬川悦生氏（横浜国立大学）、岡村和弥氏（名古屋大学、ドレスト光子研究起点）および関連の皆様に感謝いたします。そして著者の亡父母の春男と範子、さらに妹の公子にも。

本書執筆の企画立案後、出版に至るまでご協力とご援助を賜ったアドスリー編集部の皆様に感謝します。

2022年5月
大津 元一

※オフシェル科学の進展の様子は https://www.rodrep.or.jp をご覧ください。

目 次

[VI] PRESENTATIONS

IN DOMESTIC CONFERENCES

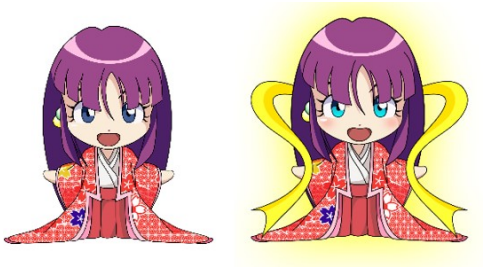

26Cp-2

SiC 空間光変調器が示す巨大偏光回転機能の評価
Evaluation of giant polarization rotation with a SiC spatial light modulator

九州大学大学院システム情報科学府 Du Haoze、竹田 晴信、竪 直也、興 雄司、林 健司
日亜化学工業株式会社 門脇 拓也、川添 忠　　ドレスト光子研究起点 大津 元一
Kyushu Univ. : H.Du, H.Takeda, N.Tate, Y.Oki, K.Hayashi
Nichia Corp. : T.Kadowaki, T.Kawazoe　Research Origin for Dressed Photon : M.Ohtsu
E-mail : duhaoze@laserlab.ed.kyushu-u.ac.jp

1. 研究の背景と目的

磁気光学効果を用いた空間光変調器（SLM）は光通信や光学記録媒体，ホログラフィなどへ広く応用されている．そのような中で近年，間接遷移型半導体を用いた SLM が開発された．すなわち Al 原子をドープした 4H-SiC 結晶にドレスト光子援用アニールを施して SiC-SLM が製作され，それは可視域において注入電流に対する巨大な偏光回転機能（ベルデ定数が 9.5×10^4 rad/T.m）を示した[1]．本発表ではハイパースペクトル計測応用を指向し，SiC-SLM の空間変調時における偏光回転機能のデバイス内空間分布を評価した結果について報告する．

2. 実験

開発された SiC-SLM（3 mm 窓径）デバイスは表面のループ状電極に励磁電流を流し入射光と平行な磁界を発生させることで偏光回転を実現する．このデバイス全面での偏光回転の空間依存性を評価するため，2 つのグラントムソンプリズムを直交させたクロスニコル光学系でデバイスを挟み，波長 457 nm の LD 励起固体レーザーの直線偏光を入射して CMOS センサーで透過画像を観測した．励磁電流源は交流変調が可能な NF-EC750SA（NF 回路設計ブロック）を用いた．

3. 結果と考察

透過光画像例を Fig.1(a)に示す．励磁電流は 600 mA で，明るい部分，暗い部分は偏光回転角が各々$n\pi$，$(2n+1)\pi/2$ と推定できる．次に画像の一部（半径 30 μm の円内）に着目して，励磁電流を三角波変調(0.05 Hz)したときの透過光強度波形を Fig.1(b)に示す．波形は異なる二つの周期での変調が重畳している様に見える．周期が短い成分を偏光回転による変化と仮定して，見積もられた偏光回転角を電流に対してプロットすると Fig.1(c)が得られた．ここでは偏光回転角の励起電流依存性が非線形を示し，さらにヒステリシス特性も示した．発表では検討している本 SiC-SLM デバイスの偏光回転モデルについても述べる．本研究は科研費(22H04952)の助成を受けて行われました．

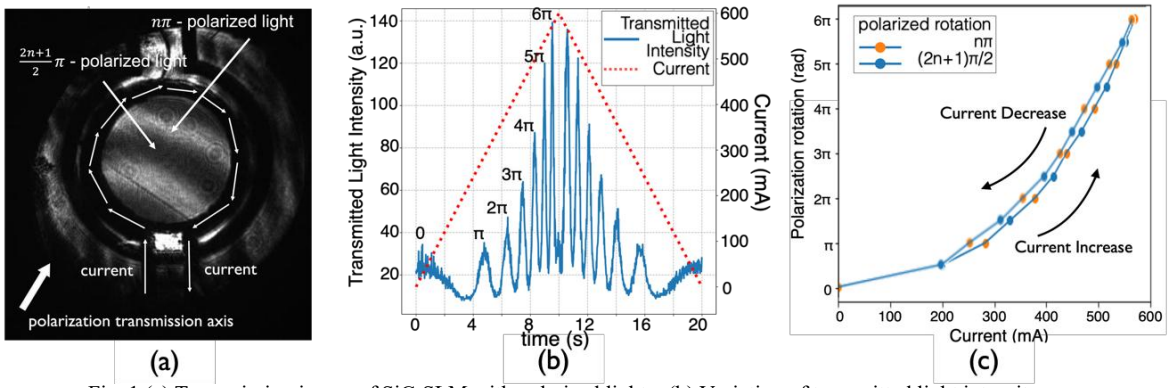

Fig. 1 (a) Transmission image of SiC-SLM with polarized light　(b) Variation of transmitted light intensity as a function of time (current)　(c) Polarization rotation angle as a function of current.

参考論文

[1] T.Kadowaki, *et. al.,* Scientific Reports, Vol. 10, 12967 (2020)

16pAS2

ドレスト光子の生成過程とそのエネルギー移動
Creation and Energy Transfer of Dressed Photon

°*大津元一
°* Motoichi Ohtsu

（一般社団法人）ドレスト光子研究起点
Research Origin for Dressed Photon
*ohtsu@rodrep.or.jp

Based on a Clebsch dual field theoretical model, it is made clear that a dressed photon (DP) originates from a transition of the spacelike momentum of the Majorana field to a timelike one. The DP energy transfer , a unique phenomenon observed as a complex system, is described by a quantum walk model. It is demonstrated that the calculated results show agreements with the experimental ones.

1. はじめに

ドレスト光子（DP）はナノ寸法の物質粒子（NP）に光を照射すると生成しNPに局在する．その寸法はNPの寸法に相当し照射光波長より小さい． 従ってその運動量は大きな不確定性を有し， DP の分散関係が定義できない． 即ち質量シェルから逸脱したオフシェルの量子場である． 更にDPはナノ寸法空間における光子， 電子， フォノンの相互作用の結果生成するので，DP場には縦クーロンモードが付随する． 一方,従来のオンシェル科学では分散関係， モードなどの概念に基づき巨視的寸法空間にて観測可能な伝搬光を扱ってきた.これは横モード光子を扱い， 縦モード光子は非物理的な量として排除されてきた． この事情からDPの発生過程を記述するには相互作用， 縦モードを記述しうる新しい科学が必要であり， それはオフシェル科学と呼ばれる． 急進展するオフシェル科学により最近では DP の生成過程が明らかになった [1)]．生成後のDPは複数のNPの間を移動することから，DPエネルギー移動は複雑系の現象として考える必要がある．その記述のために最近では量子ウォーク（QW）モデルが必要であることが明らかになった [2)]．

2. DPの生成過程

電磁場理論に縦モードを導入して相互作用を記述するためにClebsch双対（CD）場モデルが導入された．そのspacelike場とlightlike場を組み合わせて場のエネルギー・運動量テンソルが導出され，マクスウェル方程式がspacelike運動量域に解析接続された． またCD場のspacelikeディラック方程式はマヨラナ場の方程式に等しいことから， CD場はマヨラナ場に対応することが明らかになった． 以上をもとにDPの生成過程が説明された． 即ち CD 場の spacelike クライン・ゴルドン方程式に点状の摂動が加わるとspacelike運動量場とtimelike運動量場の組み合わせが生成され，特異点における光・物質相互作用の結果spacelikeマヨラナ場からtimelikeマヨラナ粒子と反粒子の対が生成する． そしてこの対の消滅によりボゾン場が発生するが，これがDPである．

3. DPのエネルギー移動

QWモデルによる解析の第一歩としてDPの生成の実験に使われるファイバプローブ先端でのDPの生成効率が求められた．DPは物質中を移動する際，原子間を跳躍（跳躍エネルギーJ）しつつ，フォノンを励振しそれと結合（結合エネルギーχ）してDPフォノン(DPP)を形成する． 今回のQWモデルでは2次元格子中を互いに反対方向に移動するDPの確率振幅と局在フォノンの確率振幅からなる3元ベクトルを扱い，これをDPPの存在確率振幅とした． この確率振幅の時間空間発展方程式を与えるユニタリ行列Uの一般化のために位相角ξを用いて複素数化した[$U(\xi)=\exp(i\xi)U$]．数値計算のパラメータはχ/Jとξである.その結果生成効率はファイバプローブ斜面からの光エネルギーの散逸を抑圧すると大きくなること，ファイバプローブ頂角の増加とともに大きくなることが導出され,これらは実験結果と整合した.

4. まとめ

オフシェル科学によりDPの生成過程が明らかになり，QWモデルによりエネルギー移動過程の特徴が記述された．その計算結果は実験結果と整合した.

参考文献

1) H. Sakuma and I. Ojima: Symmetry,**13** (2021) 593.
2) M. Ohtsu, T. Kawazoe and H. Saigo: Off-Shell Archives, Offshell 1710R. 001.v1, (2017).

16pAS3

量子ウォークが定常状態になるまでの時間
A convergence time of quantum walk

瀬川 悦生
Etsuo Segawa

横浜国立大学(環境情報)
Graduate School of Environment and Information Sciences,
Yokohama National University
segawa-etsuo-tb@ynu.ac.jp

There are similarities to the behaviors of the energy transfer of dressed photon in the stationary state of quantum walks. Then in this talk, to find more detailed mathematical structure in this dynamical system, we estimate a convergence time of quantum walks.

1. はじめに

ドレスト光子のエネルギー遷移の挙動は, 量子ウォークの定常状態の中に幾つか類似性を見出すことができる. 特に, 最大出力を得るために必要な空間構造を導出するような計算量を要する問題には, ドレスト光子ダイナミクスの素子化モデルとして, 量子ウォークが着目されつつある [1]. そこで本研究では, この量子ウォークが定常状態に収束するまでにかかる時間が, システムサイズにどのように依存するかについて評価する. ここでは, 正則グラフ上で, Grover walk と呼ばれる比較的単純なモデルでその描像を明確にする. 特に, 完全グラフの場合には, 1 つの頂点に印をつけ, そこに摂動を加え, 従来のいわゆる量子探索アルゴリズムとの比較をして考察する.

2. 結果

各頂点の特殊性を除去するため, 正則グラフの各頂点に, 毎時刻, 外部から同じだけ(ここでは 1 の)流入を受けるような設定にする. 定常状態をφ_∞ , 時刻 t での状態をφ_tとする. 正の値 θ (例えば 1)を予め定めておき, 収束時刻$t_*(\theta)$ をここでは, 次のように定義する.

$$t_*(\theta) := inf_{t>0}\{\ \left||\varphi_\infty - \varphi_s|\right|_2 < e^{-\theta}\ , for\ any\ s \geq t\}.$$

定理 1 [Ishikawa, Kubota, S, 2022+]. N 頂点, k-正則グラフの場合(N>k>1)

$$t_*(\theta) = \left\lceil \frac{\theta + \log(k\,N)}{\log\frac{k+1}{k-1}} \right\rceil.$$

定理 2[2]. N 頂点の完全グラフで, 1 頂点に印をつけ, そこに符号付き摂動を入れた場合. ($N \gg 1$)
(1) 定常状態: 印付き頂点の発見相対確率は, 定常状態で 1/2, それ以外の頂点の発見相対確率は 1/ 2(N-1).
(2) 収束時間: $t_*(\theta) \approx N \log N$.
(3) 脈動: 印付き頂点の発見相対確率を最大にする時刻は$O(\sqrt{N})$で, そのときの印付き頂点の発見相対確率は 1/2 より大きい.

3. 考察

定理 1 に,それぞれ円環と完全グラフの場合に相当する k=2, k=N-1 を代入すると, それぞれ, $O(\log N), O(N \log N)$となる. 一方で良く知られているランダムウォークの場合の混合時間はそれぞれ$O(N^2), O(1)$であるため, 収束の速さに関しては, 量子ウォークとランダムウォークの間には双対的な関係が垣間見られる. また, 従来の量子探索アルゴリズムでは, $O(\sqrt{N})$で見積もられる, 最適な時刻を逃すと, 印付きの頂点の発見を取り逃がすリスクがある. 一方で, 本研究で提案するモデルでは, 万が一, 定理 2 (3) の最適な時刻を取りに逃がしても, ペナルティとして, 定理 2(2)より, N log N だけ待たなければならないが, それだけ待てば, システムサイズ N によらない確率 1/2 で, 印付き頂点を見つけ出すことができる, 保証がついたものになっている.

参考文献

1) M. Ohtsu, A quantum walk model for describing the energy transfer of a dressed photon, DOI：2109R.001.v1
2) Yu. Higuchi, M. Sabri, E. Segawa, arXiv:2207.10633

16pAS4

ドレスト光子記述のための圏代数
Creation and Energy Transfer of Dressed Photon

°*西郷　甲矢人
°* Hayato Saigo
長浜バイオ大学
Nagahama Institute of Bio-Science and Technology
*h_saigoh@nagahama-i-bio.ac.jp

Dressed photon is the light as a quantum field interacting with nanoparticles. It is known that in mathematical physics, there is no mathematical model that describes interacting quantum fields as long as they satisfy the axioms that seem very reasonable from the conventional point of view. Simply put, one cannot fully describe a dressed photon without going beyond the framework assumed in conventional “on-shell” physics. In this talk, we will introduce a new approach based on the concepts of category algebras and states on categories.

1. はじめに

ドレスト光子はナノ粒子と相互作用する量子場としての光である。しかし、非常に妥当と思われるひと揃いの公理を仮定するだけで、それらを満たす限り相互作用する量子場を記述する数理モデルが存在しないことが数理物理学で知られている。簡単に言えば、通常の物理学で前提とされている枠組みを超えない限りドレスト光子を十全に記述することはできないのである。本講演においては、圏代数および圏上の状態[1)]の概念に基づいた演者自身による新しいアプローチ[2)]を紹介する。

2. 圏・圏代数・圏上の状態・圏上のウォーク

量子場の理論は、歴史的には相対論と量子論の融合を目指して構築された（当然非相対論的な文脈も重要であるが)。しかし、相対論的な量子場概念を公理的に考察する中で、「当然」と一見思われるひと揃いの公理を満たす限り相互作用する量子場の記述は（数学的に矛盾しない形では）不可能であることが知られている。何かを変える必要があるのだ。そこで相対論（特殊のみならず一般相対論を含めて）の物理的本質に立ち戻ってみると、それは時空とは事象とそれらの間の関係性の総体だということである。時空は単に事象の集合ではなくて、むしろその間の関係性に注目すべきではないかという考えは自然である。実際、時空多様体の構造は、事象間の「因果性」による順序構造によって分類されてしまうことも知られている。これに基づいて「因果集合」を出発点にしたアプローチも試みられている。

一方で、相互作用の記述には「因果的」でない事象の関係性が不可欠であることも、積み重なった状況証拠から確実であると考えられる。そこで、順序構造をその特殊例として含みつつ、かつ相対論的な共変性の構造をも内蔵しうるような一般概念を用いて時空構造を捉え直すべきではないかという考えが浮かぶ。実はそのような数学概念として「圏」(特に「ダガー圏」）というものがある。これは簡単に言えば「対象」（事象に対応）とそれらをつなぐ「射」(矢印、「関係性」に対応）のシステムであって、隣接している二つの矢印にはその「合成」が考えられるようなものである（「ダガー」は矢印の「ひっくり返し」に相当する)。

この圏の構造を反映した代数（「畳み込み」の代数）が「圏代数」であり、これは異なる対象の間に一本でも射が存在する限り非可換代数となる（圏がダガー圏であればスター代数となる)。これを物理量代数、すなわち量子場そのものに対応させ、 そこからの「期待値を与える汎関数」としての状態すなわち「圏上の状態」を量子場の状態と捉えると、これまでの量子場の数理研究と対応を取りながらそれらを越える道が開かれる[2)]。本講演ではこれを説明するとともに、状態の時間発展の記述として「圏上の量子ウォーク」を考えることで、相互作用する量子場、特にドレスト光子のダイナミクスを記述する試みを紹介する。

参考文献

1) H. Saigo: Symmetry,**13** (2021) 1172.
2) H. Saigo: Symmetry,**13** (2021) 1727.

16pAS5

グラフ上の量子カオス
Quantum Chaos on Graphs

°*齋藤正顕
°*Seiken Saito

工学院大学　教育推進機構
Center for Promotion of Higher Education, Kogakuin University
*saito.seiken@cc.kogakuin.ac.jp

In 1977 , M.V. Berry predicted that "in the semiclassical limit of the solution of the Schrödinger equation on the Riemann surface, the distribution of the eigenfunction values becomes Gaussian if the dynamical system is irregular". On the other hand, Anantharaman-Le Masson (2015) and others have considered "graph-theoretic analogue of the semiclassical limit" in terms of quantum ergodic properties on graphs. Based on this, we consider the graph-theoretic analogue of Berry's conjecture.

1. はじめに

リーマン面上のシュレディンガー方程式の解の半古典極限をとると，その力学系が非正則な場合には，固有関数の値分布がガウス分布になることを M.V. Berry は 1977 年の論文[2]で予想した．これは自由粒子を球とみたとき，ビリヤードの球の軌道がビリヤード台を埋め尽くすという量子カオス現象の一つである．最近の光学的な進展として，光の量子カオス現象をリアルタイムで観測したとの報告もなされている[4]．D.A. Hejhal らは，2001 年の論文[5]で，複素上半平面上の CM 型 Maass 波動形式についても，Berry の予想が成り立つ という数値実験の結果を発表している．一方で，近年，Brooks-Lindenstrauss (2013)[3], Anantharaman-Le Masson (2015)[1]などの研究では，グラフ上の量子エルゴード性の観点から「半古典極限のグラフ理論的類似」を考えている．それを踏まえて，本講演では，グラフ理論的な Berry の予想の類似を定式化し，その数値実験について報告する．まず，リーマン面上の Berry 予想は，プランク定数を 0 に近づける極限，つまりラプラシアンの固有値を発散させるという極限をとったときの固有関数の値分布に関する予想である．それに対し，グラフの場合の Berry 予想は，空間に関する極限（頂点数が発散し，ベーテ格子に収束するようなグラフの増大列．エルゴード的なグラフ）をとるときの隣接行列に関する固有関数の値分布に関する予想として定式化される．

2. 正則グラフにおける Berry 予想の数値実験

エルゴード的なグラフの代表例として「ランダム正則グラフの増大列」「Lubotzky-Phillips-Sarnak のラマヌジャングラフの列」について， 定式化に基づいて数値実験を実施し，固有関数の値分布がガウス分布となることが確認された(Fig. 1).

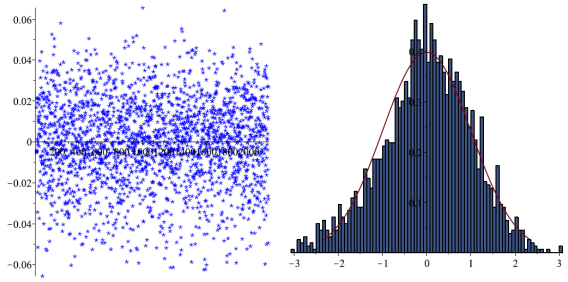

Fig. 1 Value distribution of a certain eigenfunction of the adjacency matrix of the Lubotzky-Phillips-Sarnak graph X^{5,13}.

参考文献

1) N. Anantharaman and E. Le Masson, Quantum ergodicity on large regular graphs, Duke Math. J. Vol. 164, Number 4 (2015), 723–765.
2) M. V. Berry, Regular and irregular semiclassical wavefunctions, J. Phys. A 10, 2083–2091 (1977).
3) S. Brooks and E. Lindenstrauss, Non-localization of eigenfunctions on large regular graphs, Israel J. Math. 193 (2013), 1–14.
4) L. Fan, X. Yan, H. Wang, L.V. Wang, Real-time observation and control of optical chaos, Science Advances, Vol. 7, No. 3, 13 Jan 2021.
5) D. A. Hejhal and A. Strömbergsson, On Quantum Chaos and Maass Waveforms of CM-Type, Foundations of Phys., Vol. 31, No. 3, 519–533 (2001).

16pAS6

欠陥構造を起点とするドレスト光子の状態遷移
State Transition of Dressed Photons Originating from Defect Structures

°*三宮 俊
°*Suguru Sangu
（株）リコー
Ricoh Co., Ltd.
*suguru.sangu@jp.ricoh.com

In this paper, the numerical simulation of dressed photons using the quantum density matrix is explained as an example of reproducing the dressed-photon-phonon (DPP)-assisted annealing, which is a physical phenomenon mediated by dressed photons. Numerical simulations show that multiple dressed photons contribute to the localization and energy dissipation, which are in qualitative agreement with the experimental results and prove the validity of the numerical simulation model.

1. はじめに

ドレスト光子を介在した物理的および産業的に興味深い現象が数多く報告されている [1]．本発表では，間接遷移型半導体であるシリコンを発光デバイスへ転化させる不純物（ドーパント）構造の生成プロセス（ドレスト光子フォノン(DPP)援用アニール）[2]を取り上げ，数値シミュレーションにより背景にある物理現象の再現を試みる．現在，ドレスト光子の理論検討が精力的に進められている．本研究は，従来光学理論では説明できない光学現象を数値モデル化し実験結果との整合を図ることで，理論研究を後押しするとともに定量設計・解析ツールの提供を目指すものであり，本発表では DPP 援用アニールの再現を例に，ドレスト光子シミュレーションの現状について概説する．

2. 欠陥構造へのドレスト光子局在と散逸過程

ドレスト光子の数値シミュレーションではその局在性や高速応答性を記述するために，量子性と外場への散逸を表現するモデルが必要である．Fig.1(a)は本数値シミュレーションの概念図であり，実験状況を模倣して，系全体へのドレスト光子の励起，非輻射および輻射緩和，ノード間に補足されたドレスト光子のホッピングを Lindblad 方程式と呼ばれる量子密度行列の運動方程式で記述している．また，不純物影響を同種／異種ノード間の結合強さの違いとして与えている．本数値シミュレーションにより量子密度行列を算出した結果の一例を Fig.1(b)に示す。本計算では，系内のドレスト光子が 2 個以下となるように基底状態を制限している．同様の計算をドレスト光子 1 個以下の制約のもと行うと，顕著な局在性は現われず，複数個のドレスト光子が散逸すなわち不純物の位置固定（冷却）に寄与していることが明らかとなった．

以上の結果は，DPP 援用アニールの物理描像を定性的によく表現している．計算規模の拡大，高次元化，実際の物理量との対応付けなど，残存課題は少なくないが，将来のドレスト光子介在デバイスの構造や特性の最適設計に向けた第一歩の成果と言える．

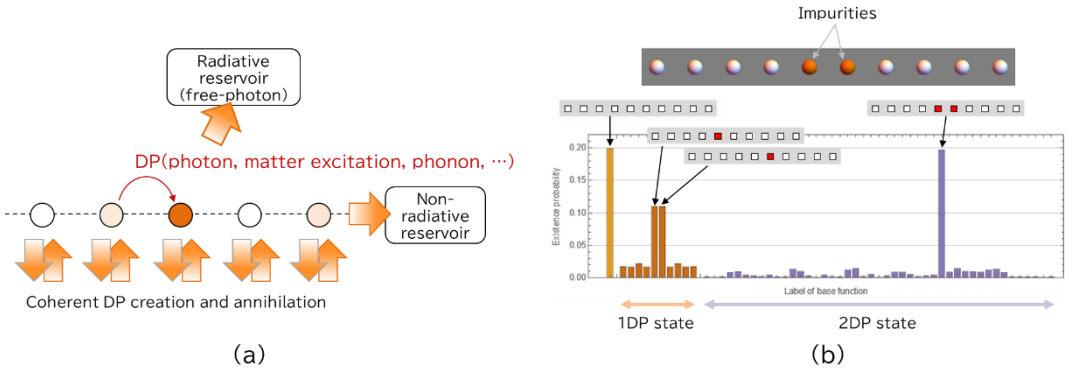

Fig. 1 (a) Simulation model (1D case) of the dressed-photon system, and (b) existence probability of the dressed-photon basis states for a vacuum, 1-dressed-photon, and 2-dressed-photon states.

参考文献

1) 大津元一，杉浦 聡：*ドレスト光子の深わかり*（ナノフォトニクス工学推進機構，2022）．
2) M. Ohtsu and T. Kawazoe: Adv. Mat. 10 (2019) 860-867.

最小作用の原理で達成される内在電磁場を伴う散逸構造の理論

Dissipative Structure with Immanent Electromagnetic Field attained by the Principle of Least Action

○坂野　斎　(山梨大院)
○Itsuki Banno　(Univ. of Yamanashi)
E-mail: banno@yamanashi.ac.jp

内在電磁場；ドレスト光子（DP）を利用した川添，大津らのフォトン・ブリーディング [1] は間接遷移型半導体から発光デバイスを作製可能にする方法であり，その発光波長は物質のバンドギャップではなくデバイス作製過程の照射光波長で決められる．このデバイスの発光を最小作用の原理をたよりに内在電磁場と電流密度がある非平衡開放系の動的状態として記述したい．

作用のやり取りができる外部自由度を，光学フォノンに伴う電流密度，遠隔場にある受光装置上の電流密度，系の外部の電流密度源とする．これらの外部自由度を絶った場合，最小作用の原理は電流，エネルギー流のない基底状態を導く．ここに外部自由度との結合を導入して，差分の作用を最小化することで，非平衡開放系の動的状態を探索する．

差分の作用には，ベクトルポテンシャルの２乗が電流密度と結合する非線型項がある．この項は通常は無視しえるほど小さいが，ベクトルポテンシャルが内在することで増大し，また，差分の作用を減らす寄与をする．内在ベクトルポテンシャルは内在電流密度を源泉とするので，外部自由度との結合の下で，この非線型項の寄与により電流密度と発光というエネルギー散逸を伴う動的状態が実現されることを示唆している．

著者は非平衡開放熱力学系の散逸構造 [2] の量子版と捉えており，熱力学系の散逸構造でのエントロピーの役割を量子系においては作用に担わせている [3]．また，散逸構造を特徴づける，散逸と非線形性は，それぞれ，外部自由度の結合，内在ベクトルポテンシャルの非線形の寄与となっている．

作用の差分を最適化するにあたり，(1) 電子の自由度を最適化してから，電磁場の自由度を最適化する方法 (2) 電磁場の自由度を最適化してから電子の自由度を最適化する方法 [4] の２とおりの段取りが考えられるが，(2) は電子の運動エネルギーの取り扱いが難しいため，本発表では (1) を用いる．(1) の見方では，物質間の相互作用を担う内在ベクトルポテンシャルは，非線型マクススェル方程式の解として得られる．

謝辞

ドレスト光子研究起点 (RODreP) での研究会のメンバーである次の方々に感謝いたします：大津元一博士 (RODreP)，小嶋泉博士 (RODreP)，佐久間弘文博士 (RODreP)，川添忠博士 (日亜化学)，西郷甲矢人博士 (長浜バイオ大学)，岡村和弥博士 (名古屋大学)，瀬川悦生博士 (横浜国立大学)，松岡雷士博士 (広島工業大学)，三宮　俊博士 (リコー)，門脇拓也博士 (日亜化学)，結城謙太氏．この研究の一部はドレスト光子研究起点からの援助を受けています．

参考文献

[1] T. Kawazoe and M. A. Mueed and M. Ohtsu, Appl. Phys. B, 104 p.747–754(2011).
[2] G. ニコリス，I. プリゴジーヌ,「散逸構造 – 自己秩序形成の物理学的基礎」(岩波書店，1980).
[3] 坂野　斎,「フォトンブリーディングと散逸構造 その 2」2021 年秋季学術講演会，12a-N202-4.
[4] 坂野　斎,「ドレスト光子 / 内在電磁場と最小作用の原理」2022 年春季学術講演会，22a-E103-1.

ドレスト光子研究が拓く”オフシェル科学”：一具体例の考察

"Off-shell science" opened up by dressed photon studies: a tangible example

ドレスト光子研究起点、○佐久間弘文
RODreP, Hirofumi Sakuma
E-mail: sakuma@rodrep.or.jp

物理学では、世界の構成要素を大きく次の様に分類している。（1）粒子状の物質と（2）物質の相互作用を担う力の場という事である。最近の研究では、これに加え、entanglement による量子相関が時空を創発するのではという事も言われている。量子力学を学ぶ時に出会う最初の”衝撃”は、粒子は古典的な意味の粒子ではなく、波動性も伴う存在で、その事の深い意味は誰も理解していないという説明である。量子場理論の専門家が加わり、現在推進しているドレスト光子（DP）の研究活動は、この量子性の深い意味を、DP現象を切り口として、改めて考えて見るという挑戦である。

難解な議論を横に置き、素朴な直観に従えば、時空という存在は、局所性を有する粒子的な存在の”環境”と言えるものである。そうであるなら、存在としての”場”は局所的な粒子性と非局所的な”時空性”の二つを兼ね備えていると考えるのは至極自然な事であろう。量子力学が対象とする量子場がその様な”場”と直結しているなら、上で触れた”衝撃”は、じつは神秘でもなんでもなく、むしろ当然そうあるべき自然の姿と言えるのではないだろうか？

実は、相互作用する場が持つ局所的な time-like 性と非局所的な spacelike 性はどちらも重要であるという事は、公理論的量子場理論に関しての定理の形で証明されているが [1]、これまで後者は、場の粒子性が過度に強調される物理学界の一般的風潮の中では、Einstein 因果律を破る非物理的なものという（粒子的な）見方により排除される傾向が強く、その正当性にあまり注意が向けられて来なかった経緯がある。**RODreP が推進する”オフシェル科学”とは、今後の科学の更なる発展の為に、超光速の位相速度を持つ波動場として表現される後者が果たす役割の重要性を深く理解する事を目指すものである。**

ここ数年の RODreP が推進して来た”オフシェル科学”研究により、DP 現象という未解明の研究テーマに大きな進展があり、現在もその研究活動は益々の広がりを見せている。（圏代数による量子場理論の再考や量子ウォークモデルによる DP 現象の記述等）講演者自身の研究としては、電磁場理論における Maxwell 方程式を spacelike な運動量域に拡張する事により、DP の基本理論が、前回の発表で報告した（i）”回折しないスピンゼロの光の存在”や、（ii）現代宇宙論の未解明テーマである、ダークマター及びダークエネルギーと深く関係する事を示し、更には、最新の研究 [2] によって重力場が有する熱力学特性が、時空が有するスピンネットワークという属性から如何に創発されるのかという新理論を提示した。

本発表においては、[2] の成果を用いて、まず、”オフシェル科学”という視点から見た場合の電磁場理論と重力場理論の簡単な対比を説明する。より具体的に言えば、局所性を有する粒子的な場とその環境として存在する非局所的な場という双対性の観点から、電磁場と重力場をみた場合、その類似性と違いは何かという事である。もちろん、量子重力場の理論が完成されていない現段階での比較は、大まかな比較ではあるが、古典理論におけるニュートン重力と電磁場のクーロン力との相似を考えれば、その様な比較は大いに意味のある事であると思われる。そのような比較を議論する中で、広義の電磁場理論から説明される DP は、定性的に重力場理論に関わるダークマターに類似した存在であることを示す。

参考文献
[1] ここからはじまる量子場、大津元一、小嶋泉（編著）朝倉書店、2020。
[2]H. Sakuma, I. Ojima, H. Saigo and K. Okamura, http://arxiv.org/abs/2203.09763.

オフシェル科学への圏代数アプローチ

A category algebraic approach to off-shell sciences

○西郷　甲矢人 (長浜バイオ大学)

○Hayato Saigo (Nagahama Institute of Bio-Science and Technology)

E-mail: h_saigoh@nagahama-i-bio.ac.jp

本講演では、圏代数と圏上の状態の概念 [3, 4] に基づくオフシェル科学へのアプローチについて概説する。

2022 年春の本学会における講演では、量子場とその状態を、部分的な対合構造をもつ圏上の圏代数とその上の状態として定義することにより、圏論的構造としての相対論的構造と非可換確率構造としての量子論的構造を直接に統合できることを示し、代数的量子場理論や位相的量子場理論などの先行するアプローチとの概念的関係についても論じた。

その後、内部自由度を持つ状態空間の取り扱い（それは熱力学における状態空間の圏論的な取り扱いと結びつく）を通じて、このアプローチがオフシェル科学への量子ウォークからのアプローチやネットワーク上の「(一般化された) 生成消滅演算子」を活用するアプローチとも深く関連していることが明らかとなった。

本講演においてはこれらについての物理的なアイデア、特にドレスト光子 [1] やミクロ・マクロ双対性 [2] との関連の議論に重点をおくが、もし時間が許せば位相や測度の構造を入れることで見えてくる数学的諸概念との関連についても紹介したい。

Acknowledgments

本研究は（社）ドレスト光子研究起点の助成を得た。

参考文献

[1] M. Ohtsu: *Dressed Photons* (Springer, Berlin Heidelberg 2014)

[2] 小嶋泉：量子場とミクロ・マクロ双対性 (丸善出版, 東京 2013)

[3] Saigo, H. Category Algebras and States on Categories. *Symmetry* **2021**, *13* 7, 1172. https://doi.org/10.3390/sym13071172

[4] Saigo, H. Quantum Fields as Category Algebras. *Symmetry* **2021**, *13* 9, 1727. https://doi.org/10.3390/sym13091727

ドレスト光子の量子ウォークモデル: 1次元の場合

Quantum Walks related to Dressed Photons: the 1-dimensional case

○齋藤 正顕[1] (工学院大) 瀬川 悦生[2] (横国大)

○Seiken Saito[1] (Kogakuin Univ.) Etsuo Segawa[2](Yokohama Nat. Univ.)

ドレスト光子 (DP) を説明するモデルとして, 大津 [2], 瀬川によって3状態の量子ウォーク (QW) モデル (ドレスト光子の量子ウォークモデル) が提案されている. 大津–瀬川–結城 [3] は, 2次元の場合のシミュレーションを実施し, その数値的な挙動を調べている. しかし, 次元が2以上の場合, 遷移が複雑で, 定常状態など理論的な性質は謎が多いままである. そこで, 本研究では, ドレスト光子の QW モデルについて, まず1次元の場合を検討したので報告する. 先行研究 [1] の手法を応用し, 3状態のユニタリ行列 H が [2] で提案されている行列 H_{DP} に等しい場合に考察した. 本研究の QW では, M 個の欠陥があり, 初期状態 $\Psi_0(x)$ を $x \leq 0$ においては $\Psi_0(x) = z^x|R\rangle$, $x > 0$ においては0とする. ここで, $R = [0,1]^T$, $z = e^{i\xi}$ ($\xi \in \mathbb{R}$) である. この入力パラメータ z が変わると QW の挙動が変化する. 本稿では「量子ウォークの定常状態での振幅が内部で指数関数的に減衰する」ことを量子ウォークが内部に対して嫌忌的と呼ぶ. 我々は z について次の結果を得た:

Theorem 1 量子ウォークを与えるユニタリ行列を

$$H := \begin{bmatrix} a_{LL} & a_{LO} & a_{LR} \\ a_{OL} & a_{OO} & a_{OR} \\ a_{RL} & a_{RO} & a_{RR} \end{bmatrix}, \quad H_{DP} := \begin{bmatrix} \varepsilon_L & \chi & J \\ \chi & \varepsilon_{phonon} & \chi \\ J & \chi & \varepsilon_R \end{bmatrix} = \begin{bmatrix} -\cos^2\theta & \frac{\sin 2\theta}{\sqrt{2}} & \sin^2\theta \\ \frac{\sin 2\theta}{\sqrt{2}} & \cos 2\theta & \frac{\sin 2\theta}{\sqrt{2}} \\ \sin^2\theta & \frac{\sin 2\theta}{\sqrt{2}} & -\cos^2\theta \end{bmatrix}$$ とする. $H = H_{DP}$ のとき, z の偏角 ξ (振動数) が

$$\xi \notin [2\cos^{-1}\tfrac{\sqrt{1+\cos^2\theta}}{2}, 2\cos^{-1}\tfrac{\sqrt{1-3\cos^2\theta}}{2}] \cup [2\pi - 2\cos^{-1}\tfrac{\sqrt{1-3\cos^2\theta}}{2}, 2\pi - 2\cos^{-1}\tfrac{\sqrt{1+\cos^2\theta}}{2}]$$

を満たすならば, 量子ウォークが内部に対して嫌忌的である.

上記ドレスト光子の QW を含むより一般の1次元3状態の QW について (つまり $H = H_{DP}$ とは限らない一般の場合に) 以下を得た:

Theorem 2 量子ウォークを与えるユニタリ行列 H に対し, 入力パラメータ z が $z = \Delta\frac{\bar{a}_{RR}}{a_{LL}}$ を満たすならば, 完全反射が起こる. ここで, $\Delta = -(\det H)\, z\frac{|z - a_{OO}|^2}{(z - a_{OO})^2}$. とする. 特に, DP の場合, つまり $H = H_{DP}$ のとき, $z = 1$ または $\cos^2\theta = 1$ ならば, 完全反射が起こる.

上記より, DP の場合, 量子ウォークを嫌忌的にさせる振動数 ξ のうち, ちょうど真ん中に位置する $\xi = 0$ においては, 完全反射が起こる. この振動数は, 我々の扱っている M が有限の場合と裏腹に M が無限の場合の3状態 QW の局在化を起こす固有値に対応していることは興味深い. また, [1] で扱っている1次元2状態の QW では完全反射は起こらないが, 本研究の QW ではそれが起こることも注意しておく.

謝辞 この研究の一部はドレスト光子研究起点の支援を受けています.

参考文献

[1] K. Higuchi, T. Komatsu, N. Konno, H. Morioka and E. Segawa, *A discontinuity of the energy of quantum walk in impurities*, Symmetry, 2021, 13, 1134.

[2] M. Ohtsu, *A quantum walk model for describing the energy transfer of a dressed photon*, preprint, 2021, Offshell: 10.14939/2109R.001.v1.

[3] 大津元一, 瀬川悦生, 結城謙太, 「量子ウォークモデルによるドレスト光子エネルギー移動の数値計算」, 2022年第83回応用物理学会秋季学術講演会.

量子ウォークとランダムウォークの収束の速さの双対性

Estimation of speed of convergence of quantum walks

○瀬川 悦生 (横国大)

○Etuo Segawa(Yokohama Nat. Univ.)

流出入のある量子ウォークは, ドレスト光子の挙動とよく似た挙動を示すことが知られており [1, 2] 流入の振動数が境界によらない場合, 定常状態に収束する [3]. 本研究ではこの定常状態に収束するまでの時間について, 議論する.

内部グラフを $G = (V, A)$ として, この全ての頂点に半無限長のパス (=tail) を接続する. この半無限グラフを $\tilde{G} = (\tilde{V}, \tilde{A})$ とする. この量子ウォークの全空間はこの有向辺によって生成されるベクトル空間 $\mathbb{C}^{\tilde{A}}$ となる. 初期状態 $\psi_0 \in \mathbb{C}^{\tilde{A}}$ は一定値が各頂点に毎時時刻流入するようにとる. 収束にかかるまでの時刻を次のように定義する.

$$t_*(\theta) = \min_{t \geq 0}\{d(s) < e^{-i\theta} \text{ for any } s > t\}$$

ここで, $d(s)$ は内部グラフに関する定常状態と時刻 s での状態との全変動距離である. つまり, $t_*(\theta)$ は, この時刻以降, $e^{-\theta}$ よりもこの全変動距離が小さくなるような時刻である. すると, 本研究では次のようなことを証明した.

Theorem 1 内部グラフが κ-正則グラフのとき, 任意の $\theta > 0$ に対して

$$\frac{1}{\log \frac{\kappa+1}{\kappa-1}} (\log \kappa N + \theta) \leq t_*(\theta) \leq \frac{1}{\log \frac{\kappa+1}{\kappa-1}} \log 2\kappa N.$$

このことから, ランダムウォーク的な直観に反して, 次数が多ければ多いほど, 量子ウォークでは収束が遅くなるという現象が起きていることがわかる. 例えば, この定理よりサイクルの場合, 量子ウォークでは収束の時間は $O(\log N)$ であるのに対して, ランダムウォークでは $O(N^2)$ [4] であり, ランダムウォークよりも非常に収束が早くなる. その一方で, 完全グラフの場合, 量子ウォークでは $O(N \log N)$ であるのに対して, ランダムウォークでは $O(1)$ [4] であり, ランダムウォークよりも非常に収束が遅くなるというある種の双対的な描像になっている.

実は今回の量子ウォークの収束に関する結果の中に, 内部グラフの次数と頂点数の情報しか現れてこないのは, どの正則グラフの隣接行列も最大固有値が k でその最大固有ベクトルが一定であるという非常に基本的な事実が反映されている. 入力としてどの頂点も特殊性をなくすために、それなりにリーズナブルに見える一様な入力を採用したが、収束を最も遅くするよな入力にした場合の見積もりは, この事実を使うことができないので, 量子性から誘導されたグラフの内部構造などが抽出されることが期待される, 今後の楽しみな課題である.

謝辞 この研究の一部はドレスト光子研究起点の支援を受けています.

参考文献

[1] M. Ohtsu, Dressed Photons, Springer-Verlag, Berlin Heiderberg (2014).

[2] M. Hamano, H. Saigo, Electronic Proceedings in Theoretical Computer Science **315** pp. 93–99.

[3] Yu. Higuchi, E. Segawa, Journal of Physics A: Mathematical and Theoretical **52** (39) (2019).

[4] D. A. Levin, Y. Peres, American Mathematical Society (2017)

量子ウォークモデルによるドレスト光子エネルギー移動の数値計算

Numerical calculation of a dressed photon energy transfer by a quantum walk model

ドレスト光子[1]，横浜国大[2]，Middenii[3]　○大津元一[1]，瀬川悦生[2]，結城謙太[3]

Res. Origin Dressed Photon[1], Yokohama Ntnl. Univ[2], Middenii[3]

°Motoichi Ohtsu[1], Etsuo Segawa[2], Kenta Yuki[3]

E-mail: ohtsu@rodrep.or.jp

【まえがき】ドレスト光子（DP）は光子とナノ粒子（NP）中の電子との相互作用により生成されNP に局在するオフシェル場である[1]。生成されたDP が近隣のNP に移動する際、その時間的振る舞いの高速性、空間的振る舞いの特性から[2]、本計算では量子ウォーク（QW）モデルを用いる。

【方法】近隣のNP 間を両方向に移動するDP とNP に局在するフォノンからなるドレスト光子フォノン（DPP）の確率振幅ベクトルを計算する。その時空発展方程式中の実数ユニタリ行列Uに位相項ξを付加し$U(\xi)=\exp(i\xi)U$を用いる。行列の非対角成分J、χは各々DP のNP 間跳躍エネルギー、DP-フォノン相互作用エネルギーである。ξ、χ/Jをパラメータとし、ファイバプローブを表す直角二等辺三角形の2 次元格子について計算した。すなわち底辺の全サイト（サイト数n）に入力信号を加え、格子中の各サイト、頂点での確率振幅を求めた。

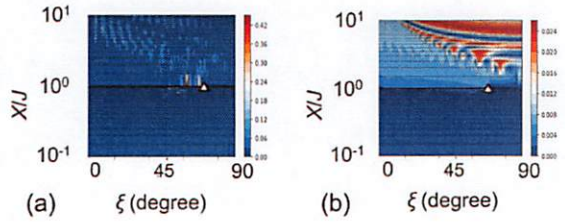

図1. 存在確率Pのパラメータξ、χ/J依存性。斜面でのエネルギー散逸無し(a)、有り(b)。（n=41 の場合）

【結果と考察】図1 は頂点でのDPP の存在確率Pのξ、χ/J依存性を表す。(a)は斜面でのエネルギー散逸のない場合である。入力サイト数nが小さいときは斜面での反射による内部干渉効果が表れるが、nの増加とともにそれは消滅する。実験結果との比較によりこれは妥当である。(b)はエネルギー散逸のある場合で、内部干渉は無いが赤色帯領域ではPの値が大きい。この赤色帯は局在フォノンの特性に起因する。この帯の中とその周辺ではPの値は各パラメータに対して急激かつ不規則に変化する。この領域は$\chi/J>>1$にて表れる。数値計算には$\chi/J=1$ とするのが標準的であり、それはこの赤色帯の影響をうけない。その場合、Pの値は$\xi\fallingdotseq67.5$ 度（図1 中の△の位置）で最大値を取る。これはnの値によらない。またPが定常値に至るまでの時間的振る舞いは格子の全サイト数に依存し、QW 理論の結果と整合した[3]。

【まとめ】パラメータの最適値$\xi\fallingdotseq67.5$ 度、$\chi/J=1$が見出された。

【文献】

[1] H. Sakuma and I. Ojima, *Symmetry* **2021**, 13, 593.

[2] M. Ohtsu, *Off-Shell Applications In Nanophotonics*, Elsevier, Amsterdam (2021).

[3] M. Sabri、瀬川、第69 回応物学会春季講演会（2022 年3 月）、22a-E103-4

不純物を含む系におけるドレスト光子の振る舞い

Behavior of Dressed Photons in Systems Containing Impurities

(株)リコー[1]，長浜バイオ大[2]，ドレスト光子研究起点[3] ○三宮 俊[1]，西郷 甲矢人[2]，大津 元一[3]

Ricoh Co., Ltd.[1], Nagahama Inst. Bio-Sci. Tech.[2], Res. Origin Dressed Photon[3],
○Suguru Sangu[1], Hayato Saigo[2], Motoichi Ohtsu[3]

E-mail: suguru.sangu@jp.ricoh.com

1. はじめに

ナノ領域に局在する光子を介在した物理現象として、特異な発光現象[1]や巨大磁気光学効果[2]を示す実験結果が報告されている。これらの現象は、ドレスト光子フォノン(DPP)援用アニールと呼ばれる、光を外部より照射しながらドーパント（不純物）を空間分布させる加工法を用いて作製したデバイスにおいて発現する。本論文の目的は、DPP 援用アニールにおける不純物(対)の位置決め機構を推定するドレスト光子の数値シミュレーションモデルを構築することである。前回発表[3]では、量子密度行列を用いた数値シミュレーションにより二次元系における不純物配置の影響を考察したが、不純物の拡散状態から固定(冷却)状態への遷移を説明するには至らなかった。本論文では、一次元系モデルに立ち返り、複数の不純物を含む系におけるドレスト光子局在現象のメカニズムを考察し、不純物の自律的な位置決め機構へのつながりについて議論する。

2. 数値シミュレーション結果

Fig. 1 に、一次元格子上に 2 つの不純物を設けた場合のドレスト光子の存在確率として、特徴的な 2 つの配置における結果を示す。不純物による影響はドレスト光子を表わすサイト間のホッピング結合強さの差異で表現し、本シミュレーションでは異種物質間の結合を 0.1 倍として与えている。Fig. 1(a)は不純物を 2 サイト離して配置した場合の結果であり、不純物位置にドレスト光子が局在する。一方、Fig. 1(b)は不純物を 3 サイト離して配置した場合の結果であり、不純物サイト間の中央位置においてドレスト光子が最も局在し、一次元かつ 2 不純物を含む系におけるドレスト光子の存在確率が最大となる構成であった。

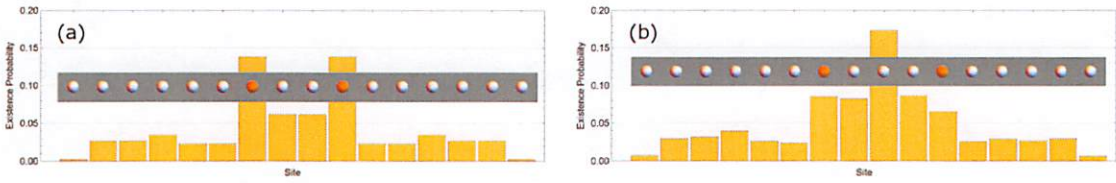

Fig.1: 一次元光子系における不純物位置とドレスト光子存在確率

3. 考察

Fig. 1 の結果は、わずかな不純物配置の違いにより、ドレスト光子の存在確率が劇的に変化し得ることを示している。サイト間の結合強さや同種・異種物質間の結合強さの調整により、ドレスト光子の局在性をさらに高める構成が存在するものと推察される。不純物の位置決め機構を表わすモデルとして、特定の不純物配置におけるドレスト光子の誘導放出の影響が指摘されている[1]。発表では、ドレスト光子の局在メカニズムの詳細を議論するとともに、局在性と誘導放出(多体効果)とのかかわりについても言及したい。

参考文献

[1] M. Ohtsu and T. Kawazoe, Adv. Mat. Lett. 10 (2019) 860.
[2] N. Tate, et al., Sci. Rep. 5 (2015) 12762.
[3] 三宮・他，2022 年第 69 回応用物理学春季学術講演会 (2022) 22a-E103-6.

日本物理学会北陸支部特別講演会

講師： 大津元一（一般社団法人）ドレスト光子研究起点代表理事
演題： オフシェル科学の展開
場所： オンライン（Zoom）
以下の URL に氏名と電子メールアドレスを登録して頂きますと，
Zoom ミーティングのログイン情報が通知されます（自動応答）。
講演会開催中でも登録（途中参加）可能です。
[登録サイト URL]
https://us06web.zoom.us/meeting/register/tZAkcu-prDkoH9GrONbfQciZlCS5gkLsMWDO
講演日時：2021 年 8 月 12 日（金）9:00 ～ 10:00
担当教員：守安 毅（福井大学）<moriyasu@u-fukui.ac.jp>

講演概要：
ナノ寸法空間での光子と電子、さらにはフォノンとの相互作用により生成されるドレスト光子（DP）の実験研究その応用技術は大きく進展したが、その理論研究はこれまで発展途上であった。それは DP の持つオフシェル性に起因するが、さらなる基本的問題は従来のオンシェル科学では生成の源となる光・物質相互作用に関する理論が未開発であることであった。
本講演ではそれを解決するために我々が開拓したオフシェル科学について解説する。
電磁場を spacelike 運動量場に拡大することにより、相互作用を記述し DP の生成機構を明らかにした。また生成にはマヨラナフェルミオンの粒子・反粒子対が関与することを見出した。その結果、DP には最大寸法があり、それはハイゼンベルグ・カットに対応すること、さらに DP から変換される伝搬光は回折フリーの粒子性を有することを見出した。本講演ではこれらの特性を実験結果と対比して提示する。

正則グラフにおける non-backtracking cycle の個数の誤差項の分布

齋藤正顕　(工学院大学)*

概　要

$(q+1)$-正則グラフの長さ m の non-backtracking cycle の個数 N_m について, 絶対値が $2\sqrt{q}$ 未満の (隣接行列の) 固有値が寄与している項 t_m を考える (ここでは N_m の誤差項とよぶ). 本研究では, データ t_m $(m=1,2,\dots)$ の分布について調べ, そのモーメント母関数を与えた. また, これを応用して, 正則グラフの増大列がある条件をみたすとき, $t_m/\sqrt{n}$ (n は絶対値が $2\sqrt{q}$ 未満の固有値の個数) の極限分布が正規分布となることを示した. 尚, 本研究は, 長谷川武博氏 (滋賀大学), 西郷甲矢人氏 (長浜バイオ大学), 杉山真吾氏 (日本大学), 谷口哲也氏 (金沢工業大学) との共同研究に基づく.

1. Non-backtracking cycle の個数の誤差項

$G=(V,E)$ を有限単純連結グラフとし, V をその頂点集合, E を辺集合とする. G の隣接する2つの頂点 $v,w\in V$ に対し, $vw=wv\in E$ を v, w を端点とする (無向) 辺とし, v を始点, w を終点とする有向辺を (v,w) と表す. $e:=(v,w)$ の逆向きの有向辺を $\overline{e}:=(w,v)$ とする. $D(G):=\{(v,w),(w,v)\mid vw\in E\}$ を有向辺の全体とする. G の有向辺 $e\in D(G)$ に対し, a の始点と終点をそれぞれ $o(e)$, $t(e)$ とおく. G の長さ m の路 (path) $C=e_1\cdots e_m$ とは $e_1,\dots e_m\in D(G)$ かつ $t(e_i)=o(e_{i+1})$ $(i=1,\dots,m-1)$ のときをいう. とくに, $t(e_m)=o(e_1)$ のとき, C は閉路 (closed path) あるいはサイクル (cycle) といわれる. 本稿では, グラフ G のサイクル $C=e_1\cdots e_m$ が以下の条件を満たすとき, non-backtracking cycle とよぶ:

- $e_{i+1}\neq\overline{e}_i$, $(i=1,\dots,m-1)$. つまり, C には後戻りがない.
- $e_1\neq\overline{e}_m$. つまり C の最初の辺が最後の辺の逆になっていない.

自然数 m に対し, N_m を G の長さ m の non-backtracking cycle の個数とする. N_m の母関数 $Z_G(u)=\exp\left(\sum_{m\geq1}\dfrac{N_m}{m}u^m\right)$ はグラフ G の伊原ゼータ関数とよばれる ([2]). $(q+1)$-正則グラフ G に対し, N_m は A の固有値よって次のように表される ([1]).

$$N_m=2q^{m/2}\sum_{\lambda\in\mathrm{Spec}(A)}T_m\left(\frac{\lambda}{2\sqrt{q}}\right)+ne_m(q-1).$$

ここで, T_m は第1種チェビシェフ多項式 (つまり $T_m(\cos\theta)=\cos m\theta$) とし, e_m は m が偶数のときは 1, それ以外のときは 0 と定義する. このとき, N_m について, 絶対値が

本研究は科研費 (基盤研究 (C) :19K03608) の助成を受けたものである. また, 本研究は (社) ドレスト光子研究起点の助成を得た.
2020 Mathematics Subject Classification: 05C38, 05C50
キーワード：non-backtracking cycles, regular graphs
* 〒192-0015　東京都 八王子市 中野町 2665-1 工学院大学　教育推進機構　基礎・教養科
e-mail: saito.seiken@cc.kogakuin.ac.jp

$2\sqrt{q}$ より小さい A の固有値の寄与を t_m で表す.

$$t_m := \frac{1}{2q^{m/2}}\{N_m - 2q^{m/2}\sum_{\substack{l\in\sigma(A)\\ |\lambda|\geq 2\sqrt{q}}} T_m\left(\frac{\lambda}{2\sqrt{q}}\right) m_\lambda - n(q-1)e_m\} = \sum_{i=1}^{l} m_{\lambda_i}\cos m\theta_i.$$

ここで, $\sigma(A)$ は G の隣接行列 A の相異なる固有値全体の集合, $\{\lambda_1,\ldots,\lambda_l\} := \{\lambda \in \sigma(A) \mid |\lambda| < 2\sqrt{q}\}$, m_λ は A の固有値 λ の重複度とする. 特に, G が $|\lambda| = 2\sqrt{q}$ なる固有値 λ をもたない $(q+1)$-正則 Ramanujan グラフのときは, $t_m = \frac{1}{2q^{m/2}}\{N_m - n(q-1)e_m\}$ である. 我々は, N_m の（主要部でないという意味での）"誤差項" t_m の分布について調べた. t_m は隣接行列の固有値で表され, グラフの頂点数が増大するとき固有値の極限分布は Kesten-McKay 分布となる. よってグラフの頂点数が増大するとき, t_m の分布が正規分布に近づくように見えることは中心極限定理の観点から理解できる. しかし, 固有値の間には代数的な関係があるので注意が必要である.

2. 誤差項の分布とモーメント母関数

Theorem 1 (主結果1: グラフの増大列における $\frac{t_m}{\sqrt{n_\nu}}$ の極限分布) $(G_\nu)_{\nu\in\mathbf{Z}_{\geq 1}}$ を $(q+1)$-正則グラフの列とし, A_ν を G_ν の隣接行列とする.

$$\begin{aligned}\{\lambda_1,\ldots,\lambda_{l_\nu}\} &:= \{\lambda\in\sigma(A_\nu) \mid |\lambda| < 2\sqrt{q}\},\\ \theta_i &:= \arccos\tfrac{\lambda_i}{2\sqrt{q}} \in (0,\pi) \quad (i=1,\ldots,l_\nu),\\ n_\nu &:= |\{\lambda\in\mathrm{Spec}(A_\nu) \mid |\lambda| < 2\sqrt{q}\}|\end{aligned}$$

とおく. 以下を仮定する. $\lim_{\nu\to\infty} n_\nu = \infty$ かつ

$$(*)_\nu \qquad \text{各 } \nu \text{ について } \tfrac{\theta_1}{2\pi},\ \ldots,\ \tfrac{\theta_{l_\nu}}{2\pi} \text{ は } \mathbf{Q} \text{ 上1次独立.}$$

このとき, $\frac{1}{\sqrt{n_\nu}}t_m$ $(m\in\mathbf{Z}_{\geq 1})$ の極限分布は平均が 0, 分散が 1/2 の正規分布 $N(0,1/2)$ である.

Theorem 2 (主結果2: t_m の分布は逆正弦則の畳み込み) G を $(q+1)$-正則グラフとし, $\{\lambda_1,\ldots,\lambda_l\} := \{\lambda\in\sigma(A) \mid |\lambda| < 2\sqrt{q}\}$, $\theta_i := \arccos\frac{\lambda_i}{2\sqrt{q}} \in (0,\pi)$ $(i=1,\ldots,l)$ とおく. t_m の d 次モーメントを M_d, モーメント母関数を $\varphi(x) := \sum_{d=0}^{\infty}\frac{M_d}{d!}x^d$ とすると,

$$\varphi(x) = \sum_{\substack{k_1,\ldots,k_l\in\mathbf{Z}\\ \sum_{h=1}^{l}k_h\theta_h\in 2\pi\mathbf{Z}}} \prod_{h=1}^{l} I_{k_h}(m_{\lambda_h}x).$$

ここで, $I_k(x)$ は第1種変形ベッセル関数である.

Corollary 1 $\frac{\theta_1}{2\pi},\ \ldots,\ \frac{\theta_l}{2\pi}$ が $\mathbf{Q}$ 上1次独立ならば, $\varphi(x) = \prod_{k=1}^{l} I_0(m_{\lambda_k}x)$.

参考文献

[1] T. Hasegawa, T. Komatsu, N. Konno, H. Saigo, S. Saito, I. Sato and S. Sugiyama, The limit theorem with respect to the matrices on non-backtracking paths of a graph, arXiv:2005.09341v2 [math.CO], 22 Aug 2021.

[2] Y. Ihara, On discrete subgroups of the two by two projective linear group over p-adic fields, J. Math. Soc. Japan 18 (1966), 219–235.

ドレスト光子 / 内在電磁場と最小作用の原理

Dressed Photon / Immanent Electromagnetic Field and the Principle of Least Action

○ 坂野　斎　(山梨大院)

○Itsuki Banno　(Univ. of Yamanashi)

E-mail: banno@yamanashi.ac.jp

量子電気力学のダイナミクスは最小作用の原理により決められる．作用は根本的な場の量で書かれたラグランジアン密度を時間・空間積分して求められる．相対論系を対象とする場合，場においても，座標においても時間成分と空間成分は対等に扱われる．非相対論系においては対称性の低下はあるものの，同様の扱いが合理的である．

しかし，非相対論系を扱う物質科学（物性物理学や分子化学）におけるダイナミクスの追跡は，通常，エネルギー・運動量演算子の時間成分であるハミルトニアンに頼って行う．また，電磁場の摂動による遷移振幅の計算においては長波長近似が多用され，電磁場の空間構造は捨象される．空間積分は遷移行列要素を求める手続きに込められ，時間積分はエネルギー共鳴を導く．このような時間成分と空間成分の対等でない扱いの原因には，量子論が原子・分子という小さな物質への適用から始まったという歴史的経緯と実用上重要なエネルギー共鳴の記述ができるという成功体験への心理的依存もあるように思う．

さらに，上記の扱いでの摂動は電場・磁場と考えられることが多い．物質から遠方での電場・磁場は人間が操作できる自由度であり，かつ，ゲージ変換不変量であることが理由だろう．ここで，人間が操作できない内在電磁場を広い意味でドレスト光子（DP）と捉えると，それが関わる現象の記述には，根本的自由度であるベクトルポテンシャルとスカラーポテンシャルに基づき高次の摂動的扱い，または，非摂動的扱いをすることが相応しい．強調すべきは，ベクトルポテンシャルの横成分はゲージ変換不変量であり，超伝導体のマイスナー効果やコヒーレントな電子ビームのアハラノフ-ボーム効果だけでなく，近接場光学系や DP 系のエネルギー非共鳴条件下で直接物理現象に関わりうることである [1].

ここで，DP が関わる顕著な現象として，フォトン・ブリーディング [2] がある．間接遷移型半導体から発光デバイスを作製可能にする方法であり，その発光波長は物質のバンドギャップではなくデバイス作製過程の照射光波長で制御される．このデバイスの発光は非平衡開放系で DP が関わる量子現象であるが，著者は非平衡開放熱力学系の散逸構造 [3] の量子版と捉えており，熱力学系の散逸構造でのエントロピーの役割を量子系においては作用に担わせることを考えている [4].

DP が関わる非平衡開放量子系を，電磁ポテンシャルと座標の時間成分と空間成分の対等な扱いの下，最小作用の原理を指導原理として記述することを目的に，内在電磁場に関する因果律・反因果律の運用，電流注入と光の放射を考慮をした作用積分の表式を議論する．

謝辞

ドレスト光子研究起点 (RODreP) での研究会のメンバーである次の方々に感謝いたします：大津元一博士 (RODreP)，小嶋泉博士 (RODreP)，佐久間弘文博士 (RODreP)，川添忠博士 (日亜化学)，西郷甲矢人博士 (長浜バイオ大学)，岡村和弥博士 (名古屋大学)，瀬川悦生博士 (横浜国立大学)，松岡雷士博士 (広島工業大学)，三宮　俊博士 (リコー)，門脇拓也博士 (日亜化学)，結城謙太氏．この研究の一部はドレスト光子研究起点からの援助を受けています．

参考文献

[1] 坂野　斎,「物質系の非相対論性とドレスト光子」IMI 研究所研究会 Basic mathematical studies on dressed photon phenomen (2020 年 2 月); マス・フォア・インダストリ研究，No.19, p.152 (2020).

[2] T. Kawazoe and M. A. Mueed and M. Ohtsu, Appl. Phys. B, **104** p.747–754(2011).

[3] G. ニコリス，I. プリゴジーヌ,「散逸構造 – 自己秩序形成の物理学的基礎」(岩波書店，1980).

[4] 坂野　斎,「フォトンブリーディングと散逸構造 その 2」2021 年秋季学術講演会，12a-N202-4.

圏代数としての量子場

Quantum Fields as Category Algebras

○ 西郷　甲矢人 (長浜バイオ大学)

○Hayato Saigo (Nagahama Institute of Bio-Science and Technology)

E-mail: h_saigoh@nagahama-i-bio.ac.jp

本講演では、圏代数と圏上の状態の概念に基づく量子場への新しいアプローチを提起する。我々は量子場とその状態を、部分的な対合構造をもつ圏上の圏代数とその上の状態として定義する。

圏代数と圏上の状態の概念を用いることにより、圏論的構造としての相対論的構造と非可換確率構造としての量子論的構造を直接に統合できる。代数的量子場理論や位相的量子場理論などの先行するアプローチとの概念的関係についても論じる。

2021 年春の本学会における講演においては、マクロに可視化されうる「可能な事象」を対象とし、それらの間の可能な遷移（さらに一般には事象間の潜在的な関係性を射とする圏を考え（この発想の原型は「モビリティの圏」[2] において導入された)、その圏上の「圏代数」を考えることを提唱した。また、その上のある種の線型汎関数として、一般化された状態の概念が定式化できるが、これは物理量（「非可換な確率変数」）に対しその「期待値」を対応させるものである（この定式化の物理的意味は、系と環境の「インターフェイスとしての状態」[1] という見方によって明確となる）とした。また、2021 年秋の本学会における講演においては、量子場を圏代数としてとらえ、その（局所）状態たちを圏代数上の状態たちとして捉えるアイデアを提唱した。

本講演においては、これらの講演において先行的に提起されたアイデアを定式化した論文 [3, 4] に基づき、この新しいアプローチの現状と展開について述べる。

Acknowledgments

本研究は（社）ドレスト光子研究起点の助成を得た。

参考文献

[1] 小嶋泉：量子場とミクロ・マクロ双対性 (丸善出版, 東京 2013)

[2] H. Saigo, M. Naruse, K. Okamura, H. Hori and I. Ojima: Complexity 2019 1490541:1-1490541:12 (2019).

[3] Saigo, H. Category Algebras and States on Categories. Symmetry 13(7), 1172. (2021). https://doi.org/10.3390/sym13071172

[4] Saigo, H. Quantum Fields as Category Algebras. Symmetry 13(9), 1727. (2021). https://doi.org/10.3390/sym13091727

C*-代数的量子論におけるシュレディンガー描像

On the Schrödinger picture in C*-algebraic quantum theory

ドレスト光子[1]，名大情報[2]　○岡村 和弥[1,2]

Dressed Photon[1], Nagoya Univ.[2], ○Kazuya Okamura[1,2]

E-mail: k.okamura.renormalizable@gmail.com

本講演では，C*-代数的量子論におけるシュレディンガー描像について議論する。量子論には，通常量子力学系と呼ばれる有限自由度量子系と，量子場に代表される無限自由度量子系がある。量子力学系に対してはヒルベルト空間論を用いた解析が有効であるが，無限自由度量子系では非有界作用素の解析の難しさのみならず表現論的な困難もあって様々な処方箋が必要となる。その一つが作用素代数（operator algebra）に基づく量子論の定式化であり，最も一般的な枠組みがC*-代数を駆使するC*-代数的量子論である。

よく知られているように，シュレディンガー描像では,（系とその環境の）動力学によって引き起こされる系の状態遷移を扱う。本講演では，C*-代数的量子論特有の事情を考慮し，数学だけでなく物理としても概念的に掘り下げる必要がある。ここでは、遷移確率の概念が中心的な役割を果たす [1]。ディラックの遷移確率は，ボルンの統計公式とは異なり，遷移先の状態の指定をも含む概念である。遷移確率を一般的に定義することにより，量子系における様々な状態遷移を記述することを今回可能にした。そして，遷移確率を用いてシュレディンガー描像での状態変化を圏論的に定式化した。

さらに、遷移確率の理論を量子測定理論と結びつける。確率的に様々な状態へと遷移する状況を，測定によって測定装置のメーターから出力される値と状態を結びつけることで実現可能であるとする自然な直観に基づくアプローチである。量子測定の公理的アプローチ [2] はシュレディンガー描像に基づいている（ハイゼンベルク描像での定式化 [3] も物理的には同等に重要である）。今回，C*-代数的量子論においてセクター理論と整合的な量子測定理論の定式化を行った [4]。量子測定理論の中心概念であるインストルメントがC*-代数の設定においてはセクターの分離を行う機能まで担うことになる。

以上の議論は，物理系だけでない「モビリティの圏」[5] から着想を得たものである。ただし，「モビリティの圏」とは圏の対象についての扱いが少しだけ異なる。

参考文献

[1] 岡村 和弥, RIMS kokyuroku **2010**, (2016) 69–77. http://hdl.handle.net/2433/231579

[2] K. Okamura and M. Ozawa, J. Math. Phys. **57** (2016), 015209. https://doi.org/10.1063/1.4935407

[3] K. Okamura, “Measuring processes and the Heisenberg picture,” pp. 361–396 in Reality and Measurement in Algebraic Quantum Theory, edited by M. Ozawa et. al,, (Springer, Singapore, 2018).

[4] K. Okamura, Symmetry **13**, (2021) 1183. https://doi.org/10.3390/sym13071183

[5] H. Saigo, M. Naruse, K. Okamura, H. Hori, and I. Ojima, Complexity **2019** (2019), 1490541. https://doi.org/10.1155/2019/1490541

量子ウォーク・ドレスト光子の摂動に対する感受性

Sensitivity of quantum walk and dressed photon to perturbtion

Mohamed Sabri(東北大), ○ 瀬川 悦生 (横国大)

Mohamed Sabri(Tohoku Univ.), ○Etuo Segawa(Yokohama Nat. Univ.)

ドレスト光子においては, 空間的に特異な場所で強く光ることが良く知られているが [1], その挙動の類似性を再現させる量子ウォークモデル [2, 3] を考える. この量子ウォークモデルは定常状態に収束する離散時間量子ウォークで, 本研究ではグラフの中から一つ頂点 u_* を選び, そこに摂動を加えたものを特異な場所としてみなす. 時間が十分に経過したときに、この摂動を加えれらた頂点における相対確率がどのようになるかについて考察する.

内部グラフを $G = (V, A)$ として, この全ての頂点に半無限長のパス (=tail) を接続する. この半無限グラフを $\tilde{G} = (\tilde{V}, \tilde{A})$ とする. この量子ウォークの全空間はこの有向辺によって生成されるベクトル空間 $\mathbb{C}^{\tilde{A}}$ となる. 時間発展は各頂点で Grover matrix と呼ばれるもので状態が混ざりあい, u_* のところだけ -1 の符号を課すような $\mathbb{C}^{\tilde{A}}$ 上のユニタリ作用素である. 初期状態 $\psi_0 \in \mathbb{C}^{\tilde{A}}$ は一定値が各頂点に毎時時刻流入するようにとる. すると内部グラフ G に制限すると, 力学系となり固定点に収束する [3]. すると, 本研究では次のようなことを証明した.

Theorem 1 マークされた頂点 u_* の相対確率を最大にする時刻を t_N とおく. 完全グラフ K_N に対して,

1. $t_N = O(\sqrt{N})$
2. 定常相対確率は次のようになる.

$$\mu_\infty(u) = \begin{cases} 1/2 & : u = u_* \\ 1/(2(N-1)) & : otherwise \end{cases}$$

3. ステップ数 $n > N \log c^2 N/\epsilon^2$ ならば (c は有限な定数), $||\psi_\infty - \psi_n|| < \epsilon$.

1 つ目の主張により, マークされた頂点の相対確率を最大にする時刻を逃さなければ, その時刻は $O(\sqrt{N})$ であり, 従来の量子探索アルゴリズムにおけるスピードと同じオーダーである. また, そのときの発見確率は少なくと 1/2 以上である. そして万が一, このタイミングに乗り遅れても, 2 つ目の主張により, マークされた頂点での相対確率が定常状態の中で安定して得られることになるから, しばらくずっと待ち続けていればよい. どの位待ち続けているべきかは, $O(N \log N)$ 程度であるというのが 3 つ目の主張になる. いわゆる量子探索アルゴリズムにおいては, マークされた頂点の存在確率は, 漸近的に $O(\sqrt{N})$ の周期で周期的になるのに対して [4], 本研究では, 最適な時刻に乗り遅れた場合は, 安定して発見できることと引き換えに, 乗り遅れたことに対する “報い” としてスピードが遅くなるというトレードオフがある.

謝辞 この研究の一部はドレスト光子研究起点の支援を受けています.

参考文献

[1] M. Ohtsu, Dressed Photons, Springer-Verlag, Berlin Heiderberg (2014).

[2] M. Hamano, H. Saigo, Electronic Proceedings in Theoretical Computer Science **315** pp. 93–99.

[3] Yu. Higuchi, E. Segawa, Journal of Physics A: Mathematical and Theoretical **52** (39) (2019).

[4] L. K. Grover, Proc., 28th ACM Symposium on the Theory of Computing 212 (1996).

出口付き量子ウォークネットワークにおける有理数の残留振幅

The amplitude distribution of rational numbers trapped in quantum walk networks with exit sinks

広工大工[1]，フリーランサー[2]，Blocksize Capital GmbH[3]，横浜国大[4]
○松岡 雷士[1]，結城 謙太[2]，Hynek Lavička[3]，瀬川 悦生[4]
Hiroshima Inst. of Tech.[1], Freelancer[2], Blocksize Capital GmbH[3], Yokohama Nat. Univ.[4]
○Leo Matsuoka[1], Kenta Yuki[2], Hynek Lavička[3], Etsuo Segawa[4]
E-mail: r.matsuoka.65@cc.it-hiroshima.ac.jp

流入・流出を考慮したネットワーク型の量子ウォークモデルは定常状態の形成など、ドレスト光子との対応を考えるための直観的な糸口を多数含んでいる。我々は量子ウォークの時間発展によって、出口 (Sink) 付きネットワークの最短経路に振幅が残留する性質を発見した[1]。講演ではこの残留振幅の大きさが概して有理数に収束するいう数値計算結果を示し、ネットワーク構造との関係を考察する。

図はネットワークのスタート地点に初期振幅をおき、量子ウォークの時間発展を繰り返した結果の残留振幅の分布の例である。(a) においては経路上のエッジの振幅の大きさがそれぞれおよそ 1/6 に収束している。経路には 4 本の双方向エッジと 2 本のセルフループエッジが含まれており、1/6 の分母はこのエッジ本数に対応していることが推察される。一方で(b)においては、最短経路上で 1/7, 遠回りの経路上では 1/14, セルフループ上では 3/14 に振幅が収束しており、経路間の距離に振幅が反比例することなどが示されている。構造との完全な対応付けは難しいものの、より複雑なネットワークにおいても有理数の残留振幅が観測されることは同様である。

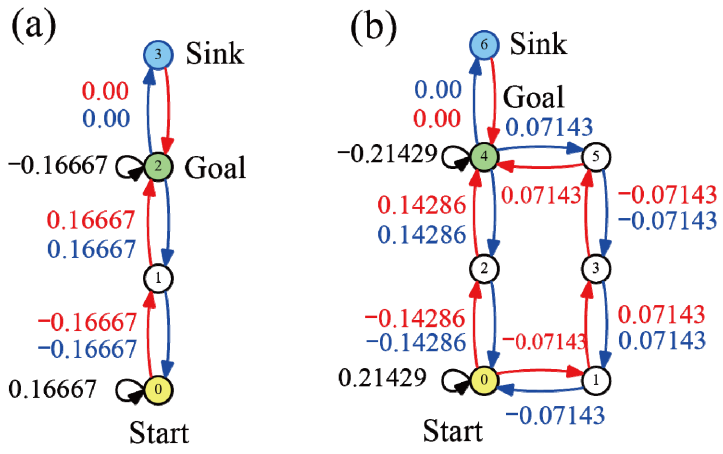

Fig. 1. Examples of the trapped amplitude distribution.

謝辞　この研究の一部はドレスト光子研究起点の支援を受けています.

[1] L. Matsuoka, K. Yuki, H. Lavička, and E. Segawa, *Symmetry* **13**, 2263 (2021).

ドレスト光子エネルギー移動における不純物配置の影響

Effect of Impurity Configuration on Dressed-Photon Energy Transfer

(株)リコー[1]，長浜バイオ大[2]，ドレスト光子研究起点[3] ○三宮 俊[1]，西郷 甲矢人[2]，大津 元一[3]

Ricoh Co., Ltd.[1], Nagahama Inst. Bio-Sci. Tech.[2], Res. Origin Dressed Photon[3],
○Suguru Sangu[1], Hayato Saigo[2], Motoichi Ohtsu[3]

E-mail: suguru.sangu@jp.ricoh.com

1. はじめに

ドレスト光子の概念により説明される幾つかの光機能がある。例えば、間接遷移型半導体であるシリコンの発光現象[1]や、非磁性体である酸化亜鉛による巨大磁気光学効果[2]などが知られている。これらの光機能はドレスト光子フォノン(DPP)援用アニールと呼ばれる、光を外部より照射しながらドーパント（不純物）を空間分布させる加工法を用いて作製したデバイスにおいて観察され、ドレスト光子を介した不純物の自律的な位置決め機構が光機能発現の重要な役割を担っている。本論文ではこの自律的な位置決め機構について、これまで検討を進めてきた数値シミュレーション解析手法[3]の立場からその物理現象の解読を試みる。具体的には、欠陥を構成する複数の異種原子を含む系におけるドレスト光子の局在状態および散逸過程を視覚化し、特異な原子配置が誘発されるメカニズムについて考察する。

2. 数値シミュレーション

本論文の数値シミュレーションでは、ドレスト光子をノードに束縛された調和振動子と見なし、ドレスト光子がノード間を湯川関数で与えられる有限相互作用を介して移動する様子を、一粒子状態を基底状態とした量子密度行列の時間発展方程式により表現する[3]。ここで、不純物による非一様性を欠陥ノードにおける湯川関数の減衰長すなわちドレスト光子質量の差異として与える。Fig. 1 は、2 つの欠陥ノードを、背景ノードを一つ挟んで配置した場合について、ドレスト光子存在確率（定常状態）の空間分布を算出した結果である。また、Fig. 2 はその特徴的な空間モードの幾つかを、量子密度行列の対角化操作（基底変換）により抽出した結果（確率の大きさ）を示している。欠陥ノード自身に加え、欠陥ノードの外縁や欠陥ノード間の孤立点にドレスト光子の停留する空間モードが活性化される様子が確認できる。

3. 考察

DPP 援用アニールはドレスト光子を、コヒーレントフォノンを含む混合励起とし、その誘導放出が不純物の運動エネルギーを奪い、所定の位置に固定するものと解釈されている[1]。上述の数値シミュレーションでは誘導放出の影響までは含めておらず、実験状況の再現にはやや不十分さが残り、現在改良を進めている。一方、不純物の配置に依存した空間モードの選択制は、そのエネルギー散逸の経路に関わる情報を捉えている可能性がある。講演では、より詳細な数値解析を追加し、不純物の自律的な位置決め機構について議論を進める。

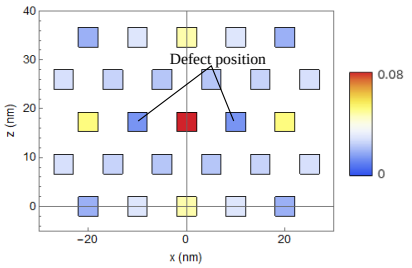

Fig. 1: ドレスト光子存在確率の空間分布

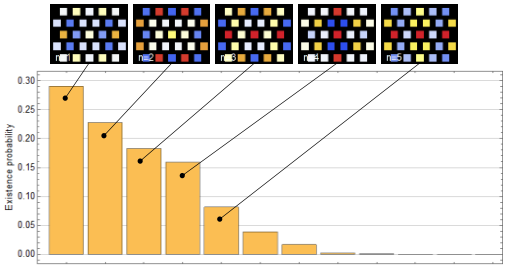

Fig. 2: 基底変換後の主要な空間モード

参考文献

[1] M. Ohtsu and T. Kawazoe, Adv. Mat. Lett. 10 (2019) 860.
[2] N. Tate, et al., Sci. Rep. 5 (2015) 12762.
[3] S. Sangu and H. Saigo, Symmetry 13 (2021) 1768.

ドレスト光子を用いた赤外 Si-LED の時間分解 PL 測定

Time-resolved photoluminescence of Si light-emitting diode for infrared wavelength using dressed photons

日亜化学工業(株)[1]，ドレスト光子研究起点[2]
○門脇 拓也[1]，川添 忠[1]，菅田 雅樹[1]，大津 元一[2]，佐野 雅彦[1]，向井 孝志[1]
Nichia Corporation[1], Research Origin for Dressed Photon[2]
○Takuya Kadowaki[1], Tadashi Kawazoe[1], Masaki Sugeta[1], Motoichi Ohtsu[2], Masahiko Sano[1], Takashi Mukai[1]
E-mail: takuya.kadowaki@nichia.co.jp

【はじめに】これまで我々はドレスト光子(DP)技術により Si 結晶を用いた赤外域の発光素子、受光素子の開発を行い、その受発光特性について報告してきた[1, 2]。一方で、Si 発光素子の時間領域に関する報告例は少ない。これは赤外領域での Si 発光素子の従来報告例がなく、かつ赤外領域で時間分解できる受光素子の種類が限られるためである。今回、超電導単一光子検出器(SSPD)を用いて我々の開発した赤外 Si-LED の時間分解 PL 測定を行った。

【素子作製】n 型の Si 基板に B 原子をイオン注入し p 型に変換した後、電極を形成し、1 mm 角に素子化した。作製した素子に DP を効率よく発生させるため、DP アニールと呼ばれる製作法を用いた。これは電流注入によるジュール熱アニールとレーザー光照射（波長 1.3 μm）による誘導放出に起因する冷却とを同時に行い、最適な B 原子分布の自律的形成を促すものである。その結果、作製された素子は DP を介した誘導放出が生じ、DP アニールの際の照射光エネルギーに支配される発光（光子ブリーディング：PB）が可能となった。

【実験・考察】代表的な DP Si-LED の PL スペクトルを Fig.1 に示す。図中の黒線は計測結果を示し、緑線はバンド間遷移と DP アニールに用いた波長(図中矢印)のピークでガウス曲線でフィッティングした結果を示す。PB 効果として、DP アニールの照射波長の位置に発光帯が表れていることが分かる。次に、作製した素子をピコ秒パルスレーザ(波長 800nm、繰り返し 80MHz、パルス幅 2ps)で励起し、SSPD と TAC を用いた時間相関光子計数測定を行った。Fig.2 に(a)DP Si-LED と(b)一般的な pn 接合をもつ Si 結晶の PL 減衰特性を示す。DP アニールした素子の発光緩和寿命は 0.36 ns であり、一般的な間接遷移半導体の Si の発光緩和寿命より著しく短くなっている。これは、DP を介したフォノン散乱により誘導放出が生じるので、発光再結合が起こりやすくなるためであると考える。

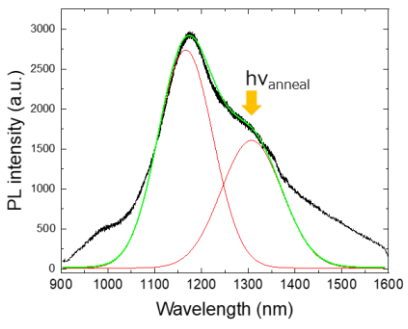

Fig.1 PL spectra of DP Si-LED

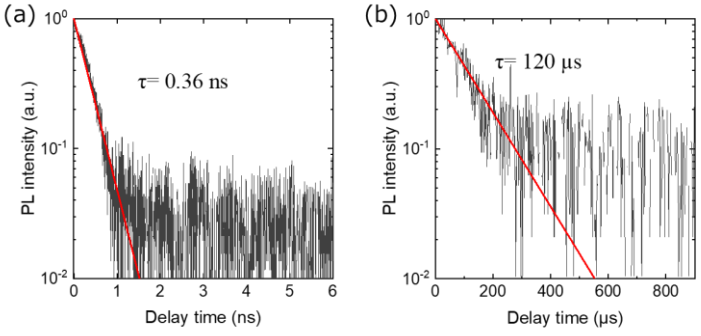

Fig.2 Decay curve of time resolved measurements. (a) DP Si-LED. (b) Si p-n crystal.

[1] 門脇、川添、大津　他　第 67 回応用物理学会春季学術講演会(2020 年 3 月) 14p-B309-16
[2] 門脇、川添、大津　他　第 82 回応用物理学会秋季学術講演会(2021 年 9 月) 12a-N202-1

DPP アニールで作製した高感度 Si 温度計

A highly sensitive thermometer fabricated by using DPP annealing

日亜化学工業(株)[1], ドレスト光子研究起点[2]、○川添 忠[1]、門脇拓也[1]、大津元一[2]、佐野 雅彦[1]、向井孝志[1]
Nichia Corp[1], RODreP[2], ○T. Kawazoe[1], T. Kadowaki[1], M. Ohtsu[2], M. Sano[1], T. Mukai[1]
E-mail: tadashi.kawazoe@nichia.co.jp

ドレスト光子フォノン(DPP)アニールは順方向電流印加によって起こるドーパントの拡散を同時照射するレーザー光で制御、再配列させることができるアニール法である。この結果間接遷移型半導体である Si(シリコン)が発光材料としての性質を獲得するとともに、バンドギャップよりも長波長側に受光感度特性が広がる。昨年の春の応用物理学会にて DPP アニール後の素子の電気特性は大きな温度依存性を有し、温度計探針として機能する事、その感度は計測電流にも依存するが 10 倍以上高い事、大きな温度依存性の要因は黒体輻射光の受光であるとの可能性を報告した。今回、より実用に近い使い方として市販の高感度温度計を用いて比較対照実験を行ったので報告する。

Si-pn 接合素子に波長：1.3 μm、光パワー：160mW のレーザー光を照射し、注入順方向電流 150mA を印加する条件で DPP アニールを行った。(素子の IV 特性や温度依存性等は 2021 年春の応用物理学会予稿集を参照)。作製した素子の温度依存性は温度 30～40℃の範囲で通常のサーミスタの 10 倍ほど大きくなった。

今回、比較対象とした市販高感度温度計は FLUKE 社 Super-DAQ1586A である。また、この装置を利用した時に最も高精度な温度計測が可能な公称 10KΩのサーミスタを比較対象にした。この場合の温度表示分解能は 100μ℃、計測精度は 2m℃である。当初 DPP アニールによって作製した素子の抵抗値に対して温度依存性を校正し温度精度として比較する事を考えていたが、①温度精度が校正によって左右されること、②温度校正が基本的に Steinhart-Hart equation を用いて行われるため、それとは異なる依存性になる DPP アニールで作製された温度計は正確な校正が難しい事、の二つの理由から、Super-DAQ1586A の抵抗計測モードを用いて比較した。

計測方法は室温を数分計測しその後、室温＋5℃に設定したホットプレート(28℃)に接触させた。なお、本計測において Super-DAQ1586A は定電流 10μA での抵抗値を検出している。Fig.1.にその計測結果を示す。縦軸は規格化された抵抗値であり、この測定結果は最適化された電流でない Super-DAQ1586A による計測にもかかわらず市販温度プローブの場合より感度が 2 倍高かった。

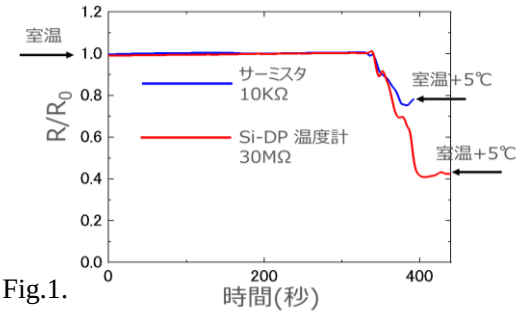

Fig.1.

次に素子の計測安定度を室温の計測によって行った結果を報告する。Fig.2.に実験結果を示す。図から分かるように専用サーミスタの安定度を示すバラツキ(計測結果の標準偏差)は DPP アニールにより作製された温度計と比較して凡そ 1/2 であったが感度が 1/2 であることを考慮すると同等であることが分かった。

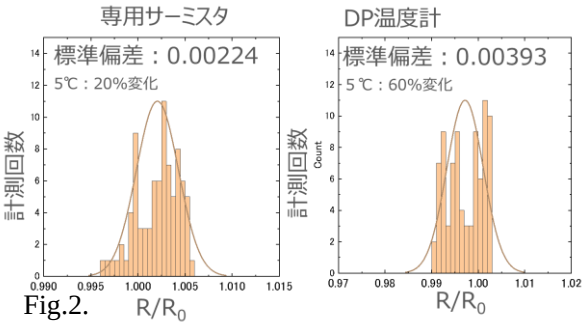

Fig.2.

[1] T. Kawazoe & M. Ohtsu, Appl. Phys. A, **115**, 127-133, (2014).
[2] T. Kawazoe, et al., Appl. Phys. B-Lasers and Optics, **98**, 5-11 (2010). also **107**, 659-663 (2012).
[3] H. Tanaka, et al., Appl. Phys. B-Lasers and Optics, **108**, 51-56 (2012).
[4] Y. Tanaka, and K. Kobayashi, J. Microscopy **229** 228-232(2008).
[5] 川添忠、橋本和信、杉浦聡、大津 元一、2017 年第 78 回秋季応用物理学会、福岡 講演番号 7a-A405-5.
[6]川添忠他 2021 年第 68 回応用物理学会春季学術講演会、オンライン、講演番号 17p-Z14-9

Off-shell mathematical science toward system's analysis and designing

解析から設計に向けたオフシェル数理科学

I-1 Keynote speech

M. Ohtsu (RODREP), "Recent progresses in experimental studies of dressed photons for off-shell science theories."

Abstract: This presentation presents recent experimental results derived for promoting theoretical studies of off-shell science. It focuses on two essential phenomena. They are generation and energy transfer of dressed photons (DP). The former is found by evaluating the features of the light emitted from a silicon light-emitting diode; it exhibited antibunching in spite that it is composed of multiple photons. These photons imply the boson with spin 0, as have been theoretically identified by Sakuma. The latter is the experimental evaluations of DP generation efficiency of fiber probes. It agrees with the numerically simulated results based on the specific quantum walk (QW) model developed by Segawa. This agreement suggests that the QW model can be used as a powerful tool for analyzing the autonomous DP energy transfer that has been observed by a series of experiments.

【基調講演】

大津元一(ドレスト光子研究起点)、「オフシェル科学理論のためのドレスト光子実験研究の進展」

講演概要：本講演ではドレスト光子（DP）に関する二つの本質的現象（DPの生成とエネルギー移動）に関する実験結果を提示し、オフシェル科学理論の裏付けとして供する。前者はシリコン発光ダイオードから出射する光が複数の光子からなり、かつ全体として光子アンチバンチングの特徴を示す実験結果である。これは佐久間が開拓したDP生成理論で裏付けられているスピン0のボゾン場に対応する。後者はファイバ プローブの先端でのDP発生効率の実験結果である。これは瀬川により開発された量子ウォークモデルに基づく数値計算結果と整合しており、ファイバプローブ中のDPの自律的エネルギー移動の機構の解明に役立つと考えられる。

Off-shell mathematical science toward system's analysis and designing

解析から設計に向けたオフシェル数理科学

I-2 Invited speech

S. Sangu (Advanced Technology R&D Division, Ricoh Co., Ltd.),"Considerations on dressed and free photon conversion and nanostructure formation."

Abstract: It has been experimentally shown that chemical processing and dopant annealing under light irradiation induce autonomous nanostructure formation, and that the dressed photons play important role in the structure formation. On the other hand, the theory to explain these experimental situations are still inadequate, and a development of practical theory is expected for applications such as device design and optimization of device fabrication conditions. In this presentation, the conceptual model for the conversion between dressed and free photons is applied to the formation of a nanostructure mediated by the dressed photons, based on numerical simulations.

【民間セクターからの招待講演】

三宮俊（株式会社リコー 先端技術研究所）、「ドレスト光子―自由光子の変換とナノ構造形成に関する考察」

講演概要：光を照射しながら化学的な加工やドーパントのアニール処理を行うことで自律的な構造形成が引き起こされ、この構造形成にドレスト光子が重要な役割を果たしていることが実験的に示されている。一方、このような実験状況を説明する理論は未熟であり、デバイス設計やデバイス作製条件などの観点から、実用可能な理論の構築が期待されている。本発表では、これまで検討を進めてきたドレスト光子と自由光子の変換に関わる概念モデルを、ドレスト光子を介在したナノ構造形成に適用することを、数値シミュレーションを基軸に検討する。

Off-shell mathematical science toward system's analysis and designing

解析から設計に向けたオフシェル数理科学

I-3

I. Banno (Yamanashi Univ.), "Theory of Quantum Dissipative Structure associated with Dressed Photons."

Abstract: The photon-breeding (PB) process [T. Kawazoe, M. A Mueed and M. Ohtsu, Appl. Phys. B **104**, p.747(2011)] makes light emitting diode from the indirect-type semiconductors. For a long time, such the materials had been believed unsuitable for light emitting devices. The present theory describes the light emitting from the photon-breeding device, referring to the non-equilibrium thermodynamical theory of dissipative structure [G. Nicolis and I. Prigogine, "Self-Organization in Nonequilibrium Systems", Wiley (1977)]. The dissipative structure appears far from the equilibrium by balance between the entropy production in the system and the entropy dissipation out of the system. As suggested by the original theory, it is essential for the quantum version theory to treat the non-linear and open system. Our theory starts from the action integral in the non-relativistic quantum electrodynamics, and considers the nonlinearity employing the immanent vector potential, that is, dressed photon, and adjusts the causality and anti-causality together with the gauge function of the open system.

坂野斎（山梨大学工学部）、「ドレスドフォトンが関わる量子的散逸構造の理論」

講演概要：フォトンブリーディング製作過程［T. Kawazoe, M. A Mueed and M. Ohtsu, Appl. Phys. B 104, p.747(2011)］は，長い間発光デバイスに不向きであると信じられてきた間接遷移型半導体から発光ダイオードをつくることを可能にした．発表する理論はフォトンブリーディングデバイスからの発光を，非平衡熱力学の散逸構造の理論［G. Nicolis and I. Prigogine, "Self-Organization in Nonequilibrium Systems", Wiley (1977)］をモチーフに記述するものである．散逸構造は系内でのエントロピー生成と系外へのエントロピー散逸のバランスに よって平衡から遠いところに現れる．量子版の散逸構造の理論構築のためには，元の理論から示唆されるように，非線形系かつ開放系を扱うことが必要になる．この理論は非相対論系の電磁量子力学の作用積分から出発し，内在ベクトルポテンシャル，つまり，ドレスドフォトンにより非線形性を考慮し，また，因果律と反因果律の調整，及び，ゲージ関数の調整を行うことで開放系を記述する．

Off-shell mathematical science toward system's analysis and designing

解析から設計に向けたオフシェル数理科学

II-1

E. Segawa (Yokohama National Univ.), "Comfortability of quantum walk."

Abstract: A response from the surface of the internal graph is obtained by sequential input of quantum walks to the graph. This response tells some information on the graph structure. In this study, we will observe not only the information on the surface but also its interior induced by quantum walks. To this end, we introduce the notion of "comfortability" which gives how quantum walkers are stored in this graph for large time step; that is, how quantum walkers feel comfortable to this graph. We show that the comfortability can be expressed by some quantity of the graph geometry induced by quantum walk.

瀬川悦生（横浜国立大学）、「量子ウォークの Comfortability」

講演概要 : 内部グラフに対して量子ウォークの打ち込みを続けることにより、そのグラフの表面から応答が得られる。この応答から、内部グラフの構造の情報を得ることができる場合がある。この研究ではさらに進んで、このグラフの量子ウォークによる「表面上の様子」だけではなく、その「内面」についても観察したい。そのための一つの手段としてComfortabilityという概念を導入し、量子ウォーカーが十分に時間経過したときに、どの位そのグラフに蓄積されているか、つまり、どのくらいこのグラフを居心地よく感じているかに着目する。すると、この量が量子ウォークによって誘導されるグラフのある幾何的な構造を表す量によって表現されることがわかったので、報告する。

Off-shell mathematical science toward system's analysis and designing

解析から設計に向けたオフシェル数理科学

II-2

L. Matsuoka (Hiroshima Institute of Technology), "Maze-solving behavior in the quantum walk model on networks."

Abstract: The study of the autonomous energy transfer of the Dressed Photons is in progress based on the specific quantum walk model. In this presentation, we show the recent progress of the study of the quantum walk model on the network mazes where the shortest path is exhibited autonomously. We found the amount of the remained amplitude on the shortest path is expressed by rational numbers in most cases, which implies the existence of the mathematical rule corresponding to the network structure.

松岡雷士(広島工業大学)、「ネットワーク量子ウォークモデルにおける迷路解決挙動」

講演概要：量子ウォークモデルに基づくドレスト光子の自律的エネルギー移動の研究が進んでいる。本講演では迷路状に構成されたネットワーク上で時間発展させた量子ウォークが、あたかも迷路の最短経路を導き出すような挙動を示すことについて、最新の研究結果を報告する。数値計算の結果、最短経路に残留する振幅の絶対値はほぼ全て何らかの有理数で表現できることがわかっており、ネットワーク構造と対応する明確な数学的規則の存在が示唆される。

Off-shell mathematical science toward system's analysis and designing

解析から設計に向けたオフシェル数理科学

III-1

H. Saigo (Nagahama Institute of Bio-Science and Technology), "Quantum Fields as Category Algebras."

Abstract: In the present talk, we propose a new approach to quantum fields in terms of category algebras and states on categories. We define quantum fields and their states as category algebras and states on causal categories with partial involution structures. By utilizing category algebras and states on categories instead of simply considering categories, we can directly integrate relativity as a category theoretic structure and quantumness as a noncommutative probabilistic structure. Conceptual relationships with conventional approaches to quantum fields, including Algebraic Quantum Field Theory (AQFT) and Topological Quantum Field Theory (TQFT), are also discussed.

西郷甲矢人（長浜バイオ大学）、「圏代数としての量子場」

講演概要 : 本講演においては、圏代数および圏上の状態の概念に基づく量子場への新しいアプローチを提起する。われわれは、量子場およびその状態を部分的に定義された対合構造をもつ「因果的な圏」の上の圏代数および状態として定義する。単に圏を用いるだけではなく圏代数と圏上の状態を用いることにより、圏論的構造としての相対性と非可換確率構造としての量子性を直接的に統合できる。代数的量子場理論や位相的量子場理論との概念的な関係性についても議論する。

Off-shell mathematical science toward system's analysis and designing

解析から設計に向けたオフシェル数理科学

III-2

K. Okamura (RODREP/Nagoya Univ.), "On the Schrodinger picture in C*-algebraic quantum theory."

Abstract: We discuss the Schrodinger picture in C*-algebraic quantum theory. In the Schrodinger picture, we treat the state change of the system caused by the dynamics (of the system and its environment). Dirac's notion of transition probability plays a central role in this context. We formulate the Schrodinger picture using transition probability in a category theoretical way. Furthermore, we connect the theory of transition probability with quantum measurement theory. The axiomatic approach to quantum measurement in C*-algebraic quantum theory is consistent with sector theory and gives good examples of transition probability in the category theoretical setting.

岡村和弥(ドレスト光子研究起点/名古屋大学)、「C*-代数的量子論におけるシュレディンガー描像」

講演概要：C*-代数的量子論におけるシュレディンガー描像について議論する。シュレディンガー描像では、(系とその環境の) 力学によって引き起こされる系の状態変化を扱う。ここでは、Diracの遷移確率の概念が中心的な役割を果たします。遷移確率を用いてシュレディンガー像を圏論的に定式化する。さらに、遷移確率の理論を量子測定理論と結びつける。C*-代数的量子論における，セクター理論と整合的な量子測定の公理的アプローチは，圏論的な設定における遷移確率の良い例を与える。

Off-shell mathematical science toward system's analysis and designing

解析から設計に向けたオフシェル数理科学

IV-1

H. Sakuma (RODREP), "On the role of duality field for understanding "off-shell physics."

Abstract: In the comparison of "on-shell vs. of-shell fields", we think that the former corresponds to physical objects or systems under consideration, while the latter to a background to which we won't pay special attention. This simple view can be likened to the relation between a given physical system under consideration and spacetime as a "background" with which we describe the system. In the context of relativistic situations, we know that these two elements exist in a special interdependent way which may be called a kind of specific "duality". In this talk, we discuss a possibility of opening up a novel view in pursuing off-shell science by reconsidering such a specific "duality".

佐久間弘文（ドレスト光子研究起点）「オフシェル物理における双対場の役割について」

講演概要：「オンシェル場―オフシェル場」という対比においては、前者は「見えるもの」としての「図」、後者は「図」を「下支えする」「地」という見方が可能であると思われる。この見方は、着目する「物理系」とそれを記述する為に必須な「時空」という対比に例える事ができる。特に、相対論の文脈では、両者は相互に関わりあう、独特な"双対"関係を呈している事が知られているが、ここでは、その"双対"関係を再吟味する事で、如何なる「新たな見方」が可能であるかを議論する。

シンポジウム

ドレスト光子とそのオフシェル科学としての展開
---実験と理論の対応のために、今何が求められているか？---

Dressed photon and its development as off-shell science

--- What are required for comparing experiments and theories? ---

大津　元一（一般社団法人　ドレスト光子研究起点）

Motoichi OHTSU (Research Origin for Dressed Photon)

1.　はじめに

ドレスト光子（DP）が関与する新規の光学現象が多数観測され、応用されている[1-6]。それは従来の光科学の理論では説明不可能である。なぜならばDPはナノ寸法領域での光・物質相互作用により生成する量子場であるが、このように相互作用する量子場は古くから知られているように量子力学・非相対論など、オンシェル科学での常識とはかけ離れた性質を持つからである[7-9]。この問題を解決するためにオフシェル科学の研究が始まった[10]。その結果、これまでにDPの生成機構と、それがもたらす独特な現象が明らかになった。

生成されたDPのエネルギーは多数のナノ物質間を移動する。それがもたらす新規現象が多く観測されているが、それはランダムウオークモデルでは記述できない。このような複雑系の記述にもオフシェル科学が必要であることから量子確率論、量子ウオーク(QW)などの手法が適用されるようになった。またその過程でカオス現象の発現の可能性も指摘されている。

本シンポジウムの目標の一つはDPの実験結果を理論的に説明するために、理論に何が求められているかを議論することであり、そのための導入として本講演を供する。

2.　DPの生成過程

DPの生成には電磁場の縦方向成分およびMinkoswki空間でのspacelike 4-momentumが寄与する相互作用が必要である[11]。すなわちまずspacelikeのKlein-Gordon (KG)方程式を満たすspacelikeベクトル場と点状源との相互作用により timelike Majorana粒子と反粒子の対が生成する。これらの粒子場は非伝搬であり、いち早く対消滅して小さな光場を生成する。これこそがDP場なのである。上記の理論モデルの対称性が数学的観点から考察されている[12]。

点状源により乱されるKG方程式の解のtimelikeモードの空間成分は湯川型関数で与えられ、DPの空間局在性を表す。DPはそのエネルギーの最小単位を使って量子化される。その最小単位はDP定数と呼ばれ、その逆数はDPの最大寸法に相当する。実験によるとその最大寸法は50-70nmである[11]。DPが関与する現象はこれ以下の寸法の空間で生ずるのである。

なお、上記の対のスピンが反平行の場合、この対が消滅するとスピン0のDPが生成し、それは電気的性質を持つ。平行スピンの対が消滅するとスピン±1のDPが生成し、それは磁気的性質をもつ。

エネルギーの励起状態にあるDPがフォノン場の揺らぎにより脱励起すると伝搬光（自由光子）を生成するが、DPのスピンが0の場合、その伝搬光のスピンも0、したがって粒子場のように弾丸状の光の場が自由空間を伝搬していく。これは単一光子相当のanti-bunching性を示し、それが多数集まってDPクラスター光となっていることが実験により確認されている[13,14]。すなわちそれは回折のない光ビームである。DPのスピンが±1の場合、生成された伝搬光は磁気光学効果に関与するが、この現象は大きな磁気光学定数を持つ偏光制御素子に応用されている[15]。

3.　DPエネルギーの移動の特性

DPのエネルギーが多数のナノ物質間を移動する現象を記述するためのQWの研究が進んでいる[16,17]。たとえばDPのエネルギー移動の特性を評価する実験結果に表れた移動の自律性の特徴[18]と同様の結果はQWモデルの一つ、Groverウオークモデルにより独立に得られている。この成果をもとにDP用の2次元（図1）、3次元のQWモデルと空間時間発展方程式が得られた[19]。

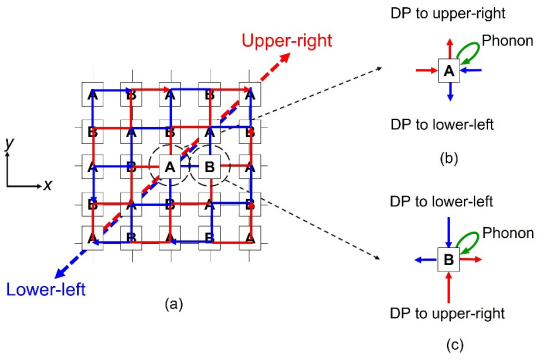

図1　DPに対する2次元QWモデルの概念図

この方程式を用い、DP がファイバプローブのテーパ部を移動し先端に到達する様子を推定した結果、ファイバ内での DP エネルギーの空間分布には軸非対称性が現れた。この事実は高効率のファイバプローブ開発の時代に採用された技術と整合している。その当時、非対称性を持つファイバプローブを作り、テーパ部に HE_{11} モードを励起して効率を飛躍的に向上させたのであった [20]。HE_{11} モードなる術語はオフシェル科学が存在しない時代に、DP の発生に至るテーパ部の電磁場の振る舞いを表現するための窮余の策であった。QW モデルを使うとそのような非対称性にかかわる現象が自動的に無理なく再現されたのである。

4. 関連する基礎理論

前節までの理論を展開するための基礎となる理論研究が次のように並行して進められている。

(1) ミクロ系で生成した DP をマクロ系で観測するための量子測定理論の構築を目指した研究が進展している [21]。これには C*-代数で記述される量子系に対する測定理論が利用される。さらに、DP を記述する「ネットワーク量子場」を展開するうえで 必要となるグラフの性質、およびネットワーク量子場のダイナミクスが検討されている。

(2) DP の特性記述のための圏論代数の構築が進展している [22-24]。すなわちオフシェル科学の基礎として「物理量」や「状態」の概念の適切な定式化が必要なことから、量子場を圏代数として捉え、その局所状態を圏代数上の状態として捉える。これにより圏上の QW の概念を通じてオフシェル量子場の動力学のモデル化の構築が進められている。

5. おわりに

これまでの実験研究で見いだされた DP の関わる新規な現象の起源・その特徴がオフシェル科学の理論研究の進展により遂に記述可能となった。それは DP にとどまらず宇宙論に至る広範な理論とつながっている [11]。オフシェル科学により新しい学問体系が拓かれることが期待されている。そのための今後の課題として第 4 節に記した基礎理論研究を進めること、さらに第 2,3 節の理論との統合による体系的理論の形成が重要である。その試みとしてネットワーク量子場、圏論代数と QW との関係づけが検討されている。

なお、以上のようなオフシェル科学の急進展を反映し、学術誌 Symmetry では Special Issue “Quantum Fields and Off-Shell Sciences” が企画され、筆者がその Guest Editor と務めた。本稿の参考文献 11,12,16,17,21-24 はその投稿論文である。

謝辞

当法人の小嶋泉顧問、佐久間弘文理事をはじめ、共同研究を推進して下さっている研究者諸氏、特に本稿執筆に際しご助力を賜った西郷甲矢人氏（長浜バイオ大）、岡村和弥氏（名古屋大）、瀬川悦生氏（横浜国大）に深く感謝致します。

参考文献

1) M. Ohtsu, *Dressed Photons* (Springer, Heidelberg, 2013).
2) M. Ohtsu, *Silicon Light-Emitting Diodes and Lasers* (Springer, Heidelberg, 2016).
3) M. Ohtsu, *Progress in Nanophotonics 5*, ed. by T. Yatsui (Springer, Heidelberg, 2018) 1-51.
4) M. Ohtsu, *Opto-Electronic Advances*, **3** (2021) 190046
5) M. Ohtsu, *Off-shell Application in Nanophotonics* (Elsevier, Amsterdam, 2021).
6) M. Ohtsu, et al., *Progress in Optics,* 64, ed. by T.D. Visser (Elsevier, Amsterdam, 2019) 45-97.
7) R. R. Haag: *Local Quantum Physics: Fields, Particles*, Algebras (Springer, Heidelberg,1996).
8) R.F. Streater and A.S. Wightman: *PCT, Spin and Statistics, and All That*, (Princeton Univ. Press, Princeton, 2000).
9) R. Jost: *The General Theory of Quantum Fields* (American Mathematics Soc., 1965).
10) 大津元一、小嶋泉 編著：ここからはじまる量子場（朝倉書店、東京、2020）.
11) H. Sakuma and I. Ojima, *Symmetry* **13** (2021) 593.
12) H. Ochiai, *Symmetry* **13** (2021) 1283.
13) 川添忠、他、第 82 回応物会秋季講演会（2021 年 9 月）講演番号 12a-N202-2
14) 佐久間弘文、川添忠、第 82 回応物会秋季講演会（2021 年 9 月）講演番号 12a-N202-3
15) T. Kadowaki et al., *Sci. Reports*, **10** (2020) 12967.
16) K. Higuchi, et al., *Symmetry* **13** (2021) 1134.
17) N. Konno, et al., *Symmetry* **13** (2021) 1169.
18) W. Nomura, et al., Appl. Phys. B, **100** (2010) 181.
19) M. Ohtsu, *Off-shell Archive* (September, 2021) OffShell: 2109R.001.v1
20) T. Yatsui, et al., Appl. Phys. Lett., **71** (1997) 1756.
21) K. Okamura, *Symmetry* **13** (2021) 1183.
22) H. Saigo, *Symmetry* **13** (2021) 1172.
23) H. Saigo and J. Nohmi, *Symmetry* **13** (2021) 1573.
24) H. Saigo, *Symmetry* **13** (2021) 1727.

招待講演

量子ウォーク力学系とドレスト光子の実験結果との比較

Dynamical system of quantum walks and experimental results on dressed photon

瀬川 悦生(横浜国立大学)

Etsuo Segawa (Yokohama National University)

1. はじめに

ナノ粒子系と光の相互作用によって生じるドレスト光子によって誘導される数多くの独特な光学現象[1]の事例を説明するため, オフシェル科学の研究が行われている[2]. その中で, 量子ウォークモデルを用いたドレスト光子ダイナミクスを簡略化した数理的研究がおこなわれるようになってきている[3,4].

量子ウォークの時間発展は, グラフ上の状態推移を各時刻ユニタリ変換によって与えられる. この原型は [5]の中にも既に与えられており, 量子シミュレータや高速化を実現する量子探索アルゴリズムを担う数理モデル[6]の候補としても着目されている. 特に特出すべき性質として, 線形的拡がりと局在化の相反する 2 つの性質の共存が明らかになっている[7]. これを説明するために, 対応するランダムウォークを考える. ランダムウォークにおいては, 時刻 n に対して, スタート地点から大体 $n^{1/2}$ のオーダーの区間に粒子は多く観測される. また, どの頂点での発見確率は長時間では 0 に収束する. これはいわゆる中心極限定理によって明示的に表現され, ガウス分布が特徴づけている. 一方で, 量子ウォークの場合もこの中心極限定理に対応するものが存在する. スタート地点から n のオーダーの区間に観測される線形的拡がりと, また摂動箇所周辺では長時間においても正の発見確率となる局在化を表す. これをドレスト光子の事例に翻ると, ファイバープローブの先端という空間的に特異な場所で強く光るというドレスト光子の振舞いと, この量子ウォークの摂動部分における局在化の間に関係性はないだろうか？

2. 量子ウォーク力学系

このような動機から, 量子ウォークモデルによるドレスト光子解釈のチャレンジが始まっている. 実験系にモデルをより寄せるにあたり, 1 つ量子ウォーク数理として越えなければいけない問題がある. それは, システムサイズの有限性である. 時間発展がユニタリであるため, 全ての固有値の絶対値が 1 なので, 状態は全ての固有モードが主張し続け, いつまで経っても収束しないのである. 実験結果はあるリミットサイクルでの状態で与えられているとするのであれば, これは大きな問題である. そこで考案されたのが量子ウォーク力学系である[8].

量子ウォーク力学系は, 与えられた有限グラフに境界を与えて, そこに外界との流出入を繰り返すモデルである. これまでの研究では量子ウォークの空間は基本的に 2 乗加算和な関数空間で考えられていたが, それに対し, 本研究では常に流入が繰り返されていることに表れているように, 一様有界な関数空間まで拡げて考えることがポイントである. 実際, もし外界込みで考えると, システム全体の時間発展はユニタリ時間発展作用素になるが, 一方で内部グラフに制限すると, 実は固有値が半径 1 の複素円盤の内側に存在する作用素になることが示せる. これは外界へ量子ウォーカーが流出していることを表している.

したがって, 真に固有値の大きさが 1 以下であることが原因で時刻の経過とともに減衰する分が, 外界からの流入により補われ, 最終的にある固定点もしくはリミットサイクルに収束させるという力学系の描像に当てはめることが期待される. 実際入力の振動数がすべての頂点で一定の場合(下で現れている数式の $\alpha(v)$=const. に対応), そのことが数学的に厳密に証明されている[8].

このようにして量子ウォークとドレスト光子との繋がりを探したいという目的を発端に, 一様有界な関数空間上の量子ウォークダイナミクスを内部グラフに制限することにより, 外界からの影響をうける力学系モデルとして量子ウォークをデザインする量子ウォーク力学系の研究がはじまった. 本研究では ϕ_n を時刻 n での状態としたときに, 次のようなモデルを考える.

$$\phi_{n+1} = E\ \phi_n + \rho_n,\ \phi_0 = 0$$

ここで, E は外界も含めた系全体の量子ウォークの無限次元ユニタリ時間発展作用素 U を内部グラフに制限した有限作用素, ρ_n を時刻 n での外界からの流入量とする. このユニタリ作用素の切頂作用素 E は, 正規性どころか, 代数的重複度と幾何的重複度が異なる場合もあり, 対角化可能性も保証されず, 従来の正規性を前提とした伝統的な解析手法が当てはまらず, ドレスト光子を始めとするオフシェル科学を動機とした, 新しい手法の開発の研究が進められている.

3. 幾つかの事例

量子ウォークの中でも量子探索アルゴリズムの中で現れる Grover walk とよばれるものに限定したときに, 流入量 ρ_n に関して特別な場合で, 解

招待講演

ったことがあるので, それを本研究で報告する. 各境界頂点 v が, 時刻 n で

$$r(v)\exp(2\pi i\,\alpha(v)\,n)$$

の流力を受けるとする, ここで r(v) > 0, α(v) は境界頂点 v に依存した実数値である.

(1) 境界頂点によらず振動数 0 のとき(一定入力)

【定理 1】
(i) 境界頂点を{1,…,r}とラベル付けして, そこからの流入値と時刻無限大での出力値をそれぞれ $\boldsymbol{\alpha}$:=(α_1,… α_r), $\boldsymbol{\beta}$:=(β_1,…, β_r)とすると

$$\boldsymbol{\beta} = \mathrm{Gr}(r)\ \boldsymbol{\alpha}.$$

ここで Gr(r) は r 次元の Grover 行列.
(ii) 内部グラフ G に時刻無限大で滞在している量子ウォーカーの量を定常状態の二乗加算和と定義し, C(G)とする. 境界の個数 r=2 の場合, 次のように表される.

$$C(G) = |E(G)| + \tau_2(G) / \tau_1(G).$$

ここで, |E(G)|はグラフ G の枝の本数, τ_j(G) (j=1,2) は, グラフ G の全域木や全域森の個数に関係するものであるが詳細は省く.

(2) 境界頂点によらず振動数πのとき(交代入力)

元の ϕ_nの代わりに, ϕ_n:= $(-1)^n\phi_n$を考え, この定常状態を考察する.

【定理 2】
(i) (1)と同様な状況で
もしグラフ G が二部グラフのとき, 頂点を X と Y に分割して, 入力と出力のベクトルもその順番に並べると,

$$\boldsymbol{\beta} = -\sigma_z\,\mathrm{Gr}(r)\,\sigma_z\,\boldsymbol{\alpha}.$$

ここでσ z はパウリ行列
もしグラフ G が二部グラフでないと

$$\boldsymbol{\beta} = \boldsymbol{\alpha}\ \text{(完全反射)}$$

(ii) (1)と同じ状況で
もしグラフ G が二部グラフのときは(1)(i)と一致する.
一方でもしグラフ二部グラフではないときは,

$$C(G) = \iota_2(G) / \iota_1(G).$$

ここで, ι_j(G) (j=1,2) はグラフ G の奇閉路を１つだけ含む連結成分と木の連結成分による全域部分グラフを数え上げることよって得られる量である.

(3) 振動数が各場所で異なるとき(一般の入力)

数学の研究としてまだ本格的に行われていない状況ではあるが, そのとりかかりとして, レーザーカオス分野と結びつきが見えてきそうな興味深い数値実験の結果があるのでそれを紹介する. 頂点数 4 のサイクルグラフにおいて, 頂点 1,2,3 を境界とする頂点数 4 のサイクルグラフにおける頂点 1 から出てくる出力の時間推移をプロットする. 左の図は入力の振動数が全て有理数で与えられたものに対し, その隣の図は振動数が無理数で与えられたものである. すると, 入力の振動数が有理数で与えられたものは時刻が十分に経過すると周期的な振舞いになっているのに対して, 無理数を入力すると非周期的になり, カオティックな時間推移になっていることが見て取れる.

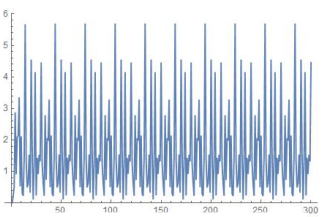

図 1: α(u)が有理数のとき

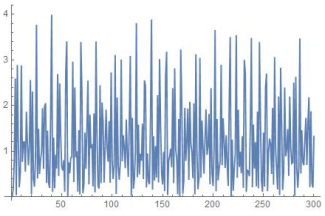

図 2: α(u)が無理数のとき

4. 終わりに

定常状態の二乗加算和は, α で特徴づけられて流入してきたドレスト光子が, 与えられたグラフ内部に対して「どの位居心地よく感じているか」を表す量ともいえる. すると, 入力の振動数が頂点によらずに 0 かπのときは, 与えられたグラフを注意深く眺めるだけで, 表されることを示した. さらにまた, 入力が無理数で表されると, カオス的になることが, 数値計算で示唆された. 逆にどの位で脱出するかを考察する研究もおこなわれており, sink と source との距離が離れているほど, むしろ脱出がし易くなる場合があるという非直観的な現象が, ドレスト光子の[9]の実験結果と一致する. このようにドレスト光子の実験の事例とこの量子ウォークモデルによる数学的結果が示すことを今後より吟味していく.

参考文献

[1] 大津元一: ドレスト光子(朝倉書店, 東京, 2013)
[2] 大津元一・小嶋泉編著, ここからはじまる量子場 (朝倉書店, 東京, 2020).
[3] M.Hamno H. Saigo, Electronic Proceedings in Theoretical Computer Science 315, 2020, pp. 93-99
[4] M. Ohtsu, Off-shell Archive (2021) OffShell: 2109R.001.v1
[5] R.P.Feynman, A.R.Hibbs, Dover Publications, Inc., Mineola, NY, emended edition (2010).
[6] A.Ambainis, Internatioanl Journal of Quantum Information 1 (2003) pp.507–518.
[7] N.Inui, N. Konno, E. Segawa, Phys. Rev. E, 72,. 056112.
[8] Yu. Higuchi. E. Segawa, Journal of Physics A: Mathematics and Theoretical 52 (39) 395202 (2019).
[9] W. Nomura, T. Yatsui, T. Kawazoe, M. Naruse,and M. Ohtsu, Appl. Phys. B 100 (2010) pp.181-187.

シンポジウム

ドレスト光子の記述のための圏代数

Category Algebras for the Description of Dressed Photons

°西郷　甲矢人 (長浜バイオ大学)
Hayato SAIGO (Nagahama Institute of Bio-Science and Technology)

1.　はじめに

ドレスト光子は、ナノ粒子系と量子電磁場である光が相互作用をつうじて一種の「合成系」をなすことで生まれる「物質励起によって装いを得た」光であり、数多くの実験結果ともに様々な工学的応用が進んでいる（文献1）。

一方で、その数理的取り扱いは従来の物理学の標準的な観点からは原理的な困難を有している。何よりも、「相互作用する量子場」の数理が現在も発展中であること、そして「物理学的に当然」と考えられがちな諸公理をみたす量子場のモデルが本質的に自由場のみになってしまうといった数理的事実が、その困難のうちでもっとも本質的なものである（文献2）。

こうした困難を乗り越えるためには、従来の物理学の枠を超えた斬新なモデル化が必要であり、非可換確率論（量子確率論）や量子ウォークを用いたモデル化をはじめ、近年ますます盛んな研究が進んできている。

本講演においては、そうしたこれまでの具体的な研究をある意味で包括しつつ、「相互作用する量子場」を正面から扱えるようにすることが期待できる新たなアプローチ（文献3）を紹介したい。このアプローチは、非可換確率論と圏論の新たな融合としての「圏代数とその状態」の概念枠組み（文献4）に基づく。

2.　圏代数としての量子場

量子場の理論は、歴史的には相対論と量子論の融合を目指す中で生まれた（もちろん、非相対論的文脈も当然重要であり、物性物理の基盤のひとつをなしているが）。

では相対論の本質とは何かといえば、変換とその間の関係性であり、それは通常「群」の概念を用いて捉えられる（実際には、群をさらに一般化した「亜群」を考えているとみたほうが適切な場合も多いのだが）。一方で、相対論の本質としての因果構造を見逃すわけにはいかない。こちらは「順序集合」の概念を用いて捉えられる。

したがってそれらをともに包含する一般的構造はないか？と考えるのは自然であろう。それが「圏」である。圏にまで拡張すると、通常の順序集合の観点からはどうしても漏れ落ちてしまいがちな量子場の「オフシェル」性をきちんと取り込むことができるし、一般の不可逆過程をも排除せずに「相対論の本質」を相当に一般的に（当然ながら一般相対論や、離散時空のような文脈にまで）広げて理解することが可能である（なお、非相対論的な文脈も、違う圏を考えればよいだけである）。

一方、量子論の本質は非可換代数およびその上の状態であるといえる。状態は、非可換代数の元である「物理量」に対し「期待値」を対応させる汎関数として定義され、それらの組からは通常のヒルベルト空間論的な枠組みも再構築が可能である。

問題は、「相対論」的な変換構造・因果構造・オフシェル的特性などを反映した非可換代数がどのように定義できるか？ということであるが、それがまさに「圏代数」なのである。

圏代数は、圏の「合成」構造を反映させた「畳み込み」代数であり、関数のなす代数・多項式代数・行列代数といった「身近な」代数を例として含む（群の表現論等で重要な「群環」も圏代数の一例である）。圏の構成要素である「射」という矢印を「不定元」とみなしたようなものともいえる。もし圏に（部分的な）「向きを反転する構造」があれば、圏代数もまた「エルミート共役」的な構造をもつ。

3.　量子場の状態＝圏上の状態

そのような圏代数の上の状態を考えると、これは本質的に「不定元としての射」に付値する一種の「重みづけ」と解釈できる。つまり、圏というダイナミクスの基本構造に定量的な重みを加えたようなものなのである。これが「圏上の状態」の概念である。

そして本講演では、この「圏上の状態」がまさしく量子場の状態にあたるものであることを、物理的な洞察および「代数的量子場理論」や「位相的量子場理論」などの先行研究とのかかわりを明らかにすることで、なぜこの枠組みが適切だと考えられるかを論じていく。

4.　展望

さらに時間が許せば、この新アプローチがいかなる意味で量子ウォーク等の近年進んでいる研究と関係するのかにも触れるとともに、一般相対論や宇宙論といった「まさかそんなところと関係するとは信じられない」と一見思えるような話が、たしかにドレスト光子の数理と関連していることの深い理由についても述べたい。

参考文献

1) 大津元一: ドレスト光子(朝倉書店, 東京, 2013)
2) 大津元一・小嶋泉編著: ここからはじまる量子場(朝倉書店, 東京, 2020)
3) Saigo, H. Quantum Fields as Category Algebras. *Symmetry* **2021**, *13*(9), 1727.
4) Saigo, H. Category Algebras and States on Categories. *Symmetry* **2021**, *13*(7), 1172.

シンポジウム